Characterization of the Zr-polymeryl Species Present during Ethylene and Propylene Polymerizations by Homogeneous Zirconocene Catalysts

By Mihaela Vatamanu

A thesis submitted to the Department of Chemistry

in conformity with the requirements for

the degree of Doctor of Philosophy

Queen's University

Kingston, Ontario, Canada

December 2008

Abstract

A detailed investigation of Zr-polymeryl intermediates, present during ethylene and propylene polymerization by metallocene and non-metallocene catalysts, is presented. In this regard, the potential use of bromine as a quenching agent to give polymers with brominated end groups is investigated. Using NMR spectroscopy, these groups can be identified as primary or secondary and quantified, thus providing information on the nature of the Zr-polymeryl linkage(s) and their relative concentration(s). Bromine quenching was examined for ethylene polymerization by $Cp_2ZrMe_2/B(C_6F_5)_3$, and for propylene polymerization by $Cp_2ZrMe_2/B(C_6F_5)_3$, $(indenyl)_2ZrMe_2/B(C_6F_5)_3$, and *rac*-$\{C_2H_4(1\text{-indenyl})_2\}ZrMe_2/B(C_6F_5)_3$. Polymers with primary alkyl bromide end groups were obtained. In the case of propylene polymerization by [ONNO]$Zr(CH_2C_6H_5)_2$/MAO/2,6-di-^{t}butylphenol, both primary and secondary alkyl bromide end groups were detected. Primary alkyl bromide end groups result from the cleavage by bromine of primary Zr-CH_2~polymeryl linkages while secondary alkyl bromides are the result of the cleavage by bromine of secondary Zr-$CH(Me)CH_2$~polymeryl linkages. The concentration of Zr-CH_2~polymeryl intermediates was found to be low, suggesting that the catalyst deactivates during the polymerization.

A second objective of this research is to investigate the formation of Cp_2Zr^+-allyl complexes as these species are proposed to arise during the polymerization and deactivate the catalyst. Compounds of type $[Cp_2ZrMe]^+$ were found to react with vinylidene compounds of type $CH_2=C(Me)R$, (R = CH_2CHMe_2 and $CH_2CH(Me)C_3H_7$), to form methane and Cp_2Zr^+-allyl complexes. The reaction of $Cp_2ZrMe_2/[Ph_3C][B(C_6F_5)_4]$ with

CH_2=C(Me)CH_2CHMe_2 involves the unprecedented [Cp_2Zr(Me)(CH_2CMeCH_2CHMe_2)]$^+$ intermediate, detected by low temperature one- and two-dimensional NMR spectroscopy. The observation of this intermediate represents the first direct experimental evidence for a d^0 metal-alkyl-olefin complex. The dynamic behavior and the kinetics of formation of Cp_2Zr^+-allyl complexes were also investigated by NMR spectroscopy. *In situ* propylene polymerization studies indicate that Cp_2Zr^+-allyl polymeryl intermediates form under catalytic conditions when either $Cp_2ZrMe_2/B(C_6F_5)_3$ or $Cp_2ZrMe_2/[Ph_3C][B(C_6F_5)_4]$ are used. Formation of Zr-allyl species occurs in the early stages of the polymerization process, even before the [Cp_2ZrMe]$^+$ catalyst is completely consumed, by recoordination of the polypropylene-containing vinylidene end groups, which are the normal products of chain transfer reactions via β-H elimination, to the active catalyst.

Acknowledgements

The input provided by Dr. Michael C. Baird, Dr. Kim B. McAuley, and Dr. Ralph A. Whitney during my Ph. D program is thankfully acknowledged. I want to thank Dr. Francoise Sauriol for her assistance with NMR spectroscopy and Dr. Bernd Keller for his help with mass spectrometry. I also want to thank Dr. Natalie M. Cann and Dr. Richard F. Jordan for useful input provided by in finalizing this thesis. I would acknowledge the encouragement, friendship and support provided by my family and friends as very important.

Statement of Originality

The research reported in this thesis was carried out by the author in the Department of Chemistry at Queen's University under the supervision of Dr. M.C. Baird.

This research reports on an investigation into the identities and relative concentrations of various Zr-polymeryl species present during ethylene and propylene polymerization by zirconium-based catalysts. It also reports on the synthesis and characterization of various $Cp_2Zr^+(\eta^3\text{-allyl})$ complexes which can serve as model compounds for similar Zr-allyl species which may form during the olefin polymerization. Furthermore, it reports on the first direct observation of a Cp_2Zr^+(alkyl)(olefin) intermediate during a reaction. d^0 metal-alkyl-alkene intermediates have been proposed to play a key role in Ziegler-Natta polymerization of olefins.

Table of Contents

Abstract……... i

Acknowledgements……. iii

Statement of Originality…….. iv

Table of Contents…… v

List of Schemes……... xi

List of Figures……. xv

List of Abbreviations…….. xxi

1. Introduction

1.1. General Introduction…… 1

1.2. Ziegler-Natta Polymerization Mechanism……... 4

1.2.1. Precursor Catalyst Activation……..... 4

1.2.2. Initiation……. 5

1.2.3. Propagation…… 6

1.2.4. Chain Transfer…… 7

1.2.5. Termination…… 11

1.3. Homogeneous Group IV Olefin Polymerization Catalysts…….. 12

1.3.1. Metallocene-based Catalysts…….. 12

1.3.2. Diamine bis(phenolate) Catalysts…….. 16

1.4. Cocatalysts……... 19

1.4.1. Methylaluminoxane……... 20

1.4.2. Boron-based Cocatalysts…… 22

1.5. Polymers Involved in this Thesis……. 26

1.5.1. Polyethylene……... 26

1.5.2. Polypropylene……..... 29

1.6. Aims of the Present Research…….. 31

References……... 33

2. An Investigation into the Zr-polymeryl Intermediates Present during Ethylene and Propylene Polymerizations by Zirconocene-based Catalysts

2.1. Introduction…….. 36

2.2. Results and Discussion…… 43

2.2.1. Model Compounds……. 43

2.2.2. Ethylene Polymerization…… 50

2.2.3. Propylene Polymerizations…… 54

2.2.4. The Analysis of Unsaturation in Atactic Polypropylene obtained from the $(indenyl)_2ZrMe_2/B(C_6F_5)_3$ catalyst system……... 62

2.2.5. The Presence of Zr-allyl Intermediates and Deactivation of the Catalyst…… 68

2.3. Summary…….. 76

2.4. Experimental Section……... 79

2.4.1. General Considerations…….. 79

2.4.2. Synthesis of Dimethylzirconocene……. 80

2.4.3. Synthesis of Bis(π-indenyl)dimethylzirconium……. 81

2.4.4. Synthesis of *rac*-ethylenebis(1-indenyl)dimethylzirconium…….. 82

2.4.5. Synthesis of Tris(pentafluorophenyl)boron……... 82

2.4.6. Ethylene Polymerization by $[Cp_2ZrMe][MeB(C_6F_5)_3]$…….. 83

2.4.7. Propylene Polymerization by $[Cp_2ZrMe][MeB(C_6F_5)_3]$…… 84

2.4.8. Propylene Polymerization by $[(indenyl)_2ZrMe][MeB(C_6F_5)_3]$…….. 85

2.4.9. Propylene Polymerization by

$[rac\text{-}\{C_2H_4(1\text{-indenyl})_2\}ZrMe][MeB(C_6F_5)_3]$……. 86

2.4.10. Synthesis of $BrCH_2CH(Me)(CH_2)_8CH_3$…….. 87

2.4.11. Synthesis of $BrCH_2CH(Me)CH_2CH(Me)CH_2CH_2CH_3$……... 88

2.4.12. *In situ* Reaction between

$[Cp_2Zr(\eta^3\text{-}CH_2C(CH_2CHMe_2)CH_2)][MeB(C_6F_5)_3]$ and bromine……. 89

2.4.13. ^{1}H NMR Spectroscopic Data of $BrCH_2(CH_2)_9CH_2Br$……. 89

2.4.14. ^{1}H NMR Spectroscopic Data of $CH_3CH(Br)(CH_2)_7CH_3$……. 90

2.4.15. ^{1}H NMR Spectroscopic Data of $CH_2=C(Me)CH_2CH(Me)CH_2CH_2CH_3$ 90

References…….. 91

3. An Investigation into the Zr-polymeryl Intermediates Present during Propylene Polymerizations by Nonmetallocene Catalysts

3.1. Introduction…….. 97

3.2. Results and Discussion……. 101

3.3. Summary…….. 109

3.4. Experimental Section……... 110

3.4.1. General Considerations…….. 110

3.4.2. Preparation of 2-cumyl-4-methyl-phenol ……. 111

3.4.3. Preparation of [ONNO] ligand…….. 111

3.4.4. Preparation of tetra(benzyl) zirconium…….. 112

3.4.5. Preparation of [ONNO]Zr($CH_2C_6H_5$)$_2$…….. 113

3.4.6. Propylene Polymerization…….. 113

References……... 115

4. Formation and characterization of various types of Zr-allyl complexes obtained from the reaction of [Cp_2ZrMe]$^+$ with $CH_2C(Me)(R)$, (R = H, CH_2CHMe_2, $CH_2CH(Me)(C_3H_7)$). Identification of [$Cp_2Zr(Me)(CH_2C(Me)CH_2CHMe_2)$]$^+$ as a reaction intermediate

4.1. Introduction…….. 118

4.2. Results and Discussion……. 123

4.2.1. Synthesis and Characterization of [$Cp_2Zr(\eta^3$-allyl)]$^+$ species……... 123

4.2.1.1. Reaction of [Cp_2ZrMe][$MeB(C_6F_5)_3$] with 2,4-Me_2-1-pentene…. 123

4.2.1.2. Reaction of [Cp_2ZrMe][$MeB(C_6F_5)_3$] with 2,4-Me_2-1-heptene…. 132

4.2.1.3. Reaction of [Cp_2ZrMe][$B(C_6F_5)_4$] with 2,4-Me_2-1-pentene: Identification of [$Cp_2ZrCH_2C(Me)CH_2CHMe_2$][$B(C_6F_5)_4$] as an Intermediate in the Formation of the Allyl Complex [$Cp_2Zr(\eta^3$-$CH_2C(CH_2CHMe_2)CH_2$][$B(C_6F_5)_4$]…… 142

4.2.2. The Dynamic Behavior of $Cp_2Zr(\eta^3$-allyl) Species……... 152

4.2.3. Kinetic Study on Cp_2Zr^+-allyl Species Formation……. 167

4.2.4. *In situ* Polymerization of Propylene by Borane-derived Cationic Zirconocene Catalyst: Identification of Cp_2Zr^+-allyl Polymeryl Intermediates……... 174

4.3. Summary…….. 189

4.4. Experimental Section……... 191

4.4.1. General Considerations…….. 191

4.4.2. *In situ* Reaction between $[Cp_2ZrMe][MeB(C_6F_5)_3]$ and 2,4-dimethyl-1-pentene…… 192

4.4.3. *In situ* Reaction between $[Cp_2ZrMe][MeB(C_6F_5)_3]$ and 2,4-dimethyl-heptene…… 194

4.4.4. *In situ* Reaction between $[Cp_2ZrMe][B(C_6F_5)_4]$ and 2,4-dimethyl-1-pentene…… 195

4.4.5. *In situ* Reaction between $[Cp_2ZrMe][MeB(C_6F_5)_3]$ and CD_3CN……... 196

4.4.6. General procedure for Variable Temperature NMR experiments…….. 197

4.4.7. General Procedure for Kinetics experiments……. 197

4.4.8. *In situ* Propylene polymerization by $[Cp_2ZrMe][MeB(C_6F_5)_3]$……. 199

4.4.9. *In situ* Propylene polymerization by $[Cp_2ZrMe][B(C_6F_5)_4]$…….. 199

4.4.10. General procedure for ESI-MS/MS experiments……. 200

4.4.11. ^{1}H NMR Spectroscopic Data of 2,4-Me_2-1-pentene…… 200

4.4.12. ^{1}H NMR Spectroscopic Data of 2,4-Me_2-1-heptene…… 201

References……... 202

5. Conclusions…… 207

Appendix A: ^{1}H NMR spectrum of atactic polypropylene obtained from (indenyl)$_2$ZrMe$_2$/B(C$_6$F$_5$)$_3$ in chlorobenzene after CD$_3$OD quenching…….... 213

Appendix B: ^{13}C NMR spectrum in aliphatic region of iPP obtained from propylene polymerization by [ONNO]Zr(CH$_2$C$_6$H$_5$)$_2$/MAO/2,6-di-^{t}butylphenol….. 214

List of Schemes

Scheme 1.1. Activation of the precursor catalyst by $B(C_6F_5)_3$…….. 5

Scheme 1.2. Initiation mechanism…….. 6

Scheme 1.3. Propagation mechanism……. 6

Scheme 1.4. Propylene insertion modes……. 7

Scheme 1.5. Chain transfer via β-hydrogen elimination……. 8

Scheme 1.6. Olefinic end groups formed as a result of β-hydrogen elimination reactions…… 9

Scheme 1.7. Chain transfer via β-Me elimination…….. 9

Scheme 1.8. Chain transfer via hydrogenolysis…….. 10

Scheme 1.9. Termination reaction using methanol……. 11

Scheme 1.10. General structure of a zirconocene catalyst…….. 12

Scheme 1.11. Correlation between the structure of the precursor zirconocene catalyst and the polymer microstructure (X = Cl, Me)……. 15

Scheme 1.12. General structure of a diamine bis(phenolate) zirconium complex….. 17

Scheme 1.13. Generation of the catalytically active species $[Cp_2ZrR]^+$……. 19

Scheme 1.14. Proposed structures for MAO……... 20

Scheme 1.15. Alkylation of the zirconocene dichloride precursor catalyst by MAO. 21

Scheme 1.16. Activation of the precursor catalyst by MAO…….. 22

Scheme 1.17. Activation of the precursor catalyst by $[Ph_3C][B(C_6F_5)_4]$…… 24

Scheme 1.18. The structure of the dimeric $[(Cp_2ZrMe)_2(\mu\text{-Me})][B(C_6F_5)_4]$ species.. 25

Scheme 1.19. Schematic representation of different types of polyethylenes: low density polypropylene (LDPE), high density polyethylene (HDPE), and linear low density polyethylene (LLDPE)……. 28

Scheme 1.20. General structures of isotactic and syndiotactic polypropylenes……. 30

Scheme 2.1. Bromine quenching scheme……... 41

Scheme 2.2. The brominated end groups of (a) isotactic polypropylene and (b) syndiotactic polypropylene.…….….. 49

Scheme 2.3. The brominated end groups of atactic polypropylene...……. 49

Scheme 2.4. Formation of internal vinylidene groups on a polymer chain via a Zr-allyl intermediate…….. 64

Scheme 2.5. Formation of isobutenyl groups on the polymer chain via a Zr-allyl intermediate…… 65

Scheme 2.6. Formation of isobutenyl end groups via a tertiary Zr-polymeryl intermediate…… 66

Scheme 2.7. Acidic isomerization of the vinylidene end group……. 67

Scheme 2.8. Olefinic groups present in atactic polypropylene obtained from the (indenyl)$_2$ZrMe$_2$/B(C$_6$F$_5$)$_3$ catalytic system in chlorobenzene……... 68

Scheme 2.9. Structures of deuterated end groups expected on the polymer chain as a result of the cleavage by CD$_3$OD of a (a) primary (1,2) Zr-polymeryl bond, (b) secondary (2,1) Zr-polymeryl bond, and (c-e) Zr-allyl bond……..…… 73

Scheme 3.1. Propylene insertion modes…… 98

Scheme 3.2. The [ONNO]Zr(CH$_2$C$_6$H$_5$)$_2$ catalyst…….. 100

Scheme 3.3. Mechanism of initiation for propylene polymerization using [ONNO]Zr($CH_2C_6H_5)_2$ catalyst……. 103

Scheme 4.1. Possible mechanisms for formation of Zr-allyl species during propylene polymerization. …… 121

Scheme 4.2. The structures of Zr-allyl complexes which may form from the reaction of [Cp_2ZrMe][$MeB(C_6F_5)_3$] with 2,4-dimethyl-1-pentene…... 123

Scheme 4.3. The NMR spectroscopic data of the η^3-$CH_2C(CH_2CHMe_2)CH_2$ ligand of complex **A** (chlorobenzene-d_5, 0°C, 600 MHz).…… 128

Scheme 4.4. The NMR spectroscopic data of the η^3-$CH_2C(Me)CHCHMe_2$ ligand of complex **B** (chlorobenzene-d_5, 0°C, 600 MHz)……. 132

Scheme 4.5. The structures of Zr-allyl complexes which may form from the reaction of [Cp_2ZrMe][$MeB(C_6F_5)_3$] with 2,4-dimethyl-1-heptene…... 135

Scheme 4.6. The NMR spectroscopic data of the η^3-$CH_2C(CH_2CH(Me)CH_2CH_2CH_3)CH_2$ ligand of complex **C** (chlorobenzene-d_5, 0°C, 600 MHz)…… 139

Scheme 4.7. The NMR spectroscopic data of the η^3-$CH_2C(Me)CHCH(Me)CH_2CH_2CH_3$ ligand of complex **D** (chlorobenzene-d_5, 0°C, 600 MHz)…… 142

Scheme 4.8. Reaction between [Cp_2ZrMe][$B(C_6F_5)_4$] and 2,4-Me_2-1-pentene (R is CH_2CHMe_2 and X^- is either $[B(C_6F_5)_4]^-$ or C_6D_5Cl)…….. 148

Scheme 4.9. The intramolecular exchange of the two terminal vinylidene hydrogens of the coordinated olefin of complex **F**…… 149

Scheme 4.10. Dynamic behavior of metal-allyl complexes via η^3/η^1 allyl interconversion…….. 153

Scheme 4.11. Dynamic behaviour of metal-allyl complexes via rotation of the η^3-coordinated allyl ligand about the metal-allyl bond……. 153

Scheme 4.12. Proposed mechanism of *syn-anti* hydrogen exchange and apparent Cp ligand exchange in complex **A**…… 156

Scheme 4.13. Proposed mechanism for apparent Cp ligand exchange in complex **A**……. 158

Scheme 4.14. The equilibrium between the η^1- and η^3-coordinated allyl complexes of **B**…… 160

Scheme 4.15. Proposed mechanism of *syn-anti* hydrogen exchange and apparent Cp ligand exchange in complex **C**…… 164

Scheme 4.16. Possible mechanism for formation of an internal olefinic group of the type -C(Me)=CHCH$_2$CH$_2$CH$_2$-……... 178

Scheme 4.17. Possible mechanism for formation of a CH$_3$CH$_2$CH=C(Me)- end group……... 179

List of Figures

Figure 2.1. ^{1}H NMR spectra in the brominated region of (a) $BrCH_2(CH_2)_9CH_2Br$ in CD_2Cl_2 (400 MHz) and (b) $CH_3CH(Br)(CH_2)_7CH_3$ in C_6D_5Cl (600 MHz)…… 44

Figure 2.2. ^{1}H NMR and ^{1}H-^{13}C HSQC spectra of $BrCH_2CH(Me)(CH_2)_8CH_3$ in the brominated end group region (CD_2Cl_2, 600 MHz)…….. 47

Figure 2.3. ^{1}H NMR and ^{1}H-^{13}C HSQC spectra of $BrCH_2CH(Me)CH_2CH(Me)(CH_2)_2CH_3$ in the brominated end group region (CD_2Cl_2, 600 MHz)……... 48

Figure 2.4. ^{1}H NMR spectrum of brominated polyethylene in C_6D_5Cl (400 MHz, 120°C)…….. 50

Figure 2.5. APT-^{13}C NMR spectrum of a sample of brominated polyethylene obtained after a 50 second polymerization time…….. 53

Figure 2.6. ^{1}H NMR spectrum of atactic polypropylene obtained from $(indenyl)_2ZrMe_2/B(C_6F_5)_3$ after quenching with bromine (CD_2Cl_2, 400 MHz)…… 56

Figure 2.7. ^{1}H NMR and ^{1}H-^{13}C HSQC spectra in the brominated end group region of brominated atactic polypropylene (CD_2Cl_2, 600 MHz)……... 57

Figure 2.8. ^{1}H NMR and ^{1}H-^{13}C HSQC spectra in the brominated end group region of low isotactic polypropylene……. 58

Figure 2.9. Variation of the relative concentrations of primary Zr-polymeryl groups with polymerization time (two runs)…… 61

Figure 2.10. ^{1}H NMR spectra (CD_2Cl_2, 25°C) in the olefinic region of atactic polypropylene obtained from (indenyl)$_2ZrMe_2/B(C_6F_5)_3$, (a) 300 MHz and (b) 500 MHz…… 63

Figure 2.11. ^{1}H NMR spectrum (C_6D_5Cl, 600 MHz) of the reaction products obtained from *in situ* reaction of $Cp_2Zr^{+}(\eta^{3}\text{-}CH_2C(CH_2CHMe_2)CH_2)$ with bromine at room temperature……. 70

Figure 2.12. (a) ^{2}H NMR spectrum (600 MHz, 25°C, CH_2Cl_2) of atactic polypropylene obtained from (indenyl)$_2ZrMe_2/B(C_6F_5)_3$ in chlorobenzene after CD_3OD quenching and (b) ^{1}H NMR spectrum (600 MHz, 25°C, CD_2Cl_2) of 2,4-dimethyl-1-heptene…….. 74

Figure 3.1. ^{1}H NMR spectrum of isotactic polypropylene obtained from propylene polymerization by [ONNO]Zr($CH_2C_6H_5)_2$/MAO/2,6-di-^{t}butylphenol after 1 min polymerization time (1,1,2,2-tetrachloroethane-d_2, 120°C, 400 MHz).…… 102

Figure 3.2. Variation of Mn (determined using ^{1}H NMR spectroscopy) as a function of polymerization time for propylene polymerization by [ONNO]Zr($CH_2C_6H_5)_2$/MAO/2,6-di-^{t}butylphenol in chlorobenzene at room temperature…… 104

Figure 3.3. ^{1}H NMR spectrum in the brominated end group region of isotactic polypropylene obtained following quenching the polymerization with bromine (1 min polymerization time, 1,1,2,2-tetrachloroethane-d_2, 120°C, 600 MHz)……. 105

Figure 3.4. ^{1}H NMR and ^{1}H-^{13}C HSQC spectra in the brominated end group region of isotactic polypropylene (1,1,2,2-tetrachloroethane-d_2, 120°C, 600 MHz)……. 106

Figure 4.1. ^{1}H NMR spectra of the *in situ* reaction between $[Cp_2ZrMe][MeB(C_6F_5)_3]$ (1 equivalent) and 2,4-dimethyl-1-pentene (1.5 equivalents) in chlorobenzene-d_5 at room temperature (600 MHz)…… 124

Figure 4.2. ^{1}H NMR spectrum of the *in situ* reaction between $[Cp_2ZrMe][MeB(C_6F_5)_3]$ (1 equivalent) and 2,4-Me_2-1-pentene (1 equivalent) in C_6D_5Cl at 0°C (600 MHz)……. 126

Figure 4.3. ^{1}H NMR spectrum of the *in situ* reaction between $[Cp_2ZrMe][MeB(C_6F_5)_3]$ (1 equivalent) and 2,4-dimethyl-1-pentene (1 equivalent) in chlorobenzene-d_5. (600 MHz, -40°C)…… 130

Figure 4.4. ^{1}H NMR spectra of the *in situ* reaction between $[Cp_2ZrMe][MeB(C_6F_5)_3]$ and 2,4-dimethyl-1-heptene (1:1 mole ratio) in chlorobenzene-d_5 at room temperature (600 MHz). …… 133

Figure 4.5. ^{1}H NMR spectrum of the *in situ* reaction between $[Cp_2ZrMe][MeB(C_6F_5)_3]$ and 2,4-Me_2-1-heptene in chlorobenzene-d_5 at 0°C: (a) expansion of the Cp region and (b) expansion of the allylic region…….. 136

Figure 4.6. ^{1}H NMR spectra (600 MHz) of (a) *in situ* generated chlorobenzene-d_5 solution of $[Cp_2ZrMe][B(C_6F_5)_4]$ and (b) *in situ* reaction between $[Cp_2ZrMe][B(C_6F_5)_4]$ and 2,4-Me_2-1-pentene in chlorobenzene-d_5 at room temperature, after 5 minutes reaction time……. 144

Figure 4.7. ^{1}H NMR spectrum of the reaction between $[Cp_2ZrMe][B(C_6F_5)_4]$ and 2,4-Me_2-1-pentene in chlorobenzene-d_5 at -45°C…… 145

Figure 4.8. The ROESY spectrum (600 MHz, -45°C, chlorobenzene-d_5) showing the exchange cross peaks between the two terminal CH_2= hydrogens of 2,4-Me_2-1-pentene at ~4.87 and 4.80 ppm and the weak broad resonance at ~3.5 ppm…… 146

Figure 4.9. The ROESY spectrum (600 MHz, -45°C, chlorobenzene-d_5) showing the exchange cross peak between the Zr-Me resonance of $[Cp_2ZrMe][B(C_6F_5)_4]$ at 0.67 ppm and the proton resonance at ~0.3 ppm……. 147

Figure 4.10. ^{1}H NMR spectra of vinylidene resonance of complex **F** at (a) -50°C, (b) -55°C, (c) -60°C…… 150

Figure 4.11. Variable temperature ^{1}H NMR spectra of the mixture of **A** and **B** complexes (counterion, $[MeB(C_6F_5)_3]^-$) in the Cp and allylic regions…. 155

Figure 4.12. The NOESY spectrum of complex **A** at 0°C, showing the exchange between the *syn* and *anti* hydrogens of the allylic CH_2 groups and the exchange between the two Cp ligands……... 157

Figure 4.13. Variation of H_{syn} and H_{anti} resonances of the **A** and **B** complexes with temperature……. 159

Figure 4.14. Variable temperature ^1H NMR spectra of the mixture of **C** and **D** complexes in the allyl region in chlorobenzene-d_5, 600 MHz (counterion, $[MeB(C_6F_5)_3]^-$)……... 162

Figure 4.15. (a) The NOESY spectrum of complex **C** in the allylic region, under slow exchange regime (at 0°C). (b) The chemical structure of complex **C**, with chemical shift assignments……. 163

Figure 4.16. Plots of $[10^{-3}/(a_0-b_0)]\ln(ab_0/a_0b)$ versus time for the formation of $[Cp_2Zr(\eta^3\text{-}C_7H_{13})]^+$ from $[Cp_2ZrMe][MeB(C_6F_5)_3]$ and 2,4-Me_2-1-pentene in chlorobenzene-d_5……. 169

Figure 4.17. Arrhenius plot for the formation of $[Cp_2Zr(\eta^3\text{-}C_7H_{13})]^+$ from $[Cp_2ZrMe][MeB(C_6F_5)_3]$ and 2,4-Me_2-1-pentene in chlorobenzene-d_5. 170

Figure 4.18. Plots of $[10^{-3}/(a_0-b_0)]\ln(ab_0/a_0b)$ versus time for the formation of $[Cp_2Zr(\eta^3\text{-}C_7H_{13})]^+$ from $[Cp_2ZrMe][B(C_6F_5)_4]$ and 2,4-Me_2-1-pentene in chlorobenzene-d_5……. 172

Figure 4.19. Arrhenius plot for the formation of $[Cp_2Zr(\eta^3\text{-}C_7H_{13})]^+$ from $[Cp_2ZrMe][B(C_6F_5)_4]$ and 2,4-Me_2-1-pentene in chlorobenzene-d_5….. 173

Figure 4.20. ^{1}H NMR spectra of the *in situ* propylene polymerization by $[Cp_2ZrMe][MeB(C_6F_5)_3]$ in chlorobenzene-d_5 (room temperature, 600 MHz). (a) The $[Cp_2ZrMe][MeB(C_6F_5)_3]$ ion pair, (b) after addition of 5 equivalents of propylene, (c) after addition of 10 equivalents of propylene..... 175

Figure 4.21. ^{1}H NMR spectra, in the olefinic end group region of atactic polypropylene oligomers obtained from $[Cp_2ZrMe][MeB(C_6F_5)_3]$ in chlorobenzene-d_5 at room temperature, using (b) 5 equivalents of propylene and (c) 10 equivalents of propylene..... 176

Figure 4.22. ^{1}H NMR spectra of the *in situ* propylene polymerization by $[Cp_2ZrMe][B(C_6F_5)_4]$ in chlorobenzene-d_5 (room temperature, 600 MHz). (a) the $[Cp_2ZrMe][B(C_6F_5)_4]$ ion pair, (b) after addition of 5 equivalents of propylene, (c) after addition of 10 equivalents of propylene..... 182

Figure 4.23. Positive mode ESI-MS spectrum of a polypropylene oligomer mixture in chlorobenzene..... 184

Figure 4.24. (a) Positive mode ESI-MS spectrum of the peak at m/z 237, (b) The theoretical isotopic product distribution of $C_{10}H_{10}ZrOH$..... 185

Figure 4.25. Positive mode ESI-MS/MS spectrum of the oligomeric zirconocene intermediate cation of m/z 275..... 186

Figure 4.26. Positive mode ESI-MS/MS spectrum of the distribution of oligomeric zirconocene intermediate cations of m/z 275, 317, 359, 401, 443, and 485..... 188

List of Abbreviations

Å	Angstrom
Ar	aryl
atm	atmosphere
br	broad
CID	Collision-Induced Dissociation
cm	centimeter
COSY	the homonuclear COrrelation SpectroscopY
Cp	cyclopentadienyl, η^5-$C_5H_5^-$
Cp'	substituted cyclopentadienyl
d	doublet
dd	doublet of doublet
δ	chemical shift in parts per million
°C	degree Celsius
DSC	Differential Scanning Calorimetry
e.g.	(latin: “exempli gratia”) for the sake of example
equiv.	equivalent
ESI-MS	ElectroSpray Ionization Mass Spectrometry
ESI-MS/MS	ElectroSpray Ionization tandem Mass Spectrometry
g	gram
η	hapticity
h	hour

HDPE	high density polyethylene
HMBC	Heteronuclear Multiple Bond Correlation
HSQC	Heteronuclear Single Quantum Coherence
Hz	Hertz
i.e.	(latin: “id est”) that is
J	coupling constant (NMR) in Hz
J	Joule
K	Kelvin
kJ	kilojoule
L	liter
LDPE	low density polyethylene
LLDPE	linear low density polyethylene
m	*meso*
m-	*meta*-
μL	microliter
μmole	micromole
M	molar
m	multiplet (NMR)
MAO	methylaluminoxane
Me	methyl group
mg	miligram
MHz	megahertz
min	minutes

mL	milliliter
mmol	millimole
Mn	number average molecular weight
m/z	mass to charge ratio
NOE	Nuclear Overhouser Effect
NOESY	Nuclear Overhouser Effect SpectroscopY
NMR	Nuclear Magnetic Resonance
o-	*ortho*-
p-	*para*-
ppm	parts per million
r	*racemo*
rac-	racemic
ROESY	Rotational nuclear Overhauser Effect SpectroscopY
s	singlet
sec	seconds
t	triplet
TMA	trimethyl aluminum
UHMWPE	ultrahigh molecular weight polyethylene
v	volume
wt%	weight percent

Chapter 1

Introduction

1.1. General Introduction

Polymeric materials are omnipresent in modern society having found applications in almost every aspect of our daily life such as food packaging, clothing, appliances, construction, transportation, and communications.[1] In the polymer industry, polyolefins (such as polyethylene and polypropylene) represent by far the most important class of synthetic polymers.[2]

Polyethylene was synthesized industrially for the first time during the second World War, one of its applications being for submarine cables.[3] It was obtained by a free radical polymerization process at temperatures of 150-230°C and pressures of 1,000-3,000 atm.[1,3] However, the extreme reaction conditions required for the polymerization process, and the fact that only highly branched polyethylene can be obtained via a radical polymerization process, drove research toward finding new, more efficient means to polymerize olefins.[3]

The major breakthrough in the polyolefin industry was, however, the discovery of transition metal mediated polymerization of ethylene and propylene in the middle 1950's by Karl Ziegler and Giulio Natta.[1,3] In this regard, Ziegler successfully developed a heterogeneous catalytic system based on titanium tetrachloride and aluminum alkyls which can polymerize ethylene under mild conditions of temperature and pressure (room temperature and 1 atm.) to yield highly linear polyethylene. Shortly after Ziegler's discovery, Natta used similar catalytic systems to investigate the polymerization of propylene and obtained for the first time isotactic polypropylene.[1a,2b,3] These major breakthroughs have revolutionized the polyolefin industry. In acknowledgement of their contributions, a catalytic system consisting of a combination of a transition metal complex catalyst with a main group metal alkyl compound is known as a Ziegler-Natta catalyst. It is also known as a coordination catalyst to reflect that the polymerization reaction occurs via coordination of an olefin to the active transition metal centre, followed by a migratory insertion into the metal-alkyl bond.[3] Both Ziegler and Natta shared the Nobel Prize in Chemistry in 1963 for their pioneering work in the transition metal mediated polymerization of olefins.[1,3]

The discovery of Ziegler-Natta catalysts for olefin polymerization forms the basis of the present polyolefin industry.[3,4] Classical Ziegler-Natta catalysts are quite efficient in olefin polymerization and can produce a large variety of commercially important polymers.[1] However, these catalysts are complex systems having multiple active sites that yield polymers with broad molecular weight distributions and non-uniform stereochemistries. Also, the heterogeneous nature of these catalysts has hindered their detailed characterization making them unsuitable candidates for mechanistic studies.[4b,5]

In order to overcome the limitations of classical Ziegler-Natta catalysts, extensive research has been directed toward the development of new, homogeneous olefin polymerization catalysts.[5] Homogeneous metallocene catalysts, able to catalyze ethylene polymerization upon activation with aluminum alkyls, were known as early as 1957.[6] However, these early homogeneous catalytic systems received limited attention due to their low catalytic activity in polymerizing ethylene.[4b,c] The big momentum in olefin polymerization by homogeneous single-site metallocene catalysts emerged in the 1980s with the discovery that the partially hydrolyzed trimethylaluminum (also called methylaluminoxane, MAO), in connection with group 4 metallocene catalysts form highly active catalysts for the polymerization of ethylene and α-olefins.[4b,c] In contrast with classical heterogeneous Ziegler-Natta catalysts, metallocene-based catalysts display superior performance in achieving higher activity and stereoselectivity, and polymers of narrower molecular weight distributions. Moreover, the single-site nature of the metallocene catalysts allows detailed mechanistic studies, thus making correlations between the catalyst structure and polymer structure possible.[5] Metallocene catalysts have revolutionized the polyolefin industry, making possible new polymeric materials which could not be achieved by classical heterogeneous Ziegler-Natta catalysts.[4c,5]

Following significant advances in understanding the polymerization process, the search for new, single-site olefin polymerization catalysts that are able to produce high performance polymers is now extended toward the development of new classes of cyclopentadienyl-free catalysts, also referred to as non-metallocene catalysts. Of special interest are those catalysts able to induce living polymerization of olefinic monomers, and by this, to further extend the range of polymeric materials now available.[2a]

The experiments in this thesis are primarily based on ethylene and propylene polymerization by homogeneous zirconium-based polymerization catalysts. Discussed below are some general aspects on the Ziegler-Natta polymerization mechanism, the catalytic systems (i.e., precursor catalysts and cocatalysts) used in the experiments described in this thesis, as well as the polymers involved in this thesis. At the end, the aims of the present research are described.

1.2. Ziegler-Natta Polymerization Mechanism

Transition metal mediated polymerization of olefins and α-olefins has become an important technology in the polyolefin industry since the discovery of Ziegler-Natta catalysts, about 50 years ago.[3,4] Extensive research in this area has resulted in a consensus regarding the general polymerization mechanism. The main steps involved in the Ziegler-Natta polymerization reaction consist of catalyst activation, initiation, propagation, chain transfer and termination. These steps will be discussed below.

1.2.1. Precursor Catalyst Activation

The general consensus is that the catalytically active species in the Ziegler-Natta polymerization of olefins is a coordinatively unsaturated cationic alkyl complex of type $[Cp_2ZrMe]^+$.[7] This active species is generated *in situ* by the reaction of a catalyst precursor, for this particular case Cp_2ZrMe_2, with a strong Lewis acid, as, for example, $B(C_6F_5)_3$. In this reaction, $B(C_6F_5)_3$ abstracts a methyl anion from the Cp_2ZrMe_2 to form the electron deficient cationic intermediate $[Cp_2ZrMe]^+$, able to coordinate an olefin molecule. The $[MeB(C_6F_5)_3]^-$ anion remains weakly coordinated to the cationic

zirconocene catalyst $[Cp_2ZrMe]^+$ (Scheme 1.1).[7] (In all schemes in this Section, the square identifies the vacant coordination site where olefin can coordinate).

Scheme 1.1. Activation of the precursor catalyst by $B(C_6F_5)_3$

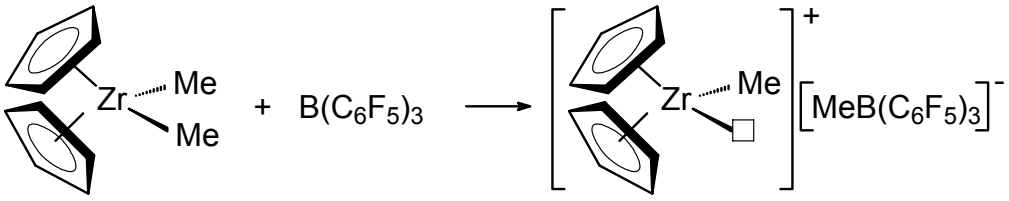

1.2.2. Initiation

Once the active species is generated, the initiation takes place by coordination of the olefin to the vacant site at the transition metal center. This is followed by a migratory insertion of the olefin into the metal-carbon σ-bond. The migratory insertion is believed to occur by a *cis* opening of the carbon-carbon double bond[7b] followed by the alkyl group migration to the olefin through a four-membered transition state,[7c] as shown in Scheme 1.2. A new free coordination site at the position of the former alkyl ligand, is thus created.[7] This coordination-insertion mechanism was proposed for the first time by Cossee in 1964.[8] Although the d^0 metal-alkyl-olefin complex, considered the key intermediate in the Ziegler-Natta olefin polymerization, has never been directly observed in an active polymerization system,[9] nowadays the olefin coordination-insertion mechanism remains the most widely accepted mechanism for olefin polymerization by Ziegler-Natta catalysts.[7b,c]

Scheme 1.2. Initiation mechanism

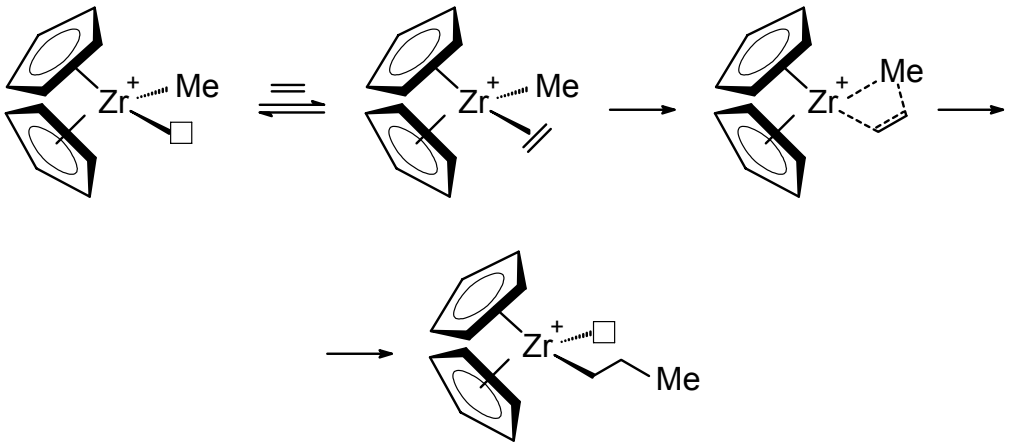

1.2.3. Propagation

After the polymerization is started, propagation of the polymer chain takes place by successive olefin coordination and insertion into the Zr-polymeryl chain[7] as depicted in Scheme 1.3.

Scheme 1.3. Propagation mechanism

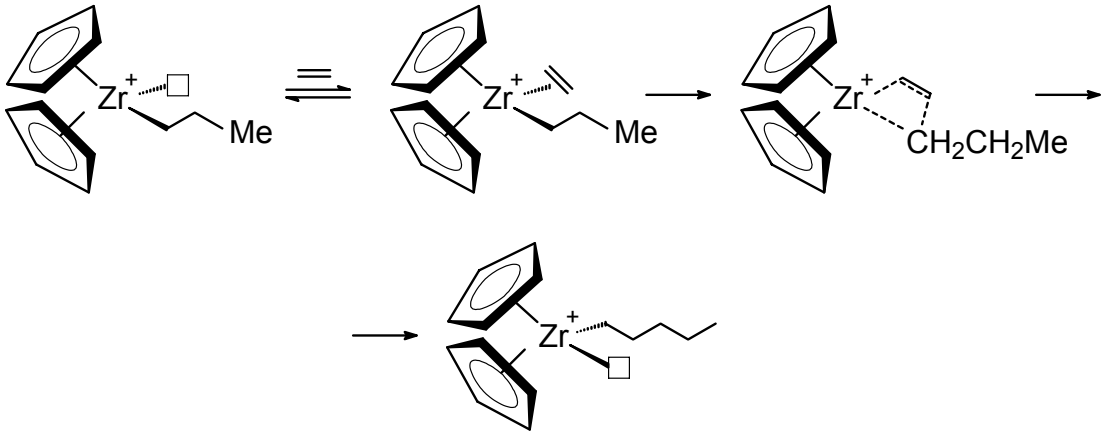

In the case of propylene, the insertion takes place, generally, in a 1,2-fashion to give primary (1,2) Zr-polymeryl groups; however, secondary (2,1) insertions are also possible (Scheme 1.4).[10]

Scheme 1.4. Propylene insertion modes

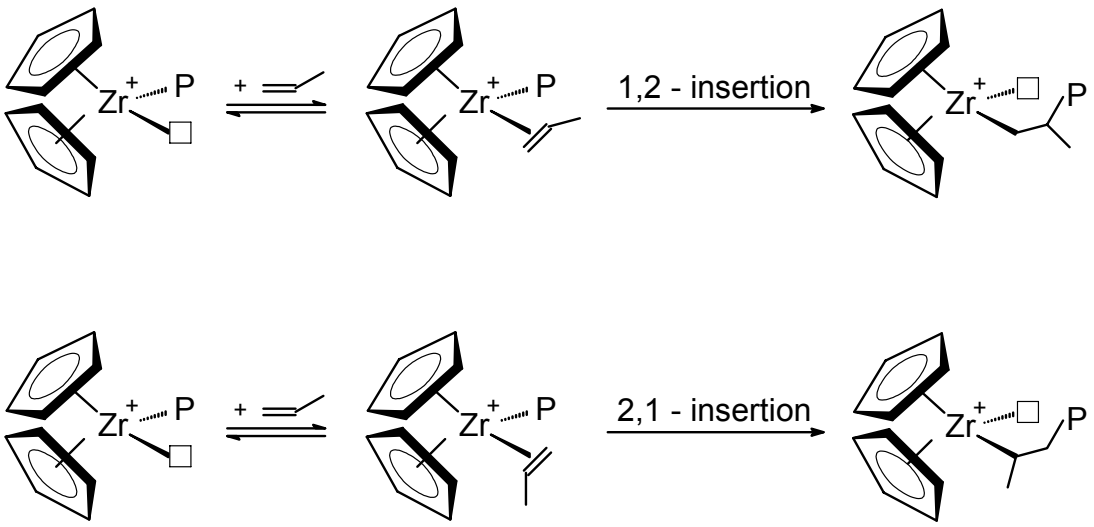

Propagation of a polymer chain does not occur infinitely. There are other competing reactions that limit the polymer chain growth, namely chain transfer and termination reactions.

1.2.4. Chain transfer

Chain transfer reactions are those reactions in which a polymer chain is released from the active catalyst and a new metal-hydride or metal-alkyl species with an open coordination site is produced. This new species is able to reinitiate the olefin

polymerization reaction. Therefore, the chain transfer reactions terminate the polymer chain growth but do not deactivate the catalyst. The mechanisms of chain transfer reactions are usually inferred from the structure of the polymer end groups.[7b,11] The chain transfer reactions discussed in this section are: β-hydrogen elimination, β-methyl elimination, chain transfer to aluminum, and the hydrogenolysis reaction.

The most common chain transfer reaction is β-hydrogen elimination. In this reaction, a hydrogen on a carbon atom placed in the β-position of the growing polymer chain relative to the transition metal center is transferred to the vacant site on the metal center, as depicted in Scheme 1.5. As a result, a cationic metal-hydride species, which can reinitiate the olefin polymerization, is produced while a polymer chain with an olefinic end group is released.

Scheme 1.5. Chain transfer via β-hydrogen elimination

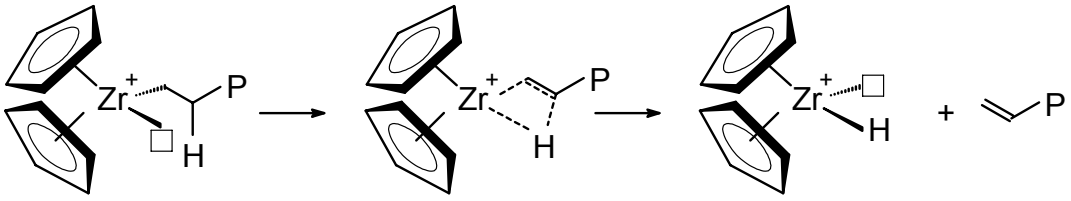

The growing polymer chain can also transfer a β-hydrogen atom to a coordinated monomer. This reaction pathway again yields a polymer chain with an olefinic end group and a cationic metal-alkyl complex able to initiate polymer chain growth. In the case of ethylene polymerization, a polymer chain with an allyl end group is formed. In the case of propylene polymerization, the presence of a vinylidene end group is diagnostic for β-

hydrogen elimination after a primary insertion, while the presence of a cis-2-butenyl end group is indicative of β-hydrogen elimination after a secondary insertion. In Scheme 1.6, the olefinic end groups formed following a β-hydrogen elimination reaction are presented.

Scheme 1.6. Olefinic end groups formed as a result of β-hydrogen elimination reactions

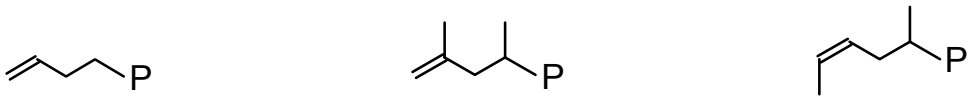

(a) allyl (b) vinylidene (c) cis-2-butenyl

In the β-Me elimination reaction, a Me group attached to the β carbon atom of a metal-polymeryl species is transferred to the vacant site at the metal center to form a cationic metal-methyl active species, as depicted in Scheme 1.7. The polymer chains released from β-Me elimination reactions are terminated by an allyl group (Scheme 1.7).

Scheme 1.7. Chain transfer via β-Me elimination

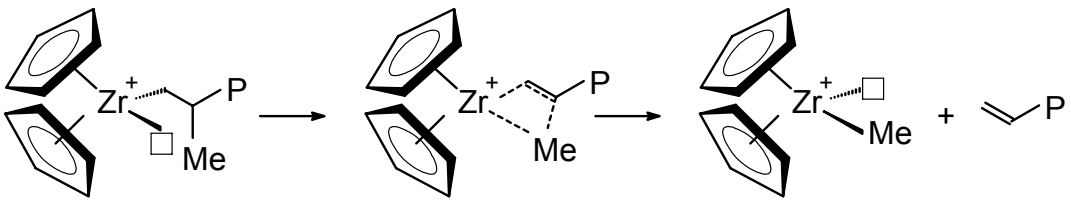

Chain transfer to aluminum, also known as a transalkylation reaction, is another common chain transfer reaction that occurs in the catalytic systems in which the precursor catalyst was activated by an aluminum based cocatalyst, such as MAO.[7b] The transalkylation reaction results in an aluminum terminated polymer and a new cationic transition metal-alkyl complex which can reinitiate the polymer chain growth.[11b] Upon hydrolysis, the aluminum terminated polymer is converted to a polymer with a saturated end group.[7b]

The growing polymer chain can also be transferred to an added chain transfer agent, different from AlR_3 (where R is an alkyl). The most widely used chain transfer agent in Ziegler-Natta polymerization is molecular hydrogen.[7b] In this reaction, H_2 coordinates to the vacant site of the metal center to form a dihydro complex $[Cp_2Zr(H_2)(polymeryl)]^+$, from which a saturated polymer chain is released. As in the previously described chain transfer reactions, a catalytically active metal-hydride species is formed.[12] The hydrogenolysis reaction is depicted in Scheme 1.8.

Scheme 1.8. Chain transfer via hydrogenolysis

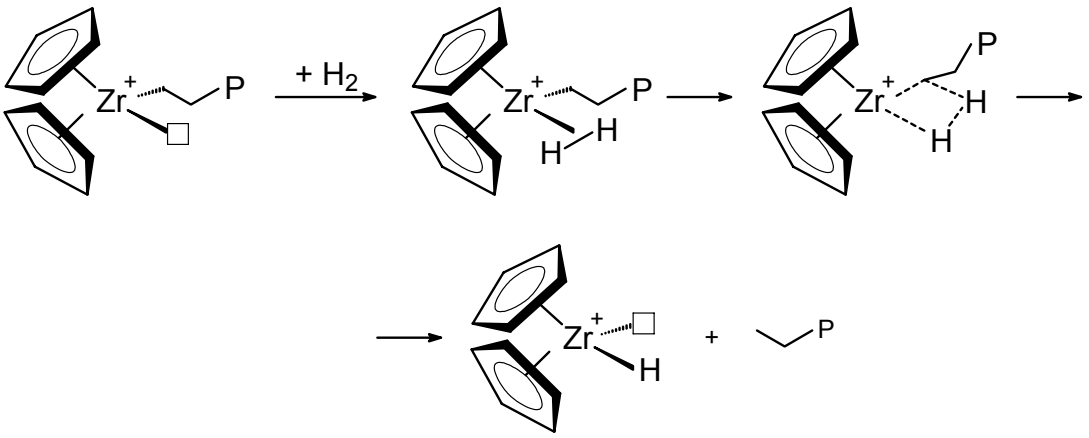

The addition of small amounts of H_2 during olefin polymerization by Ziegler-Natta catalysts is usually used as a way to control the molecular weight of polymers. It is also used as a method to increase the catalyst activity.[7b]

1.2.5. Termination

Termination of Ziegler-Natta polymerization is usually achieved by addition of polar compounds, such as methanol, to the polymerization mixture. The acidic proton is transferred to the growing polymer chain. This reaction yields a polymer chain with a saturated end group and a metal-alkoxide complex that is incapable of reinitiating polymer chain growth (Scheme 1.9).

Scheme 1.9. Termination reaction using methanol

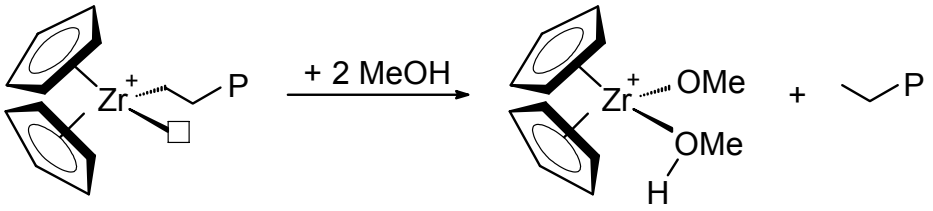

Quenching with methanol results in deactivation of all catalyst active sites simultaneously.[13]

1.3. Homogeneous Group IV Olefin Polymerization Catalysts

1.3.1. Metallocene-based Catalysts

Metallocenes are organometallic compounds in which a Group 4 transition metal atom (Ti, Zr, and Hf) bears two aromatic η^5-cyclopentadienyl type ligands and two σ-ligands. The two aromatic five-membered ring ligands are also called 'ancillary' ligands as they remain bound to the metal center during polymerization. The two σ-bonded ligands, on the other hand, are removed during the polymerization such that the two coordination sites can be occupied by a polymeryl chain and an olefin which exchange their place after each insertion. The most common η^5-cyclopentadienyl type ligands are cyclopentadienyl itself (Cp, $C_5H_5^-$), indenyl (Ind, $C_9H_7^-$), and fluorenyl (Flu, $C_{13}H_9^-$). The carbon atoms of the η^5-cyclopentadienyl type ligands can in turn bear different substituents (i.e., alkyl, aryl) which can change the steric and electronic environment at the active site. The most commonly encountered metallocene catalysts are zirconocenes (Scheme 1.10).[7a,b]

Scheme 1.10. General structure of a zirconocene catalyst

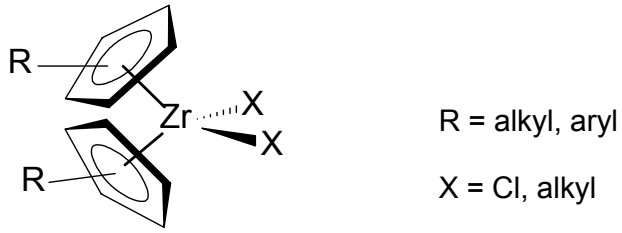

Neutral metallocenes by themselves are not active in olefin polymerization. In order to catalyze the olefin polymerization reaction, they are mixed with an activating agent (cocatalyst) able to abstract an alkyl or halide ligand and thus to generate a vacant site at the metal center available for olefin coordination. This is why the neutral metallocenes are also referred to as the precursor catalysts.[7a]

Compared with classical Ziegler-Natta catalysts, metallocenes are well-defined compounds which are soluble in most organic solvents. Upon activation they form only one type of active site (single-site catalysts) and as a result they produce polymers with narrow molecular weight distribution and uniform stereochemistry.[5] The homogeneous single-site nature of the metallocene catalysts also allows detailed mechanistic studies and allows one to accurately predict the structures of the resulting polymers.[2b,c,5a] This thesis reports results for such mechanistic studies.

A significant additional advantage of the homogeneous, single-site metallocene catalysts, as compared to the classical Ziegler-Natta catalysts, is that the well-defined structure of the active species of these catalysts enables efficient control of the polymer stereochemistry by tuning the coordination environment of the metal centre via rational ligand design. Specifically, systematic modification of the structure of the two η^5-cyclopentadienyl type ligands gives rise to various steric effects at the active site which in turn have a major influence on the polymer microstructure.[14] Some common examples of how the polymer stereospecificity is related to the precursor zirconocene catalyst chemical structure are shown in Scheme 1.11.

Propylene is a prochiral olefin which can, in principle, coordinate and insert into the metal-polymeryl bond in four different ways: in a primary (1,2) or secondary (2,1)

fashion each of which can occur on either of the two coordination faces (enantioface). The steric environment created about the active metal center of the metallocene catalyst by the ligands attached to the metal is responsible for the accessibility of the incoming monomer to the active reaction center. Moreover, as stated above, it will induce a preferential orientation of the incoming monomer and therefore can determine the polymer regio- and stereochemistry. With metallocene catalysts, propylene polymerization occurs predominantly via primary (1,2) insertion, leading to highly regioregular polymers. The polymer stereochemistry, on the other hand, is determined by the catalyst active site preference for a particular olefin enantioface.

Scheme 1.11. Correlation between the structure of the precursor zirconocene catalyst and the polymer microstructure (X = Cl, Me)

(a)

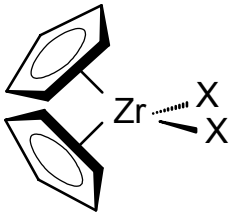

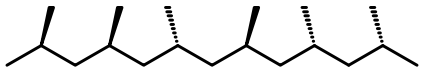

atactic polypropylene

(b)

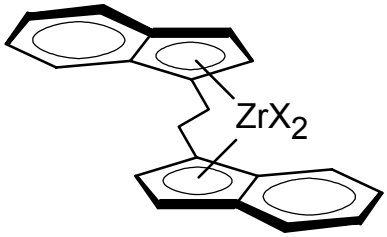

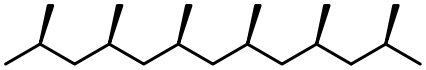

isotactic polypropylene

(c)

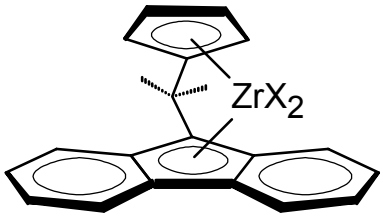

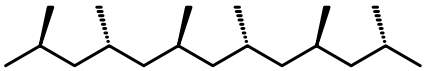

syndiotactic polypropylene

For instance, Cp_2ZrX_2 (Scheme 1.11(a)) is an achiral catalyst that contains two identical, small Cp ligands. In this case, propylene can coordinate to the active site of the catalyst on either enantioface with roughly equal probability leading to an atactic polypropylene. *rac*-C_2H_4(1-indenyl)$_2ZrX_2$ (Scheme 1.11(b)), on the other hand, is a chiral catalyst

containing two identical, bulky indenyl ligands arranged in a rigid, staggered configuration. The active site of such a catalyst will have a high preference for successive coordination of the same propylene enantioface leading to an isotactic polypropylene. The $Me_2C(Cp)(9\text{-fluorenyl})ZrX_2$ precursor catalyst (Scheme 1.11(c)), contains two different ancillary ligands mutually connected via a Me_2C bridge in a rigid configuration. Propylene will coordinate to the catalyst vacant site such as to minimize the steric interactions between the benzene ring of the fluorenyl ligand and the Me group on the propylene. For this particular case, this can be done by successive coordination of the opposite enantioface of propylene which results in a syndiotactic polypropylene. Addition of various substituents on the η^5-cyclopentadienyl type ligands will further change the steric environment at the active catalytic site to produce polymers of different architectures. A description of atactic, isotactic, and syndiotactic polypropylene is done in Section 1.4.2.

The zirconocene catalysts used in the research presented in this thesis are Cp_2ZrMe_2, $(indenyl)_2ZrMe_2$ and *rac*-$C_2H_4(1\text{-indenyl})_2ZrMe_2$.

1.3.2. Diamine bis(phenolate) catalysts

Diamine bis(phenolate) group IV (Ti, Zr) complexes constitute a new class of homogeneous, single-site olefin polymerization catalysts introduced for the first time by Kol and co-workers in 2000.[15] In these complexes, the transition metal atom is attached to one dianionic tetradentate diamine bis(phenolate) [ONNO] ancillary ligand and two labile benzyl ligands in a slightly distorted octahedral geometry. In all characterized structures, the two oxygen atoms of the $[ONNO]^{2-}$ ancillary ligand adopt a trans

configuration, while the two benzyl ligands are disposed in a cis configuration.[16] In Scheme 1.12, the general structure of a diamine bis(phenolate) zirconium dibenzyl complex is presented (R_1 and R_2 are alkyl or aryl groups).

Scheme 1.12. General structure of a diamine bis(phenolate) zirconium complex

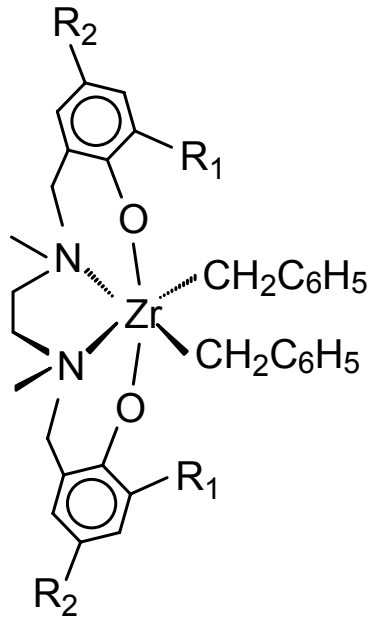

The diamine bis(phenolate) group IV complexes are not active in olefin polymerization by themselves; in order to form the catalytically active species, they need first to be activated by a suitable cocatalyst, similar to the activation of metallocene precursor catalysts. As these complexes are cyclopentadienyl-free systems, they are also referred to as "non-metallocene" precursor catalysts.[16]

As outlined in the previous section, an advantage of the homogeneous, single-site precursor catalysts is that the well-defined structure of these catalysts enables precise

control over polymer microstructure through fine tuning of the coordination environment around the active metal centre via rational design of the catalyst structure. For the [ONNO]MBn_2 complexes, where M = Ti or Zr and Bn = benzyl, the *ortho*-phenolate substituent (R_1 in Scheme 1.12) was found to be the key substituent to control the polymer stereochemistry. The *para*-phenolate substituent on the other hand, (R_2 in Scheme 1.12), which is far from the active site, has practically no effect on the polymer stereochemistry. In this regard, it has been shown[17] that an increase in steric bulk of the R_1 substituent resulted in an increase of the polymer stereoregularity, from an atactic polymer when the [ONNO]$ZrBn_2$ catalyst bears a methyl group at the R_1 position, to a highly isotactic polymer when the R_1 position is occupied by a much bulkier substituent, such as ^{t}butyl or cumyl.[17] All diamine bis(phenolate) catalysts to date have been shown[16b] to polymerize α-olefins predominantly with primary (1,2) regiochemistry.

What is truly remarkable about the diamine bis(phenolate) precursor catalysts, and non-metallocene catalysts in general, is their ability to induce living polymerization of olefins at ambient temperature. Living polymerizations are characterized by fast (instantaneous) initiation and a lack of chain transfer or termination reactions.[1] These characteristics enable synthesis of precisely controlled polymers such as monodisperse polymers, block copolymers, and end-functionalized polymers. Olefin polymerizations by non-metallocene catalysts, however, are not truly living polymerization reactions. For these systems, the terms "quasi-living"[18] or "controlled"[17a,c] polymerization reactions are also used to reflect a polymerization process in which chain initiation is fast relative to propagation, and chain transfer and termination reactions are "negligible" or slow on the time scale of the experiment. The non-metallocene catalysts are thus useful for the

synthesis of a variety of polyolefinic materials that display unique microstructures, all of which are anticipated to possess novel properties.

The research presented in Chapter 3 involves the use of a diamine bis(phenolate) zirconium complex, in which R_1 and R_2 as shown in Scheme 1.12 is a cumyl and a methyl group, respectively, as a precursor catalyst for controlled polymerization of propylene.

1.4. Cocatalysts

As already mentioned in Section 1.1, it is commonly accepted that the catalytically active species in olefin polymerization by metallocene catalysts is the electron-deficient, coordinatively unsaturated cationic alkyl complex $[Cp'_2ZrR]^+$, where Cp' is a cyclopentadienyl-type ligand and R is an alkyl group, stabilized by a weakly coordinating anion.[7] In order to form the active catalyst, the neutral zirconocene complex is reacted with a suitable activating species, also referred to as a cocatalyst, able to abstract an alkyl or halide ligand, as depicted in Scheme 1.13 (R = alkyl, R' = alkyl or halide, X = counteranion).[7, 19]

Scheme 1.13. Generation of the catalytically active species $[Cp_2ZrR]^+$

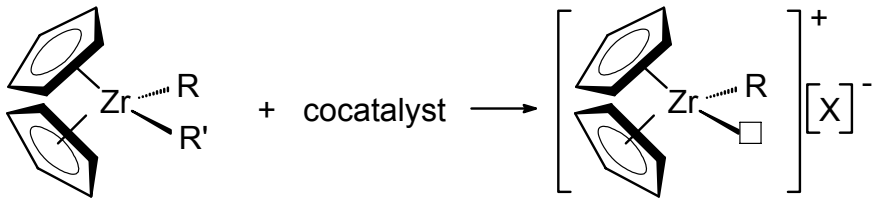

The most commonly used cocatalysts to date are methylaluminoxane (MAO), and boron-based compounds, such as perfluoroaryl boranes and borates.[19] In the following some general considerations on the cocatalysts used in this thesis are presented.

1.4.1. Methylaluminoxane

Methylaluminoxane (MAO) is the most widely used cocatalyst in metallocene-catalyzed olefin polymerization systems.[4c] It is commonly prepared by the controlled hydrolysis of trimethyl aluminum (TMA) and is believed to consist of oligomeric $[-Al(Me)-O-]_n$ moieties (n= 5-20), arranged in various structures.[19] Although it has been intensively investigated in both industry and academia,[19a] the exact structure of MAO is still not fully understood and it seems to largely depend on the synthesis conditions. The MAO structure is further complicated by the presence of small amounts of unreacted TMA, which cannot be completely eliminated. Two examples of proposed structures for MAO are depicted in Scheme 1.14 (n = 5-20).[19,20]

Scheme 1.14. Proposed structures for MAO

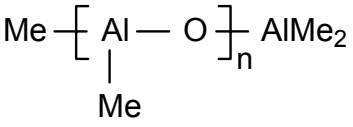

linear

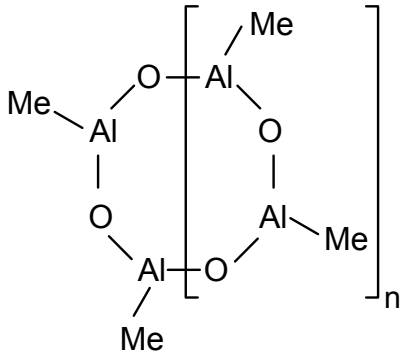

cyclic

The main role of MAO is to activate the metallocene precursor catalyst but it also acts as a scavenger as it reacts with polar impurities present in the reaction medium.

It is generally assumed that activation starts with the alkylation of the zirconocene dichloride precursor catalyst by MAO generating the corresponding methyl zirconocene chloride which can further react with excess MAO to produce dimethyl zirconocene species (Scheme 1.15).[5b,19a]

Scheme 1.15. Alkylation of the zirconocene dichloride precursor catalyst by MAO

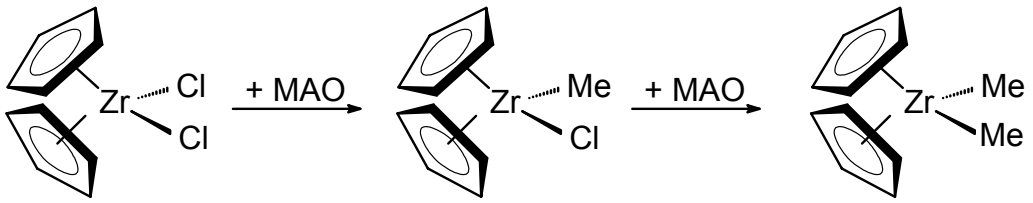

Next, either the chlorine ligand of $Cp_2Zr(Me)(Cl)$ or the methyl ligand of the Cp_2ZrMe_2, is abstracted by a Lewis acidic center of MAO to form the cationic methyl zirconocene active species $[Cp_2ZrMe]^+$ stabilized by the weakly coordinating $[Cl\text{-}MAO]^-$ or $[Me\text{-}MAO]^-$ anion, respectively (Scheme 1.16). To date, little is known about the true nature of the activating species in MAO.[4c,19a]

Scheme 1.16. Activation of the precursor catalyst by MAO

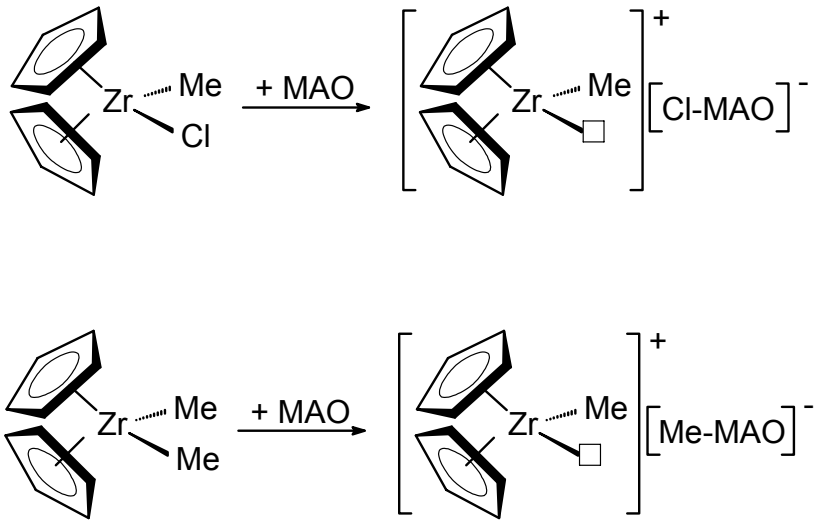

Although MAO is the most widely used cocatalyst in metallocene catalyzed olefin polymerization, the high cost associated with the large excess of MAO required for high catalyst activity is a major drawback. Typically, a ratio Al/Zr > 1000 is required in order to obtain optimum catalytic activity.[19] In this thesis, MAO is used as an activating agent for the [ONNO]$ZrBn_2$ precursor catalyst.

1.4.2. Boron-based Cocatalysts

Compared with MAO whose structure is highly variable and poorly defined, boron-based cocatalysts are structurally well defined species that can be isolated and characterized. Moreover, these cocatalysts react with dialkyl zirconocene precursor catalysts in a 1:1 catalyst-cocatalyst ratio. In this reaction, they abstract one of the two alkyl groups and form well defined ion pairs consisting of the cationic alkyl zirconocene species stabilized by a weakly coordinating anion.[19]

An example of a boron based cocatalyst is trispentafluorophenylborane, $B(C_6F_5)_3$. Although this compound was reported for the first time in 1964 by Massey and Park,[21] it was not of much interest until the 1990s when its potential as an activating agent for metallocene dialkyls was discovered.[22a] In this regard, trispentafluorophenylborane, which is a strong Lewis acid, was found (by NMR) to react rapidly and quantitatively with a variety of metallocene dimethyls to form the catalytically active $[Cp'_2ZrMe][MeB(C_6F_5)_3]$ ion pair, where Cp' is a cyclopentadienyl-type ligand, as already shown in Scheme 1.1.[22] Several such products were isolated and characterized crystallographically by Marks *et al.*[22] which allowed a better understanding of the nature of the active catalyst.

Extensive research on olefin polymerization by metallocene catalysts showed that interaction between the cationic alkyl metallocene complex and the counteranion, for a given precursor catalyst, has a strong effect on the catalyst activity.[19] In order to act as an efficient olefin polymerization catalyst, the counteranion has to be only weakly coordinated to the active center such that it does not compete with the monomer for the active site. Although $B(C_6F_5)_3$ is a widely used cocatalyst in metallocene catalyzed olefin polymerization,[19] the catalytic activity of the resulting activated metallocene complex is tempered to some degree by the interaction (although weak) between the cationic active center and the $[MeB(C_6F_5)_3]^-$ anion.[23] Therefore, researchers have been interested in the synthesis of new cocatalysts able to form catalytic systems in which the anion-cation interaction is much weaker. This will permit easier olefin coordination to the metal center and therefore an even higher catalytic activity. In practice, this can be achieved by using cocatalysts which, upon activation, provide counteranions which are bulkier, less

nucleophilic, and with a high degree of charge delocalization.[19b,23,24] Examples of such cocatalysts are tris(2,2',2''-perfluorobiphenyl)borane (PBB), bis(pentafluorophenyl)(2-perfluorobiphenyl)borane (BPB), and tris(β-perfluoronaphthyl)borane (PNB).[19]

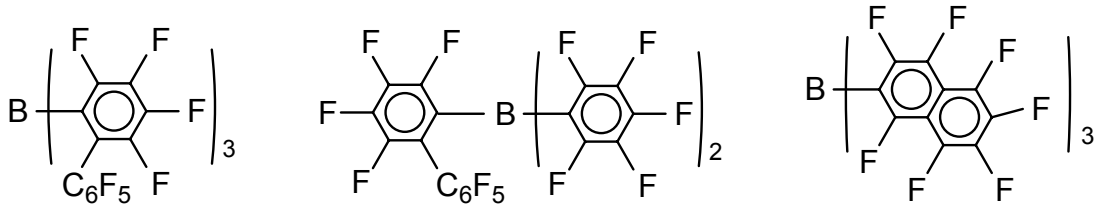

PBB BPB PNB

Another strategy to obtain highly reactive metallocene catalysts is the use of triphenylcarbenium tetrakis(pentafluorophenyl)borate, $[Ph_3C][B(C_6F_5)_4]$.[25] The trityl cation Ph_3C^+ is a strong alkyl abstracting reagent that, in combination with a dimethyl zirconocene precursor catalyst, can easily abstract a methyl group to form Ph_3C-Me and the loosely coordinated ion pair $[Cp_2ZrMe][B(C_6F_5)_4]$, as shown in Scheme 1.17.[19] The tetrakis(pentafluorophenyl)borate anion of $[Cp_2ZrMe][B(C_6F_5)_4]$ is among the least coordinating anions due to steric shielding and to low nucleophilicity originating from the extensive delocalization of the negative charge.[23]

Scheme 1.17. Activation of the precursor catalyst by $[Ph_3C][B(C_6F_5)_4]$

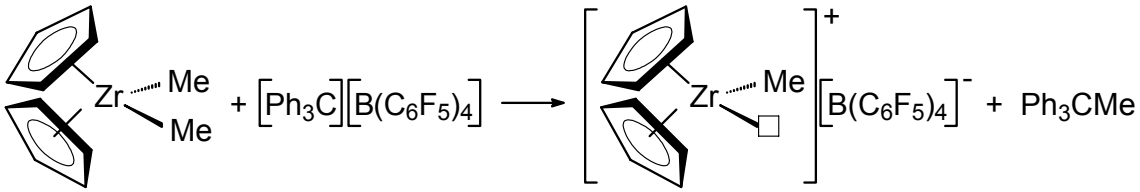

A drawback associated with the use of very weakly coordinating anions is associated with the relatively poor stability of the resulting ion pair. Thus, in these systems, the neutral dimethyl zirconocene species competes with the counteranion for the strongly electrophilic metallocene cation[19] and, as a result, small amounts of dimeric μ-Me species $[(Cp'_2ZrMe)_2(\mu\text{-}Me)][X]$, where X is a weakly coordinating counteranion (Scheme 1.18), are also formed in addition to the monomeric $[Cp'_2ZrMe][X]$ species. Such dimeric species were proposed to be inactive during the polymerization; however, they can become active by dissociation following an increase in the temperature.[19b]

Scheme 1.18. The structure of the dimeric $[(Cp_2ZrMe)_2(\mu\text{-}Me)][B(C_6F_5)_4]$ species

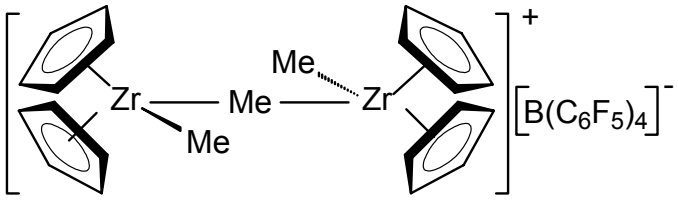

In this thesis, two boron-based cocatalysts, namely $B(C_6F_5)_3$ and $[Ph_3C][B(C_6F_5)_4]$, were used as activators for the dimethyl zirconocene catalysts.

1.5. Polymers Involved in this Thesis

1.5.1. Polyethylene

In its simplest form, polyethylene is a macromolecular chain composed of a large number of $-C_2H_4-$ repeating units arranged in a linear manner as illustrated below. The index n indicates the number of repeating units.

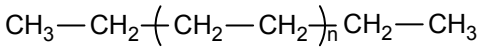

In the case of commercial polyethylenes, however, the polymer chains do not have the simple, linear structure as shown above, but they contain varying amounts of side groups (i.e., branches) of different chain length, ranging from methyl to octyl or even longer alkyl chains. In these polymers, n may vary from 400 to more than 50,000. The presence of different types of side-chain branches has a strong impact on the polymer properties and thus account for the large variety of commercially available polyethylene types, each with its own particular properties and uses.[26a] Polyethylenes are usually classified as low density polyethylene, high density polyethylene, and linear low density polyethylene.

Low density polyethylene (LDPE) is a highly branched polymer made by a free radical polymerization reaction at very high temperatures (130-350°C) and pressures (1,200-3,000 atm.). Due to the nature of the polymerization process, neither the length nor the distribution of branching can be controlled. Typical commercial LDPE contain 15-25 short chain branches per 1,000 carbon atoms. A schematic representation of a LDPE chain is presented in Scheme 1.19. The high degree of branching hinders the packing of the macromolecules into a crystal structure. Typical commercial LDPEs have

densities of 0.916-0.930 g/cm^3 and melting temperatures of 105-115°C. Major applications of LDPE include resins for many types of films, coatings, and insulators for power and communication cables.[26a]

High density polyethylene (HDPE) is a highly linear polymer which contains a very low amount of short chain branches (less than 2-3 methyl groups per 1,000 carbon atoms). The general structure of a HDPE chain is shown in Scheme 1.19. These polymers are obtained by Ziegler-Natta polymerization. Due to their linear structure, the macromolecules can pack side by side to form dense, crystalline regions in the solid material. Typically, HDPEs have densities in the range of 0.950-0.968 g/cm^3 and melting temperatures between 125 and 135°C. HDPEs are commonly employed in food and drug packaging applications. Other uses include housewares, toys, food containers, paper coatings, spray coatings, printing inks, crayons, and wax polishes.[26b]

Linear low density polyethylene (LLDPE) consists of linear polyethylene chains that have randomly attached short alkyl chains. They are synthesized by copolymerization of ethylene with small amounts of α-olefins, such as 1-butene, 1-hexene, and 1-octene via a Ziegler-Natta polymerization process. The general structure of LLDPE is shown in Scheme 1.19.[1b] The presence of branches on the macromolecules hinders crystallization to some degree; as a result, LLDPEs have a lower density and melting point than their corresponding homopolymers. In regards to commercial uses, LLDPE usually shares the same market with LDPE.[26c]

Scheme 1.19. Schematic representation of different types of polyethylenes: low density polypropylene (LDPE), high density polyethylene (HDPE), and linear low density polyethylene (LLDPE)

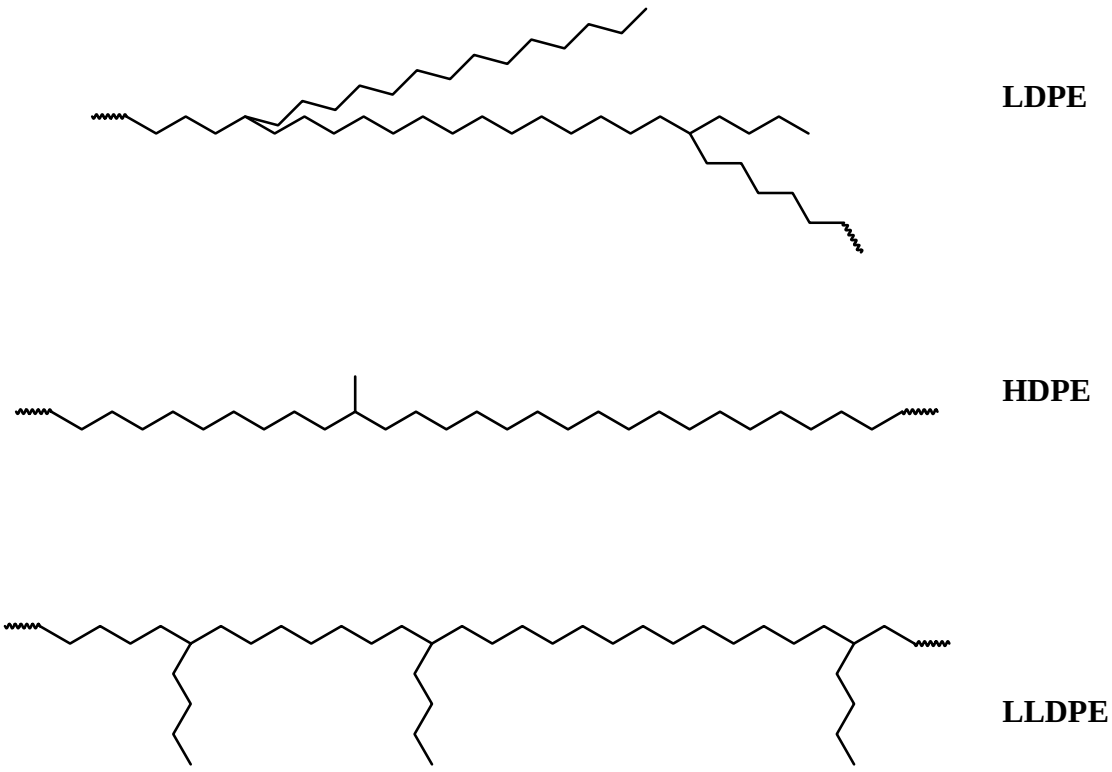

HDPE are typically obtained with molecular weight up to 50,000 g/mol. However, HDPE of much higher molecular weight, between $3x10^6$ and $6x10^6$ g/mol can also be obtained. These polymers are referred to as ultrahigh molecular weight polyethylene (UHMWPE). The extremely high molecular weight confers special properties to these polymers which make them useful in the lumber industry, for medical implants, recreational equipment, textiles, and transportation.[26d]

1.5.2. Polypropylene

Polypropylene is a thermoplastic material prepared by Ziegler-Natta polymerization of propylene. The general placement of the monomer units along the polymer chain is "head-to-tail", i.e. in which every other carbon atom of the chain bears a methyl group. "Head-to-head" or "tail-to-tail" monomer unit placement can also occur although in very low concentration; these "wrong" placements are usually referred to as regiodefects.[1b]

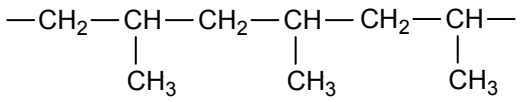

"head-to-tail"

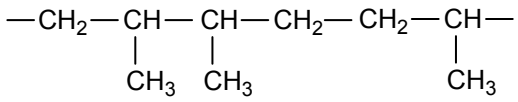

"head-to-head" or "tail-to-tail"

Occasional "head-to-head" or "tail-to-tail" monomer unit placements onto the polymer chain disrupt the crystalline structure of the polymer and lower its melting point.

Polypropylene can have different stereoregularity depending on the spatial orientation of the methyl groups on adjacent methyne carbons. If all methyl substituents are oriented on the same side of the polymer backbone, the polymer is called "isotactic". If the methyl substituents have alternate positions along the polymer chain, then the polymer is called "syndiotactic". An "atactic" polymer is a polymer in which the methyl substituents are randomly oriented along the polymer chain.

Commercially available polypropylene is neither 100% isotactic nor 100% syndiotactic. The degree of stereoregularity of a polymer is generally defined by the proportion and sequence of tactic x-ads (diads, triads, tetrads, and so on). A diad refers to the relative configuration between two consecutive repeating units, a triad refers to the relative configuration between three consecutive repeating units, and so on. If two

consecutive repeating units of a diad have the same configuration, the diad is called a *meso* diad (*m*). If the two consecutive repeating units of a diad are oriented in opposition, then the diad is called a *racemo* diad (*r*). Usually, the degree of stereoregularity of a polymer is associated with the content of [*mmmm*] or [*rrrr*] pentad sequences of that polymer (Scheme 1.20).[1]

Scheme 1.20. General structures of isotactic and syndiotactic polypropylenes

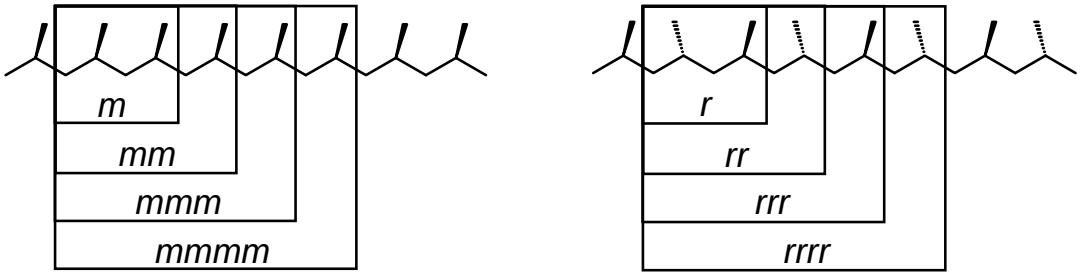

isotactic polypropylene syndiotactic polypropylene

The polymer stereoregularity has a huge impact on the polymer morphology, which in turn, influences the polymer properties and uses. Stereoregular polypropylenes have a high degree of crystallinity and therefore high melting temperatures (~165°C for isotactic polypropylene and ~135°C for syndiotactic polypropylene), while stereoirregular polypropylenes (atactic polypropylenes) are amorphous, viscous materials at room temperature, and this limits their uses. Most commercially available polypropylenes are in the isotactic form, having applicability in the plastics industry, fibers, automotive and electronic industries, and packaging film.[27]

1.6. Aims of the Present Research

Homogeneous Ziegler-Natta catalysts have revolutionized the polyolefin industry, making possible new polymeric materials through control of polymer molecular weights and microstructure. The large amount of theoretical and experimental work so far on metallocene catalysts has led to a widespread consensus on the overall of olefin and α-olefin polymerization mechanism but there is still much to be learned about intimate details of the polymerization process. For instance, although d^0 metal-alkyl-olefin complexes have been proposed key intermediates in Ziegler-Natta olefin polymerization even since 1964, so far they have never been directly observed in an active polymerization system. Also, there is now evidence that not all of the metal added as e.g. Cp_2ZrMe_2 is present as identical, equally active catalyst species, and that much of the metal may actually be tied up as dormant species. Actually, there is very little direct experimental information available about all these and there is currently much interest in identifying the intermediates present in the polymerization system and determining the concentrations of the catalyst actively involved in polymer chain growth at any one time.

One of the objectives of this research is to obtain information about various Zr-polymeryl intermediates present during ethylene and propylene polymerization by homogeneous zirconium-based olefin polymerization catalysts. Two main strategies have been used in order to gain such information. The first one involves the quenching of a polymerization reaction with different quenching agents followed by an analysis of the resulting polymers using NMR spectroscopy. In this regard, the potential of bromine as a quenching agent capable of efficiently replacing the metal moiety of a metal-polymeryl intermediate with bromine is investigated in Chapters 2 and 3. Aside from bromine,

conventional quenching agent CH_3OH and the deuterium-labeling agent CD_3OD, are also used. The second strategy involves direct observation of Zr-polymeryl intermediates in the polymerization mixture by the use of *in situ* ^1H NMR and ESI-MS/MS techniques (Chapter 4).

Another issue of interest in coordination (Ziegler-Natta) polymerization of olefins is related to the observation that these processes are adversely affected by the conversion of the active catalyst to dormant or even unreactive species. One of the mechanisms proposed to account for catalyst deactivation consists of formation of Zr-allyl polymeryl intermediates; these are considered to accumulate in the polymerization mixture as dormant species rather than propagate. Although recently the presence of Zr-allyl polymeryl intermediates in a polymerization mixture has been demonstrated, the literature on this topic is still scarce. Thus, another objective of this research is to obtain information about the formation and characterization of Zr-allyl complexes. The Zr-allyl complexes of interest were synthesized from the reaction of the active catalyst Cp_2Zr^+Me with vinylidene terminated compounds (Chapter 4). These complexes can be used as model compounds for similar Zr-allyl polymeryl species present in the polymerization systems.

References

1. (a) Elias, H. -G. *An Introduction to Polymer Science*, 1st ed., VCH Publishers, Inc., New York, **1997**. (b) Rempp, P.; Merrill, E. W. *Polymer Synthesis*. Huethig & Wepf Verlag Basel, Heidelberg, New York, **1986**.
2. (a) Coates, G. W.; Hustad, P. D.; Reinartz, S. *Angew. Chem. Int. Ed. Engl*. **2002**, *41*, 2236. (b) Kaminsky, W. *Cat. Today* **2000**, *62*, 23. (c) Kaminsky, W.; Laban, A. *Appl. Cat. A: General* **2001**, *222*, 47.
3. *Comprehensive Organometallic Chemistry: The Synthesis, Reactions and Structures of Organometallic Compounds.* editor, Wilkinson, G. S.; deputy editor, Gordon, F., Stone, A.; executive editor, E. W. Abel. 1st ed., Vol. 3, Oxford, New York, Pergamon Press, **1982**.
4. (a) Kim, S. H.; Somorjai, G. A. *Proc. Natl. Acad. Sci. USA* **2006**, *103*, 15289. (b) Bochmann, M. *J. Chem. Soc., Dalton Trans.* **1996**, 255. (c) Kaminsky, W. *Macromol. Chem. Phys.* **1996**, *197*, 3907.
5. (a) Coates, G. W. *Chem. Rev*. **2000**, *100*, 1223. (b) Brintzinger, H. H.; Fischer, D.; Mülhaupt, R.; Rieger, B.; Waymouth, R. M. *Angew. Chem. Int. Ed. Engl.* **1995**, *34*, 1143.
6. (a) Natta, G.; Pino, P.; Mazzanti, G.; Giannini, U. *J. Am. Chem. Soc*. **1957**, *79*, 2975. (b) Breslow, D. S.; Newburg, N. R. *J. Am. Chem. Soc*. **1957**, *79*, 5072.
7. (a) Alt, H. G.; Köppl, A. *Chem. Rev*. **2000**, *100*, 1205. (b) Resconi, L.; Cavallo, L.; Fait, A.; Piemontesi, F. *Chem. Rev.* **2000**, *100*, 1253. (c) Müller, G.; Rieger, B. *Prog. Polym. Sci*. **2002**, *27*, 815.
8. Cossee, P. *J. Cat.* **1964**, *3*, 80.

9. (a) Wu, Z.; Jordan, R. F. *J. Am. Chem. Soc*. **1995**, *117*, 5867. (b) Stoebenau, E. J. III.; Jordan, R. F. *J. Am. Chem. Soc*. **2006**, *128*, 8162. (c) Casey, C. P.; Carpenetti II, D. W.; Sakurai, H. *J. Am. Chem. Soc*. **1999**, *121*, 9483.

10. (a) Correa, A.; Talarico, G.; Cavallo, L. *J. Organomet. Chem*. **2007**, *692*, 4519. (b) Guerra, G.; Longo, P.; Cavallo, L.; Corradini, P.; Resconi, L. *J. Am. Chem. Soc.* **1997**, *119*, 4394.

11. (a) Resconi, L.; Camurati, I.; Sudmeijer, O. *Topics in Catalysis* **1999**, *7*, 145. (b) Rappé, A. K.; Skiff, W. M.; Casewit, C. J. *Chem. Rev*. **2000**, *100*, 1435.

12. Fagan, P. J.; Manriquez, J. M. ; Maatta, E. A. ; Seyam, A. M. ; Marks, T. J. *J. Am. Chem. Soc.* **1981**, *103*, 6650.

13. G. Stojcevic. *PhD Thesis*, Queen's University, **2008**.

14. Möhring, P. C.; Coville, N. J. *J. Organomet. Chem*. **1994**, *479*, 1.

15. Tshuva, E. Y.; Goldberg, I.; Kol, M. *J. Am. Chem. Soc*. **2000**, *122*, 10706.

16. (a) Gibson, V. C.; Spitzmesser, S. K. *Chem. Rev*. **2003**, *103*, 283. (b) Busico, V.; Cipullo, R.; Pellecchia, R.; Ronca, S.; Roviello, G.; Talarico, G. *Proc. Natl. Acad. Sci. USA* **2006**, *103*, 15321.

17. (a) Busico, V.; Talarico, G.; Cipullo, R. *Macromol. Symp*. **2005**, *226*, 1. (b) Busico, V.; Cipullo, R.; Ronca, S.; Budzelaar, P. H. M. *Macromol. Rapid. Commun*. **2001**, *22*, 1405. (c) Busico, V.; Cipullo, R.; Friederichs, N.; Ronca, S.; Talarico, G.; Togrou, M.; Wang, B. *Macromolecules* **2004**, *37*, 8201.

18. Busico, V.; Cipullo, R.; Friederichs, N.; Ronca, S.; Togrou, M. *Macromolecules* **2003**, *36*, 3806.

19. (a) Chen, E. Y.-X.; Marks, T. J. *Chem. Rev*. **2000**, *100*, 1391. (b) Pédeutour, J. –N.; Radhakrishnan, K.; Cramail, H. ; Deffieux, A. *Macromol. Rapid Commun.* **2001**, *22*, 1095.

20. Soga, K.; Shiono, T. *Prog. Polym. Sci*. **1997**, 1503.

21. Massey, A. G.; Park, A. J. *J. Organomet. Chem*. **1964**, *2*, 245.

22. (a) Yang, X.; Stern, C. L.; Marks, T. J. *J. Am. Chem. Soc.* **1991**, *113*, 3623. (b) Yang, X.; Stern, C. L.; Marks, T. J. *J. Am Chem. Soc.* **1994**, *116*, 10015.

23. Piers, W. E.; Chivers, T. *Chem. Soc. Rev*. **1997**, *26*, 345.

24. Strauss, S. H. *Chem. Rev*. **1993**, *93*, 927.

25. Chien, J. C. W.; Tsai, W. –M.; Rausch, M. D. *J. Am. Chem. Soc*. **1991**, *113*, 8570.

26. (a) Doak, K. W. *Concise Encyclopedia of Polymer Science and Engineering*, Kroschwitz, J. I. Ed., John Wiley & Sons, **1990**, 350. (b) Beach, D. L.; Kissin, Y. V. *Concise Encyclopedia of Polymer Science and Engineering*, Kroschwitz, J. I. Ed., John Wiley & Sons, **1990**, 354. (c) James, D. E. *Concise Encyclopedia of Polymer Science and Engineering*, Kroschwitz, J. I. Ed., John Wiley & Sons, **1990**, 352. (d) Coughlan, J. J.; Hug, D. P. *Concise Encyclopedia of Polymer Science and Engineering*, Kroschwitz, J. I. Ed., John Wiley & Sons, **1990**, 357.

27. Lieberman, R. B.; Barbe, P. C. *Concise Encyclopedia of Polymer Science and Engineering*, Kroschwitz, J. I. Ed., John Wiley & Sons, **1990**, 914.

Chapter 2

An Investigation into the Zr-polymeryl Intermediates Present during Ethylene and Propylene Polymerizations by Zirconocene-based Catalysts

2.1. Introduction

In recent years, there has been considerable research into the utilization of metallocene complexes of the type $[Cp'_2ZrR]^+X^-$ (Cp' = substituted η^5-cyclopentadienyl group, R = alkyl group, and X^- = weakly coordinating anion) as homogeneous catalysts for coordination (Ziegler-Natta) polymerization of olefins.[1] There is widespread consensus with respect to mechanisms of the general processes involved in the initiation, propagation, chain transfer and termination steps, and it is believed that these catalysts function as in Equation 2.1, where ~P is either a long chain alkyl, or a polymeryl group. The methyl group is being converted to a long chain, primary polymeryl group via repeated ethylene insertion steps.[1] Chain transfer then may involve β-hydrogen migration, as shown in Equation 2.2, to release a polymer with a terminal olefinic end

group. A reinsertion-deinsertion of the terminal olefinic end group (Equation 2.3) can result in both secondary polymeryl groups and internal olefins.[1]

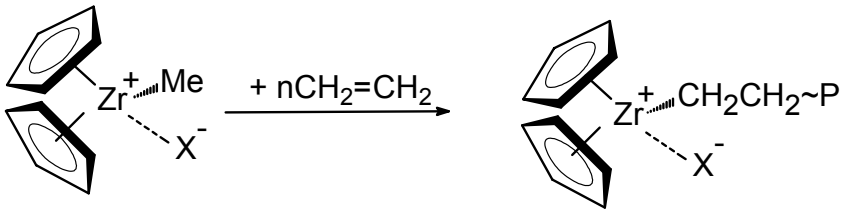

(**2.1**)

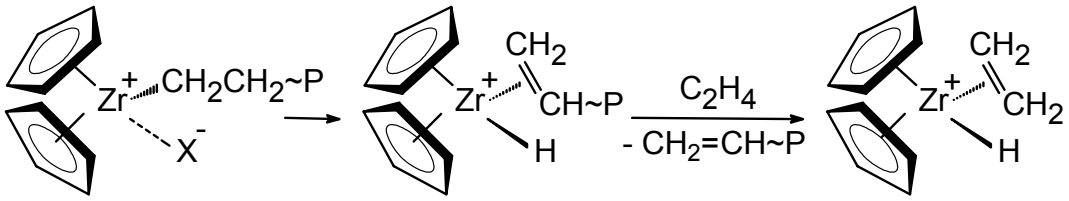

(**2.2**)

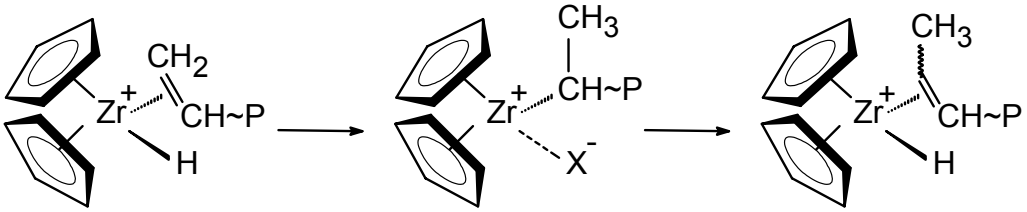

(**2.3**)

Alternatively, reinsertion of the terminal olefinic products CH_2=CH~P into a propagating polymer chain can result in long chain branching, as in Equation 2.4 (where P_1 and P_2 are different chain length polymeryl groups).

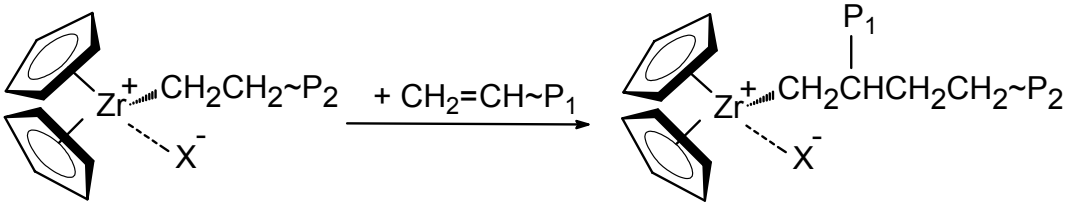

(**2.4**)

In fact, there is actually very little direct experimental information available concerning these and other possible species, and there remains much to be learned about intimate details of the polymerization process, as for example, the intermediates present during polymerization and the concentration of the catalyst actively involved in polymer chain growth at any one time.

Experimentation designed to gain such information has taken several approaches, and it has recently been shown that it is possible to observe some such species directly.[2] Thus, by use of *in situ* ^{1}H and ^{13}C NMR spectroscopic studies, the latter involving ^{13}C-enriched catalyst and/or monomer, the presence of the primary Zr-$CH_2CH(R)$-polymeryl species during the polymerization reaction (R = H, CH_3, C_4H_9, C_7H_{15}, C_8H_{17}) has been demonstrated.[2] More recently, direct evidence of the presence of Zr-allyl oligomers during *in situ* propylene and 1-^{13}C-1-hexene polymerization, respectively, by chiral zirconocene catalysts, has also been obtained.[3]

A complementary general approach has involved the use of quenching agents containing radioactive labels such as CH_3O^3H and ^{14}CO.[4,5] The former is believed to cleanly and efficiently replace the metal of a $[Cp'_2MCH_2CH_2{\sim}P]^+$ moiety with a single tritium to give ^3H -CH_2CH_2~P, which can be quantified and related to the sum of the concentrations of all species present which contain metal-carbon σ bonds.[4] Carbonylation reactions, on the other hand, are expected to result in coordination of ^{14}CO to the vacant

site of the metal in the $[Cp'_2MCH_2CH_2{\sim}P]^+$ moiety followed by a migratory insertion to give an acyl species of the type $[Cp'_2M^{14}COCH_2CH_2{\sim}P]^+$ (Equation 2.5).[5a]

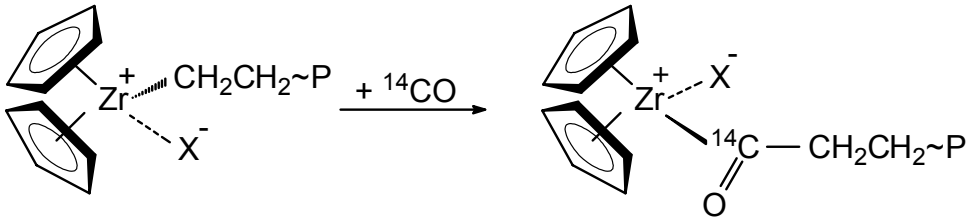

(**2.5**)

It was anticipated that protic cleavage of the resulting acyl species would result in the formation of labeled aldehyde, whence again the sum of the concentrations of the $[Cp'_2MCH_2CH_2{\sim}P]^+$ propagating species could be determined.[5] Although these methods have been generally accepted and used for quantification of metal-polymeryl groups, they do have the limitation that they do not yield information concerning the nature of the end groups bearing the radioactive labels. Moreover, it has been demonstrated[6] that CO does not necessarily terminate polymerization, but that it can participate in alkene-CO copolymerization such that more than one CO molecule is absorbed per metallocene unit.[5b,6] If this were the situation generally, then estimates of numbers of active sites obtained using ^{14}CO would be higher than those obtained using CH_3O^3H and thus the general applicability of this method remains suspect.

Recently, to complement a kinetics study,[7] CH_3OD has been utilized as a quenching agent to determine the nature and relative concentrations of intermediates present during catalysis at the time of quench by using ^2H NMR techniques. In one particular case, involving 1-hexene polymerization using *rac*-{C_2H_4(1-

indenyl)$_2$}Zr(Me)(μ-Me)B(C_6F_5)$_3$, the -CH_2D end group resulting from termination following a 1,2-insertion was the only end group detected. In addition, estimations of its concentration made it possible to show that the number of active sites was approximately equal to the catalyst concentration for the system under study. However this method suffers from poor sensitivity of ^{2}H NMR techniques and, taking into account all the above observations, clearly a general and efficient method for identification of Zr-polymeryl intermediates and determination of the relative concentrations of the propagating polymeryl species is still needed.

In this Chapter, the results of an investigation into the nature and relative concentrations of Zr-polymeryl intermediates present in solution during ethylene polymerization by Cp_2ZrMe_2 catalyst and propylene polymerization by Cp_2ZrMe_2, (indenyl)$_2$ZrMe_2 and *rac*-{C_2H_4(1-indenyl)$_2$}ZrMe_2 catalysts activated with B(C_6F_5)$_3$ are discussed.

Specifically, with a view to developing a simple, rapid method for the identification and quantification of metal-polymeryl groups present during a polymerization reaction, the use of bromine to label the polymer chain ends is explored in the first part of this chapter (Sections 2.2.1-2.2.3). Bromine has long been known to rapidly cleave metal-carbon σ bonds,[8a] the products being organic bromides and the corresponding metal bromides as in Equation 2.6 (where M = metal, R = alkyl group, and L = ligand).

$$L_nM\text{-}R + Br_2 \longrightarrow L_nM\text{-}Br + R\text{-}Br \qquad (\mathbf{2.6})$$

Zirconocene compounds of the type $Cp_2Zr(R)(Cl)$ have been shown to be cleaved similarly,[8b,c] and thus bromine would be expected to react with polymerization reaction mixtures containing Cp_2Zr^+-polymeryl linkages, as in Scheme 2.1, to form Br-polymeryl end groups which may be identified as primary or secondary alkyl bromides on the basis of chemical shifts.[9]

Scheme 2.1. Bromine quenching scheme.

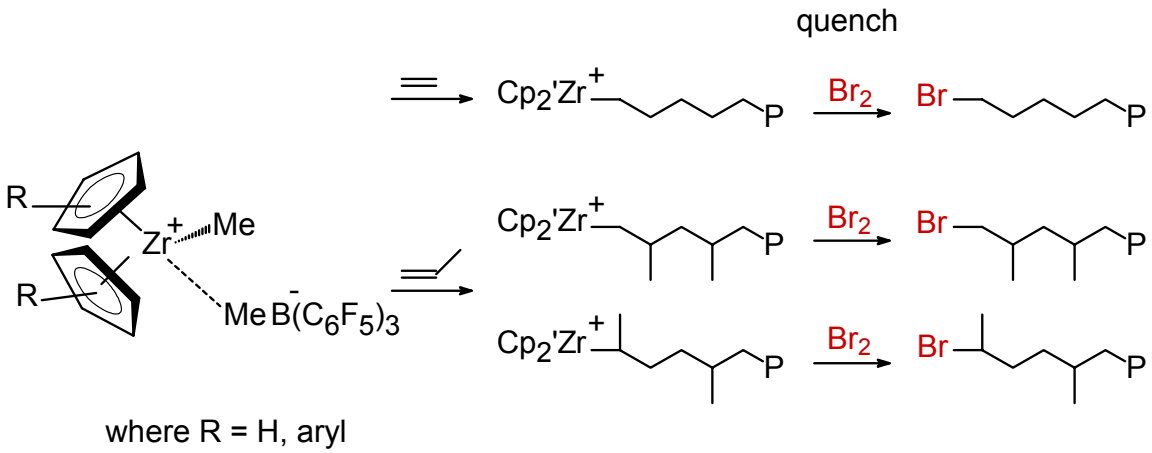

The method of quenching a polymerization reaction by bromine was previously reported by Boden.[10a] As a test of the procedure, a series of *in situ* bromination reactions of Cp_2ZrMe_2 and $[Cp_2ZrMe][MeB(C_6F_5)_3]$ in different solvents were performed.[10] The study showed that the Zr-C σ bond cleavage reactions are fast and quantitative as in Equations 2.7 and 2.8.

$$Cp_2ZrMe_2 + 2Br_2 \longrightarrow Cp_2ZrBr_2 + 2MeBr \quad (\mathbf{2.7})$$

$$[Cp_2ZrMe][MeB(C_6F_5)_3] + 2Br_2 \longrightarrow Cp_2ZrBr_2 + 2MeBr + B(C_6F_5)_3 \quad (\mathbf{2.8})$$

These results are important because they imply that species of the type Cp_2Zr^+-polymeryl present in the polymerization mixture will also be cleaved rapidly and quantitatively by bromine to give Cp_2ZrBr_2 [11] and Br-polymeryl, confirming the validity of this method. Furthermore, the integration of a ^1H NMR spectrum of a reaction mixture would result in an estimate of the amounts of all Br-polymeryl groups in solution and hence in quantitative estimates of all Cp_2Zr^+-polymeryl species in solution at the time of quenching. Thus, in principle, the method should make it possible to identify and quantify every type of Zr-C σ bonded moiety in solution at the time of termination.

The methodology seems rather more appealing than e.g. termination reactions which replace the metal with ^2H or ^3H as the protocol utilizes ^1H NMR spectroscopy rather than the inherently less sensitive ^2H NMR spectroscopy and, of course, it does not require the use of radioactive materials. Also, losses to evaporation of alkyl bromide oligomers are less critical than would possibly be the case with the hydrocarbon analogues obtained via polymeryl labeling with ^2H or ^3H; thus the quantification of polymeryl species would be more reliable. In Sections 2.2.1-2.2.3, the bromine quenching method is applied to ethylene polymerization by Cp_2ZrMe_2[12a,b] catalyst and propylene polymerization by Cp_2ZrMe_2, $(indenyl)_2ZrMe_2$[12a,c] and *rac*-$\{C_2H_4(1\text{-indenyl})_2\}ZrMe_2$[12d,e] catalysts activated with $B(C_6F_5)_3$[12f] in chlorobenzene. The assignments of the brominated polymer chain ends, as primary or secondary, are

facilitated by the use of different model compounds. Specifically, comparisons with the NMR spectra from brominated hydrocarbons is used to identify the end groups.

Additionally, in Section 2.2.4, an analysis of unsaturation in atactic polypropylene obtained from the $(indenyl)_2ZrMe_2/B(C_6F_5)_3$ catalyst is presented. This provides further information on the Zr-polymeryl intermediates present during the polymerization. Of particular interest is the presence of Zr-allyl intermediates which are considered to accumulate in the polymerization mixture rather than to propagate and therefore to deactivate the catalyst. The presence of Zr-allyl intermediates is further confirmed from the analysis of the deuterium-labeled polymer chain ends obtained following quenching of propylene polymerization by CD_3OD (Section 2.2.5).

A summary of the results is presented in Section 2.3 while Section 2.4 presents experimental details.

2.2. Results and Discussion

2.2.1. Model Compounds

Cleavage of Zr-polymeryl σ-bonds by bromine would invariably yield bromine terminated polymer chains. In the case of ethylene polymerization, the polymer backbone is mainly made by methylenic units and, in this case, the assignment of a bromine terminated polyethylene chain arising from the cleavage of a $Zr\text{-}CH_2CH_2\sim P$ bond seems straightforward. In the case of propylene polymerization, however, the assignment of the brominated end groups of the polypropylene chains becomes more complicated due to the presence of the methyl side groups on the polymer chain. In this case, several factors have to be taken into consideration: the stereochemical configuration of the polymer

chain end, the propylene insertion mode into the Zr-polymeryl linkage, and the fact that a polymer is obtained as a mixture of polymer chains of different stereochemical configurations.

In order to identify different types of brominated end groups of the polymer chains, a series of model compounds which contain brominated moieties with chemical structures close to those of the corresponding brominated polymer chain ends to be assigned were used. Comparison between the NMR spectra of the alkyl bromide end groups of the polymer chains and the spectra of the model compounds allows direct assignment of the different types of alkyl bromide end groups on the polymer chain.

The commercially available 1,11-dibromoundecane and 2-bromodecane were used as model compounds for a primary alkyl bromide end group of a polyethylene chain and a secondary alkyl bromide end group of a polypropylene chain, respectively. The brominated end group regions of 1,11-dibromoundecane and 2-bromodecane are shown in Figure 2.1(a) and (b), respectively.

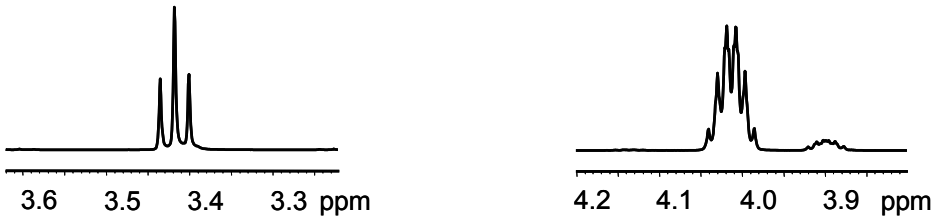

(a) (b)

Figure 2.1. ^{1}H NMR spectra in the brominated region of (a) $BrCH_2(CH_2)_9CH_2Br$ in CD_2Cl_2 (400 MHz) and (b) $CH_3CH(Br)(CH_2)_7CH_3$ in C_6D_5Cl (600 MHz).

From Figure 2.1 it can be seen that the primary alkyl bromide group (BrC**H**$_2$-) resonance of 1,11-dibromoundecane appears as a triplet at 3.42 ppm, while the methyne resonance (-C**H**Br-) of the secondary alkyl bromide group of 2-bromodecane appears as a multiplet at ~4.01 ppm. The weak multiplet at ~3.9 ppm in Figure 2.1(b) is due to traces of 3-bromodecane in the commercially available 2-bromodecane.

As model compounds for a primary alkyl bromide terminated polypropylene chain, 1-bromo-2-methyl-undecane and 1-bromo-2,4-dimethyl-heptane were used. These compounds were chosen as they are small enough to allow for an accurate characterization by NMR spectroscopy but large enough to capture the stereochemical configuration of the polypropylene chain ends. Also, they are obtained as a mixture of stereoisomers which make them suitable as model compounds for mixtures of polymer chains of differing configurations.

1-bromo-2-methyl-undecane and 1-bromo-2,4-dimethyl-heptane were prepared via hydrozirconation[8] of the appropriate α-olefins with $Cp_2Zr(H)(Cl)$, followed by the bromination of the intermediate zirconocene alkyl chloride complexes[8b,c] as depicted in Equations 2.9 and 2.10, respectively (R is an alkyl chain).

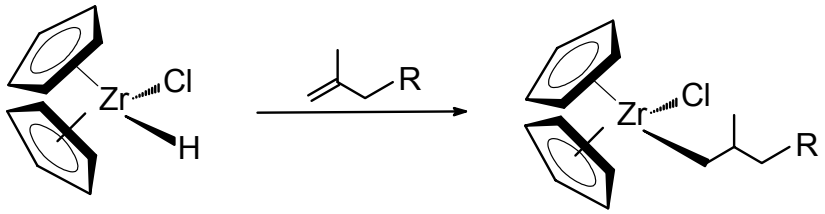

(**2.9**)

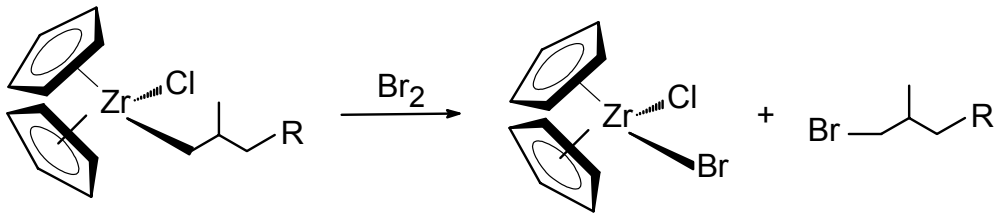

(**2.10**)

In particular, 1.2 equivalents of $Cp_2Zr(H)(Cl)$ was reacted with 1 equivalent of $CH_2=C(Me)(CH_2)_8CH_3$ or $CH_2=C(Me)CH_2CH(Me)CH_2CH_2CH_3$ in dry chlorobenzene to yield $Cp_2Zr(Cl)(CH_2CH(Me)(CH_2)_8CH_3)$ or $Cp_2Zr(Cl)(CH_2CH(Me)CH_2CH(Me)C_3H_7)$, respectively. The above zirconium alkyl chloride complexes were not isolated but further reacted with bromine to give the corresponding primary alkyl bromide compounds which were characterized by NMR spectroscopy.

The ^1H NMR spectrum of $BrCH_2CH(Me)(CH_2)_8CH_3$ in dichloromethane-d_2 in the brominated end group region shows the presence of two doublets of doublets at 3.34 and 3.42 ppm which were assigned to the two diastereotopic hydrogens of the Br**C**$\mathbf{H}_2$-terminal group. The assignment of the primary alkyl bromide group hydrogens was confirmed by an HSQC experiment which shows the presence of two cross peaks between the two hydrogen resonances at 3.34 and 3.42 ppm and a carbon resonance at 41.6 ppm. The ^1H NMR and ^1H-^{13}C HSQC spectra of $BrCH_2CH(Me)(CH_2)_8CH_3$ in the brominated end group region is displayed in Figure 2.2.

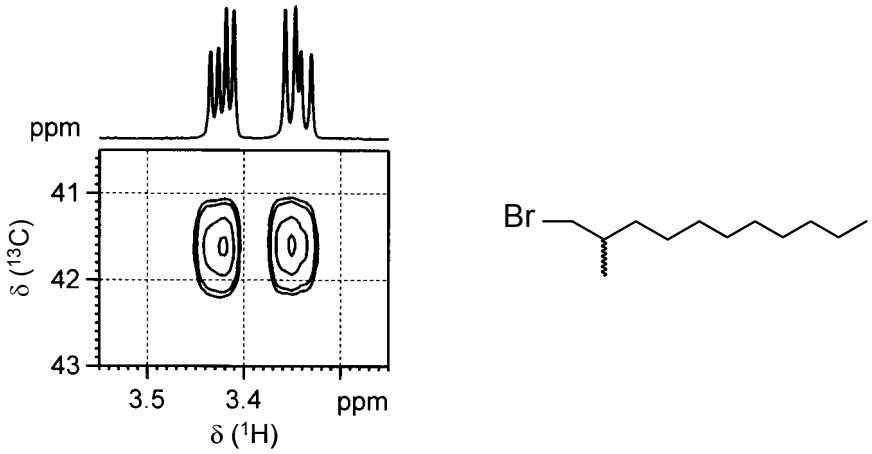

Figure 2.2. ^{1}H NMR and ^{1}H-^{13}C HSQC spectra of Br**H**$_2$CH(Me)(CH$_2$)$_8$CH$_3$ in the brominated end group region (CD_2Cl_2, 600 MHz).

The ^{1}H NMR spectrum of the BrCH$_2$CH(Me)CH$_2$CH(Me)CH$_2$CH$_2$CH$_3$ model compound in the brominated end group region, on the other hand, is more complicated due to the presence of a second chiral center in the molecule (see Figure 2.3). In this case, the BrCH$_2$CH(Me)CH$_2$CH(Me)CH$_2$CH$_2$CH$_3$ compound is obtained as a mixture of stereisomers containing *m* (meso) and *r* (racemic) diad terminal groups in about 1:1 molar ratio. Since the Br**H**$_2$CH(Me)- group hydrogens are sensitive to the nature of the adjacent *m* or *r* diad unit, for a mixture of *m* and *r* diad terminated 1-bromo-2,4-dimethyl-heptane diastereomers, they appear as two overlapping pairs of doublets of doublets. This can be seen from an HSQC experiment (Figure 2.3) in which the pair of doublets of doublets at 3.44 and 3.34 ppm is correlated with a carbon resonance at 41.7 ppm, while the pair of doublets of doublets at 3.40 and 3.32 ppm is correlated with a carbon resonance at 42.2 ppm.

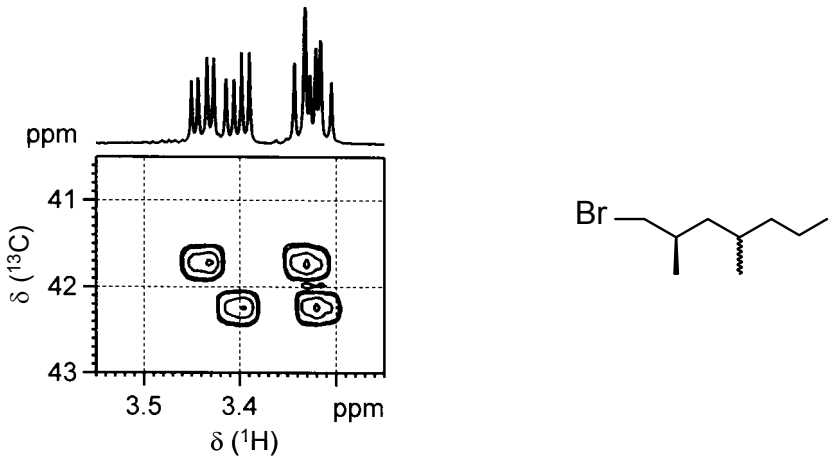

Figure 2.3. ^{1}H NMR and ^{1}H-^{13}C HSQC spectra of Br**C**$\mathbf{H}_2$CH(Me)CH_2CH(Me)$(CH_2)_2CH_3$ in the brominated end group region (CD_2Cl_2, 600 MHz).

Based on the spectra of the brominated end groups of 1-bromo-2-methyl-undecane and 1-bromo-2,4-dimethyl-heptane model compounds, the pattern of the primary alkyl bromide end groups of a polypropylene obtained following the cleavage of a primary Zr-CH_2CH(Me)~P linkage can be easily predicted. Thus, for highly isotactic polypropylene, in which most of the polymer chains will be *m* diad terminated (i.e., most of the polymer chains will have the same stereochemical configuration of the brominated chain ends) as shown in Scheme 2.2(a), the ^{1}H NMR and ^{1}H-^{13}C HSQC spectra of the primary alkyl bromide end groups will show the presence of only one set of Br**C**$\mathbf{H}_2$CH(Me)- resonances, as depicted in Figure 2.2. Likewise, the ^{1}H NMR and ^{1}H-^{13}C HSQC spectra of highly syndiotactic polypropylene, in which most of the polymer chains will be *r* diad terminated (Scheme 2.2(b)), will show the presence of only one set of Br**C**$\mathbf{H}_2$CH(Me)- resonances.

Scheme 2.2. The brominated end groups of (a) isotactic polypropylene and (b) syndiotactic polypropylene. Three polymer chains are shown in each case.

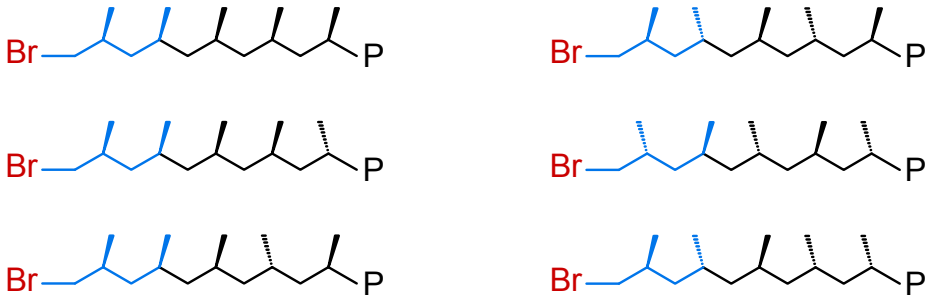

(a) (b)

On the other hand, for an atactic polypropylene, which is actually composed of a mixture of polymeryl chains containing *m* and *r* terminal diads in almost equivalent amounts (see Scheme 2.3), the NMR spectra of the primary alkyl bromide end groups are expected to show the presence of two overlapping sets of resonances similar to those shown in Figure 2.3.

Scheme 2.3. The brominated end groups of atactic polypropylene. Four polymer chains are shown in this case.

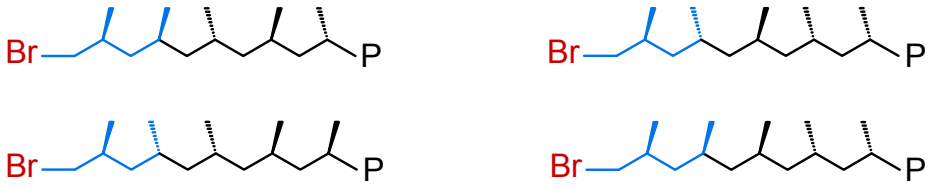

For a polymer of intermediate degree of stereospecificity, the relative intensities of the two pairs of hydrogens of the primary alkyl bromide end groups next to *m* and *r* terminal diads, respectively, are expected to change according to the degree of stereospecificity of the polymer.

2.2.2. Ethylene Polymerizations

Ethylene polymerization was performed at room temperature, under 1 atmosphere of ethylene, using the $Cp_2ZrMe_2/B(C_6F_5)_3$ polymerization system[2a,13] in chlorobenzene. Polymerizations were typically carried out for 10-60 seconds in order to obtain data for the early stages of the process, and stopped by quenching with a solution of bromine in methylene chloride. After quenching, polyethylene was precipitated in methanol, filtered, dried and purified by reprecipitation from hot chlorobenzene. ^{1}H NMR spectra of the resulting polyethylene were run at 120°C in chlorobenzene-d_5, and a typical ^{1}H NMR spectrum of a brominated polyethylene obtained after 10 seconds of polymerization time is presented in Figure 2.4.

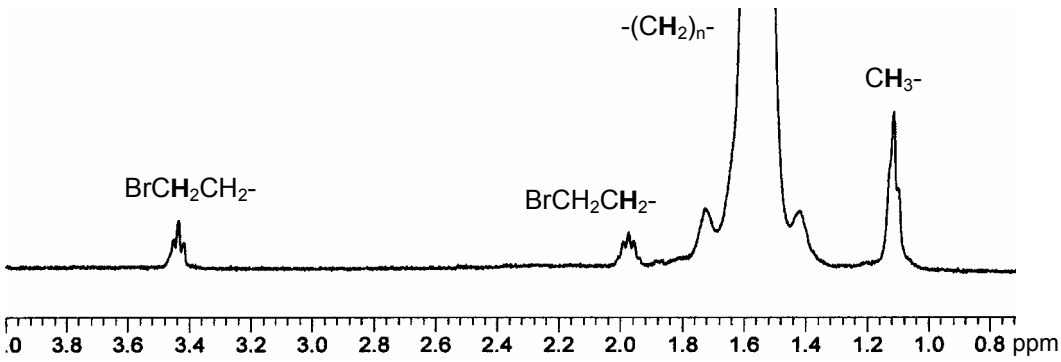

Figure 2.4. ^{1}H NMR spectrum of brominated polyethylene in C_6D_5Cl (400 MHz, 120°C).

In addition to the methylene polymer backbone resonance at 1.57 ppm (singlet) and the terminal methyl resonance at 1.11 ppm (broad triplet), a weak triplet at 3.44 ppm and a multiplet at 1.97 ppm are attributed, respectively, to the anticipated $BrC\mathbf{H}_2CH_2{\sim}P$ and $BrCH_2C\mathbf{H}_2{\sim}P$ end group hydrogens.

In order to obtain estimates of the concentrations of Cp_2Zr^+-$CH_2{\sim}P$ groups during these polymerization reactions, the concentration of the $BrCH_2{\sim}P$ groups relative to the amount of catalyst used was obtained from ^1H NMR spectrum (120°C, C_6D_5Cl) using 1,1,2,2-tetrachloroethane (5.80 ppm) as an internal standard. In this regard, integrations of the resonance at 3.44 ppm of several such polymeric products and comparison of their intensities with that of the 1,1,2,2-tetrachloroethane at 5.80 ppm showed that the Zr-polymeryl concentrations were low, in the range 4-10%. There appeared to be no correlation of Zr-polymeryl concentration with time, but it seemed quite likely that entrapment of zirconium-containing compounds in the precipitating polyethylene may have resulted in reduced concentrations of Zr-polymeryl groups. Thus, both uninitiated catalyst (Cp_2Zr^+-Me) and Zr-polymeryl species which were entrapped into precipitating polymer (and therefore inactive) may have not been cleaved by bromine upon quenching but by traces of water during reprecipitation from hot chlorobenzene resulting in methane and methyl terminated polymeryl chains, respectively.

Similar results were obtained by Boden[10] who performed ethylene polymerization in the presence of the $Cp_2ZrMe_2/B(C_6F_5)_3$ polymerization system in toluene. In this case, after quenching by bromine, all volatiles were removed from the reaction mixtures and ^1H NMR spectra of unpurified samples of polymers which retained the Cp_2ZrBr_2 product were run in 1,1,2,2-tetrachloroethane-d_2 at 100°C. Peak areas, obtained from integration

of the BrC**H**$_2$- resonance of several such polymeric products, were compared with those of the Cp resonance of the Cp_2ZrBr_2 present at 6.55 ppm. Again the Zr-polymeryl concentrations were low, in the range 0.5-5 % of the total catalyst present.[10]

These results seem reasonably consistent with those of Busico *et al.*,[14] who studied ethylene polymerization by the *rac*-Me_2Si(2-Me-4-Ph-1-indenyl)$_2ZrCl_2$/MAO catalyst system and deduced Zr-polymeryl relative concentrations of 5-25%.

For all polymer samples obtained in chlorobenzene, the ratio of the relative intensity of the methyl resonance to that of the BrC**H**$_2$- group resonance varied from 2:1 at 10 seconds to 32:1 at 60 seconds. Similarly, for polymer samples obtained in toluene,[10] the ratio of the intensity of the methyl resonance to that of the BrC**H**$_2$- group resonance was always >>3:2, varying from ~10:1 at 10 seconds to ~40:1 at 60 seconds. These observations, coupled with observations that the NMR spectra of the brominated polymers exhibited weak or no ^{1}H NMR resonances of vicinal dibromides,[9] and that polyethylene obtained via conventional methanol quenching contained no, or very weak, olefinic end groups, imply that while a significant degree of chain transfer via β-hydrogen elimination to form α-olefins does occur, the thus formed α-olefins must be efficiently incorporated into the growing polymer chains as long chain branches (Equation 2.4). Cleavage of Zr-polymeryls entrapped into precipitating polyethylene by traces of water during reprecipitation may also account for part of the methyl terminated polymer chains.

To investigate the possibility for long chain branch incorporation, $^{13}C\{^1H\}$ NMR spectra of brominated polyethylene samples were obtained in 1,1,2,2-tetrachloroethane-d_2 at 120°C. A typical APT-^{13}C NMR spectrum of a sample of brominated polyethylene,

obtained after 50 seconds polymerization time in chlorobenzene, is shown in Figure 2.5, with assignments.

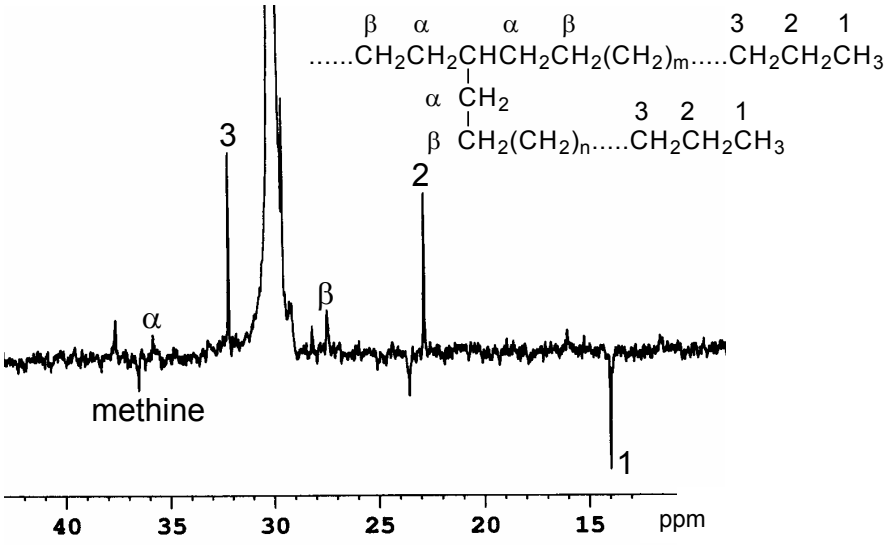

Figure 2.5. APT-^{13}C NMR spectrum of a sample of brominated polyethylene obtained after a 50 second polymerization time ($C_2D_2Cl_4$, 120°C, 400 MHz).

As can be seen, the spectrum exhibits a weak resonance at 36.5 ppm which indicates the presence of a methine group; in conjunction with the α and β methylene resonances at 35.8 and 27.4 ppm, respectively, there is firm evidence for long chain branching.[15a-d] Interestingly, resonances of short chain methyl, ethyl, propyl and butyl chain branches[15] were not observed in this spectrum, although there is an as yet unassigned methyl resonance at 23.5 ppm.[15e] The presence of branches in the polyethylene can also be confirmed from DSC analysis as it is known that branches affect the crystalline structure of the polymer and as a result the melting temperature and crystallinity of the polymer are reduced.[16a] Thus, melting point measurements showed

that the polyethylene samples prepared in chlorobenzene all melted at 128.6 ±1.3 °C, values indicative of high density polyethylene (HDPE) containing small amounts of long chain branches.[16b]

These results are in themselves interesting as it is generally believed that polymers containing olefinic end groups should be major species in this type of polymerization reaction[1] *unless* the polymerizations involve alkyl aluminum co-catalysts such as MAO. For the latter, polymeryl transfer to aluminum followed by hydrolysis can result in saturated polymers,[17a-c] and observation of the latter tends to be taken as evidence for processes involving chain transfer to aluminum.[14,15a] In fact our observations suggest that this interpretation may not always be correct: saturated polymers can be obtained in the absence of alkyl aluminum compounds and the presence of saturated polymers need not necessarily require chain transfer to aluminum.

2.2.3. Propylene Polymerizations

This study was then continued with propylene polymerization by the $Cp_2ZrMe_2/B(C_6F_5)_3$[13a,b] and $(indenyl)_2ZrMe_2/B(C_6F_5)_3$[12a,c] catalyst systems which are known to give atactic polypropylene;[13a,b,18,19] the latter is quite soluble in different solvents at room temperature and therefore easier to investigate than polyethylene. In these experiments the anticipated brominated end groups would be $BrCH_2CH(Me)CH_2CH(Me)$~P (~3.3-3.5 ppm, Figure 2.3), following a 1,2-insertion, although the presence of $BrCH(Me)CH_2CH_2CH(Me)$~P (~4.0-4.2 ppm, Figure 2.1(b)) end groups,[9] resulting from an ultimate 2,1-insertion would also be possible (see Scheme 2.1).

Polymerizations were generally begun at room temperature, under 1 atmosphere of propylene, and terminated with excess bromine after reaction times varying from 10 seconds to 4 minutes. After termination, the volatiles were removed under reduced pressure and the residues were extracted with hexanes and passed through a short silica column to remove catalyst. The solvent was then removed to give oily, atactic polypropylene which was characterized on the basis of comparisons with model compounds as discussed below, using ^{1}H NMR and correlation spectroscopy.

The ^{1}H NMR spectra of the brominated polymeric products all exhibited the expected methyne (~1.6 ppm), methylene (~0.8–1.4 ppm), and methyl (~0.83 ppm) backbone resonances. In addition, the Br-C**H$_2$**CHMe~polymeryl group resonances in the region 3.3-3.5 ppm appear as three broad, unresolved multiplets with an approximately 1:1:2 ratio of intensities (Figure 2.6).

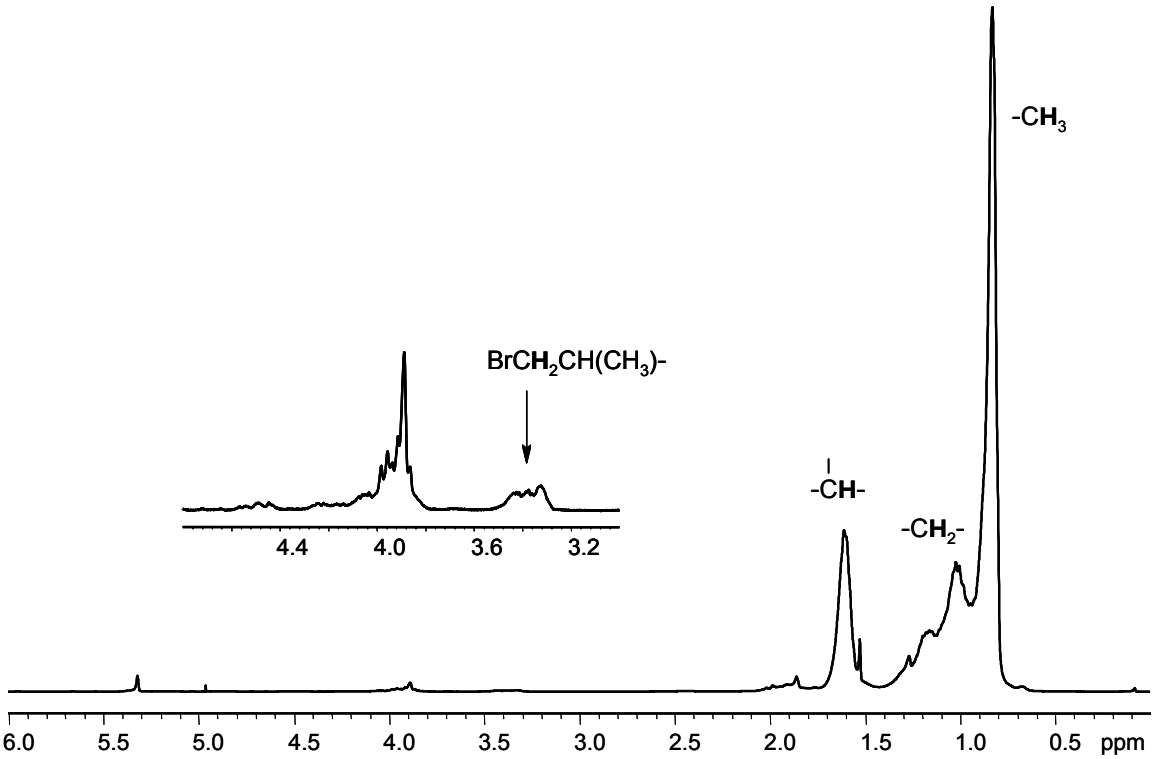

Figure 2.6. ^{1}H NMR spectrum of atactic polypropylene obtained from (indenyl)$_2$ZrMe$_2$/B(C$_6$F$_5$)$_3$ after quenching with bromine (CD_2Cl_2, 400 MHz).

This pattern arises, as expected, from the overlapping of two pairs of multiplets, as shown by an HSQC experiment (Figure 2.7) in which one pair of protons at about 3.34 and 3.44 ppm was found to correlate with a carbon resonance at 41.7 ppm and the other pair of protons at about 3.32 and 3.40 ppm with a carbon resonance at 42.2 ppm.

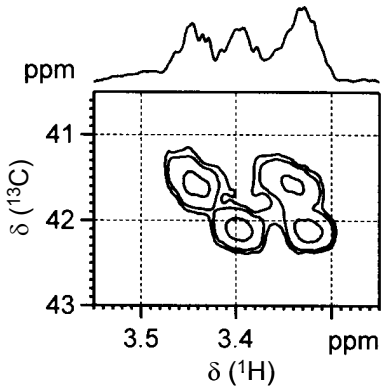

Figure 2.7. ^{1}H NMR and ^{1}H-^{13}C HSQC spectra in the brominated end group region of brominated atactic polypropylene (CD_2Cl_2, 600 MHz).

The presence of the primary alkyl bromide group was also confirmed on the basis of comparison with the spectrum of the model compound $Br(CH_2CHMe)_2(CH_2)_2Me$ (see Figure 2.3), for which two overlapping pairs of doublets of doublets attributable to the diastereotopic Br**H**$_2$CH(Me)- hydrogen atoms are also observed at 3.3-3.45 ppm. The greater complexity in the case of the spectrum of the polymeric sample reasonably results from the presence of various pentads terminated by *r* and *m* diads, a stereochemical feature which is not present in the model compound which contains only two chiral centers.

The primary alkyl bromide group results from the cleavage of the Zr-C bond after a primary (1,2) insertion and two overlapping pairs of multiplets (*m* and *r* terminal diads) of approximate 1:1 ratio for this group in the brominated polypropylene are consistent with an atactic polymer.

In order to assign the two terminal diads as *m* or *r*, a propylene polymerization in the presence of *rac*-{C_2H_4(1-indenyl)$_2$}$ZrMe_2$/$B(C_6F_5)_3$[2b,c,4e] was carried out in

chlorobenzene and quenched with bromine as above. This catalytic system was chosen as it preferentially gives isotactic polypropylene[4e,20] and therefore, by quenching the propylene polymerization with bromine, a change in the relative intensities of the above mentioned pairs of resonances was expected to occur. On the basis of relative intensities in the ^{1}H NMR and ^{1}H-^{13}C HSQC spectra of the resulting polymer (Figure 2.8), the pair of peaks at 3.32 and 3.40 ppm (^{13}C resonance at 42.2 ppm) was assigned to the Br**H**$_2$CH(Me)- hydrogens next to an *r* terminal diad while the pair of peaks at 3.34 and 3.44 ppm (^{13}C resonance at 41.7 ppm) was assigned to the Br**H**$_2$CH(Me)- hydrogens next to an *m* terminal diad.

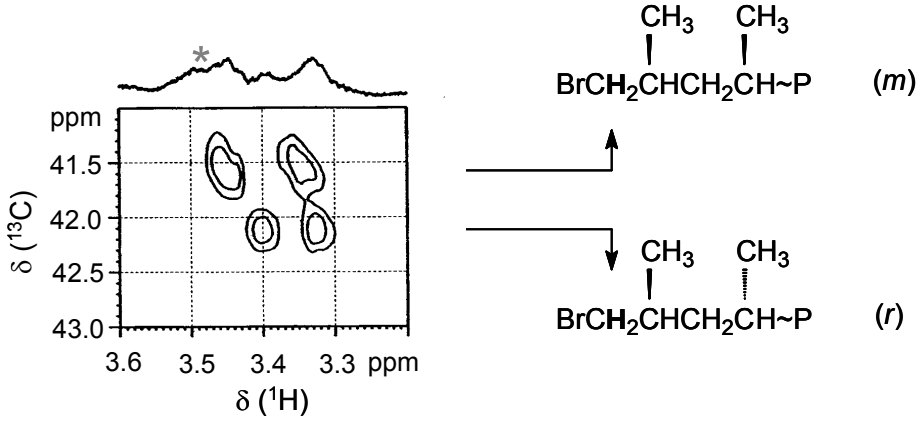

Figure 2.8. ^{1}H NMR and ^{1}H-^{13}C HSQC spectra in the brominated end group region of low isotactic polypropylene. The peak marked with asterisk (*) is due to traces of $BrCH_2CH_2Br$.

While the two achiral catalysts studied have generally been found to be highly regiospecific in favor of primary (1,2) insertion,[18a,21] occasional secondary (2,1) insertions[22] are also possible and would result in secondary Zr-polymeryl linkages.

Although the latter have long been considered to represent likely dormant species because of the probability of steric hindrance to further propylene coordination,[23] there is in fact no direct evidence of their presence in polymerization mixtures and their existence has only been implied from analyses of polymer microstructures[24] and end groups.[19,25] Interestingly, however, a recent study by Landis *et al.*[2d] showed that a secondary Zr-butyl compound was not particularly inert to insertion of propylene and thus the dormancy of secondary Zr-polymeryl species is currently under debate.

On addition of bromine to our propylene polymerization mixtures, any secondary Zr-polymeryl species present would cleave to give secondary alkyl bromide end groups; these are expected to give resonance at about 4.0-4.2 ppm on the basis of the ^{1}H NMR spectrum of 2-bromodecane as a model compound and literature data.[9] However, the polymers formed contained various types of olefinic (vinylidene and isobutenyl) groups (see Section 2.2.4) which on addition of bromine would also brominate to give the corresponding brominated products. In addition, as it will be shown in Section 2.2.5, different types Zr-allyl intermediates are also present in the polymerization mixture. Upon bromine quenching, the Zr-allyl linkages would also cleave to yield the corresponding alkyl tribromide products. Hence all of our ^{1}H NMR spectra exhibited a plethora of relatively intense resonances in the region 3.8-4.6 ppm (Figure 2.6), completely obscuring the 4.0-4.2 ppm region. No attempt to identify all of the resonances in the region 3.8-4.6 ppm was done. However, while an HSQC experiment with 2-bromodecane showed that the $CH_3C\mathbf{H}(Br)CH_2$- resonance at 4.16 ppm couples with the C-2 resonance of the $CH_3\mathbf{C}H(Br)$- unit at 52 ppm, similar experiments on several of the polymers obtained using $Cp_2ZrMe_2/B(C_6F_5)_3$ and $(indenyl)_2ZrMe_2/B(C_6F_5)_3$ revealed no

coupling of any proton resonances in the region 3.8-4.5 ppm with carbon resonances in the region 46-55 ppm. Furthermore no 2-butenyl end groups, the products anticipated from β-H elimination after a secondary insertion,[19] were detected in the olefinic region of polymers when propylene polymerization was quenched with methanol. Thus for $Cp_2ZrMe_2/B(C_6F_5)_3$ and $(indenyl)_2ZrMe_2/B(C_6F_5)_3$, at least, we find no evidence for Zr-polymeryl products of secondary 2,1-insertion. These results are consistent with *in situ* $^1H\{^{13}C\}$ NMR experiments[2,3] in which the presence of only primary Zr-polymeryl and Zr-allyl polymeryl species have been detected.

In order to estimate the relative concentrations of the $Zr\text{-}CH_2CHMe\sim P$ groups present during propylene polymerization, the multiplet at 3.3-3.5 ppm was integrated relative to the peak of an added internal standard, 1,1,2,2-tetrachloroethane (5.91 ppm). Accordingly, with $Cp_2ZrMe_2/B(C_6F_5)_3$ as catalyst, the relative concentration of the primary Zr-polymeryl groups was found to be low, about 10%, and almost constant for polymerization times from 20 to 60 seconds. With $(indenyl)_2ZrMe_2/B(C_6F_5)_3$, on the other hand, a relatively high value of 84% was reached within 20 seconds, after which it decreased to much lower values for longer polymerization times (32% after 4 minutes, see Figure 2.9).

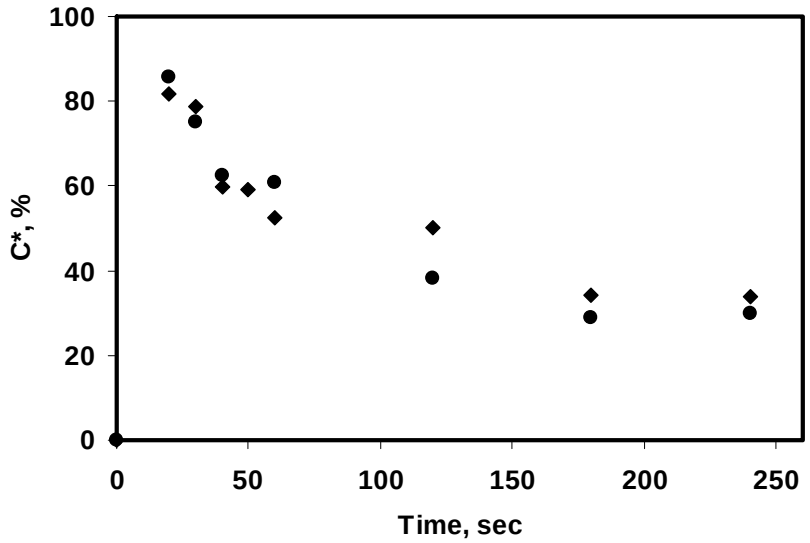

Figure 2.9. Variation of the relative concentrations of primary Zr-polymeryl groups with polymerization time (two runs).

The higher values with the $(indenyl)_2ZrMe_2/B(C_6F_5)_3$ than with the $Cp_2ZrMe_2/B(C_6F_5)_3$ catalyst system may be related to the faster initiation and higher polymerization activity of the former, which generally gave polymer yields several times greater than did the latter. Similar results have been reported elsewhere.[1a,26] Although propylene polymerization with the $Cp_2ZrMe_2/B(C_6F_5)_3$ and $(indenyl)_2ZrMe_2/B(C_6F_5)_3$ catalyst systems have been well investigated with respect to the polymerization mechanism, kinetics, end group analyses and catalyst activities,[1a,d,j,2a,13b,26,27] to our knowledge there are no reports on the concentration of active species during propylene polymerization with these particular systems and thus a direct comparison of our results is not possible at this time. However, our results are quite reproducible and are therefore reliable.

Somewhat similar values have, however, been reported for propylene polymerization by stereoselective catalysts. Specifically, Landis *et al*. used a quench methodology to obtain a value of 25% for propylene polymerization by *rac*-{C_2H_4(indenyl)$_2$}$ZrMe_2/B(C_6F_5)_3$ at 20°C,[2b] although much lower values were obtained by Chien *et al*. using *rac*-{C_2H_4(indenyl)$_2$}$ZrMe_2$ activated with $[Ph_3C][B(C_6F_5)_4]$ at 0°C.[4e] We were, in fact, unable to detect any $BrCH_2CHMe$~P end groups at all in reactions carried out at 0°C and lower, consistent with previous reports that Zr-polymeryl concentrations increase with increasing temperature.[4a,5b]

2.2.4. The Analysis of Unsaturation in Atactic Polypropylene Obtained from the (indenyl)$_2$ZrMe$_2$/B(C$_6$F$_5$)$_3$ catalyst system

Important mechanistic information about different events occurring at the metal site can also be obtained from the analysis of polymer chain unsaturation. Specifically, the olefinic groups present on the polymer chain give information about various reactions occurring at the transition metal center during the polymerization, which in turn provide information about potential Zr-polymeryl intermediates. Thus, in order to get more information about Zr-polymeryl intermediates present in the polymerization system, a series of propylene polymerizations as catalyzed by (indenyl)$_2ZrMe_2/B(C_6F_5)_3$ in chlorobenzene was performed and the polymerization reactions were terminated after a specific reaction time (20 sec – 2 min) by quenching with CH_3OH. The olefinic region of the ^{1}H NMR spectrum of an atactic polypropylene sample obtained after quenching the polymerization with CH_3OH is shown in Figure 2.10.

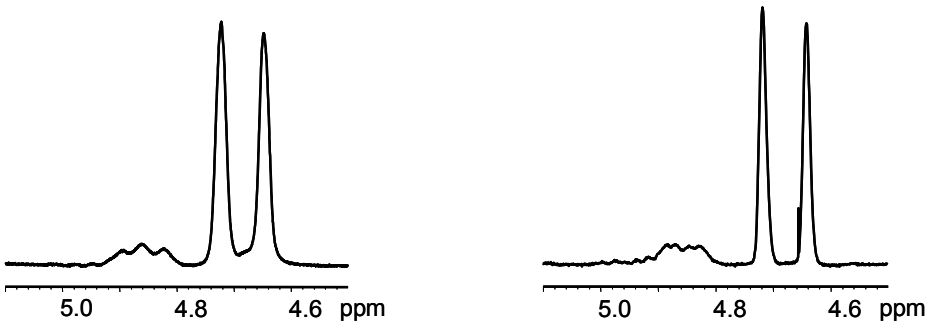

(a) (b)

Figure 2.10. ^{1}H NMR spectra (CD_2Cl_2, 25°C) in the olefinic region of atactic polypropylene obtained from (indenyl)$_2ZrMe_2/B(C_6F_5)_3$, (a) 300 MHz and (b) 500 MHz.

As can be seen from Figure 2.10, the ^{1}H NMR spectrum in the olefinic region of atactic polypropylene shows the presence of two strong resonances at 4.64 ppm (singlet) and 4.72 ppm (singlet) which can be easily attributed to vinylidene end group resonances.[19] Vinylidene end groups are the most common type of olefinic end groups in polypropylene[28] and they arise from β-hydrogen elimination of a Zr-polymeryl species after a primary (1,2) insertion.

For the vinylidene end groups, peak integration shows that the intensity of the lower field vinylidene resonance is higher than that of the higher field one. The increase in intensity of the lower field vinylidene resonance was proposed by Resconi *et al.*[19,29] to be the result of an overlap of the lower field terminal vinylidene resonance with another nearly symmetrical, internal vinylidene resonance of the type $^{i}Bu\text{-}C(=CH_2)CH_2CH(CH_3)CH_2P$.[19,29a] The nonequivalent intensities of the two vinylidene end group resonances in atactic polypropylene is noteworthy as this feature of the vinylidene groups is usually observed in isotactic polypropylenes obtained from

isospecific zirconocene.[19,29,30] The internal vinylidene group was proposed to arise via the intermediacy of a Zr-allyl intermediate as depicted in Scheme 2.4.[31]

Scheme 2.4. Formation of internal vinylidene groups on a polymer chain via a Zr-allyl intermediate.

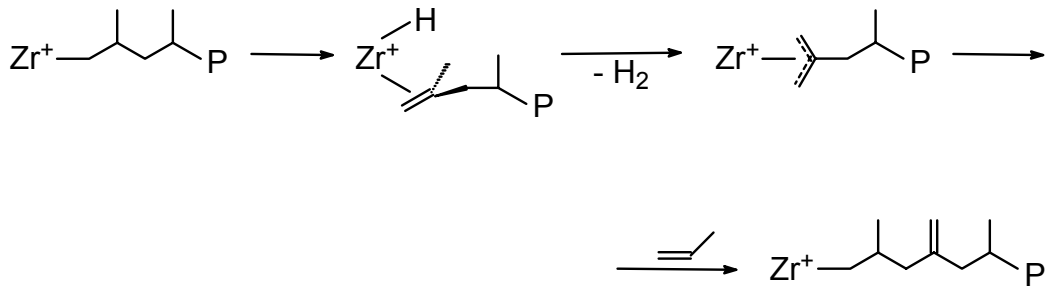

According to this scheme, β-hydrogen elimination of a primary (1,2) Zr-polymeryl species followed by allylic C-H activation of the coordinated vinylidene chain end at the methyl group and dissociation of molecular hydrogen yields a cationic Zr(η^3-$CH_2C(CH_2CH(Me)(P))CH_2$) species. The new cationic Zr-allyl species formed can further insert propylene[19] to give a polymer chain with an internal vinylidene group.[31a]

Figure 2.10 also shows the presence of isobutenyl end group resonances at 4.84 ppm (doublet) and 4.88 ppm (doublet).[19] There are several mechanisms proposed for formation of the isobutenyl end groups. The first one, presented in Scheme 2.5, involves β-hydrogen elimination of a primary Zr-polymeryl species followed by allylic C-H activation of the olefin chain end at the methylene group and dissociation of molecular hydrogen to form a cationic Zr(η^3-$CH_2C(Me)CHCH(Me)(P)$) species.

Scheme 2.5. Formation of isobutenyl groups on the polymer chain via a Zr-allyl intermediate.

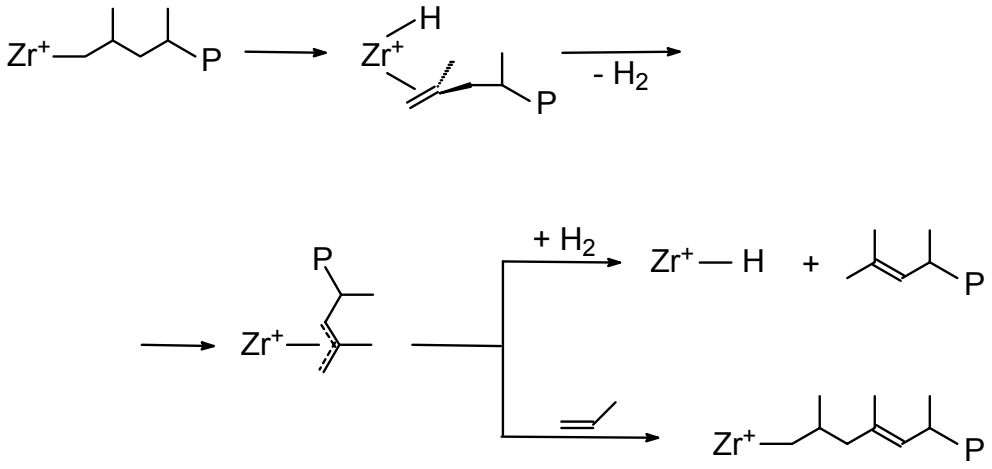

The dihydrogen molecule generated *in situ* in the C-H allylic activation process can then act as a chain transfer agent to release a polymer chain with an isobutenyl end group.[19] Alternatively, the cationic Zr-allyl species can further insert propylene to yield a polymer chain with an internal isobutenyl group.[19] The internal isobutenyl groups, if present, give rise to resonances in the same region of the ^{1}H NMR spectrum as the terminal isobutenyl groups[19] and therefore their presence on the polymer chain usually goes unnoticed.

A second mechanism for the formation of an isobutenyl end group was proposed by Resconi *et al.*[29a] and involves the intermediacy of a tertiary Zr-polymeryl species as shown in Scheme 2.6.[29a,31a]

Scheme 2.6. Formation of isobutenyl end groups via a tertiary Zr-polymeryl intermediate.

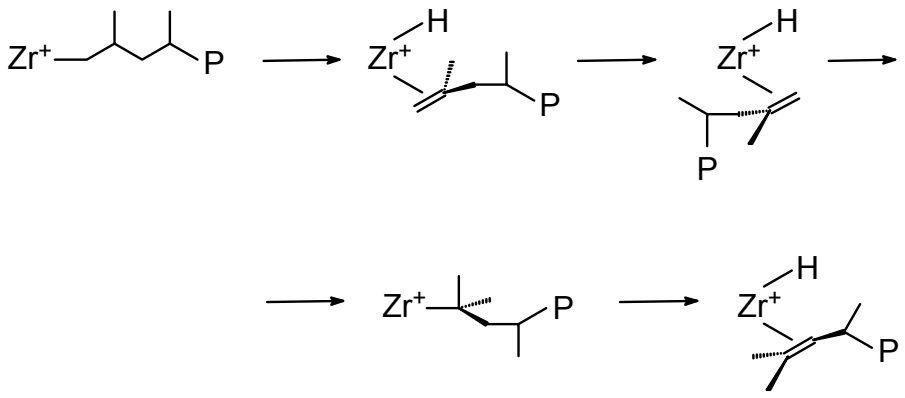

According to this mechanism the coordinated vinylidene fragment, obtained following the β-hydrogen elimination of a primary Zr-polymeryl species, rotates and then reinserts into the Zr-H bond in a secondary (2,1) fashion to give the Zr-$C(Me)_2CH_2CH(Me)$P species. This species can further undergo β-hydrogen elimination from the methylene group to yield a polymer chain with an isobutenyl end group. The tertiary Zr-polymeryl species were proposed to represent key intermediates for the epimerization/isomerization of Zr-polymeryl intermediates.[2b,28a,29a] However, *in situ* experiments conducted by Gou *et al.*[28b] showed that cationic hydride $[(C_5H_4Me)_2Zr(H)(THF)][BPh_4]$ complex undergoes only primary (1,2) insertion of isobutylene and in this case it seems unlikely that a secondary (2,1) insertion of an α,α-disubstituted olefinic end group of a polymer chain into a Zr-H bond with formation of a Zr-$C(Me)_2$-polymeryl species may occur.[29b]

Another mechanism which may account for isobutenyl end group formation is acidic isomerization of a vinylidene end group (Scheme 2.7).[19]

Scheme 2.7. Acidic isomerization of the vinylidene end group.

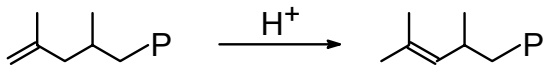

In the case of propylene polymerization by $(indenyl)_2ZrMe_2/B(C_6F_5)_3$ in chlorobenzene, the vinylidene and isobutenyl end group resonances are present in ^1H NMR spectra of both crude and pure atactic polypropylene and the ratio of their relative intensities does not change either after purification or in time. This indicates that the isobutenyl end group is not the result of acidic isomerization during the NMR analysis or polymer work-up but it was formed during the polymerization reaction.[19]

A summary of the unsaturated groups present in the atactic polypropylene obtained from the $(indenyl)_2ZrMe_2/B(C_6F_5)_3$ catalytic system in chlorobenzene is presented in Scheme 2.8.

Scheme 2.8. Olefinic groups present in atactic polypropylene obtained from the $(indenyl)_2ZrMe_2/B(C_6F_5)_3$ catalytic system in chlorobenzene.

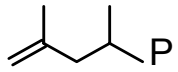

vinylidene end group

(80 – 87%)

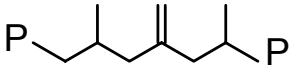

internal vinylidene group

(0.5 – 5%)

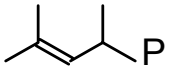

isobutenyl end group

(10 – 18%)

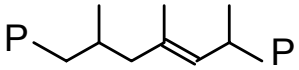

internal isobutenyl group (possibly)

As discussed above, the presence of these olefinic groups in atactic polypropylene implies that aside from the primary (1,2) Zr-polymeryl species, which were already detected in the polymerization mixture by the use of bromine quenching method, cationic $Zr(\eta^3\text{-}CH_2C(CH_2CH(Me)(P))CH_2)$ and $Zr(\eta^3\text{-}CH_2C(Me)CHCH(Me)(P))$ complexes are also formed during the polymerization.

2.2.5. The presence of Zr-allyl Intermediates and Deactivation of the Catalyst

Of particular interest is the implication that the cationic Zr-allyl polymeryl intermediates form during the propylene polymerization by $(indenyl)_2ZrMe_2/B(C_6F_5)_3$ as these intermediates are considered to accumulate in the polymerization mixture as dormant species rather than to propagate and therefore to deactivate the catalyst. The

presence of Cp_2Zr^+-allyl oligomers was actually observed in *in situ* propylene polymerization by $Cp_2ZrMe_2/B(C_6F_5)_3$ and $Cp_2ZrMe_2/[Ph_3C][B(C_6F_5)_4]$ catalysts, respectively, in chlorobenzene–d_5, as will be shown in Chapter 4. On quenching the polymerization reaction with bromine, any Zr-allyl intermediate present in the polymerization mixture would also cleave; the anticipated reaction products are dibromozirconocene and polymer chains containing alkyl tribromide end groups, as shown in Equations 2.11 and 2.12.

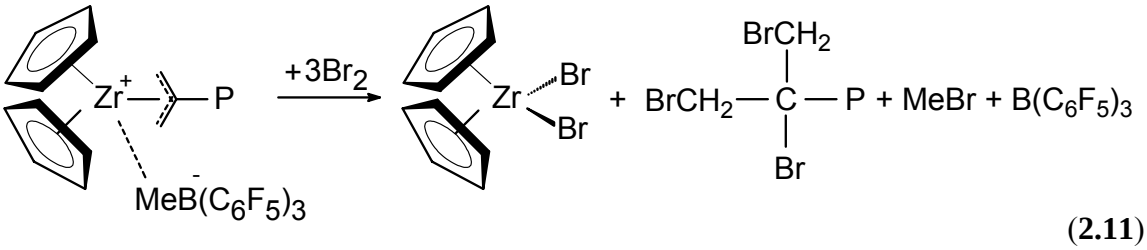

(**2.11**)

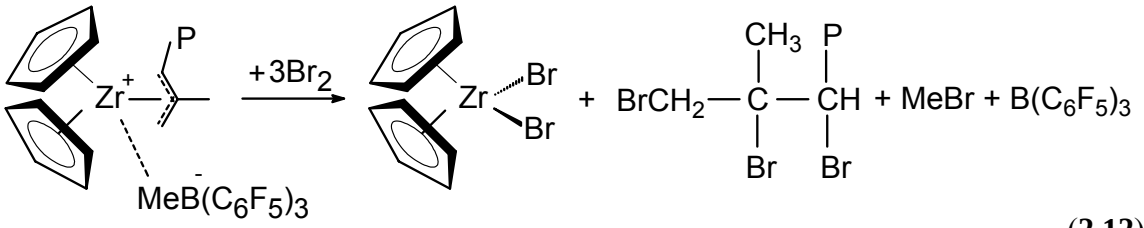

(**2.12**)

In order to get some insight on the potential brominated end groups which would arise from the reaction of Zr-allyl polymeryl intermediates with bromine, the cationic $Cp_2Zr^+(\eta^3\text{-}CH_2C(CH_2CHMe_2)CH_2)$ complex, obtained *in situ* from the reaction of $[Cp_2ZrMe][MeB(C_6F_5)_3]$ with 2,4-dimethyl-1-pentene at room temperature in chlorobenzene-d_5 in addition to methane, was reacted with bromine as shown in Equation

2.11. The expected reaction products, $BrCH_2C(Br)(CH_2Br)CH_2CHMe_2$ and Cp_2ZrBr_2, were identified by NMR spectroscopy. The ^1H NMR spectrum of the *in situ* bromination reaction products is shown in Figure 2.11.

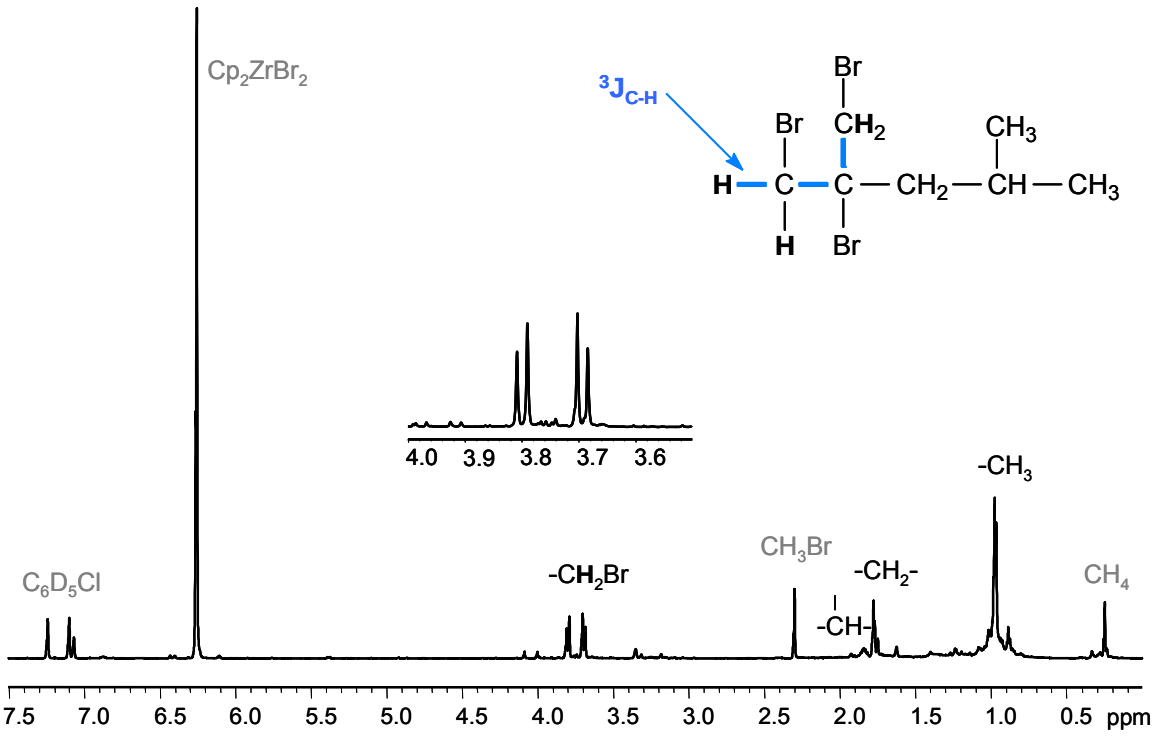

Figure 2.11. ^1H NMR spectrum (C_6D_5Cl, 600 MHz) of the reaction products obtained from *in situ* reaction of $Cp_2Zr^+(\eta^3\text{-}CH_2C(CH_2CHMe_2)CH_2)$ with bromine at room temperature.

In this spectrum, the two diastereotopic hydrogen resonances of the two -C**H**$_2$Br groups of BrC**H**$_2$C(Br)(C**H**$_2$Br)CH_2CHMe_2 are present at 3.7 ppm (doublet) and 3.8 ppm (doublet), while the methylene, methyne and methyl group resonances appear at 1.78 ppm (doublet), 1.84 ppm (multiplet), and 0.97 ppm (doublet), respectively. Also present in the ^1H NMR spectrum of the *in situ* bromination reaction product mixture are the

resonances of the **Cp**$_2$ZrBr$_2$ (6.25 ppm, singlet), C**H**$_3$Br (2.30 ppm, singlet) and C**H**$_4$ (0.25 ppm, singlet) byproducts. Traces of brominated 2,4-Me$_2$-1-pentene and decomposition products are also observed.

Confirmation of the brominated end group assignments of BrCH$_2$C(Br)(CH$_2$Br)CH$_2$CHMe$_2$ comes from correlation spectroscopy. Thus, the two hydrogen resonances of the terminal -C**H**$_2$Br group at 3.7 ppm (doublet) and 3.8 ppm (doublet) are coupled to each other as indicated by a COSY experiment and by the AB spin system pattern and they are attached to a carbon which gives rise to a resonance at 40.1 ppm as shown by the ^{1}H-^{13}C HSQC spectrum. The long-range ^{1}H–^{13}C correlation spectrum (HMBC) shows that the two C**H**$_2$Br resonances at 3.7 and 3.8 ppm are correlated with a carbon resonance at 40.1 ppm, which indicates that there are two equivalent terminal CH$_2$Br groups which are correlated to each other by long (^{3}J) carbon-proton correlations (see Figure 2.11). Also, the two C**H**$_2$Br resonances at 3.7 and 3.8 ppm are correlated with a carbon resonance at 67.7 ppm which was assigned to the (BrCH$_2$)$_2$**C**(Br)(alkyl) carbon.

As it can be seen from Figure 2.11, the Cp$_2$Zr$^+$(η^3-CH$_2$C(CH$_2$CHMe$_2$)CH$_2$) complex reacts cleanly with bromine to produce well identifiable tribromide alkyl species of type **(BrCH$_2$)$_2$C(Br)**(CH$_2$CHMe$_2$). Likewise, the cleavage of a Cp$_2$Zr$^+$(η^3-CH$_2$C(Me)CH~P) complex by bromine is expected to result in a polymer chain containing a **BrCH$_2$C(Br)**(Me)**CH(Br)-** end group. However, the bromination of the vinylidene and isobutenyl groups of the polymer chains would also produce polymers containing a **BrCH$_2$C(Br)**(Me)- terminal moiety and/or –**C(Br)**(Me)**CH(Br)-** moiety, respectively. Due to the close similarity of the various brominated groups of the polymer

chains obtained following the bromination of the Zr-allyl polymeryl intermediates and the bromination of the olefinic groups present on polymer chains, respectively, it seems reasonable to assume that the various Br-C**H**$_2$ and Br-C**H** hydrogens, respectively, of the brominated groups would give rise to (very) close chemical shift resonances in the ^{1}H NMR spectra of the brominated polymers. Therefore for polymerizations where the chain transfer reactions by β-elimination are predominant (i.e. the presence of olefinic groups on polymer chains are predominant), the quenching of the polymerization by bromine cannot actually provide information about the presence of Zr-allyl polymeryl intermediates in the polymerization mixture.

In order to ascertain whether or not the Zr-allyl polymeryl intermediates are present in the polymerization system under study, an alternative method, quenching the polymerization with CD_3OD, was used.[7] The deuterium labeling method is expected to give rise to distinctively different deuterium labeling patterns on the polymer chain depending on the type of Zr-polymeryl bond to be cleaved, as shown in Scheme 2.9.[7,15]

Scheme 2.9. Structures of deuterated end groups expected on the polymer chain as a result of the cleavage by CD_3OD of a (a) primary (1,2) Zr-polymeryl bond, (b) secondary (2,1) Zr-polymeryl bond, and (c-e) Zr-allyl bond.

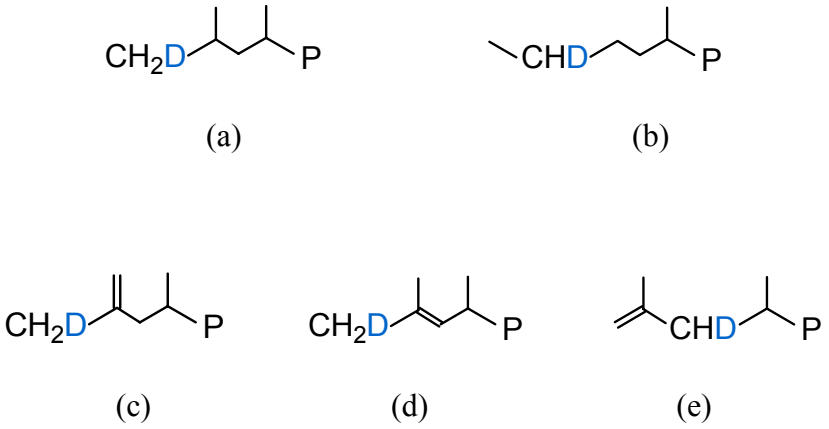

(a) (b) (c) (d) (e)

Thus, in a separate experiment, propylene polymerization was performed at room temperature, under 1 atmosphere of propylene, in the presence of $(indenyl)_2ZrMe_2/B(C_6F_5)_3$ in chlorobenzene. After 1 min polymerization time, the propylene feed was interrupted and part of the polymerization reaction mixture was transferred into another flask and quenched with CD_3OD under argon while the rest of the polymerization reaction mixture was quenched with a solution of bromine in CH_2Cl_2. The polymerization mixtures were stirred for 10 more min, and then the solvent was removed *in vacuo*. The polymerization products were extracted with hexane, purified by passage through a short silica column, and analyzed by ^1H and ^2H NMR spectrocopy.

The ^1H NMR spectrum of atactic polypropylene obtained following bromine quenching showed the presence of Br-C**H**$_2$CH(Me)- end groups (3.3-3.5 ppm) arising from the cleavage of the primary Zr-CH_2CH(Me)~polymeryl linkages by bromine, as

expected. Likewise, the ^{1}H NMR spectrum of atactic polypropylene obtained following the CD_3OD quenching showed the presence of vinylidene end groups (major) as well as internal vinylidene and isobutenyl groups (minor) (see Appendix A).

The ^{2}H NMR spectrum of the atactic polypropylene obtained after quenching the polymerization with CD_3OD is displayed in Figure 2.12(a).

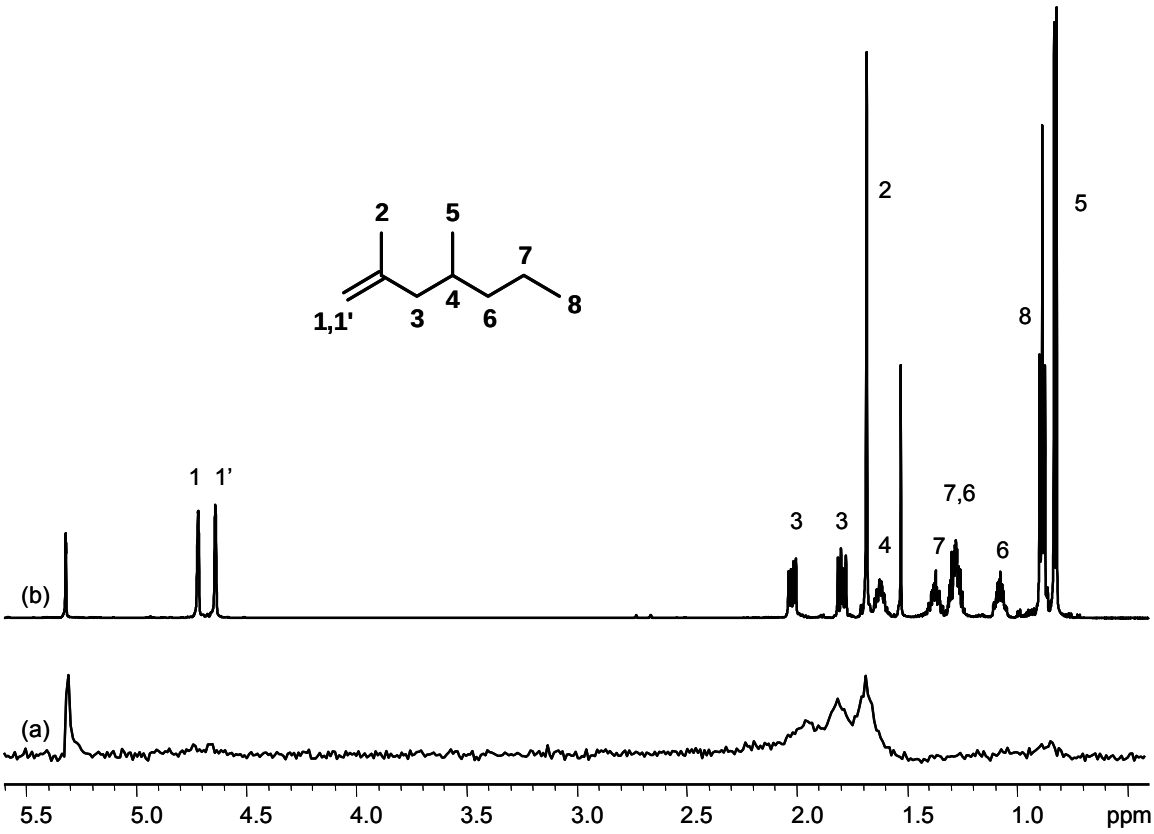

Figure 2.12. (a) ^{2}H NMR spectrum (600 MHz, 25°C, CH_2Cl_2) of atactic polypropylene obtained from (indenyl)$_2ZrMe_2/B(C_6F_5)_3$ in chlorobenzene after CD_3OD quenching and (b) ^{1}H NMR spectrum (600 MHz, 25°C, CD_2Cl_2) of 2,4-dimethyl-1-heptene.

As can be seen from Figure 2.12(a), the aliphatic region of the ^{2}H NMR spectrum of atactic polypropylene obtained after CD_3OD quenching displays three strong broad resonances between 1.5 and 2.1 ppm and a much weaker broad signal at about 0.9 ppm. Based on the ^{1}H NMR spectrum of 2,4-dimethyl-1-heptene as a model compound (Figure 2.12(b)), it seems clear that ^{2}H enrichment occurs almost exclusively at the methyl and methylene groups next to a double bond (1.65–2.1 ppm) (structures (c)–(e) in Scheme 2.9) and to a lesser extent at a terminal methyl (~0.9 ppm) or methylene group (1.2–1.4 ppm) (structures (a) and (b) in Scheme 2.9, respectively).

The presence of deuterium in the methyl and methylene groups next to a double bond is consistent with the cleavage of a Zr-allyl bond by CD_3OD and the high intensity of these resonances as compared with the resonance of the terminal deuterated methyl group at ~0.9 ppm, which would arise from the cleavage of a Zr-polymeryl species following a primary (1,2) insertion, reveals that actually most of the catalyst at the time of quench was found as Zr-allyl polymeryls. Moreover, the lack of ^{2}H enrichment at ~1.2-1.4 ppm corresponding to a deuterated methylene (-CHD-) group arising from the cleavage of a Zr-polymeryl species following a secondary (2,1) insertion, implies that formation of secondary Zr-CH(Me)CH_2~polymeryl intermediates as the main deactivation process in this system can be ruled out.

The much higher relative intensity of the CH_2**D**- and CH**D**-vinylidene end group resonances in the ^{2}H NMR spectrum of the CD_3OD quenched atactic polypropylene (Figure 2.12(a)) as compared with the weak relative intensity of the internal vinylidene group resonances in the ^{1}H NMR spectrum of the same polymer (see Appendix A) suggests that once formed, the Zr-allyl intermediates are slow to propagate and as a result

they accumulate in the polymerization system as dormant species. This is consistent with the results obtained by Landis and Christianson[3b] for 1-^{13}C-1-hexene polymerizations by the [(*rac*-$Me_2Si(indenyl)_2Zr(CH_2SiMe_3)$][$B(C_6F_5)_4$] ion pair in toluene-$d_8$. Also, Heijden *et al*.[32] found that the [$(C_5Me_5)(t\text{-}BuC_5H_4)Zr(\eta^3\text{-}CH_2C(Me)CH_2)$][$MeB(C_6F_5)_3$] complex does not react with α-olefins and therefore formation of Zr-allyl species during the polymerization can be considered an important pathway for deactivation of the catalyst.

2.3. Summary

This chapter presents an investigation into the nature and relative concentrations of Zr-polymeryl intermediates present in solution during ethylene polymerization by Cp_2ZrMe_2 catalyst, propylene polymerization by Cp_2ZrMe_2, $(indenyl)_2ZrMe_2$ and propylene polymerization by *rac*-{$C_2H_4(1\text{-indenyl})_2$}$ZrMe_2$ catalysts activated with $B(C_6F_5)_3$. Experimentation used to gain information about Zr-polymeryl intermediates present during polymerization involved a combination of various quenching methods followed by an analysis of the resulting polymers by NMR spectroscopy.

In the first part of this chapter, a simple, rapid procedure for the identification of Zr-polymeryl intermediates present during olefin polymerization by zirconocene catalysts has been investigated. This method consists of quenching of a polymerization reaction with bromine. By addition of bromine to a polymerization reaction mixture, this would react with all Zr-polymeryl intermediates present in the system at the time of quench to form bromine terminated polymers. The brominated end groups of the polymer chains can be identified as primary or secondary on the basis of their chemical shifts, and quantified by using ^{1}H NMR spectroscopy.

Termination with bromine of ethylene polymerization by $Cp_2ZrMe_2/B(C_6F_5)_3$, in chlorobenzene, resulted in polymers with primary alkyl bromide ($BrCH_2$-) end groups. The presence of primary alkyl bromide end groups in polyethylene is an indication of the presence of Cp_2Zr^+-CH_2~polymeryl intermediates in the polymerization mixture. The relative concentration of Zr-CH_2~polymeryl intermediates was found to be low, in the range of 4-10% of the catalyst present; no correlation between the concentration of Zr-CH_2~polymeryl intermediates and polymerization time has been found in this case.

Similarly, termination with bromine of propylene polymerization by Cp_2ZrMe_2, $(indenyl)_2ZrMe_2$, and *rac*-$\{C_2H_4(1\text{-indenyl})_2\}ZrMe_2$ catalysts activated with $B(C_6F_5)_3$, in chlorobenzene, all resulted in polymers with primary alkyl bromide ($BrCH_2CH(Me)$-) end groups. The presence of primary alkyl bromide end groups in polypropylene is an indication of the presence of Zr-$CH_2CH(Me)$~polymeryl intermediates in the polymerization mixture. In the case of propylene polymerization by $Cp_2ZrMe_2/B(C_6F_5)_3$, the relative concentration of Zr-$CH_2CH(Me)$~polymeryl intermediates was found to be low, around 10%, and almost constant for polymerization times from 20 to 60 sec. With $(indenyl)_2ZrMe_2/B(C_6F_5)_3$, on the other hand, a relatively high value of 84% was reached within 20 sec, after which it decreased to much lower values for longer polymerization times (32% after 4 min). The higher values with the $(indenyl)_2ZrMe_2/B(C_6F_5)_3$ than with the $Cp_2ZrMe_2/B(C_6F_5)_3$ catalyst system may be related to the faster initiation and higher polymerization activity of the former, which generally gave polymer yields several times greater than did the latter. These results are consistent with literature precedents.

In the case of propylene polymerization, secondary (2,1) insertions of propylene into Zr-polymeryl bonds are also possible. These would result in Zr-

$CH(Me)CH_2$~polymeryl intermediates, which, upon bromine quenching, would cleave to yield polymers with secondary alkyl bromide ($BrCH(Me)CH_2$-) end groups. No secondary alkyl bromide end groups were detected in polypropylenes obtained from either $Cp_2ZrMe_2/B(C_6F_5)_3$ or $(indenyl)_2ZrMe_2/B(C_6F_5)_3$ catalyst in chlorobenzene. Thus, at least for these catalytic systems, we find no evidence for Zr-polymeryl products of secondary insertion.

Further information about intermediates present during propylene polymerization was obtained from the analysis of olefinic end groups of atactic polypropylene obtained from $(indenyl)_2ZrMe_2/B(C_6F_5)_3$ after quenching the polymerization with CH_3OH. In this regard, the presence of internal vinylidene and isobutenyl end groups on the polymer chains, in addition to the usual vinylidene end groups, suggests that aside from the primary Zr-$CH_2CH(Me)$~polymeryl intermediates, also detected using the bromine quenching method, Zr-allyl polymeryl intermediates are also formed during the polymerization. A drawback of the bromine quenching method is that it cannot provide information about the presence of Zr-allyl polymeryl intermediates in the polymerization systems where a high degree of chain transfer reactions via β-elimination occur, due to the close structural similarity of the brominated polymer chain ends resulting from bromination of both Zr-allyl polymeryl intermediates and the olefinic groups present on the polymer chains.

Experimental information on the presence of Zr-allyl polymeryl species during the polymerization was obtained, however, from the quenching of the polymerization reaction with CD_3OD. The results indicated that, in the case of propylene polymerization

by (indenyl)$_2$ZrMe$_2$/B(C$_6$F$_5$)$_3$, a significant fraction of the catalyst was found as Zr-allyl polymeryl intermediates at the time of quenching.

2.4. Experimental Section

2.4.1. General Considerations

All chemicals were purchased from Aldrich unless stated otherwise. *rac*-C$_2$H$_4$(1-indenyl)$_2$ZrCl$_2$, (indenyl)$_2$ZrCl$_2$, Cp$_2$ZrCl$_2$, Cp$_2$Zr(Cl)(H) were purchased from Strem. 2,4-Me$_2$-1-Pentene and 2,4-Me$_2$-1-heptene were purchased from ChemSampCo. Anhydrous diethyl ether, dichloromethane, hexane and toluene were purchased from Aldrich in 18L reservoirs packaged under argon and passed through a single column of activated alumina prior to use. Chlorobenzene was dried by distillation, under argon, from calcium hydride prior to use. Deuterated solvents were obtained from Cambridge Isotope Laboratories (>99% atom %D). Dichloromethane-d$_2$, toluene-d$_8$, chlorobenzene-d$_5$ and benzene-d$_6$ were dried over CaH$_2$ or activated alumina, stored over molecular sieves and handled in a glove box. CD$_3$OD was used as received. Polymerization grade ethylene (99+% purity, Air Products) and propylene (99.5wt% purity, liquid phase, Praxair), were dried by passage through a column of activated 4 Å molecular sieves prior to use. Syntheses were carried out under purified argon using standard Schlenk line and glove box techniques.

NMR spectra were run on Bruker AV 300, 400 or 600 spectrometers, chemical shifts being referenced using the residual proton signals of the deuterated solvents. ^{1}H NMR spectra were acquired with a 45 degree pulse and 1 sec delay between pulses; 16 transients were stored for each spectrum. For the determination of the concentration of

active species, the ^{1}H NMR spectra were run at room temperature on a 400 MHz spectrometer; 32 transients were collected for each spectrum with a 40 sec delay between 45 degree pulses. ^{1}H-^{13}C HSQC spectra were collected on a 600 MHz spectrometer using Echo/Antiecho-TPPI gradient selection with decoupling during acquisition using shaped pulses for all 180 degree pulses on f2-channel. The HSQC acquisition parameters were: a 0.1705 sec acquisition time, a 10 ppm spectral window in f2, a 165.6 ppm spectral window in f1 and a 1 sec relaxation delay. The APT-^{13}C NMR spectra were run on a 400 MHz spectrometer at 120°C. The acquisition parameters were: a 0.54 sec acquisition time, a 301 ppm spectral window, and a 4 sec relaxation delay. ^{2}H NMR spectra were acquired on a 600 MHz spectrometer with a 1.111 sec acquisition time, a 0.5 sec delay between pulses, a 2 Hz line broadening and 1400-2050 transients.

Differential scanning calorimetry analyses were conducted on a Perkin-Elmer DSC-7 instrument at a heating rate of 5 °C/min. Samples were heated to 160 ºC, cooled to 30 ºC, and then a second scan was recorded.

2.4.2. Synthesis of Dimethylzirconocene

Dimethylzirconocene was prepared by a procedure similar to that described in the literature.[12a, 12g] Methyllithium (9 mL, 1.4M in diethyl ether) was added dropwise over a period of 45 min to a stirring suspension of zirconocene dichloride (1.75 g, 6 mmol) in 20 mL of dry diethyl ether under argon at -20°C and the reaction mixture was allowed to stir at this temperature for an additional 30 min. The reaction mixture was then allowed to warm at room temperature and the solvent was removed under reduced pressure. The residue was extracted with hexane, filtered, the solvent was evaporated *in vacuo* and the

product was purified by sublimation at 70°C. Alternatively, the product was purified by recrystallization from hexane. Dimethyl zirconocene was obtained as white powder in a yield of 60.4%.

^{1}H NMR (300 MHz, CD_2Cl_2): δ 6.1 (s, 10H, Cp), -0.41 (s, 6H, Me) ppm. ^{1}H NMR (400 MHz, $C_6D_5CD_3$): δ 5.7 (s, 10H, Cp), -0.21 (s, 6H, Me) ppm.

2.4.3. Synthesis of Bis(π-indenyl)dimethylzirconium

Bis(π-indenyl)dimethylzirconium was prepared by using the same procedure as Samuel and Rausch.[12a] Methyllithium (1.6 mL, 1.6M in diethyl ether) was added dropwise over a period of 15 min to a stirring suspension of bis(π-indenyl) zirconium dichloride (0.49 g, 1.25 mmol) in 10 mL of dry diethyl ether under argon at -20°C. The reaction mixture was allowed to stir at this temperature for an additional 30 min, then the reaction mixture was warmed at room temperature and stirring was continued for 3 more hours. The solvent was removed under reduced pressure and the residue was extracted with dichloromethane and filtered. The volatiles were removed under vacuo and the bis(π-indenyl)dimethylzirconium was obtained as brown crystals in a yield of 40.3%.

^{1}H NMR (300 MHz, CD_2Cl_2): δ -1.19 (s, 6H, Me), 5.98 (t, 2H, $^3J_{HH}$ = 3.3 Hz, Cp), 6.1 (d, 4H, $^3J_{HH}$ = 3.3 Hz, Cp), 7.11 (m, 4H, Ar), 7.42 (m, 4H, Ar) ppm. ^{1}H NMR (300 MHz, $C_6D_5CD_3$): δ -0.87 (s, 6H, Me), 5.6 (t, 2H, Cp), 5.76 (d, 4H, Cp), 6.86 (m, 4H, Ar), 7.17 (m, 4H, Ar) ppm. ^{1}H NMR (400 MHz, C_6D_5Cl): δ -0.81 (s, 6H, Me), 5.8 (t, 2H, Cp), 6.03 (d, 4H, Cp), 7.07 (m, 4H, Ar), 7.4 (m, 4H, Ar) ppm.

2.4.4. Synthesis of *rac*-ethylenebis(1-indenyl)dimethylzirconium

rac-ethylenebis(1-indenyl)dimethylzirconium was prepared by a procedure similar to that described in literature.[12d, 12h] Methyllithium (3.5 mL, 1.6 M in diethyl ether) was added dropwise to a stirring suspension of *rac*-$C_2H_4(1\text{-indenyl})_2ZrCl_2$ (1.05 g, 2.5 mmol) in 35 mL of dry diethyl ether at -30°C. The reaction mixture was stirred under argon at -30°C for an additional 30 min and then at room temperature for a further 3 hours after which the solvent was removed under reduced pressure leaving an orange-brown solid. The solid was extracted with dry toluene, the resulting solution was filtered, concentrated under reduced pressure, and cooled to -20°C to allow for crystallization. The solvent was transferred out and the solid was dried under *vacuo*. *rac*-$C_2H_4(1\text{-indenyl})_2ZrMe_2$ was obtained as light yellow crystals in a yield of 35%.

^{1}H NMR (400 MHz, C_6D_6): δ -0.96 (s, 6H, Me), 2.6 – 2.86 (m, 4H, C_2H_4), 5.64 (d, $^3J_{HH}$ = 3.1 Hz, 2H, Cp), 6.42 (d, $^3J_{HH}$ = 3.1 Hz, 2H, Cp), 6.8 – 4.4 (m, 8H, Ar) ppm.

2.4.5. Synthesis of Tris(pentafluorophenyl)boron

Tris(pentafluorophenyl)boron was prepared by a modified procedure of Massey and Park.[12f] A solution of butyllithium (33 mL, 53 mmol, 1.6M solution in hexane) was added dropwise over 3 hours under argon to a stirring solution of bromopentafluorobenzene (6 mL, 48.1 mmol) in 300 mL dry hexane at -78°C under stirring. The resulting white suspension was stirred at -78°C for an additional 3 hours when boron trichloride (16 mL, 16 mmol, 1M solution in hexane) was added all at once and the stirring was continued for another hour. After warming at room temperature, the reaction mixture was filtered to

remove LiCl and the solvent was removed under reduced pressure. Tris(pentafluorophenyl)boron was obtained as white crystals in a yield of 25%.

^{19}F NMR (400 MHz, CD_2Cl_2): δ -128 (br s, 6F, *o*-F), -145 (t, 3F, *p*-F), -161 (m, 6F, *m*-F) ppm. ^{19}F NMR (CD_2Cl_2, from literature[12i]): δ -128 (br s, 6F, *o*-F), -144 (t, 3F, *p*-F), -161 (m, 6F, *m*-F) ppm.

2.4.6. Ethylene Polymerization by $[Cp_2ZrMe][Me(B(C_6F_5)_3]$

a) In a typical ethylene polymerization, a solution of $B(C_6F_5)_3$ (0.11 g, 0.22 mmol) in 2 mL chlorobenzene was injected into a polymerization flask containing a solution of Cp_2ZrMe_2 (0.05 g, 0.2 mmol) in 8 mL chlorobenzene saturated with ethylene at atmospheric pressure under stirring. The polymerizations were started at room temperature; on the addition of the $B(C_6F_5)_3$, the reaction mixture became yellow and then cloudy as the polymerization mixture warmed up and the polyethylene began to precipitate. The reactions were run at constant ethylene pressure (1 atm) for 10-60 sec, and then the ethylene flow was stopped and the polymerization was quenched with a solution (0.4M) of bromine in dry CH_2Cl_2 or chlorobenzene. The reaction mixture was allowed to stir for 30 more min and then polyethylene was precipitated into methanol, filtered and dried. The polyethylene was purified by dissolution in hot chlorobenzene followed by precipitation with methanol, filtration and drying as above.

b) A solution of $B(C_6F_5)_3$ (0.11 g, 0.22 mmol) in 2 mL chlorobenzene was injected into a polymerization flask containing a solution of Cp_2ZrMe_2 (0.05 g, 0.2 mmol) in 8 mL chlorobenzene saturated with ethylene at atmospheric pressure under stirring. The

polymerizations were started at room temperature; on the addition of the $B(C_6F_5)_3$, the reaction mixture became yellow and then cloudy as the polymerization mixture warmed up and the polyethylene began to precipitate. The reactions were run at constant ethylene pressure (1 atm) for 1 min, and then the ethylene flow was stopped and the polymerization was quenched with methanol. The polyethylene was then precipitated in excess methanol, filtered, and dried. The crude polymer was purified by reprecipitation from hot chlorobenzene, as described above.

2.4.7. Propylene Polymerization by $[Cp_2ZrMe][Me(B(C_6F_5)_3]$

A solution of 0.11 g $B(C_6F_5)_3$ (0.22 mmol) in 2 mL chlorobenzene was injected into a polymerization flask containing a solution of 0.05 g Cp_2ZrMe_2 (0.2 mmol) in 8 mL chlorobenzene saturated with propylene at atmospheric pressure, under stirring. The polymerizations were generally started at room temperature; on the addition of the $B(C_6F_5)_3$, there was an immediate change in color (from yellow to brown) as the polymerization mixture warmed up. The polymerization was allowed to proceed at constant propylene pressure (1 atm) and, after a measured reaction time, the propylene feed was interrupted and polymerization was quenched with a solution of bromine in dry CH_2Cl_2. The polymerization mixture was stirred for 10 more min, and the solvent was removed *in vacuo*. The polymerization product was dissolved in hexane and purified by passage through a short silica column to give light yellow atactic polypropylene oligomers.

2.4.8. Propylene Polymerization by [(indenyl)$_2$ZrMe][Me(B(C_6F_5)$_3$]

a) In a typical propylene polymerization, a solution of B(C_6F_5)$_3$ (0.11 g, 0.22 mmol) in 2 mL chlorobenzene was injected into a polymerization flask containing a solution of (indenyl)$_2$ZrMe_2 (0.07 g, 0.2 mmol) in 8 mL chlorobenzene saturated with propylene at atmospheric pressure, under stirring. The polymerizations were generally started at room temperature; on the addition of the B(C_6F_5)$_3$, there was an immediate change in color (from yellow to dark red) as the polymerization mixture heated up. The polymerization was allowed to proceed at constant propylene pressure (1 atm) and, after a measured reaction time, the propylene feed was interrupted and polymerization was quenched with a solution of bromine in chlorobenzene. The polymerization mixture was stirred for 10 more minutes, and the solvent was removed *in vacuo*. The polymerization product was dissolved in hexane and purified by passage through a short silica column to give light yellow atactic polypropylene.

b) A solution of B(C_6F_5)$_3$ (0.11 g, 0.22 mmol) in 2 mL chlorobenzene was injected into a polymerization flask containing a solution of (indenyl)$_2$ZrMe_2 (0.07 g, 0.2 mmol) in 8 mL chlorobenzene saturated with propylene at atmospheric pressure, under stirring. The polymerizations were generally started at room temperature; on the addition of the B(C_6F_5)$_3$, there was an immediate change in color (from yellow to dark red) as the polymerization mixture heated up. The polymerization was allowed to proceed at constant propylene pressure (1 atm) and, after a measured reaction time, the propylene feed was interrupted and polymerization was quenched with methanol. The polymerization mixture was stirred for 10 more minutes, and the solvent was removed *in*

vacuo. The polymerization product was dissolved in hexane and purified by passage through a short silica column to give colorless atactic polypropylene.

c) A solution of $B(C_6F_5)_3$ (0.54 g, 1.06 mmol) in 6 mL chlorobenzene was injected into a polymerization flask containing a solution of $(indenyl)_2ZrMe_2$ (0.34 g, 0.97 mmol) in 18 mL chlorobenzene saturated with propylene at atmospheric pressure, under stirring. The polymerizations were generally started at room temperature; on the addition of the $B(C_6F_5)_3$, there was an immediate change in color (from yellow to dark red) as the polymerization mixture heated up. The polymerization was allowed to proceed at constant propylene pressure (1 atm) and, after 1 min reaction time, the propylene feed was interrupted; part of the polymerization reaction mixture (8 mL) was transferred into another flask via a syringe and quenched with CD_3OD under argon while the rest of the polymerization reaction mixture was quenched by addition of a solution of bromine in CH_2Cl_2. The polymerization mixtures were stirred for 10 more min, and then the solvent was removed *in vacuo*. The polymerization products were extracted with hexane and purified by passage through a short silica column.

2.4.9. Propylene Polymerization by [*rac*-{$C_2H_4(1\text{-indenyl})_2$}ZrMe][$MeB(C_6F_5)_3$]

A solution of $B(C_6F_5)_3$ (0.026 g, 0.05 mmol) in 1.1 mL chlorobenzene was injected into a polymerization flask containing a solution of *rac*-{$C_2H_4(1\text{-indenyl})_2$}$ZrMe_2$ (0.017 g, 0.046 mmol) in 49 mL chlorobenzene saturated with propylene at atmospheric pressure, under stirring. The polymerizations were generally started at room temperature; on the addition of the $B(C_6F_5)_3$, there was an immediate change in color (from yellow to dark

red) as the polymerization mixture heated up. The polymerization was allowed to proceed at constant propylene pressure (1 atm) and, after two minutes reaction time, the propylene feed was interrupted and polymerization was quenched with a solution of bromine in CH_2Cl_2. The polymerization mixture was stirred for 15 more minutes, when the polymer was precipitated with methanol, filtrated and dried. The crude polymer was purified by reprecipitation from hot chlorobenzene followed by precipitation with methanol, filtration and drying as above. Polymerization yields were 3 ± 0.05 g.

2.4.10. Synthesis of $BrCH_2CH(Me)(CH_2)_8CH_3$

$BrCH_2CH(Me)(CH_2)_8CH_3$ was prepared by a procedure adapted from Hart and Schwartz[8b] for similar compounds. 2-Me-1-undecene (0.22 mL, 1 mmol) was added under argon to a stirring suspension of $Cp_2Zr(Cl)H$ (0.31 g, 1.2 mmol) in 4.5 mL dry chlorobenzene at room temperature and the reaction mixture was allowed to stir under argon overnight. Bromine was slowly added to the reaction mixture until the color didn't fade, the reaction mixture was allowed to stir for an additional 30 min and the solvent was removed under reduced pressure. The $Cp_2Zr(Cl)(CH_2CH(Me)(CH_2)_8CH_3)$ intermediate could not be isolated.

^{1}H NMR (600 MHz, CD_2Cl_2): δ 0.88 (t, $^3J_{HH}$ = 6.8 Hz, 3H, CH_3), 1 (d, $^3J_{HH}$ = 6.8 Hz, 3H, CH_3), 1.15 - 1.5 (m, overlapped, 16H, CH_2), 1.78 (m, 1H, CH), 3.34 (dd, $^2J_{HH}$ = 9.6 Hz, $^3J_{HH}$ = 6.3 Hz, 1H, CH_2Br), 3.42 (dd, , $^2J_{HH}$ = 9.6 Hz, $^3J_{HH}$ = 4.8 Hz, 1H, CH_2Br) ppm.

^{1}H NMR (400 MHz, $CDCl_3$): δ 0.88 (t, $^3J_{HH}$ = 6.8 Hz, 3H, CH_3), 1 (d, $^3J_{HH}$ = 6.8 Hz, 3H, CH_3), 1.15 – 1.5 (m, overlapped, 16H, CH_2), 1.78 (m, 1H, CH), 3.32 (dd, $^2J_{HH}$ = 9.6 Hz, $^3J_{HH}$ = 6.3 Hz, 1H, CH_2Br), 3.4 (dd, $^2J_{HH}$ = 9.6 Hz, $^3J_{HH}$ = 4.8 Hz, 1H, CH_2Br) ppm.

2.4.11. Synthesis of $BrCH_2CH(Me)CH_2CH(Me)CH_2CH_2CH_3$

$BrCH_2CH(Me)CH_2CH(Me)CH_2CH_2CH_3$ was prepared by a procedure adapted from Hart and Schwartz[8b] for similar compounds. 2,4-dimethyl-1-heptene (0.28 mL, 1.68 mmol) was added under argon to a stirring suspension of $Cp_2Zr(Cl)H$ (0.54 g, 2.08 mmol) in 8 mL dry chlorobenzene at room temperature and stirring was continued overnight. Bromine was slowly added to the reaction mixture until the color didn't fade and the solvent was removed under reduced pressure. The $Cp_2Zr(Cl)(CH_2CH(Me)CH_2CH(Me)CH_2CH_2CH_3)$ intermediate could not be isolated.

a) Isomer 1:

^1H NMR (600 MHz, CD_2Cl_2): δ 3.44 and 3.34 (2dd, 2H, CH_2Br), 1.89 (m, 1H, $BrCH_2C\mathbf{H}(CH_3)$), 0.8 – 1.6 (alkyl peaks are overlapped) ppm. ^{13}C NMR (600 MHz, CD_2Cl_2): δ 41.7 (CH_2Br), 32.2 ($BrCH_2\mathbf{C}H(CH_3)$) ppm. ^1H NMR (600 MHz, $CDCl_3$): δ 3.4 and 3.3 (2dd, 2H, CH_2Br), 1.89 (m, 1H, $BrCH_2C\mathbf{H}(CH_3)$), 1.0 (d, 3H, $BrCH_2CH(C\mathbf{H}_3)$), 0.8 – 1.6 (alkyl peaks are overlapped) ppm. ^{13}C NMR (600 MHz, $CDCl_3$): δ 41.1 (CH_2Br), 32.5 ($BrCH_2\mathbf{C}H(CH_3)$) ppm.

b) Isomer 2:

^1H NMR (600 MHz, CD_2Cl_2): δ 3.41 and 3.33 (2dd, 2H, CH_2Br), 1.89 (m, 1H, $BrCH_2C\mathbf{H}(CH_3)$), 0.8 – 1.6 (alkyl peaks are overlapped) ppm. ^{13}C NMR (600 MHz, CD_2Cl_2): δ 42.2 (CH_2Br), 32.2 ($BrCH_2\mathbf{C}H(CH_3)$) ppm. ^1H NMR (600 MHz, $CDCl_3$): δ 3.37 and 3.29 (2dd, 2H, CH_2Br), 1.89 (m, 1H, $BrCH_2C\mathbf{H}(CH_3)$), 1.0 (d, 3H,

$BrCH_2CH(C\mathbf{H}_3)$), 0.8 – 1.6 (alkyl peaks are overlapped) ppm. ^{13}C NMR (600 MHz, $CDCl_3$): δ 41.6 (CH_2Br), 32.5 ($BrCH_2\mathbf{C}H(CH_3)$) ppm.

2.4.12. *In situ* Reaction between $[Cp_2Zr(\eta^3\text{-}CH_2C(CH_2CHMe_2)CH_2)][MeB(C_6F_5)_3]$ and bromine

A solution of Cp_2ZrMe_2 (10.1 mg, 40 μmole) in 0.5 mL of C_6D_5Cl was added to a solution of $B(C_6F_5)_3$ (22.5 mg, 1.1 equiv.) in 0.5 mL of C_6D_5Cl in a glovebox under nitrogen atmosphere, and the resulting yellow solution of the $[Cp_2ZrMe][MeB(C_6F_5)_3]$ ion pair was charged in an NMR tube. After the NMR tube was capped with a septum, 2,4-dimethyl-1-pentene (1 equiv.) was injected in the NMR tube via a microsyringe and the reaction was monitored by NMR spectroscopy at room temperature. After 12 hours, 4 equivalents of bromine (8 μL) was added to the above reaction mixture via a microsyringe and the reaction products were characterized by NMR spectroscopy.

The NMR spectroscopic data of $(BrCH_2)_2C(Br)(CH_2CHMe_2)$ are provided below.

^1H NMR (600 MHz, C_6D_5Cl): δ 0.97 (d, 6H, CH_3), 1.78 (d, 2H, CH_2), 1.84 (m, 1H, CH), 3.7 (d, $^2J_{HH}$ = 11 Hz, 2H, CH_2Br), 3.8 (d, $^2J_{HH}$ = 11 Hz, 2H, CH_2Br) ppm.

^{13}C NMR (600 MHz, C_6D_5Cl): δ 24.2 (CH_3), 25.9 (CH), 40.1 (CH_2Br), 46.7 (CH_2), 67.7 (C) ppm.

2.4.13. ^1H NMR Spectroscopic Data of $BrCH_2(CH_2)_9CH_2Br$

^1H NMR (400 MHz, CD_2Cl_2): δ 3.42 (t, 4H, CH_2), 1.85 (m, 4H, CH_2), 1.42 (m, 4H, CH_2), 1.29 (br. s, 10H, CH_2) ppm.

2.4.14. ^{1}H NMR Spectroscopic Data of $CH_3CH(Br)(CH_2)_7CH_3$

^{1}H NMR (600 MHz, CD_2Cl_2): δ 0.89 (t, 3H, CH_3), 1.2-1.6 (overlapped m, 12H, CH_2), 1.7 (d, 3H, CH_3), 1.76 (m, 1H, CH_2), 1.82 (m, 1H, CH_2), 4.15 (m, 1H, CHBr), 4.01 (m, CHBr in 3-Br-decane) ppm. ^{1}H NMR (600 MHz, C_6D_5Cl): δ 0.98 (t, 3H, CH_3), 1.16-1.43 (overlapped m, 12H, CH_2), 1.63 (d, 3H, CH_3), 1.65 (m, 1H, CH_2), 1.78 (m, 1H, CH_2), 4.01 (m, 1H, CHBr), 3.9 (m, CHBr in 3-Br-decane) ppm.

2.4.15. ^{1}H NMR Spectroscopic Data of $CH_2=C(Me)CH_2CH(Me)CH_2CH_2CH_3$

^{1}H NMR (600 MHz, CD_2Cl_2): δ 4.72 (s, 1H, $=CH_2$), 4.64 (s, 1H, $=CH_2$), 2.02 (dd, 1H, CH_2), 1.79 (dd, 1H, CH_2), 1.68 (s, 3H, CH_3), 1.62 (m, 1H, CH), 1.37 and 1.28 (2m, 2H, CH_2), 1.28 and 1.07 (2m, 2H, CH_2), 0.88 (t, 3H, CH_3), 0.82 (d, 3H, CH_3) ppm.

References

1. For useful reviews see: (a) Möhring, P. C.; Coville, N. J. *J. Organomet. Chem.* **1994**, *479*, 1. (b) Gupta, V. K.; Satish, S.; Bhardwaj, I. S. *J. Macromol. Sci., Rev. Macromol. Chem. Phys.* **1994**, *C34*, 439. (c) Brintzinger, H. H.; Fischer, D.; Mülhaupt, R.; Rieger, B. Waymouth, R. M. *Angew. Chem. Int. Ed.* **1995**, *34*, 1143. (d) Bochmann, M.. *J Chem. Soc., Dalton Trans*. **1996**, 255. (e) Kaminsky, W.; Arndt, M. *Adv. Polymer Sci*. **1997**, *127*, 143. (f) Scheirs J.; Kaminsky, W., editors, "Metallocene-based Polyolefins", John Wiley and Son, U.K, **1999**. (g) Coates, G. W. *Chem. Rev*. **2000**, *100*, 1223. (h) Resconi, L.; Cavallo, L.; Fait, A.; Piemontesi, F. *Chem. Rev*. **2000**, *100*, 1253. (i) Rappé,, A. K.; Skiff, W. M.; Casewit, C. J. *Chem. Rev*. **2000**, *100*, 1435. (j) Pédeutour, J.-N.; Radhakrishnan, K.; Cramail, H.; Deffieux, A. *Macromol. Rapid Commun.* **2001**, *22*, 1095.
2. (a) Tritto, I.; Donetti, R.; Sacchi, M. C.; Locatelli, P.; Zannoni, G. *Macromolecules* **1999**, *32*, 264. (b) Sillars, D. R.; Landis, C. R. *J. Am. Chem. Soc.* **2003**, *125*, 9894. (c) Landis, C. R.; Rosaaen, K. A.; Sillars, D. R. *J. Am. Chem. Soc*. **2003**, *125*, 1710. (d) Landis, C. R.; Sillars, D. R.; Batterton, J. M. *J. Am. Chem. Soc*. **2004**, *126*, 8890. (e) Baumann, R.; Schrock, R. R. *J. Organomet. Chem.* **1998**, *557*, 69. (f) Jayaratne, K. C.; Sita, L. R. *J. Am. Chem. Soc.* **2001**, *123*, 10754.
3. (a) Al-Humydi, A.; Garrison, J. C. ; Mohammed, M. ; Youngs, W. J.; Collins, S. *Polyhedron* **2005**, *24*, 1234. (b) Landis, C. R.; Christianson, M. D. *Proc. Natl. Acad. Sci. USA* **2006**, *103*, 15349
4. (a) Chien, J. C. W.; Wang, B.-P. *J. Polym. Sci., Part A.* **1989**, *27*, 1539. (b) Chien, J. C. W.; Wang, B.-P. *J. Polym. Sci., Part A.* **1990**, *28*, 15. (c) Chien, J. C. W.;

Sugimoto, R. *J. Polym. Sci., Part A.* **1991**, *29*, 459. (d) Chien, J. C. W.; Tsai, W.-M. *Macromol. Chem., Macromol. Symp.* **1993**, *66*, 141. (e) Chien, J. C. W.; Song, W.; Rausch, M. D. *Macromolecules* **1993**, *26*, 3239.

5. (a) Tait, P. J. T.; Booth, B. L.; Jejelowo, M. O. *Makromol. Chem., Rapid Commun.* **1988**, *9*, 393. (b) Han, T. K.; Ko, Y. S.; Park, J. W.; Woo, S. I. *Macromolecules* **1996**, *29*, 7305. (c) Marques, M. M.; Tait, P. J. T.; Mejzlik, J.; Dias, A. R. *J. Polym. Sci., Part A.* **1998**, *36*, 573. (d) Fukui, Y.; Murata, M. *Macromol. Chem. Phys.* **2001**, *202*, 1430.
6. (a) Busico, V.; Guardasole, M.; Margonelli, A.; Segre, A. L. *J. Am. Chem. Soc.* **2000**, *122*, 5226. (b) Budzelaar, P. H. M. *Organometallics* **2004**, *23*, 855.
7. (a) Liu, Z.; Somsook, E.; White, C. B.; Rosaaen, K. A.; Landis, C. R. *J. Am. Chem. Soc.* **2001**, *123*, 11193. (b) Liu, Z.; Somsook, E.; Landis, C. R. *J. Am. Chem. Soc*. **2001**, *123*, 2915.
8. (a) Kochi, J. K. "Organometallic Mechanisms and Catalysis", Academic Press, New York, **1978**, p. 532. (b) Hart, D. W.; Schwartz, J. *J. Am. Chem. Soc*. **1974**, *96*, 8115. (c) Labinger, J. A.; Hart, D. W.; Seibert, W. E.; Schwartz, J. *J. Am. Chem. Soc*. **1975**, *97*, 3851.
9. (a) Silverstein, R. M.; Webster, F. X. *Spectrometric Identification of Organic Compounds*, Sixth Ed., John Wiley & Sons, Inc. **1998**. (b) Pouchert, C. J.; Behnke, J. "The Aldrich Library of ^{13}C and ^{1}H NMR Spectra, Edition 1, **1993**.
10. (a) Boden, B. N. *M.Sc. Thesis* **2002**, Queen's University. (b) Vatamanu, M.; Boden, B. N.; Baird, M. C. *Macromolecules* **2005,** *38*, 9944.

11. Druce, P. M.; Kingston, B. M.; Lappert, M. F.; Spalding, T. R.; Srivastava, R. C. *J. Chem. Soc. A*, **1969**, 2106.

12. (a) Samuel, E.; Rausch, M. D. *J. Am. Chem. Soc.* **1973**, *95*, 6263. (b) Hunter, W. E.; Hrncir, D. C.; Bynum, R. V.; Penttila, R. A.; Atwood, J. L. *Organometallics* **1983**, *2*, 750. (c) Balboni, D.; Camurati, I.; Prini, G.; Resconi, L.; Galli, S.; Mercandelli, P.; Sironi, A. *Inorg. Chem.* **2001**, *40*, 6588. (d) Bochmann, M.; Lancaster, S. J. *Organometallics* **1993**, *12*, 633. (e) Chien, J. C. W.; Tsai, W.-M.; Rausch, M. D. *J. Am. Chem. Soc.* **1991**, *113*, 8570. (f) Massey, A. G.; Park, A. J. *J. Organomet. Chem.* **1964**, *2*, 245. (g) Wailes, P. C.; Weigold, H.; Bell, P. *J. Organomet. Chem*. **1972**, *34*, 155. (h) Chien, J. C. W.; Tsai, W. –M.; Rausch, M. D. *J. Am. Chem. Soc*. **1991**, *113*, 8570. (i) Ewart, S. W. *PhD. Thesis* **1998**, Queen's University.

13. (a) Yang, X.; Stern, C. L.; Marks, T. J. *J. Am. Chem. Soc.* **1991**, *113*, 3623. (b) Yang, X.; Stern, C. L.; Marks, T. J. *J. Am. Chem. Soc.* **1994**, *116*, 10015. (c) Braga, D.; Grepioni, F.; Tedesco, E.; Calhorda, M. J. *Z. Anorg. Allg. Chem.* **2000**, *626*, 462.

14. Busico, V.; Cipullo, R.; Esposito, V. *Macromol. Rapid Commun*. **1999**, *20*, 116.

15. (a) Gabriel, C.; Kokko, E.; Löfgren, B.; Seppälä, J.; Münstedt, H. *Polymer*, **2002**, *43*, 6383. (b) Galland, G. B.; Quijada, R.; Rojas, R.; Bazan, G.; Komon, Z. J. A. *Macromolecules* **2002**, *35*, 339. (c) Galland, G. B.; de Souza, R. F.; Mauler, R. S.; Nunes, F. F. *Macromolecules* **1999**, *32*, 1620. (d) Usami, T.; Takayama, S. *Macromolecules*, **1984**, *17*, 1756. (e) A resonance with this chemical shift in spectra of copolymers has been assigned to a -$CHMe_2$ group (Kissin, Y.V.; Mink, R. I.; Nowlin, T. E.; Brandolini, A. J. *Topics in Catalysis* **1999**, *7*, 69), although it is not clear how this would arise here.

16. (a) AlObaidi, F.; Zhu, S. *J. Appl. Polym. Sci.* **2005**, 96, 2212. (b) Beach, D. L.; Kissin, Y. V. *Concise Encyclopedia of Polymer Science and Engineering*, Kroschwitz, J. I. Ed., John Wiley & Sons, **1990**, 354.

17. See, for instance, (a) Leino, R.; Luttikhedde, H. J. G.; Lehmus, P.; Wilén, C.-E.; Sjöholm, R.; Lehtonen, A.; Seppälä. J. V.; Näsman, J. H. *Macromolecules* **1997,** *30*, 3477. (b) Götz, C.; Rau, A.; Luft, G. *Macromol. Mater. Eng.* **2002,** *287***, 16**. (c) Bhriain, N. N.; Brintzinger, H.-H.; Ruchatz, D.; Fink, G. *Macromolecules* **2005,** *38*, 2056 and references therein.

18. (a) Resconi, L.; Jones, R. L.; Rheingold, A. L.; Yap, G. P. A. *Organometallics* **1996**, *15*, 998. (b) Janiak, C.; Lange, K. C. H.; Marquardt, P. *J. Mol. Cat. A: Chem.* **2002**, *180*, 43.

19. Resconi, L.; Camurati, I.; Sudmeijer, O. *Topics in Catalysis* **1999**, *7*, 145.

20. (a) Rieger, B.; Mu, X.; Mallin, D. T.; Rausch, M. D.; Chien, J. C. W. *Macromolecules* **1990**, *23*, 3559. (b) Lee, I.-M.; Gauthier, W. J.; Ball, J. M.; Iyengar, B.; Collins, S. *Organometallics* **1992**, *11*, 2115.

21. (a) Resconi, L.; Piemontesi, F.; Franciscono, G.; Abis, L.; Fiorani, T. *J. Am. Chem. Soc*. **1992**, *114*, 1025. (b) Resconi, L.; Abis, L.; Franciscono, G. *Macromolecules* **1992**, *25*, 6814.

22. Borrelli, M.; Busico, V.; Cipullo, R.; Ronca, S.; Budzelaar, P. H. M. *Macromolecules* **2002**, *35*, 2835.

23. (a) Busico, V.; Cipullo, R.; Chadwick, J. C.; Modder, J. F.; Sudmeijer, O. *Macromolecules* **1994**, *27*, 7538. (b) Busico, V.; Cipullo, R.; Ronca, S.

Macromolecules **2002**, *35*, 1537. (c) Busico, V.; Cipullo, R.; Talarico, G. *Macromolecules* **1998**, *31*, 2387.

24. (a) Rieger, B.; Mu, X.; Mallin, D. T.; Rausch, M. D.; Chien, J. C. W. *Macromolecules* **1990**, *23*, 3559. (b) Grassi, A.; Zambelli, A.; Resconi, L.; Albizzati, E.; Mazzocchi, R. *Macromolecules* **1988**, *21*, 617. (c) Stehling, U.; Diebold, J.; Kristen, R.; Röll, W.; Brintzinger, H-. H.; Jüngling, S.; Mülhaupt, R.; Langhauser, F. *Organometallics* **1994**, *13*, 964. (d) Jüngling, S.; Mülhaupt, R.; Stehling, U.; Brintzinger, H-. H.; Fischer, D.; Langhauser, F. *J. Polym. Sci., Pol. Chem.* **1995**, *33*, 1305.
25. (a) Resconi, L.; Piemontesi, F.; Camurati, I.; Balboni, D.; Sironi, A.; Moret, M.; Rychlicki, H.; Zeigler, R. *Organometallics* **1996**, *15*, 5046. (b) Dang, V. A.; Yu, L.-C.; Balboni, D.; Dall'Occo, T.; Resconi, L.; Mercandelli, P.; Moret. M.; Sironi, A. *Organometallics* **1999**, *18*, 3781. (c) Resconi, L.; Fait, A.; Piemontesi, F.; Colonnesi, M.; Rychlicki, H.; Zeigler, R. *Macromolecules* **1995**, *28,* 6667.
26. (a) Giannetti, E.; Nicoletti, G. M.; Mazzocchi, R. *J. Polym. Sci., Pol. Chem.* **1985**, *23*, 2117. (b) Möhring, P. C.; Coville, N. J. *J. Org. Chem*. **1994**, *479*, 1.
27. Mashima, K.; Nakayama, A.; *Adv. Poly. Sci.* **1997**, *133*, 1.
28. (a) Busico, V.; Cipullo, R. *J. Am. Chem. Soc*. **1994**, *116*, 9329. (b) Guo, Z.; Swenson, D. C.; Jordan, R. F. *Organometallics* **1994**, *13*, 1424.
29. (a) Resconi, L.; Piemontesi, F.; Camurati, I.; Sudmeijer, O. ; Nifant'ev, J. E. ; Ivchenko, P. V.; Kuz'mina, L. G. *J. Am. Chem. Soc*. **1998**, *120*, 2308. (b) Resconi, L. *J. Molec. Catal. A: Chemical* **1999**, *146*, 167.
30. Janiak, C. *Coord. Chem. Rev*. **2006**, *250*, 66.

31. (a) Moscardi, G.; Resconi, L.; Cavallo, L. *Organometallics* **2001**, *20*, 1918. (b) Schaverien, C. J.; Ernst, R.; Schut, P.; Dall'Occo, T. *Organometallics* **2001**, *20*, 3436.

32. van der Heijden, H.; Hessen, B.; Orpen, A. G. *J. Am. Chem. Soc.* **1998**, *120*, 1112.

Chapter 3

An Investigation into the Zr-polymeryl Intermediates Present during Propylene Polymerizations by Nonmetallocene Catalysts

3.1. Introduction

The extensive research conducted so far on olefin polymerization by zirconocene catalysts has provided substantial insight into the important steps of the polymerization reaction. The generally accepted mechanism for zirconocene catalyzed olefin polymerization involves the coordination of the olefin to the vacant site of the Zr-polymeryl cation followed by migratory insertion of the coordinated olefin into the growing Zr-polymeryl chain.[1] For α-olefin polymerizations, insertion of the monomer into the Zr-C bond occurs predominantly in a 1,2-fashion to give primary Zr-polymeryl species, but secondary (2,1) insertions are also possible (Scheme 3.1, P = polymeryl chain).[1,2]

Scheme 3.1. Propylene insertion modes

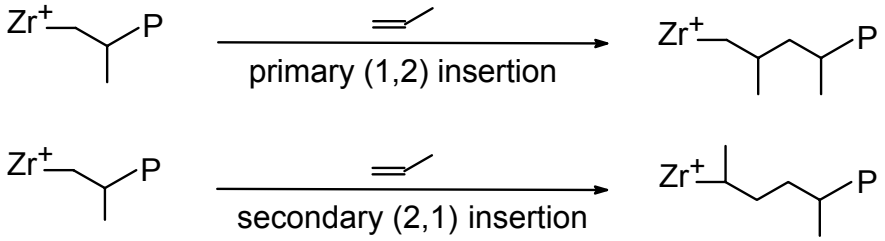

Although olefin polymerization by zirconocene catalysts has been extensively studied[1] and much is known with respect to the basic polymerization mechanism, there remains a need for detailed experimental information on the nature of the intermediates present during catalysis, and about the proportions of added catalyst actually present as active intermediate(s).

For instance, an examination of the literature on zirconocene catalyzed propylene polymerization shows that although most zirconocene-based catalysts are highly active initially, almost without exception some of the catalyst deactivates shortly after the polymerization is started.[1d,3] The catalyst deactivation is usually attributed to formation of secondary (2,1) Zr-polymeryl species, which are assumed to be slowly propagating and to therefore accumulate in the polymerization system rather than engage in subsequent propagation steps.[4] However, there is to date no direct evidence for such species in the polymerization reaction mixture, their presence being usually inferred from the microstructure analysis of the polymer chains[4c,5] and from the analysis of the polymer end groups.[1c,6]

In order to gain information about intermediates present during olefin polymerization by zirconocene catalysts, a novel method of quenching a polymerization

reaction by the use of bromine was developed.[7] This procedure allows for the rapid identification of metal-polymeryl groups present during alkene polymerization. It can distinguish between primary and secondary insertions and also allows quantification of the primary (1,2) metal-polymeryl groups which are considered the actual active species. This method has been tested on propylene polymerization in the presence of two achiral zirconocene catalysts, Cp_2ZrMe_2 and $(indenyl)_2ZrMe_2$ activated with $B(C_6F_5)_3$, as described in Chapter 2. By quenching the polymerization reactions with bromine it was found that bromine labels the growing polymer chains at the primary position only, suggesting that secondary Zr-polymeryls resulting from 2,1-insertions do not accumulate.[7]

As part of a continuing effort to find information on the nature of the Zr-polymeryl linkages present during propylene polymerization, and in particular to find evidence for the presence of secondary (2,1) Zr-polymeryl species, this research was extended to another catalytic system which is believed to undergo secondary propylene insertions. In this regard, the $[ONNO]Zr(CH_2C_6H_5)_2$[8] precursor catalyst (Scheme 3.2) activated with MAO/2,6-di-^{t}butylphenol[4a,9] was used. For this catalytic system, Busico *et al*.[8] reported that the secondary (2,1) propylene insertions into Zr-C σ-bond occur and moreover, the resulting secondary Zr-polymeryl groups accumulate in the polymerization system over time (~ 20% after 4 min polymerization time) as 'dormant' species.[4a]

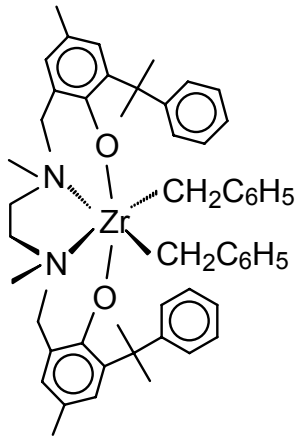

Scheme 3.2. The [ONNO]Zr($CH_2C_6H_5$)$_2$ catalyst

Additionally, this catalytic system was claimed to polymerize propylene in a "controlled" fashion: That is, chain initiation is fast as compared to propagation and chain transfer, and chain termination reactions are negligible.[4a] This catalytic system is hence expected to lead to a polypropylene polymer in which the fraction of olefinic end groups is minor. As a result, the amount of brominated vinylidene end groups obtained after quenching the polymerization reaction with bromine is expected to be reduced. In this way, any secondary alkyl bromide end groups present on the polymer chains as a result of the cleavage of the secondary Zr-polymeryl linkages by bromine, which are expected to give a resonance in the same region as the brominated vinylidene end groups, would be easier to detect by ^{1}H NMR.

3.2. Results and discussion

Polymerizations were performed at room temperature, under 1 atmosphere of propylene, in the presence of [ONNO]Zr($CH_2C_6H_5$)$_2$ activated with MAO/2,6-di-^{t}butylphenol ([Al]:[Zr] = 480) in chlorobenzene. The polymerization reactions were carried out for various polymerization times, from 40 to 360 seconds, and stopped by quenching with a solution of bromine in methylene chloride. After quenching, the polymers were precipitated with acidified methanol, filtered, dried, and subsequently purified by reprecipitation from hot chlorobenzene. The resulting polymer was characterized on the basis of comparisons with model compounds as discussed below, using NMR spectroscopy.

A typical ^{1}H NMR spectrum of an isotactic polypropylene sample obtained after quenching the polymerization reaction with bromine is presented in Figure 3.1. As can be seen, the spectrum is dominated by three groups of resonances at 1.58 ppm (multiplet), 1.27 ppm (multiplet) and 0.89 ppm (doublet) of relative intensities 1:1:4 in the aliphatic region. The multiplet at 1.58 ppm and the doublet at 0.89 ppm belong to the backbone methine and methyl group hydrogens, respectively, while the multiplet at 1.27 ppm belongs to one of the methylene (*m* diad) group hydrogens, the second methylene (*m* diad) group hydrogen resonance being overlapped by the methyl group resonance at 0.89 ppm. A very low intensity group of peaks corresponding to the methylene (*r* diad) group hydrogens is also present at 1.0-1.2 ppm. The sharp, well resolved patterns of these resonances (Figure 3.1(a)) are indicative of a highly stereoregular polymer.[10]

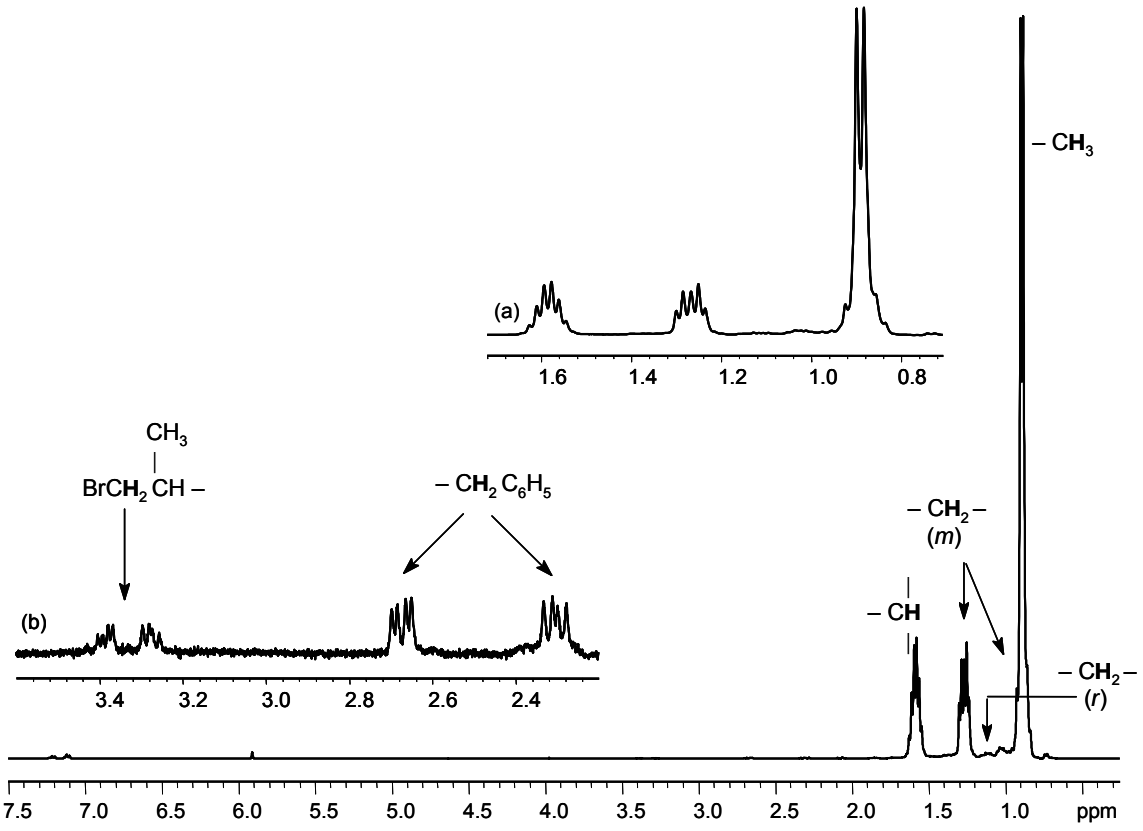

Figure 3.1. ^{1}H NMR spectrum of isotactic polypropylene obtained from propylene polymerization by [ONNO]Zr($CH_2C_6H_5$)$_2$/MAO/2,6-di-^{t}butylphenol after 1 min polymerization time (1,1,2,2-tetrachloroethane-d_2, 120°C, 400 MHz). The insets show an expanded scale of the polymer backbone (a) and the polymer end group region (b).

Aside from the strong resonances of the main chain hydrogens, the ^{1}H NMR spectrum of the brominated isotactic polypropylene also displays a series of weak resonances corresponding to the polymer chain ends. Thus, the two doublets of doublets at 2.3 and 2.67 ppm (from the ^{1}H-^{13}C HSQC spectra, these are associated with a ^{13}C resonance at 43.5 ppm) and the multiplet at 7.0 – 7.3 ppm (from the ^{1}H-^{13}C HSQC spectra, these are associated with ^{13}C resonances at 125.5, 128, and 129.1 ppm) were

assigned to the methylene and phenyl group hydrogens of the initial -$CH_2C_6H_5$ end groups, respectively. According to a COSY experiment, the two doublets of doublets at 2.3 and 2.67 ppm are correlated to each other and also with a resonance at 1.85 ppm (^{13}C resonance at 32.4 ppm), which in turn is correlated with a resonance at 1.04 ppm. On the basis of these correlations, in addition to the chemical shift values,[11] the resonances at 1.85 and 1.04 ppm were assigned to the -C**H**(Me)- and -CH(**Me**)- group hydrogens, respectively. A polymer end group of the type -$CH(Me)CH_2C_6H_5$ would arise from a primary (1,2) insertion of propylene into the Zr-$CH_2C_6H_5$ bond, as shown in Scheme 3.3. A secondary (2,1) propylene insertion into the Zr-$CH_2C_6H_5$ bond, on the other hand, would result in a –$CH(Me)CH_2CH_2C_6H_5$ end group.

Scheme 3.3. Mechanism of initiation for propylene polymerization using [ONNO]Zr$(CH_2C_6H_5)_2$ catalyst

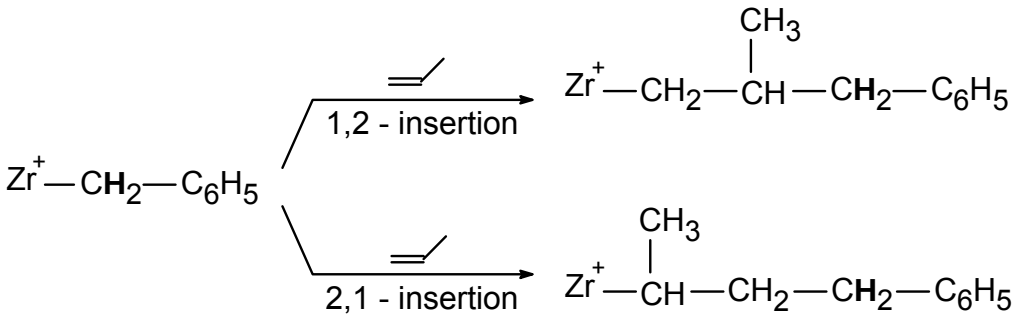

On the basis of the ^1H and ^{13}C NMR spectra of hexylbenzene as a model compound and of literature data,[11,12] the -C**H**$_2C_6H_5$ hydrogen resonance of a potential -$CH(Me)CH_2CH_2C_6H_5$ end group is expected to arise at about 2.6 ppm (^{13}C resonance at about 36 ppm). There were no COSY cross peaks between any resonance at about 2.6 ppm and any other C**H**$_2$ resonances. Also, the ^1H-^{13}C HSQC spectrum showed no

correlations between any potential hydrogen resonance at about 2.6 ppm and any carbon resonance at about 36 ppm. These observations suggest that the first insertion of propylene into the Zr-benzyl group is highly regioselective, in favor of primary (1,2) insertion.

From the ratio of the relative intensities between the -C**H**$_2$C$_6$H$_5$ end group resonances and the polymer backbone resonances, assuming that only one polymer chain per zirconium center was initiated in the time scale of the experiment, the number average molecular weight (Mn) of the polymer was calculated.[8a,13] The variation of the calculated Mn versus polymerization time is shown in Figure 3.2. There is a nearly linear increase of Mn, from about 7,800 g/mol at 40 sec polymerization time to about 44,700 g/mol at 4 min polymerization time. At longer polymerization times, the calculated Mn continues to increase but with an exponential-like deviation from the initial linear relationship of Mn versus polymerization time.

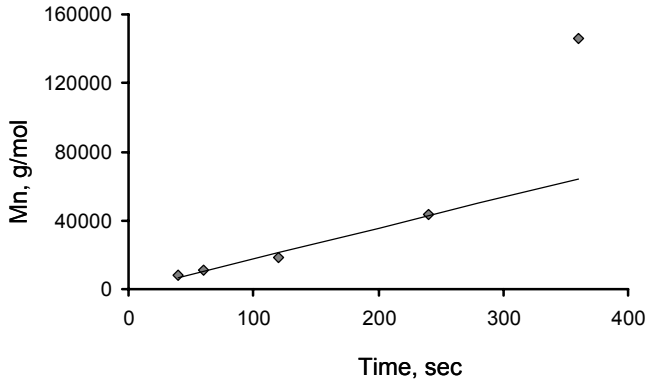

Figure 3.2. Variation of Mn (determined using ^{1}H NMR spectroscopy) as a function of polymerization time for propylene polymerization by [ONNO]Zr($CH_2C_6H_5$)$_2$/MAO/2,6-di-^{t}butylphenol in chlorobenzene at room temperature.

The deviation of calculated Mn from linearity for longer polymerization times may be due to chain transfer reactions when more than one polymer chain per catalyst center might be formed. Indeed, the end group analysis in the olefinic region of the ^{1}H NMR spectra of isotactic polypropylene obtained after quenching the polymerization reaction with acidified methanol, shows the presence of weak resonances at 4.68 and 4.74 ppm attributable to vinylidene end groups.[7a] The ratio of the relative intensities between the C**H**$_2$=C(Me)- and the -C**H**$_2$C$_6$H$_5$ end group resonances is 0.08:1 at 1 min polymerization time and 0.5:1 at 6 min polymerization time. Thus, chain transfer reactions via β-hydrogen elimination occur in the present catalytic system and they can affect the calculation of Mn for polymerization times in excess of about 4 min. The fact that the calculation of Mn using ^{1}H NMR spectroscopy is less accurate for polymers of high molecular weight is another factor which may be contributing to the deviation of Mn from linearity at longer polymerization times.

Much weaker resonances were observed in the brominated end group region of the ^{1}H NMR spectrum between 3.2 and 4.5 ppm. An expansion of the ^{1}H NMR spectrum in this region is displayed in Figure 3.3.

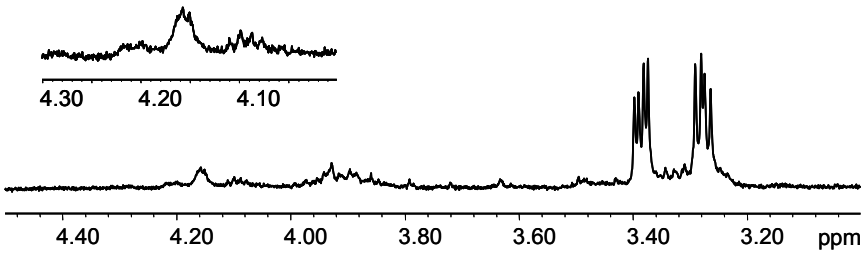

Figure 3.3. ^{1}H NMR spectrum in the brominated end group region of isotactic polypropylene obtained following quenching the polymerization with bromine (1 min polymerization time, 1,1,2,2-tetrachloroethane-d_2, 120°C, 600 MHz).

As can be seen from Figure 3.3, the ^{1}H NMR spectrum in the brominated end group region of isotactic polypropylene obtained after quenching the polymerization with bromine shows the presence of two doublets of doublets of about 1:1 ratio of relative intensities at 3.38 and 3.28 ppm. A COSY experiment indicates that the two resonances at 3.38 and 3.28 ppm are mutually correlated, while an HSQC experiment indicates that they are both bonded to a carbon atom with a ^{13}C resonance at 41.5 ppm (see Figure 3.4(a)). On the basis of the above correlations and by comparison with the spectrum of 1-bromo-2-methyl-undecane which serves as a model compound (Figure 2.2), the pair of doublets of doublets at 3.38 and 3.28 ppm was assigned to the two hydrogens of the primary alkyl bromide end groups (Br-C**H**$_2$CH(Me)-) of isotactic polypropylene.

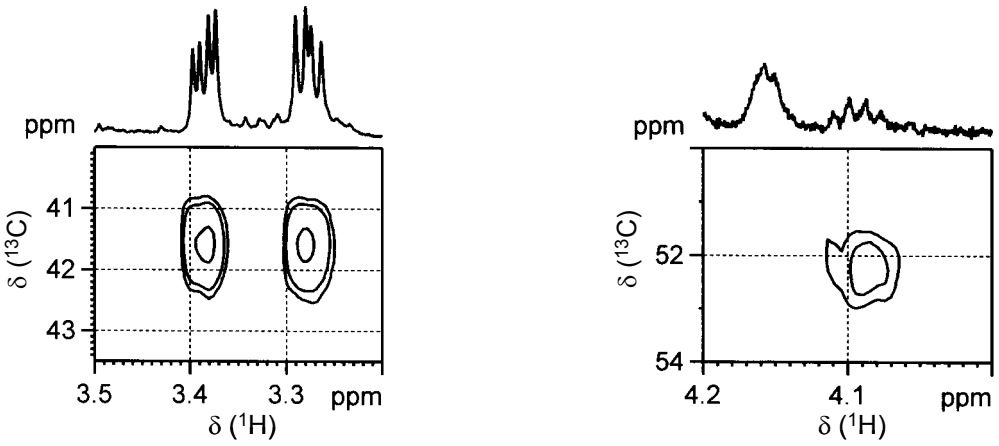

Figure 3.4. ^{1}H NMR and ^{1}H-^{13}C HSQC spectra in the brominated end group region of isotactic polypropylene (1,1,2,2-tetrachloroethane-d_2, 120°C, 600 MHz).

The primary alkyl bromide end groups result from the cleavage of a Zr-C σ-bond following a primary (1,2)-insertion and a pair of doublets of doublets for the two hydrogens of the primary alkyl bromide end groups in the brominated polymer is consistent with a highly isotactic polypropylene, in which most chains are terminated by *m* diads.

In addition to the primary alkyl bromide end groups, secondary alkyl bromide end groups arising from the cleavage of Zr-polymeryl linkages after a secondary (2,1)-insertion are also expected to be present[4a] in the ^{1}H NMR spectrum of brominated polymers. The latter would appear as a multiplet at about 4.0-4.2 ppm, according to the ^{1}H NMR spectrum of 2-bromodecane used as a model compound. As can be seen in Figure 3.3, the ^{1}H NMR spectrum in the region between 3.8 and 4.3 ppm shows the presence of a series of small resonances, in trace amounts. While no attempt to identify all these weak resonances was done, it seems reasonable that they mostly arise from the bromination of the olefinic end groups present on the polymer chain.

However, a closer look at the ^{1}H NMR spectrum in the brominated end group region shows the presence of a small multiplet resonance at ~4.1 ppm which can be tentatively attributed to a secondary alkyl bromide end group. The identity of this peak was confirmed by an HSQC experiment in which the hydrogen resonance at ~4.1 ppm is correlated with a carbon resonance at ~52 ppm (Figure 3.4(b)), as well as by comparison with the ^{1}H-^{13}C HSQC spectrum of 2-bromodecane.

It is apparent from Figure 3.3 that the relative intensity of the secondary alkyl bromide end group resonance at ~4.1 ppm is much weaker (trace amounts) as compared to that of the primary alkyl bromide end group resonances at ~3.38 and 3.28 ppm in the

polymer sample obtained after 1 min polymerization time. In the polymers obtained after longer polymerization times, the secondary alkyl bromide end group resonances are under the NMR detection limit. The ^{13}C NMR spectra of isotactic polypropylene obtained after quenching the polymerization with acidified methanol, on the other hand, revealed the presence of 2,1-regioerrors[9,4e,4f] (see Appendix B) in addition to the initial benzyl end groups[9] and the isobutyl end groups[9,4b,4f] arising from the cleavage of a primary (1,2) Zr-polymeryl bond; the peaks indicative of n-butyl end groups[9,4b] which would arise from the cleavage of a secondary (2,1) Zr-polymeryl bond were undetectable. These observations suggest that while secondary propylene insertions into Zr-C bond occur, secondary Zr-polymeryls propagate rather than accumulate in the reaction mixture for the polymerization system under investigation such that the amount of secondary Zr-polymeryl chains at the time of quenching is negligible.

From the ^{1}H NMR spectra of brominated polymer samples obtained from the [ONNO]Zr($CH_2C_6H_5$)$_2$/MAO/2,6-di-^{t}butylphenol catalytic system, it has been found that the relative intensity of the primary alkyl bromide end group (Br-C**H**$_2$CH(Me)-) resonances was always lower than that of the benzyl end group (-C**H**$_2C_6H_5$) resonances (see Figure 3.1 as an example). This observation coupled with the finding that the amount of the catalyst "trapped" as secondary Zr-polymeryl species at the time of quench is negligible, suggest that while the catalyst does deactivate during the polymerization, secondary Zr-polymeryl groups do not account for the catalyst deactivation. At present, the cause of catalyst deactivation in the polymerization system under investigation is not fully understood.

3.3. Summary

In this Chapter, the results of a study on propylene polymerization in the presence of [ONNO]Zr($CH_2C_6H_5$)$_2$ activated with MAO/2,6-di-^{t}butylphenol, in chlorobenzene at room temperature are described. The polymerization reactions were run for different polymerization times between 40 sec and 6 min and stopped by quenching with either bromine or acidified methanol.

In all cases, highly isotactic polypropylenes (as indicated by ^{1}H NMR) were obtained. Besides the initiating benzyl end groups, both primary and secondary alkyl bromide end groups were detected in the polymers obtained after quenching the polymerization with bromine. Primary alkyl bromide end groups result from the bromine cleavage of Zr-polymeryl linkages after a primary (1,2) propylene insertion and they are the major brominated end groups of the polymer chains. Secondary alkyl bromide end groups are the result of the cleavage by bromine of Zr-polymeryl linkages obtained following a secondary (2,1) propylene insertion and they were detected only in brominated polymers obtained after very short polymerization times. The amount of secondary alkyl bromide end groups on the polymer chains was found to be negligible in the polymerization system under investigation.

The analysis of the polymer end groups, performed using ^{1}H NMR spectroscopy, indicated that in all cases the catalyst deactivates during the polymerization. Although secondary insertions of propylene into a Zr-C bond were found to occur during the polymerization, the fraction of deactivated catalyst by far exceeds the fraction that could reasonably be attributed to the secondary Zr-polymeryl groups at the time of quenching and therefore, the latter cannot constitute the main cause of catalyst deactivation. At

present, the cause of catalyst deactivation in the polymerization system under investigation is not fully understood.

3.4. Experimental Section

3.4.1. General Considerations

Anhydrous diethyl ether and toluene were purchased from Aldrich in 18L reservoirs packaged under argon and passed through a single column of activated alumina prior to use. Chlorobenzene was dried by distillation under argon from calcium hydride prior to use. Deuterated solvents were obtained from Cambridge Isotope Laboratories (>99% atom %D). Benzene-d_6 was de-gassed, dried by distillation from calcium hydride, stored over molecular sieves, and handled in a glove box. Chloroform-d_1, chlorobenzene-d_5 and 1,1,2,2-tetrachloroethane-d_2 were used as received. Polymerization grade propylene (99.5 wt% purity, liquid phase, Praxair), was dried by passage through a column of activated 4 Å molecular sieves prior use. All the other chemicals were purchased from Aldrich and used as received. Synthesis and polymerizations, unless otherwise noted, were carried out under purified argon using standard Schlenk line and glove box techniques.

NMR spectra were recorded on Bruker AV 400 and 600 spectrometers, chemical shifts being referenced using the residual proton signals of the deuterated solvents. ^{1}H NMR spectra were acquired with a 45 degree pulse and 1 sec delay between pulses; 16 transients were stored for each spectrum. ^{1}H-^{13}C HSQC spectra were collected on a 600 MHz spectrometer using Echo/Antiecho-TPPI gradient selection with decoupling during acquisition using shaped pulses for all 180 degree pulses on f2-channel. The HSQC acquisition parameters were: a 0.1705 sec acquisition time, a 10 ppm spectral window in

f2, a 165.6 ppm spectral window in f1 and a 1 sec relaxation delay. The ^{13}C NMR spectra were run on a 400 MHz spectrometer at 120°C. The acquisition parameters were: a 1.625 sec acquisition time, a 200.4 ppm spectral window and a 1 sec relaxation delay.

3.4.2. Preparation of 2-Cumyl-4-methylphenol

2-Cumyl-4-methylphenol was prepared by a modified procedure from that described in literature.[8a] p-Toluenesulfonic acid monohydrate (1.9 g, 0.01 mol) was added to p-cresol (41.8 mL, 0.4 mol), under stirring, at room temperature. α-Methyl-styrene (26 mL, 0.2 mol) was then added dropwise to the above mixture under stirring over 30 min. The reaction mixture was then heated at 50°C and allowed to stir at this temperature for 5 h. After the solution was cooled at room temperature, triethylamine (1.4 mL, 0.01 mol) was added. The reaction mixture was diluted with toluene, washed several times with distilled water, dried over $MgSO_4$, filtered, and the solvent was removed under reduced pressure. The oily product was purified by vacuum fractional distillation. Pure 2-Cumyl-4-methylphenol was obtained as yellow oil in a yield of 47.4%.

^1H NMR (300 MHz, $CDCl_3$): δ 1.59 (s, 6H, $C(CH_3)_2$), 2.27 (s, 3H, CH_3), 4.09 (br.s, 1H, OH), 6.56 (d, 1H, Ar), 6.8-7.4 (m, 7H, Ar) ppm.

3.4.3. Preparation of [ONNO] ligand

The [ONNO] ligand was prepared by a procedure similar to that described in literature.[8a,14] N,N'-dimethylethylenediamine (1.12 mL, $10.5x10^{-3}$ mol) and formaldehyde (1.78 mL, $22x10^{-3}$ mol, 37 wt.% in water) were successively added to a solution of 2-cumyl-4-methylphenol (4.53 g, $20x10^{-3}$ mol) in 60 mL methanol under

stirring. The reaction mixture was refluxed for 2 days after which it was allowed to cool at room temperature. The formed solid was collected by filtration, washed with methanol and dried at 40°C under vacuum overnight. The product was obtained as white crystals with a yield of 30.6%.

^{1}H NMR (400 MHz, C_6D_6): δ 1.51 (s, 6H, NCH_3), 1.76 (s, 4H, NCH_2), 1.85 (s, 12H, $C(CH_3)_2$), 2.28 (s, 6H, CH_3), 3.04 (s, 4H, NCH_2Ar), 6.56 (br.s, 2H, Ar), 7.05 (t, 2H, Ar), 7.17 (t, 4H, Ar), 7.29 (br.s, 2H, Ar), 7.38 (d, 4H, Ar), 10.23 (br.s, 2H, OH) ppm.

3.4.4. Preparation of tetra(benzyl) zirconium

Tetra(benzyl) zirconium was prepared by a slightly modified procedure from that described in the literature.[15] Zirconium(IV) chloride (5.02 g, 0.0225 mol) was added in small portions under an argon atmosphere to a stirring solution of $C_6H_5CH_2MgCl$ (99 mL, 0.1 mol, 1M in diethyl ether) in 40 mL of dry diethyl ether at -20°C. The reaction mixture was allowed to stir at -20°C for an additional 12 h after which the resulting suspension was filtrated under vacuum and the solid was washed with 120 mL of dry diethyl ether to give a yellow-orange solution. The solvent was removed under vacuum overnight and the residue (oily orange solid) was extracted with five 15 mL fractions of hot toluene, filtrated and dried under reduced pressure. The product was purified by recrystallization from dry toluene. Pure $Zr(CH_2C_6H_5)_4$ was obtained as dark orange crystals.

^{1}H NMR (300 MHz, C_6D_6): δ 1.53 (s, 2H, CH_2), 6.37 (d, 2H, Ar), 6.95 (t, 1H, Ar), 7.05 (t, 2H, Ar) ppm.

3.4.5. Preparation of [ONNO]Zr($CH_2C_6H_5$)$_2$

[ONNO]Zr($CH_2C_6H_5$)$_2$ was prepared by a procedure similar to that described in literature.[8a,14] A solution of [ONNO] ligand (0.86 g, 0.38x10^{-3} mol) in 40 mL dry toluene was added dropwise under argon to a stirring solution of tetra(benzyl) zirconium (0.69 g, 0.38x10^{-3} mol) in 40 mL dry toluene. The reaction mixture was stirred for 3 h at 65°C after which the solvent was removed under vacuum. The pure product was obtained as yellow powder in a quantitative yield.

^{1}H NMR (300 MHz, C_6D_6): δ 0.68 (d, 2H, NCH_2), 1.16 (s, 6H, NCH_3), 1.77 (s, 6H, CH_3), 2.03, (s, 6H, CH_3), 2.11 (d, 2H, $ZrCH_2$), 2.20 (d, 2H, NCH_2Ar), 2.22 (s, 6H, CH_3), 2.36 (d, 2H, NCH_2), 2.56 (d, 2H, $ZrCH_2$), 3.53 (d, 2H, NCH_2Ar), 6.42 (br.s, 2H, Ar), 7.34 (br.s, 2H, Ar), 6.7 – 7.5 (m, 20H, Ar) ppm.

3.4.6. Propylene Polymerization

a) For a typical experiment, 2,6-di-^{t}butylphenol (0.01 mol) was charged into a Schlenk flask and dissolved in a solution of MAO (0.019 mol, 10wt% in toluene) in 50 mL dry chlorobenzene under argon at room temperature. After 1 h, 5 mL of the reaction mixture was syringed out and used to dissolve the precatalyst (0.04x10^{-3} mol, [Al]/[Zr] = 480) in a separate Schlenk flask under argon. The reaction mixture was saturated with propylene at atmospheric pressure with vigorous stirring and the polymerization was initiated by injecting in the previously prepared catalyst solution (precontact time 10 min). The polymerization was allowed to proceed at constant propylene pressure for a measured reaction time (40 – 360 sec) after which the propylene feed was interrupted and polymerization was quenched with a solution of bromine in dry methylene chloride. The

reaction mixture was allowed to stir for an additional 30 min before the polymer was precipitated with excess MeOH/HCl (10/1 v/v). The polymer was extracted in acidified methanol under stirring overnight, filtered, washed with MeOH and dried. The polymers were further reprecipitated from hot toluene in methanol, filtrated and dried under vacuum overnight at 60°C. Polymerization yields were 0.094, 0.135, 0.291, 0.466, and 0.711g for 40, 60, 120, 240, and 360 seconds, respectively.

b) 2,6-di-^{t}butylphenol (0.01 mol) was charged into a Schlenk flask and dissolved in a solution of MAO (0.019 mol, 10 wt% in toluene) in 50 mL dry chlorobenzene under argon at room temperature. After 1 h, 5 mL of the reaction mixture was syringed out and used to dissolve the precatalyst ($0.04x10^{-3}$ mol, [Al]/[Zr] = 480) in a separate Schlenk flask under argon. The reaction mixture was saturated with propylene at atmospheric pressure with vigorous stirring and the polymerization was initiated by injecting into the previously prepared catalyst solution (precontact time 10 min). The polymerization was allowed to proceed at constant propylene pressure for a measured reaction time (1 min and 6 min) after which the propylene feed was interrupted and polymerization was quenched with MeOH/HCl (10/1 v/v). The acidified methanol must be added slowly as it reacts violently with MAO. The polymer was extracted in acidified methanol under stirring overnight, filtered, washed with MeOH and dried. The polymers were further reprecipitated from hot toluene in methanol, filtrated and dried under vacuum overnight at 60°C. Polymerization yields were 0.149 and 0.551g for 1 min and 6 min, respectively.

References

1. (a) Kaminsky, W. *J. Chem. Soc., Dalton Trans*., **1998**, 1413. (b) Alt, H. G.; Köppl, A. *Chem. Rev*. **2000**, *100*, 1205. (c) Möhring, P. C.; Coville, N. J. *J. Organomet. Chem.* **1994**, *479*, 1. (d) Bochmann, M.. *J Chem. Soc., Dalton Trans*. **1996**, 255. (e) Brintzinger, H. H.; Fischer, D.; Mülhaupt, R.; Rieger, B. Waymouth, R. M. *Angew. Chem. Int. Ed.* **1995**, *34*, 1143. (f) Resconi, L.; Cavallo, L.; Fait, A.; Piemontesi, F. *Chem. Rev*. **2000**, *100*, 1253. (g) Rappé,, A. K.; Skiff, W. M.; Casewit, C. J. *Chem. Rev*. **2000**, *100*, 1435.
2. (a) Borrelli, M.; Busico, V.; Cipullo, R.; Ronca, S.; Budzelaar, P. H. M. *Macromolecules* **2002**, *35*, 2835. (b) Resconi, L.; Abis, L.; Franciscono, G. *Macromolecules* **1992**, *25*, 6814. (c) Dang, V. A.; Yu, L. –C.; Balboni, D.; Dall'Occo, T.; Resconi, L. ; Mercandelli, P. ; Moret, M. Sironi, A. *Organometallics* **1999**, *18*, 3781. (d) Guerra, G. ; Longo, P.; Cavallo, L.; Corradini, P.; Resconi, L. *J. Am. Chem. Soc.* **1997**, *119*, 4394.
3. Margl, P. M.; Woo, T. K.; Ziegler, T. *Organometallics* **1998**, *17*, 4997.
4. (a) Lin, S.; Kravchenko, R.; Waymouth, R. M. *J. Molec. Catal. A. Chem.* **2000**, *158*, 423. (b) Tsutsui, T.; Kashiwa, N.; Mizuno, A. *Makromol. Chem., Rapid Commun.* **1990**, *11*, 565. (c) Juengling, S.; Müelhaupt, R.; Stehling, U.; Brintzinger, H. –H.; Fischer, D.; Langhauser, F. *J. Polym. Sci., A. Polym. Chem*. **1995**, *33*, 1305. (d) Schaverien, C. J.; Ernst, R.; Schut, P.; Dall'Occo, T. *Organometallics* **2001**, *20*, 3436. (e) Busico, V.; Cipullo, R.; Chadwick, J. C.; Modder, J. F.; Sudmeijer, O. *Macromolecules* **1994**, *27*, 7538. (f) Busico, V.; Cipullo, R.; Ronca, S.

Macromolecules **2002**, *35*, 1537. (g) Busico, V.; Cipullo, R.; Talarico, G. *Macromolecules* **1998**, *31*, 2387.

5. (a) Rieger, B.; Mu, X.; Mallin, D. T.; Rausch, M. D.; Chien, J. C. W. *Macromolecules* **1990**, *23*, 3559. (b) Grassi, A.; Zambelli, A.; Resconi, L.; Albizzati, E.; Mazzocchi, R. *Macromolecules* **1988**, *21*, 617. (c) Stehling, U.; Diebold, J.; Kristen, R.; Röll, W.; Brintzinger, H-. H.; Jüngling, S.; Mülhaupt, R.; Langhauser, F. *Organometallics* **1994**, *13*, 964.
6. (a) Resconi, L.; Camurati, I.; Sudmeijer, O. *Top. Catal.* **1999**, *7*, 145. (b) Resconi, L.; Piemontesi, F.; Camurati, I.; Balboni, D.; Sironi, A.; Moret, M.; Rychlicki, H.; Zeigler, R. *Organometallics* **1996**, *15*, 5046. (c) Resconi, L.; Fait, A.; Piemontesi, F.; Colonnesi, M.; Rychlicki, H.; Zeigler, R. *Macromolecules* **1995**, *28*, 6667.
7. Vatamanu, M.; Boden, B. N.; Baird, M. C. *Macromolecules* **2005,** *38*, 9944.
8. (a) Busico, V.; Cipullo, R.; Friederichs, N.; Ronca, S.; Talarico, G.; Togrou, M.; Wang, B. *Macromolecules* **2004**, *37*, 8201. (b) Busico, V.; Cipullo, R.; Cutillo, F.; Friederichs, N.; Ronca, S.; Wang, B. *J. Am. Chem. Soc.* **2003**, *125*, 12402.
9. Busico, V.; Cippulo, R.; Romanelli, V.; Ronca, S.; Togrou, M. *J. Am. Chem. Soc.* **2005**, *127*, 1608.
10. Tonelli, A. E. *NMR Spectroscopy and Polymer Microstructure: The Conformational Connection*, VCH Publishers, Inc. **1989**.
11. Silverstein, R. M.; Webster, F. X. *Spectrometric Identification of Organic Compounds*, Sixth Ed., John Wiley & Sons, Inc. **1998**.
12. Busico, V.; Cipullo, R.; Friederichs, N.; Ronca, S.; Togrou, M. *Macromolecules* **2003**, *36*, 3806.

13. Lambarti, M.; Gliubizzi, R.; Mazzeo, M.; Tedesco, C.; Pellecchia, C. *Macromolecules* **2004**, *37*, 276.

14. Tshuva, E. Y.; Goldberg, I.; Kol, M. *J. Am. Chem. Soc.* **2000**, *122*, 10707.

15. (a) Zucchini, U.; Albizzati, E.; Giannini, U. *J. Organomet. Chem*. **1971**, *26*, 357. (b) Felten, J. J.; Anderson, W. P. *J. Organometal. Chem*. **1972**, *36*, 87

Chapter 4

Formation and characterization of various types of Zr-allyl complexes obtained from the reaction of $[Cp_2ZrMe]^+$ with $CH_2C(Me)(R)$, (R = H, CH_2CHMe_2, $CH_2CH(Me)(C_3H_7)$). Identification of $[Cp_2Zr(Me)(CH_2C(Me)CH_2CHMe_2)]^+$ as a reaction intermediate

4.1. Introduction

Although zirconocenes are very reactive catalytic species in coordination polymerization of α-olefins, they are also known to undergo a number of deactivating side reactions which lead to a gradual decrease in catalyst activity, and therefore productivity.[1] Despite the extensive research to date on α-olefin polymerization by zirconocene catalysts, the deactivation pathways are still poorly understood.[2] While some of the catalyst can be irreversibly deactivated due to the presence of impurities in the catalytic system, or as a result of decomposition at high temperatures,[2b] a notable fraction of the catalyst is reversibly deactivated, or in a 'dormant' state, as inferred from the observation that the catalyst activity increases when the polymerization is run in the presence of a small amount of H_2.[3]

The hydrogen activation effect was generally attributed[3] to a reactivation of Zr-polymeryl species that underwent a secondary (2,1) insertion of propylene. For steric reasons, after a secondary (2,1) insertion, subsequent propylene insertion is expected to proceed much more slowly than for a primary (1,2) Zr-polymeryl species.[4] Therefore, the secondary (2,1) Zr-polymeryl species may accumulate in the polymerization system as 'dormant' species. However, despite the extensive research conducted on zirconocene catalyzed α-olefin polymerization, attempts to detect secondary Zr-polymeryl intermediates in a polymerization mixture failed[5] and their existence has only been implied from analyses of polymer microstructures[6] and end groups.[7] Furthermore, in a recent study by Landis *et al.*,[8] a secondary Zr-butyl compound was not particularly inert to insertion of propylene and thus, the subject remains controversial.[5a,9]

A few reports also suggested that the hydrogen activation effect can be a result of the hydrogenolysis of Zr-allyl species, also proposed to arise during propylene polymerization and remain in a dormant state.[10] Compared with the previous case when hydrogenolysis of secondary Zr-polymeryl species can be easily noticed by analyzing the ^{13}C NMR spectra of the saturated end groups of the polymer chains,[3] the hydrogenolysis of Zr-allyl species would result in polymers with unsaturated end groups similar to those arising from other chain termination processes (see Equations 4.1 and 4.2; P represents a polymeryl chain and X^- is a weakly coordinating anion or a solvent molecule). Thus, while a high amount of catalyst can be trapped as Zr-allyl species during the polymerization, the hydrogen activation effect as a result of hydrogenolysis of these species can be overlooked.

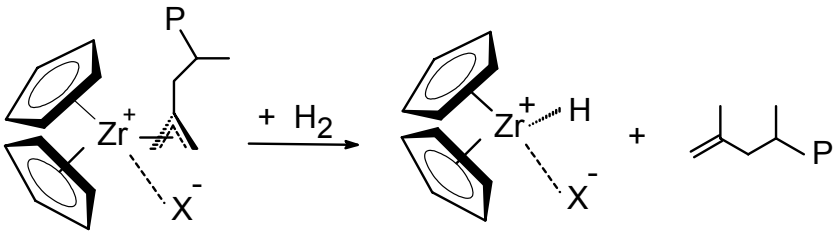

(**4.1**)

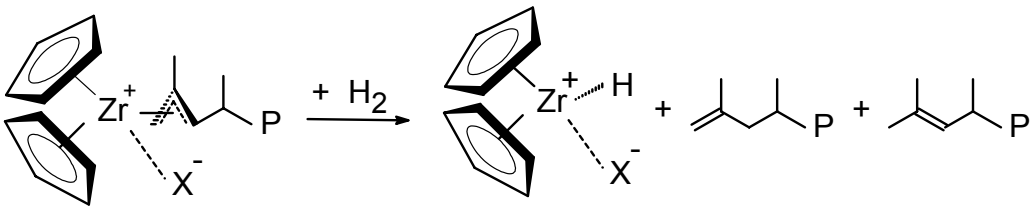

(**4.2**)

Evidence for the formation of Zr-allyl intermediates during zirconocene catalyzed propylene polymerization comes from the detection of internal unsaturation on the polymer chain (Equation 4.3).[7b,11]

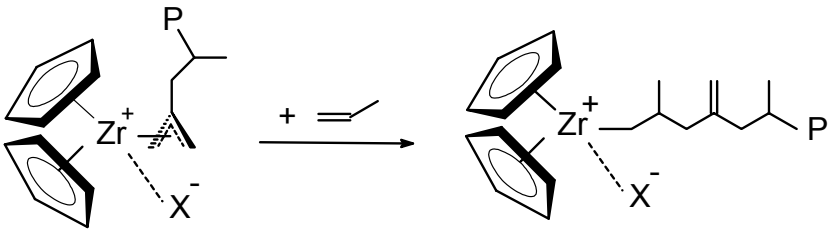

(**4.3**)

More recently, Collins *et al.*[12a] and Landis and Christianson[12b] were able to obtain direct evidence of the presence of Zr-allyl oligomers during propylene and 1-hexene polymerization, respectively, by chiral zirconocene catalysts, by using NMR spectroscopy.

A mechanism proposed to account for the formation of $[Cp'_2Zr(\eta^3\text{-allyl})]^+$ species (Cp' = η^5-cyclopentadienyl type ligand) during the polymerization is presented in Scheme

4.1(a). This mechanism involves coordination of a propylene molecule to the metal center followed by transfer of methyl hydrogen from the coordinated propylene to the Zr-polymeryl group. This leads to the formation of a Zr-allyl complex and the liberation of a polymer chain.[13] Alternatively, a zirconocene polymeryl cation can undergo a β-hydride elimination reaction to form a zirconocene(hydride)(olefin) complex from which a second hydrogen atom from Cγ position can further be transferred to form a $[Cp'_2Zr(\eta^3\text{-allyl})(\text{dihydrogen})]^+$ complex. This complex can then release the dihydrogen ligand to give a $Cp'_2Zr^+(\eta^3\text{-allyl})$polymeryl species as depicted in Scheme 4.1(b).[2b]

Scheme 4.1. Possible mechanisms for formation of Zr-allyl species during propylene polymerization. The counterion X^- has been omitted for simplicity.

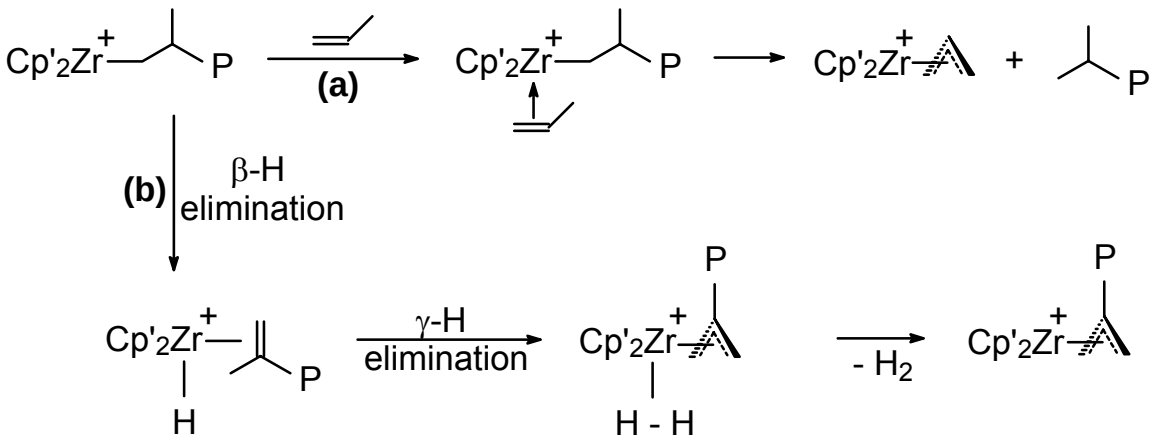

So far, particular attention both theoretically and experimentally has been given to the second mechanism. Moreover, although both mechanisms involve the formation of a $[Cp_2'Zr(R)(\text{olefin})]^+$ intermediate (R = H, alkyl), so far there is no direct characterization of such a species as a reaction intermediate.[14]

As part of an ongoing study on the nature of zirconocene containing intermediates present during propylene polymerization, the possibility of formation of Cp_2Zr^+-allyl complexes from the active catalyst $[Cp_2ZrMe]^+$ and different vinylidene terminated alkyl chains was investigated. The results of a detailed experimental study are presented in this chapter. Specifically, in Section 4.2.1, synthesis and characterization of a series of Cp_2Zr^+-allyl complexes obtained from the reaction between Cp_2ZrMe_2 activated with either $B(C_6F_5)_3$ or $[Ph_3C][B(C_6F_5)_4]$ and 2,4-Me_2-1-pentene and 2,4-Me_2-1-heptene, respectively, in chlorobenzene-d_5 are presented. These complexes can be used as model compounds for different Cp_2Zr^+-allyl polymeryl species which might arise during zirconocene catalyzed propylene polymerization reactions. Reaction of $[Cp_2ZrMe][B(C_6F_5)_4]$ with 2,4-Me_2-1-pentene involves the presence of $[Cp_2Zr(Me)CH_2C(Me)CH_2CHMe_2][B(C_6F_5)_4]$ as an intermediate in the formation of the allyl complex $[Cp_2Zr(\eta^3\text{-}CH_2C(CH_2CHMe_2)CH_2)][B(C_6F_5)_4]$, which was detected by low temperature NMR spectroscopy. The identification of the $[Cp_2Zr(Me)CH_2C(Me)CH_2CHMe_2]^+$ complex represents the first direct experimental evidence of a $[Cp_2Zr(alkyl)(alkene)]^+$ complex as a reaction intermediate. In Section 4.2.2, the Cp_2Zr^+-allyl complexes synthesized in Section 4.2.1 are characterized with respect to their dynamic behavior while in Section 4.2.3 the experimental results of a kinetic study on the $[Cp_2Zr(\eta^3\text{-}CH_2C(CH_2CHMe_2)CH_2)][X]$ complex formation (where [X] is either $[MeB(C_6F_5)_3]$ or $[B(C_6F_5)_4]$) are presented. Direct observation of different Cp_2Zr^+-allyl polymeryl intermediates formed under catalytic conditions, in *in situ* propylene polymerization by either $Cp_2ZrMe_2/B(C_6F_5)_3$ or $Cp_2ZrMe_2/[Ph_3C][B(C_6F_5)_4]$ in

chlorobenzene-d_5 at room temperature, is presented in Section 4.2.4. A summary of the results is presented in Section 4.3 while Section 4.4 presents experimental details.

4.2. Results and Discussion

4.2.1. Synthesis and Characterization of $[Cp_2Zr(\eta^3\text{-allyl})]^+$ species

4.2.1.1. Reaction of $[Cp_2ZrMe][MeB(C_6F_5)_3]$ with 2,4-dimethyl-1-pentene

The $[Cp_2ZrMe][MeB(C_6F_5)_3]$ ion pair, generated *in situ* by reacting Cp_2ZrMe_2 with 1.1 equivalents of $B(C_6F_5)_3$, was reacted with 1.5 equivalents of 2,4-dimethyl-1-pentene in chlorobenzene-d_5 at room temperature. The reaction was completed within 8 hours and resulted in a slow change in color of the reaction mixture from yellow to orange-brown. When 5 equivalents of 2,4-dimethyl-1-pentene were used the reaction was completed in less than three hours. In principle, as shown in Scheme 4.2, two kinds of $Zr(\eta^3\text{-allyl})$ species can be formed: $[Cp_2Zr(\eta^3\text{-}CH_2C(CH_2CHMe_2)CH_2)]^+$ (**A**) and $[Cp_2Zr(\eta^3\text{-}CH_2C(Me)CHCHMe_2)]^+$ (**B**)

Scheme 4.2. The structures of Zr-allyl complexes which may form from the reaction of $[Cp_2ZrMe][MeB(C_6F_5)_3]$ with 2,4-dimethyl-1-pentene.

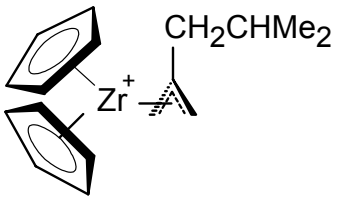

(**A**)

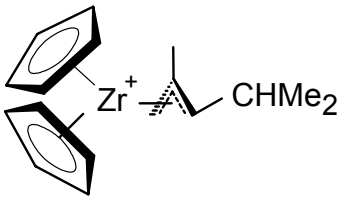

(**B**)

The *in situ* reaction between $[Cp_2ZrMe][MeB(C_6F_5)_3]$ and 2,4-dimethyl-1-pentene at room temperature was monitored by ^1H NMR spectroscopy over several hours and a plot showing the progress of the reaction is given in Figure 4.1.

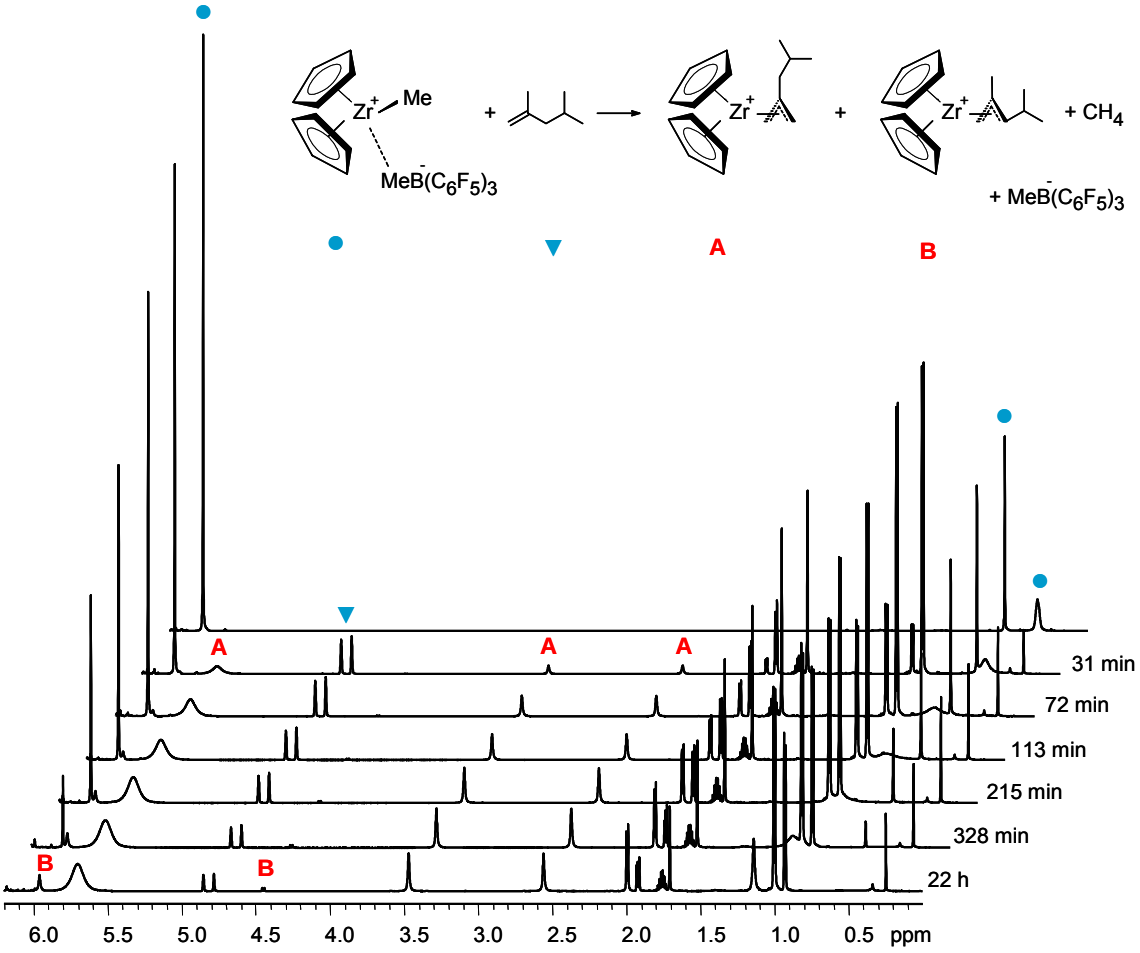

Figure 4.1. ^1H NMR spectra of the *in situ* reaction between $[Cp_2ZrMe][MeB(C_6F_5)_3]$ (1 equivalent) and 2,4-dimethyl-1-pentene (1.5 equivalents) in chlorobenzene-d_5 at room temperature (600 MHz).

As can be seen from Figure 4.1, as the reaction proceeds, the **Cp** and Zr-**Me** resonances of the $[Cp_2ZrMe][MeB(C_6F_5)_3]$ ion pair at 5.97 ppm (singlet) and 0.56 ppm

(singlet), respectively, and the 2,4-dimethyl-1-pentene resonances at 4.86 ppm (singlet, CH_2=) and 4.78 ppm (singlet, CH_2=), 1.92 ppm (doublet, CH_2), 1.77 ppm (multiplet, CH), 1.71 ppm (singlet, CH_3), and 0.93 ppm (doublet, CH_3) decrease in intensity. The **Me**-B resonance of the $[Cp_2ZrMe][MeB(C_6F_5)_3]$ ion pair at 0.34 ppm (broad singlet), on the other hand, broadens and shifts downfield to a position of free $[MeB(C_6F_5)_3]^-$. Note that the **Me**-B resonance in free $[MeB(C_6F_5)_3]^-$ appears at 1.16 ppm as determined by the reaction of $[Cp_2ZrMe][MeB(C_6F_5)_3]$ with 3 equivalents of CD_3CN in chlorobenzene-d_5 (see Section 4.4.5).

During the course of the reaction, a series of new peaks at 5.70 ppm (broad singlet), 3.47 ppm (sharp singlet), 2.56 ppm (sharp singlet), 1.99 ppm (doublet), and 0.98 ppm (doublet) appeared in addition to the singlet at 0.25 ppm, attributable to methane. The relative intensities of the resonances at 5.70, 3.47 and 2.56 ppm were 10:2:2. On this basis, and in consideration of previous reports on similar complexes,[15] the broad resonance at 5.70 ppm was attributed to the two Cp groups of the Zr-allyl complex **A** while the resonances at 3.47 and 2.56 ppm were attributed to the allyl CH_2 hydrogen atoms of the Zr-allyl complex **A**. Furthermore, the resonances at 1.99 and 0.98 ppm were attributed to the C**H**$_2$CHMe$_2$ and CH$_2$CH**Me**$_2$ groups, respectively. The CH$_2$C**H**Me$_2$ resonance could not be observed and it is likely overlapped by the analogous methyne resonance of unreacted 2,4-Me$_2$-1-pentene at 1.77 ppm.

In order to confirm the above assignments and to better characterize the $[Cp_2Zr(\eta^3\text{-}CH_2C(CH_2CHMe_2)CH_2)]^+$ complex (**A**), the sample was cooled to 0°C and further analyzed by ^{1}H NMR and correlation spectroscopy. A typical ^{1}H NMR spectrum of the reaction mixture at 0°C is shown in Figure 4.2.

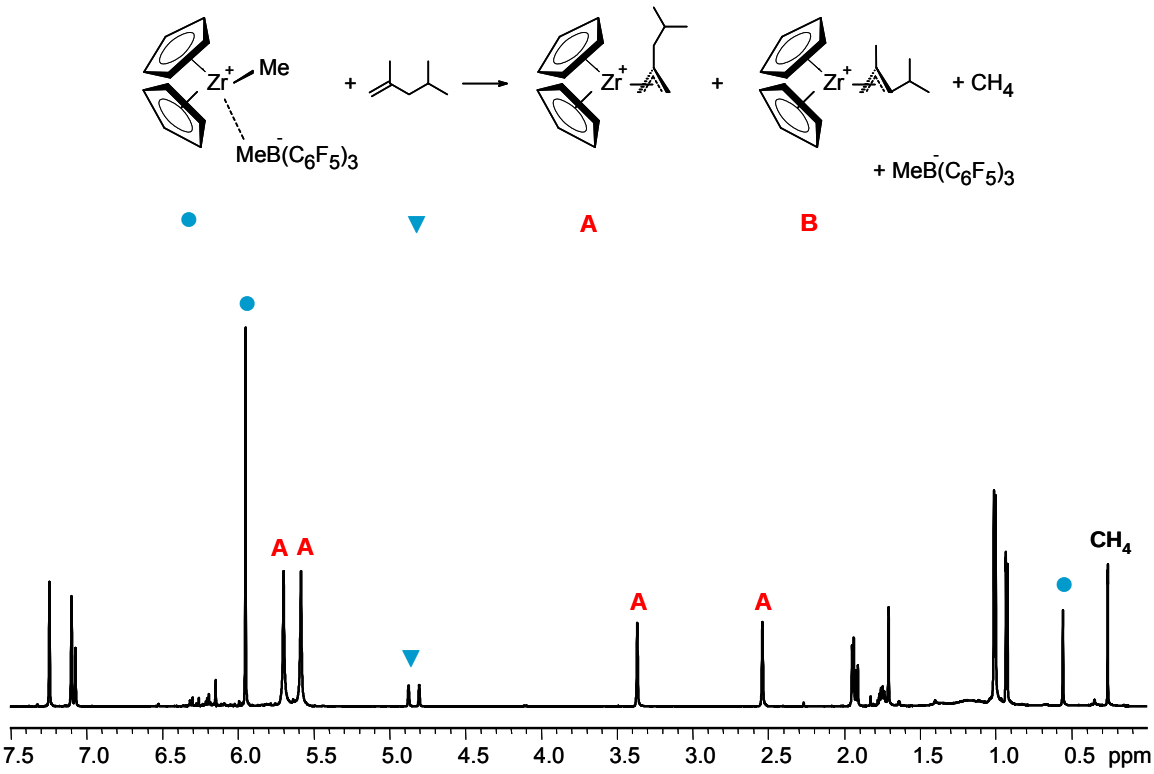

Figure 4.2. ^{1}H NMR spectrum of the *in situ* reaction between $[Cp_2ZrMe][MeB(C_6F_5)_3]$ (1 equivalent) and 2,4-Me_2-1-pentene (1 equivalent) in C_6D_5Cl at 0°C (600 MHz).

From Figures 4.1 and 4.2 it can be noticed that on cooling the reaction mixture from 25°C to 0°C, the broad Cp resonance at 5.70 ppm decoalesces to two sharp singlets of equal intensity at 5.70 and 5.58 ppm. The nonequivalence of the two Cp resonances in complex **A** at this temperature is consistent with a virtually static structure of the η^3-coordinated allyl ligand relative to the Cp_2Zr^+ moiety. This behavior was previously observed for similar complexes.[15,16]

A COSY spectrum showed that the two resonances at 2.54 and 3.36 ppm are coupled to one another while an HSQC experiment indicated that they are attached to a

carbon atom which occurs in the carbon spectrum at 67.2 ppm. Thus, the two resonances at 2.54 and 3.36 ppm can be clearly assigned to nonequivalent *syn/anti* hydrogens of a terminal CH_2 allyl group confirming the previous assignment. A long-range $^{1}H–^{13}C$ correlation spectrum (HMBC) showed that both CH_2 allyl resonances at 2.54 and 3.36 ppm exhibited cross peaks with the carbon resonance at 67.2 ppm consistent with the presence of two equivalent terminal CH_2 allyl groups which are correlated to each other by long-range (^{3}J) carbon-proton couplings. Also, the ^{1}H-^{13}C HMBC spectrum showed that the two CH_2 allyl resonances at 2.54 and 3.36 ppm and the methylene resonance at 1.94 ppm are correlated with a carbon resonance at 162 ppm which can be assigned to the central allyl carbon atom of complex **A**. The other alkyl group resonances of complex **A** could be identified following a similar procedure. The chemical shifts assigned to the η^3-coordinated allyl moiety of **A** are shown in Scheme 4.3 and are consistent with data reported in the literature for similar complexes.[15a,16a,17]

Scheme 4.3. The NMR spectroscopic data of the η^3-$CH_2C(CH_2CHMe_2)CH_2$ ligand of complex **A** (chlorobenzene-d_5, 0°C, 600 MHz). ^{13}C resonances of the allyl unit are provided between parentheses; δ in ppm.

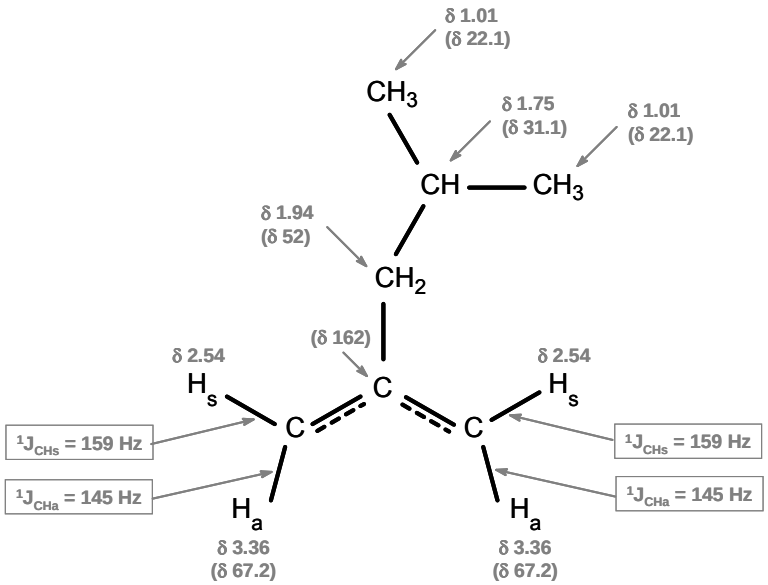

Important structural information for complex **A** can also be obtained from a NOESY experiment. The NOESY spectrum shows strong correlations between the allylic CH_2 resonance at 2.54 ppm and the methylene (1.94 ppm), methyne (1.75 ppm), and methyl (1.01 ppm) resonances of the -CH_2CHMe_2 group. In contrast, the other allylic CH_2 resonance, at 3.36 ppm, shows only very weak correlations with the methylene (1.94 ppm) and methyl (1.01 ppm) resonances. Also, no NOESY correlation between the allylic CH_2 resonance at 3.36 ppm and the methyne resonance at 1.75 ppm was detected. These observations suggest that the allylic CH_2 hydrogens which give rise to the resonance at 2.54 ppm have a *syn* arrangement with respect to the –CH_2CHMe_2 group while those which give rise to the resonance at 3.36 ppm have an *anti* configuration.

NOESY cross peaks between both Cp resonances and the two allylic CH_2 resonances and those between both Cp resonances and the methylene ($C\mathbf{H}_2CHMe_2$) resonance are also present, as expected for a η^3-allyl arrangement in complex **A**.

Further information about the structure of complex **A** was obtained from the one-bond ^{13}C - ^{1}H coupling constants of the allylic methylene groups. Thus, on the basis of an HSQC experiment without spin decoupling, the $^{1}J_{CH}$ values of 145 Hz and 159 Hz were measured for the ^{13}C - $^{1}H_{anti}$ and ^{13}C - $^{1}H_{syn}$ couplings, respectively. These one-bond ^{13}C - ^{1}H coupling constants indicate a high degree of unsaturation of the two terminal allylic CH_2 groups[18] as expected for a η^3-allyl moiety and they are in good agreement with literature data for similar η^3-allylic structures.[17,19] A larger ^{13}C-^{1}H coupling constant for *syn* hydrogens as compared with *anti* hydrogens was also previously reported for similar complexes[19] and it was explained in terms of distortions of the η^3-allyl group with respect to the Cp_2Zr^+ moiety in which *syn* hydrogens are bent from the allyl carbon plane toward the metal, while the *anti* hydrogens are bent away from the metal,[19] a feature which was also observed by X-ray analysis of similar complexes.[20]

Interestingly, as the reaction progressed, a new set of much weaker resonances arises in the ^{1}H NMR spectra in addition to the complex **A** resonances (see Figure 4.1), which suggested the presence of a second Zr-allyl species in the reaction mixture. This new set of resonances becomes more obvious in the ^{1}H NMR spectra after cooling the probe temperature to -40°C. A typical ^{1}H NMR spectrum of the reaction mixture at -40°C is depicted in Figure 4.3 where the resonances in question are identified as "**B**".

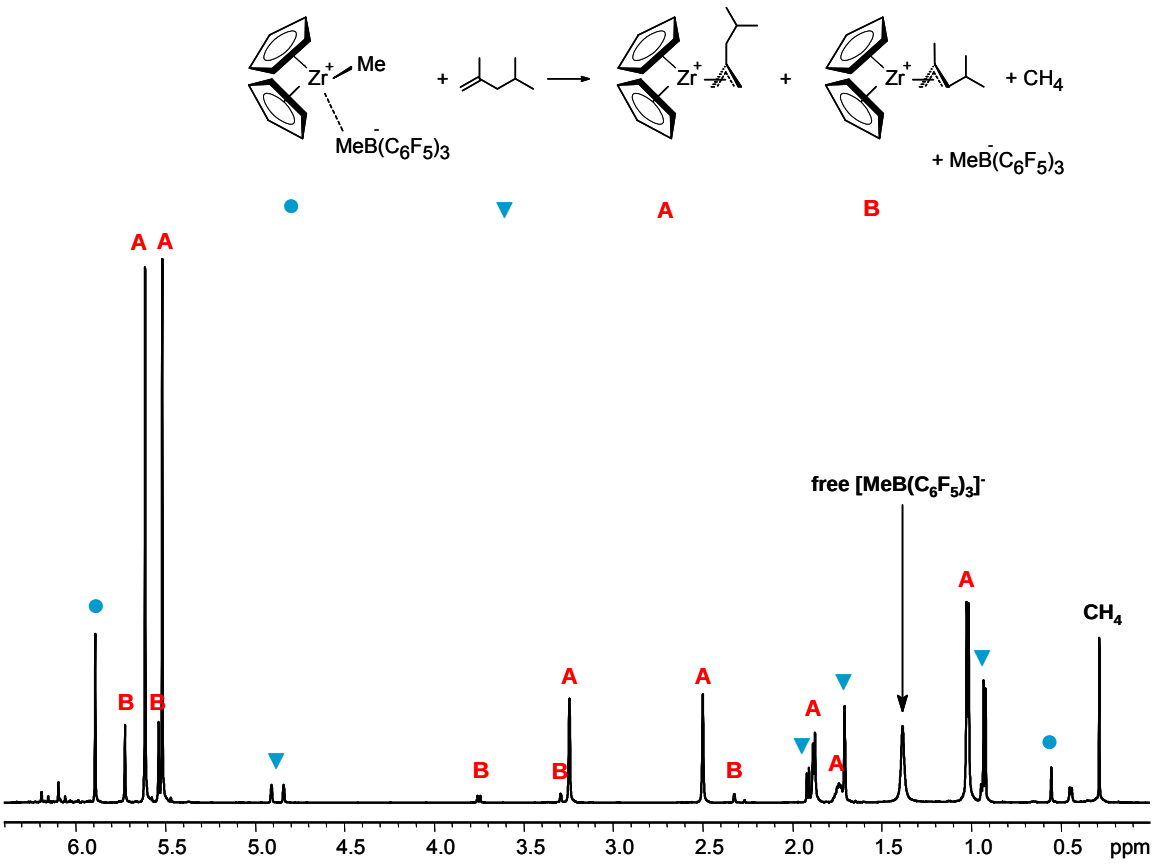

Figure 4.3. ^{1}H NMR spectrum of the *in situ* reaction between $[Cp_2ZrMe][MeB(C_6F_5)_3]$ (1 equivalent) and 2,4-dimethyl-1-pentene (1 equivalent) in chlorobenzene-d_5. (600 MHz, -40°C).

On cooling from room temperature to -40°C, the broad resonance at 5.96 ppm (at 25°C) decoalesced into two sharp singlets of comparable intensity at 5.72 and 5.54 ppm and therefore they were assigned to the two Cp groups in complex **B**. The non-equivalence of the two Cp resonances of **B** is consistent with a η^3-coordinated allylic complex in a virtually static form. Weak resonances of comparable intensity were also present in the ^{1}H NMR spectrum at 3.75 ppm (doublet, J_{HH} = 9.4 Hz), 3.29 ppm (doublet, J_{HH} = 1.9 Hz) and 2.32 ppm (doublet, J_{HH} = 1.9 Hz). The ratio of the relative intensities between the

resonances at 5.72 and 5.54 ppm and the resonances at 3.75, 3.29, and 2.32 ppm is 5:1. On this basis, as well as on the basis of proton spin coupling constants,[18] the resonances at 3.29 and 2.32 ppm were assigned to the terminal allylic CH_2 hydrogens of **B** while the resonance at 3.75 ppm was assigned to the allylic methyne hydrogen of **B**. Although the other resonances of **B** could not be clearly identified at this temperature, the ^1H NMR spectrum shows also the presence of a small doublet at 0.44 ppm (J_{HH} = 6.0 Hz). The relative intensity of the resonance at 0.44 ppm as compared with the resonances at 3.29, 2.32 and 3.75 ppm is 3:1 and it was assigned to one of the terminal methyl resonances of the $CHMe_2$ group of **B**. The other methyl resonance is partially overlapped with the terminal methyl resonance of 2,4-dimethyl-1-pentene at 0.94 ppm.

Attempts to obtain useful two-dimensional NMR spectra of complex **B** at -40°C failed. However, an HSQC experiment run at 0°C indicates that the CH allyl resonance, which at this temperature appears at 4.1 ppm, is correlated with a carbon resonance at 92 ppm ($^1J_{CH}$ = 143 Hz) while an HMBC experiment indicates long range ^1H-^{13}C correlations between the resonance at 4.1 ppm and carbon resonances at 70 and 159 ppm. On the basis of these correlations, and consistent with literature precedents,[13a,16a] the ^{13}C resonances at 70, 159 and 92 ppm were attributed to the carbon atoms of the terminal CH_2 allyl group, the central allyl carbon and the CH allyl group, respectively. Scheme 4.4 identifies the chemical shifts at 0°C assigned to complex **B**.

Scheme 4.4. The NMR spectroscopic data of the η^3-$CH_2C(Me)CHCHMe_2$ ligand of complex **B** (chlorobenzene-d_5, 0°C, 600 MHz). ^{13}C resonances of the allyl unit are provided between parentheses; δ in ppm.

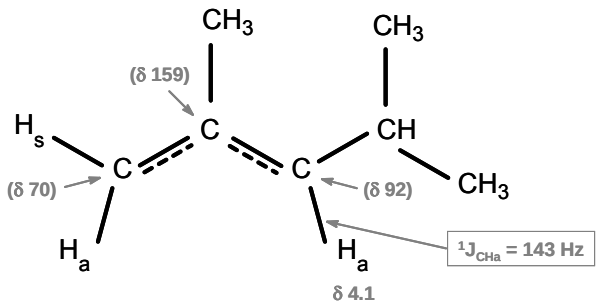

4.2.1.2. Reaction of $[Cp_2ZrMe][MeB(C_6F_5)_3]$ with 2,4-dimethyl-1-heptene

Addition of 2,4-dimethyl-1-heptene to a solution of $[Cp_2ZrMe][MeB(C_6F_5)_3]$, generated *in situ* by reacting Cp_2ZrMe_2 with 1.1 equivalents of $B(C_6F_5)_3$ in chlorobenzene-d_5 at room temperature, resulted in a slow color change of the reaction mixture from yellow to orange-brown. When equimolar amounts of 2,4-dimethyl-1-heptene and $[Cp_2ZrMe][MeB(C_6F_5)_3]$ were used, the reaction was completed within 8 hours while, when a 5-fold excess of 2,4-dimethyl-1-heptene was used, the reaction was completed within one hour.

The reaction between $[Cp_2ZrMe][MeB(C_6F_5)_3]$ and 2,4-dimethyl-1-heptene (1:1 mole ratio) was monitored by ^1H NMR spectroscopy over several hours and a typical plot showing the progress of the reaction is presented in Figure 4.4.

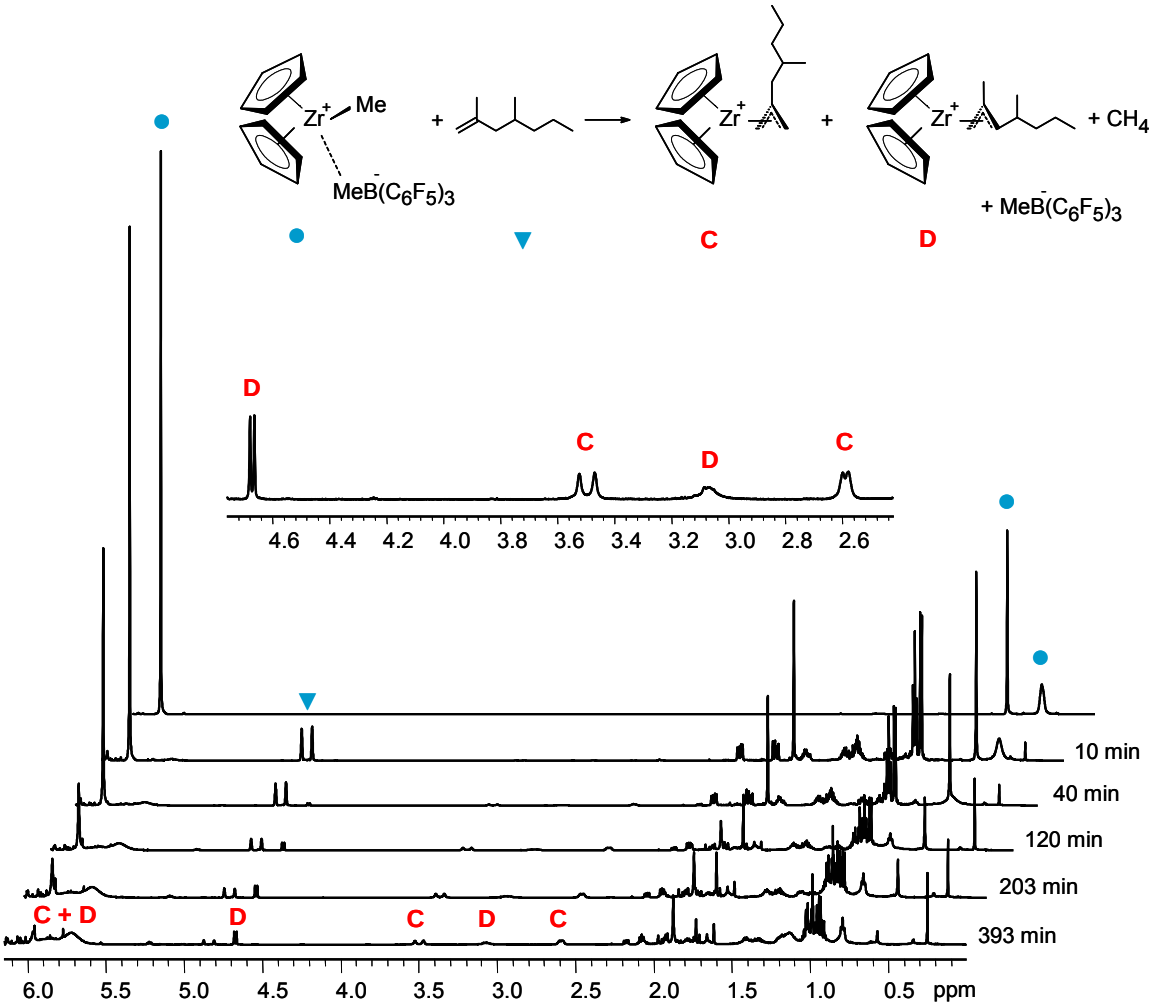

Figure 4.4. ^{1}H NMR spectra of the *in situ* reaction between $[Cp_2ZrMe][MeB(C_6F_5)_3]$ and 2,4-dimethyl-1-heptene (1:1 mole ratio) in chlorobenzene-d_5 at room temperature (600 MHz). The inset shows an expanded view of the allylic region.

During the course of the reaction, the **Cp** and Zr-**Me** resonances of the $[Cp_2ZrMe][MeB(C_6F_5)_3]$ ion pair at 5.97 and 0.56 ppm, respectively, and the 2,4-dimethyl-1-heptene resonances at 4.86 ppm (singlet, CH_2=), 4.78 ppm (singlet, CH_2=), 1.92 ppm (doublet, CH_2), 1.77 ppm (multiplet, CH), 1.71 ppm (singlet, CH_3), and 0.93 ppm (doublet, CH_3), slowly decreased in intensity. The **Me**-B resonances of the

$[Cp_2ZrMe][MeB(C_6F_5)_3]$ ion pair at 0.34 ppm, on the other hand, shifted downfield and broadened sufficiently that it eventually became undetectable.

As the reaction progressed, there appeared a series of exchange broadened resonances in the Cp (5.5–6.0 ppm) and allyl (2.5–4.7 ppm) regions of the ^{1}H NMR spectrum in addition to a singlet at 0.25 ppm, attributed to methane. A closer look at the allylic region of the ^{1}H NMR spectra revealed the presence of what appears to be two different sets of resonances, one set at 3.52 and 3.47 ppm (two peaks) and 2.60 and 2.58 ppm (two peaks), and the other set at 4.67 ppm (doublet) and 3.06 ppm (broad singlet). These two sets of resonances increase in intensity at different rates, suggesting the presence of two different Zr-allyl complexes in solution. Thus, at the beginning of the reaction the Zr-allyl complex which gives rise to the set of resonances at ~3.5 ppm (two peaks) and ~2.6 ppm (two peaks) forms faster than the one which gives rise to the set of resonances at 4.67 ppm (doublet) and 3.06 ppm (broad singlet). However, as the reaction progresses, the ratio between the two Zr-allyl complexes became almost equal and remains constant until the end of the reaction. When equimolar amounts of 2,4-dimethyl-1-heptene and $[Cp_2ZrMe][MeB(C_6F_5)_3]$ are used, the two Zr-allyl species form in a ratio of 1.2 (3.5 and 2.6 ppm) to 1 (4.67 and 3.06 ppm); yet, the reaction involving a high excess of 2,4-dimethyl-1-heptene (10 equivalents) results in formation of only the Zr-allyl complex which gives rise to the set of resonances at ~3.5 and 2.6 ppm; the reason for this behavior is not clear. The relative intensities of the resonances at ~3.5 and 2.6 ppm were 1:1 and on the basis of comparison with previously identified complex **A**, the resonances at ~3.5 and 2.6 ppm were tentatively assigned to the *syn/anti* hydrogens of the CH_2 allyl group in **C** (See Scheme 4.5). The ratio of the relative intensities of the

resonances at 4.67 and 3.06 ppm were also 1:1 and they were tentatively assigned to the allyl hydrogens of complex **D** (Scheme 4.5).

Scheme 4.5. The structures of Zr-allyl complexes which may form from the reaction of $[Cp_2ZrMe][MeB(C_6F_5)_3]$ with 2,4-dimethyl-1-heptene.

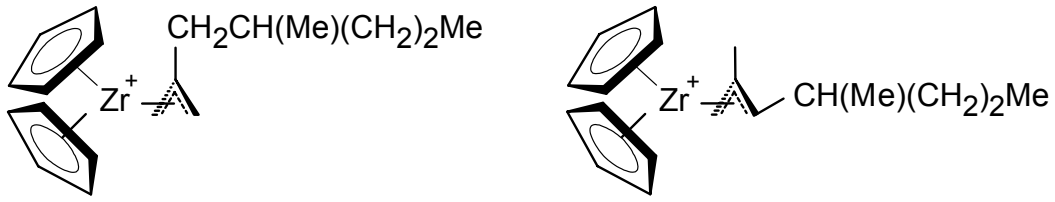

(**C**) (**D**)

In order to better identify and characterize the two Zr-allyl complexes **C** and **D**, the sample was cooled to 0°C and analyzed by ^{1}H NMR and correlation spectroscopy. Figure 4.5 provides an expanded view between 5.5 and 6.0 ppm and between 2.5 and 4.7 ppm of the ^{1}H NMR spectrum of a reaction mixture after cooling at 0°C.

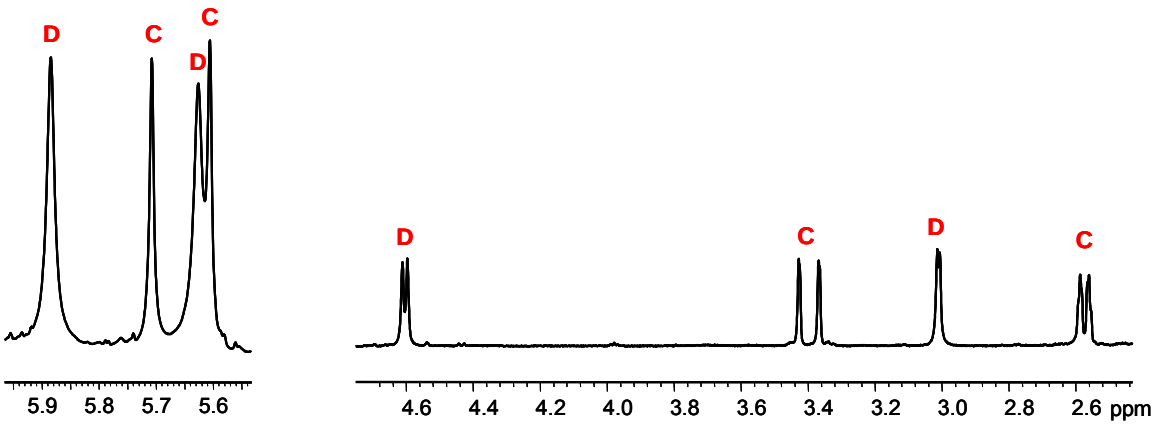

(a) (b)

Figure 4.5. ^{1}H NMR spectrum of the *in situ* reaction between $[Cp_2ZrMe][MeB(C_6F_5)_3]$ and 2,4-Me_2-1-heptene in chlorobenzene-d_5 at 0°C: (a) expansion of the Cp region and (b) expansion of the allylic region.

As can be seen from Figures 4.4 and 4.5(a), lowering the sample temperature from room temperature to 0°C resulted in decoalescence of the broad unresolved resonance between 5.5 and 6.0 ppm into four separate Cp resonances at 5.88, 5.71, 5.62, and 5.61 ppm. Two sets of Cp resonances in the ^{1}H NMR spectrum of the reaction mixture products are consistent with the presence of two separate $Cp_2Zr^{+}(\eta^{3}$-allyl) complexes in a virtually static structure.

By lowering the sample temperature to 0°C, all broad resonances in the allylic region of the ^{1}H NMR spectrum become narrow. At this temperature, the first set of allylic resonances consists of two groups of singlets of comparable intensity, one at 3.42 and 3.36 ppm and the other one at 2.58 and 2.56 ppm. The second set of allylic resonances consists of two doublets of comparable intensity at 4.60 ppm (J_{HH} = 9.1 Hz) and 3.01 ppm (J_{HH} = 4.5 Hz).

A COSY spectrum showed that the proton at 3.42 ppm is coupled to the proton at 2.58 ppm while the proton 3.36 ppm is coupled to the proton at 2.56 ppm. A complementary HSQC experiment indicated that the protons at 3.42 and 2.58 ppm are attached to a carbon atom which occurs in the carbon spectrum at 68 ppm, while the protons at 3.36 and 2.56 ppm are attached to a carbon atom which occurs in the carbon spectrum at 67 ppm. On the basis of the above correlations, and in agreement with literature data,[15a,17] the pair of peaks at 3.42 and 2.58 ppm (^{13}C resonance at 68 ppm) and the pair of peaks at 3.36 and 2.56 ppm (^{13}C resonance at 67 ppm) were assigned to the terminal CH_2 allyl groups in **C**. The slight non-equivalence of the two terminal CH_2 allyl groups is probably due to the presence of a chiral center in the allyl ligand.[18,21]

An HMBC spectrum showed long range ^{1}H-^{13}C correlations between the CH_2 allyl resonances at 3.42 and 3.36 ppm and carbon resonances at 67 and 68 ppm, respectively, indicating that the two terminal CH_2 allyl groups are connected to each other via long range correlation. In addition, the HMBC spectrum also shows long range ^{1}H-^{13}C correlations between the two CH_2 allyl resonances at 2.58 and 2.56 ppm and a carbon resonance at 162 ppm, which can be assigned to the central allyl carbon of complex **C**.

The protons of the two terminal CH_2 allyl groups all exhibited HMBC cross peaks with a carbon resonance at 50.6 ppm which in turn shows HSQC correlations with two protons at 1.89 and 2.14 ppm. On this basis, the proton resonances at 1.89 and 2.14 ppm and the carbon resonance at 50.6 ppm were attributed to C**H**$_2$CH(Me)(CH$_2$)$_2$Me and **C**H$_2$CH(Me)(CH$_2$)$_2$Me, respectively. The other alkyl group resonances of complex **C** could be identified following a similar procedure. Thus, the CH$_2$C**H**(Me)(CH$_2$)$_2$Me

resonance appears at 1.64 ppm (^{13}C resonance at 35.8 ppm), the $CH_2CH(\mathbf{Me})(CH_2)_2Me$ resonance appears 0.99 ppm (^{13}C resonance at 19 ppm) and $CH_2CH(Me)C\mathbf{H}_2CH_2Me$ resonances appear at 1.39 and 1.18 ppm (^{13}C resonance at 39 ppm). The resonances of the terminal ethyl group of $CH_2CH(Me)CH_2CH_2CH_3$ have not been assigned due to extensive overlapping with similar resonances of complex **D** and unreacted 2,4-dimethyl-1-heptene.

Further information about the structure of complex **C** comes from a NOESY experiment. Thus, a NOESY spectrum shows strong correlations between the two allylic CH_2 resonances at 2.56 and 2.58 ppm and the $CH_2CH(Me)(CH_2)_2Me$ group resonances at 2.14, 1.89, 1.64, and 0.99 ppm; the two allylic CH_2 protons at 3.42 and 3.36 ppm, on the other hand, are not correlated with the $CH_2CH(Me)(CH_2)_2Me$ group hydrogens. This implies that the two CH_2 allyl protons at 2.56 and 2.58 ppm are *syn* with respect to the $CH_2CH(Me)(CH_2)_2Me$ group while the two CH_2 allyl protons at 3.42 and 3.36 ppm are *anti*. Furthermore, the NOESY spectrum also shows correlations between the two Cp resonances at 5.71 and 5.61 ppm and the *syn* (2.56 and 2.58 ppm) and *anti* (3.42 and 3.36 ppm) hydrogens of the allylic CH_2 groups of **C**. Also there were correlations between the two Cp resonances at 5.71 and 5.61 ppm and the $C\mathbf{H}_2CH(Me)(CH_2)_2Me$ hydrogens at 1.89 and 2.14 ppm. These NOESY correlations clearly indicate that the proton resonances at 5.71 and 5.61 ppm correspond to non-equivalent Cp groups of complex **C** and that the allyl group of **C** is η^3-coordinated to the Cp_2Zr^+ moiety.

Similar to the previously characterized complex **A**, the one bond ^{13}C-^{1}H coupling constants for the *anti* hydrogens of the terminal CH_2 allyl groups of **C** (145 Hz) are smaller than those for *syn* hydrogens of the terminal CH_2 allyl groups of **C** (159 Hz). The

close similarity between the $^{1}J_{CH}$ in the two Zr-allyl complexes suggests that the η^3-allyl ligands in complexes **A** and **C** adopt a similar spatial arrangement relative to the Cp_2Zr^+ moiety. A summary of chemical shifts assigned to the η^3-allyl ligand of complex **C** are shown in Scheme 4.6.

Scheme 4.6. The NMR spectroscopic data of the η^3-$CH_2C(CH_2CH(Me)CH_2CH_2CH_3)CH_2$ ligand of complex **C** (chlorobenzene-d_5, 0°C, 600 MHz). ^{13}C resonances of the allyl unit are provided between parentheses; δ in ppm. The asterisk (*) denotes the location of the chiral carbon.

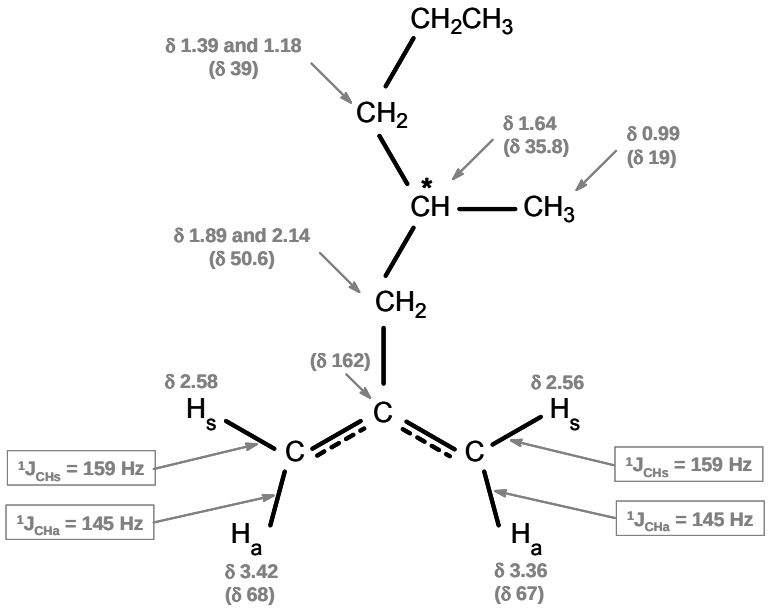

As mentioned above and shown in Figure 4.5(b), a second set of resonances are also present in the allylic region of the ^{1}H NMR spectrum of the *in situ* reaction between $[Cp_2ZrMe][MeB(C_6F_5)_3]$ and 2,4-Me_2-1-heptene in chlorobenzene-d_5 at 0°C, at 4.60 ppm

(doublet) and 3.0 ppm (doublet). The proton at 3.0 ppm is correlated in the COSY spectrum with a proton at 1.85 ppm while the proton at 4.6 ppm is correlated to a proton at 1.7 ppm. An HSQC experiment indicated that both protons at 3.0 and 1.85 ppm are attached to a carbon atom which gives a resonance at 57 ppm while the proton at 4.6 ppm is attached to a carbon atom which occurs in the ^{13}C NMR spectrum at 106 ppm. A complementary HMBC experiment indicates that the proton at 4.6 ppm exhibits long range ^{1}H-^{13}C correlation with the carbon resonance at 57 ppm while the proton at 3.0 ppm is correlated with the carbon resonance at 106 ppm. Furthermore, both protons at 3.0 and 4.6 ppm exhibit long range ^{1}H-^{13}C correlations with the carbon atoms at 158 and 23 ppm. On the basis of these correlations, the two protons at 3.0 and 1.85 ppm (^{13}C resonance at 57 ppm) were assigned to the *syn/anti* hydrogens of the terminal CH_2 allyl group of **D** while the proton at 4.6 ppm (^{13}C resonance at 106 ppm) was assigned to the substituted methyne allyl group of **D**. Moreover, the carbon resonance at 158 ppm was assigned to the central allyl carbon atom CH_2**C**(Me)CHCH(Me)Pr (Pr = propyl), while the carbon resonance at 23 ppm (^{1}H resonance at 1.82 ppm) was attributed to the methyl CH_2C(**Me**)CHCH(Me)Pr group of complex **D**.

It can be noticed that the chemical shift of the terminal CH_2 allyl carbon (57 ppm) is closer to an alkyl carbon chemical shift rather than an olefinic one (110-150 ppm);[18] likewise, the proton-proton coupling constant of the terminal CH_2 allyl hydrogen at 3.0 ppm ($^{2}J_{HH}$ = 4.5 Hz) is much larger than a typical proton-proton coupling constant between two geminal hydrogens on a =CH_2 group ($^{2}J_{HH}$ = 0-2 Hz).[18] The chemical shifts of the substitured CH allyl carbon (106 ppm) and hydrogen (4.6 ppm), on the other hand, are closer to olefinic chemical shifts.[18] This suggests a high degree of distortion of the

allyl ligand of **D** from an η^3- toward an η^1-configuration, a characteristic which was actually observed in X-ray studies of similar complexes.[22]

A NOESY spectrum shows strong correlations between the resonance at 4.6 ppm ($CH_2C(Me)C\mathbf{H}CH(Me)Pr$) and the resonances at 3.0 ppm ($C\mathbf{H}_2C(Me)CHCH(Me)Pr$) and 0.81 ppm ($^{13}C$ resonance at 20 ppm) attributed to $CH_2C(Me)CHCH(\mathbf{Me})Pr$ but no correlation between the resonance at 4.6 ppm ($CH_2C(Me)C\mathbf{H}CH(Me)Pr$) and the resonance at 1.82 ppm ($CH_2C(\mathbf{Me})CHCH(Me)Pr$). This indicates that the substituted methyne allyl hydrogen at 4.6 ppm and the CH_2 allyl hydrogen which gives rise to the resonance at 3.0 ppm are *anti* with respect to the $-CH_2C(\mathbf{Me})CHCH(Me)Pr$ group of **D** while the CH_2 allyl hydrogen at 1.85 ppm is *syn*. Also, the NOESY experiment indicates correlations between the Cp resonances at 5.88 and 5.62 ppm and the resonances at 4.6, 3.0, and 1.85 ppm, as expected for a η^3 coordination of the allyl unit to the Cp_2Zr group in **D**.

Additional structural information of the allyl unit of **D** is obtained from the one bond ^{13}C-^1H coupling constants. Thus, for the allyl CH_2 group, $^1J_{CH}$ value for C-H_{anti} (149 Hz) is different from the $^1J_{CH}$ value for C-H_{syn} (157 Hz) but both values are typical of an allyl group. The $^1J_{CH}$ value for the allyl CH group on the other hand (137 Hz) is out of range for a $^1J_{CH}$ of an olefinic group (~ 140-160 Hz),[18] although both carbon (106 ppm) and hydrogen (4.6 ppm) resonances of the allyl CH group are closer to those for the olefinic region. This unusual $^1J_{CH}$ value might be explained by further distortion of the allyl ligand relative to the Cp_2Zr^+ unit, in which the *anti* hydrogen of the substituted CH allyl group is tilted away from the metal while the electron density is accumulating on the

metal side of the allyl.[19b] A summary of the chemical shifts assigned to the η^3-allyl ligand of complex **D** are shown in Scheme 4.7.

Scheme 4.7. The NMR spectroscopic data of the η^3-$CH_2C(Me)CHCH(Me)CH_2CH_2CH_3$ ligand of complex **D** (chlorobenzene-d_5, 0°C, 600 MHz). ^{13}C resonances of the allyl unit are provided between parentheses; δ in ppm.

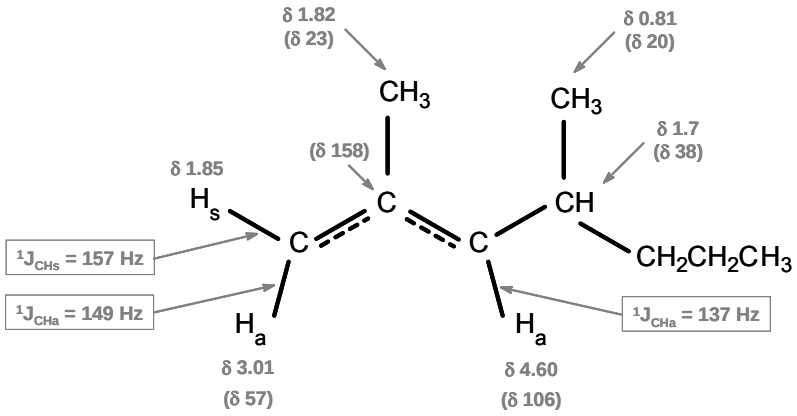

4.2.1.3. Reaction of $[Cp_2ZrMe][B(C_6F_5)_4]$ with 2,4-Me_2-1-pentene. Identification of $[Cp_2Zr(Me)(CH_2C(Me)CH_2CHMe_2)]^+$ as a Reaction Intermediate

In order to investigate the possible effect of counteranion on the formation of cationic Zr-allyl complexes, the reaction between 2,4-Me_2-1-pentene and Cp_2ZrMe_2 activated with $[Ph_3C][B(C_6F_5)_4]$ was also performed.

In a typical experiment, Cp_2ZrMe_2 was reacted with 1.0-1.1 equivalents of $[Ph_3C][B(C_6F_5)_4]$ in chlorobenzene-d_5 at room temperature to give $[Cp_2ZrMe][B(C_6F_5)_4]$ ion pair and the neutral Ph_3CMe. The resulting ^1H NMR spectrum is shown in Figure 4.6(a). In addition to the $[Cp_2ZrMe][B(C_6F_5)_4]$ resonances at 5.99 ppm (**Cp**) and 0.78

ppm (Zr-**Me**) and the Ph_3CMe resonances at 7-7.5 ppm (**Ph**) and 2.13 ppm (**Me**), the ^1H NMR spectrum of the *in situ* generated ion pair solution shows the presence of additional resonances at 0.20 and -0.89 ppm of relative intensities 6:3. On the basis of the relative intensities and by comparison with literature data,[23] the resonances at 0.2 and -0.89 ppm were attributed to the Zr-**Me** and the μ-**Me** resonances, respectively, of the bridged μ-Me binuclear species $[(Cp_2ZrMe)_2(\mu\text{-}Me)][B(C_6F_5)_4]$. The Cp resonance of the $[(Cp_2ZrMe)_2(\mu\text{-}Me)]^+$ was not observed and is presumably overlapped with the Cp resonance of $[Cp_2ZrMe]^+$.

On addition of 1.0-1.5 equivalents of 2,4-Me_2-1-pentene to the chlorobenzene-d_5 solution of $[Cp_2ZrMe][B(C_6F_5)_4]$ at room temperature, the reaction is completed in less than 10 min as indicated by the disappearance of the Zr-**Me** resonance at 0.78 ppm. Figure 4.6(b) shows the ^1H NMR spectrum obtained after 5 minutes of reaction time. After the reaction, a new set of resonances appeared at 5.76, 5.65, 3.48, and 2.57 ppm, in addition to the methane resonance at 0.25 ppm. On the basis of strong similarity to the ^1H NMR spectrum of complex **A**, the resonances at 5.76 and 5.65 ppm were attributed to the two nonequivalent Cp ligands of $[Cp_2Zr(\eta^3\text{-}CH_2C(CH_2CHMe_2)CH_2)][B(C_6F_5)_4]$ (complex **E**), while the resonances at 3.48 and 2.57 ppm were attributed to the *anti* and *syn* hydrogens, respectively, of the CH_2 allyl groups of **E**. The other resonances of **E** are present as follows: the methylene C**H**$_2$CHMe$_2$ group gives rise to a doublet at 1.99 ppm, the methyne CH_2C**H**Me_2 group appears as a multiplet at 1.77 ppm, while the terminal methyl CH_2CH**Me**$_2$ groups appear as a doublet at 1.0 ppm.

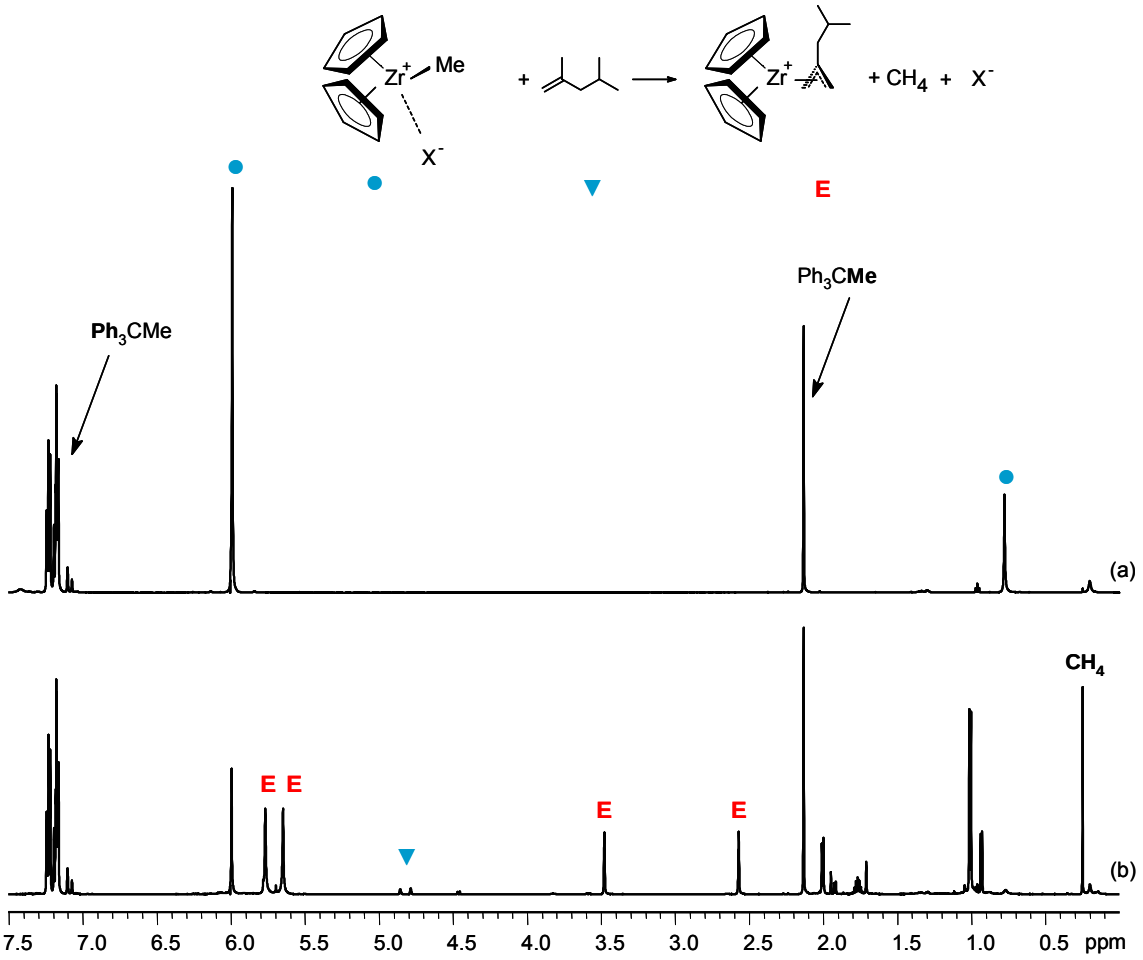

Figure 4.6. ^{1}H NMR spectra (600 MHz) of (a) *in situ* generated chlorobenzene-d_5 solution of $[Cp_2ZrMe][B(C_6F_5)_4]$ and (b) *in situ* reaction between $[Cp_2ZrMe][B(C_6F_5)_4]$ and 2,4-Me_2-1-pentene in chlorobenzene-d_5 at room temperature, after 5 minutes reaction time. X^- is either $[B(C_6F_5)_4]^-$ or a solvent molecule

The reaction rate is enhanced in this case, relative to the reaction between 2,4-Me_2-1-pentene and $[Cp_2ZrMe][MeB(C_6F_5)_3]$ which required several hours. The faster reaction is most probably due to the weaker coordinating ability of the $[B(C_6F_5)_4]^-$ counteranion as compared with $[MeB(C_6F_5)_3]^-$.[23c,24] The presence of two Cp resonances in the ^{1}H NMR spectrum of **E** at room temperature, suggests that the allyl ligand of **E** is

η^3-coordinated and relatively static at this temperature, as compared with complex **A** which shows a dynamic behavior at room temperature (see Figure 4.1). This difference is probably due to the different coordination ability of the two counteranions, as well.

Interestingly, when the reaction was carried out at lower temperatures (T ≤ -40°C) a very weak, broad resonance at ~3.5 ppm was also present in the ^{1}H NMR spectrum, in addition to the expected resonances of $[Cp_2ZrMe][B(C_6F_5)_4]$, Ph_3CMe, 2,4-Me_2-1-pentene, complex **E** and CH_4. A typical ^{1}H NMR spectrum of the reaction between $[Cp_2ZrMe][B(C_6F_5)_4]$ and 2,4-Me_2-1-Pentene in chlorobenzene-d_5 at -45°C is shown in Figure 4.7.

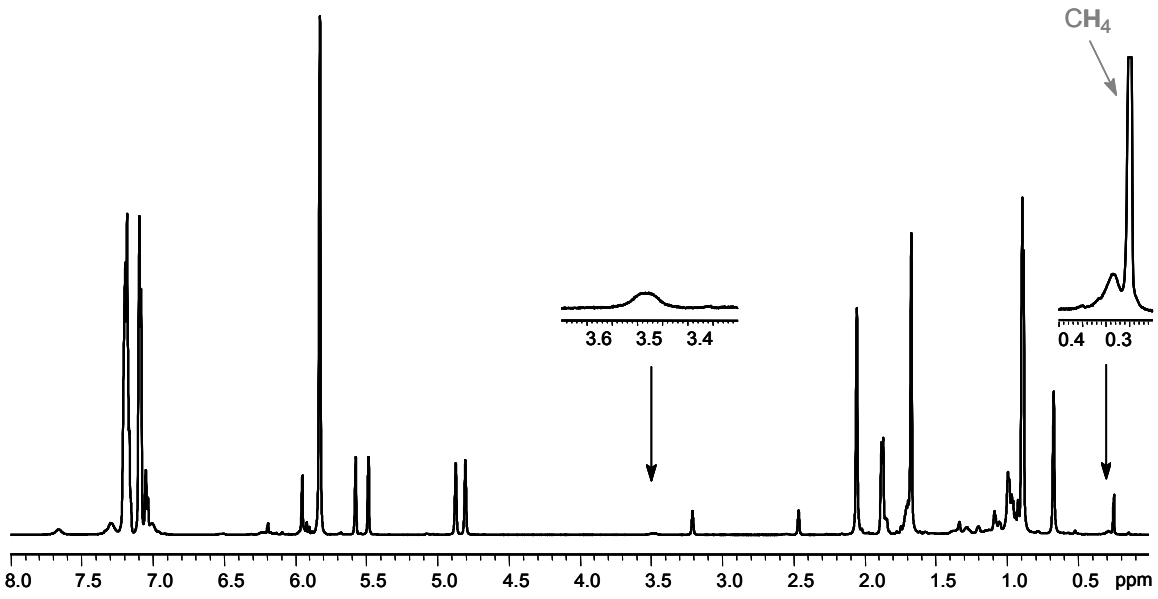

Figure 4.7. ^{1}H NMR spectrum of the reaction between $[Cp_2ZrMe][B(C_6F_5)_4]$ and 2,4-Me_2-1-pentene in chlorobenzene-d_5 at -45°C.

This resonance was ignored until a NOESY experiment at low temperature was also performed. Aside from the cross peaks expected for complex **E**, the NOESY experiment

indicated the presence of cross peaks between the two terminal C**H**$_2$= hydrogens of 2,4-Me$_2$-1-pentene at ~4.87 and 4.80 ppm and the weak broad resonance at ~3.5 ppm. The presence of these cross peaks could only be interpreted in terms of intermolecular exchange (as confirmed by a ROESY experiment)[18] between 2,4-Me$_2$-1-pentene and the species giving rise to the resonance at ~3.5 ppm. A typical ROESY spectrum showing the exchange cross peaks is shown in Figure 4.8. On the basis of these correlations, the resonance at ~3.5 ppm was attributed to the terminal vinylidene hydrogens of a coordinated 2,4-Me$_2$-1-pentene molecule of the novel $[Cp_2Zr(Me)(CH_2C(Me)CH_2CHMe_2)]^+$ (complex **F**, see Scheme 4.8)

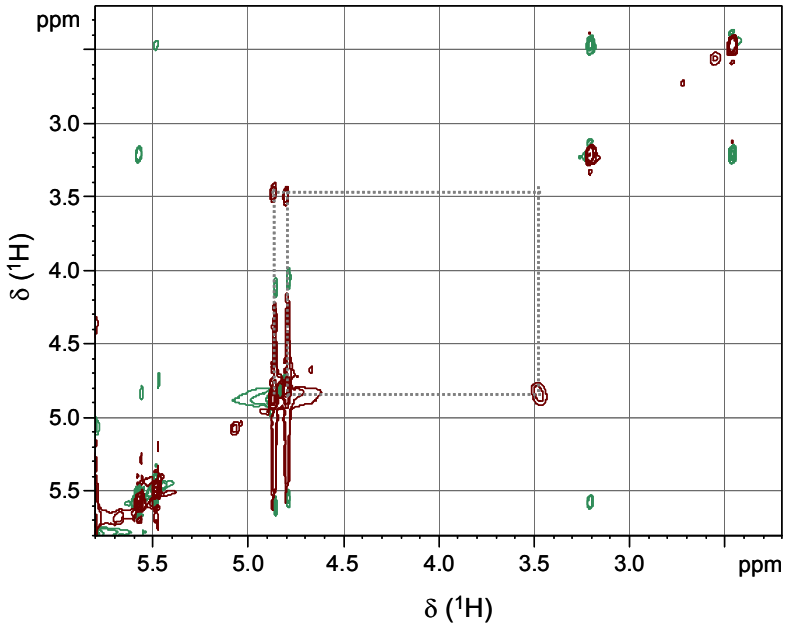

Figure 4.8. The ROESY spectrum (600 MHz, -45°C, chlorobenzene-d$_5$, mixing time = 0.3 sec) showing the exchange cross peaks between the two terminal C**H**$_2$= hydrogens of 2,4-Me$_2$-1-pentene at ~4.87 and 4.80 ppm and the weak broad resonance at ~3.5 ppm. (brown = exchange cross peaks, green = ROE cross peaks)

Although the coordinated olefin complex $[Cp_2Zr(Me)(CH_2C(Me)CH_2CHMe_2)]^+$ cannot be identified unambiguously, support for its identification comes from the observation in the NOESY/ROESY spectra of an additional cross peak between the Zr-**Me** resonance of $[Cp_2ZrMe][B(C_6F_5)_4]$ at 0.67 ppm and a proton resonance at ~0.3 ppm, as shown in Figure 4.9. This latter cross peak is an indication of intermolecular exchange between the Zr-**Me** group of $[Cp_2ZrMe][B(C_6F_5)_4]$ and the resonance at ~0.3 ppm, which can reasonably be attributed to the Zr-**Me** group of the new $[Cp_2Zr(Me)(CH_2C(Me)CH_2CHMe_2)]^+$ complex.

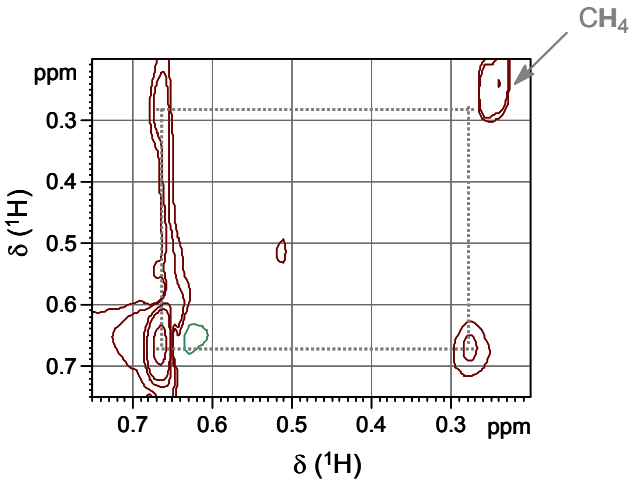

Figure 4.9. The ROESY spectrum (600 MHz, -45°C, chlorobenzene-d_5, mixing time = 0.3 sec) showing the exchange cross peak between the Zr-**Me** resonance of $[Cp_2ZrMe][B(C_6F_5)_4]$ at 0.67 ppm and the proton resonance at ~0.3 ppm (see also Figure 4.7). (brown = exchange cross peaks, green = ROE cross peaks)

Further support for the new $[Cp_2Zr(Me)(CH_2C(Me)CH_2CHMe_2)]^+$ complex comes from a low temperature ^1H NMR experiment. Thus, *in situ* monitoring of the reaction between $[Cp_2ZrMe][B(C_6F_5)_4]$ and 2,4-Me_2-1-pentene at low temperature

indicates that the resonance at ~3.5 ppm builds up in the first few minutes of the reaction, attaining a maximum level of intensity of about 5 % of that of initial alkene. It slowly decreases in time as the two reactants $[Cp_2ZrMe][B(C_6F_5)_4]$ and 2,4-Me_2-1-pentene are consumed, consistent with it being an intermediate in the formation reaction of complex **E** (Scheme 4.8). As complex $[Cp_2Zr(Me)(CH_2C(Me)CH_2CHMe_2)]^+$ was present in very low concentrations, its Cp resonance could not be identified among the several very weak singlets present in the Cp region of the ^1H NMR spectrum. Also, as a result of the very low intensity of the resonances at ~3.5 and 0.3 ppm and the short reaction time, further characterization of the new complex **F** was not possible.

Scheme 4.8. Reaction between $[Cp_2ZrMe][B(C_6F_5)_4]$ and 2,4-Me_2-1-pentene (R is CH_2CHMe_2 and X^- is either $[B(C_6F_5)_4]^-$ or C_6D_5Cl).

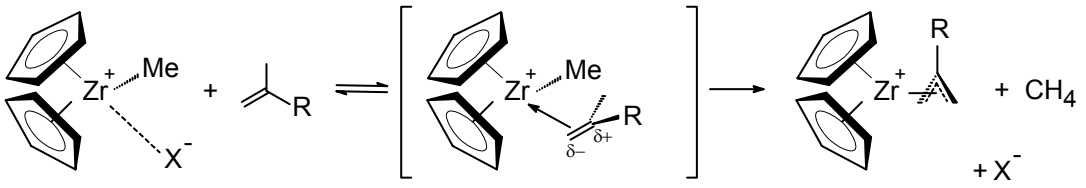

(F) (**E**)

To our knowledge, the complex $[Cp_2Zr(Me)(CH_2C(Me)CH_2CHMe_2)]^+$ represents the first experimental evidence of a d^0 zirconocene alkyl alkene complex, detectable apparently because migratory insertion does not readily occur with vinylidene ligands.[26]

Of great interest is the observation that the two vinylidene hydrogens of the $[Cp_2Zr(Me)(CH_2C(Me)CH_2CHMe_2)]^+$ complex appear as an exchange broadened

resonance at 3.5 ppm rather than two individual singlets, as expected from previous reports.[27] This suggests that the two terminal vinylidene protons undergo some kind of intramolecular exchange. The intramolecular exchange of the two terminal vinylidene hydrogens of the coordinated olefin could occur through a $Cp_2Zr(Me)CH_2C^+(Me)CH_2CHMe_2$ carbocation intermediate[27b,28] as shown in Scheme 4.9. This could only occur if the double bond of the vinylidene group of the coordinated 2,4-Me_2-1-pentene had undergone significant double bond character reduction.

Scheme 4.9. The intramolecular exchange of the two terminal vinylidene hydrogens of the coordinated olefin of complex **F**.

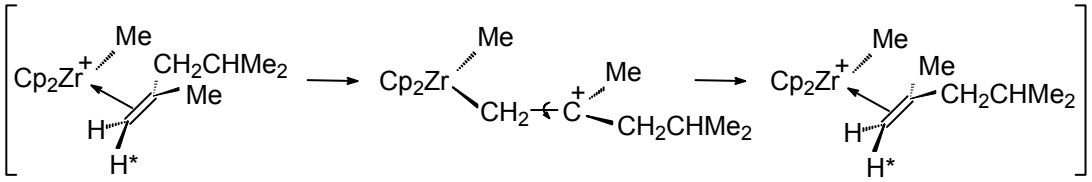

(**F_1**)

Thus, the coordinated alkene of **F** probably assumes a near η^1 structure close to **F**(1) rather than the conventional η^2 structure. This is consistent with previous reports by Jordan *et al.*[27] who investigated $[Cp_2Zr(C_6F_5)(alkene)]^+$ and $[Cp_2Zr(OBu^t)(alkene)]^+$ complexes and found that upon coordination, the olefin keeps the double bond character but it is polarized with a negative charge built up on the terminal methylene carbon and a positive charge on the internal vinylidene carbon.

As a test of this hypothesis, the sample temperature was lowered to -53°C, at which point the decoalescence of the broad resonance at ~3.5 ppm was observed. By further lowering the temperature to -60°C, the decoalescence resulted in two separated resonances (Figure 4.10). This behaviour is a clear indication that the two terminal vinylidene protons undergo intramolecular exchange by a carbocation intermediate of type $\mathbf{F}_1$ (Scheme 4.9).

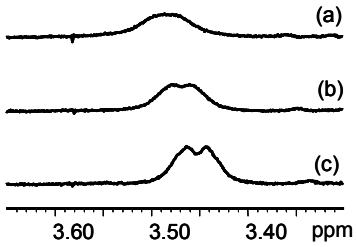

Figure 4.10. ^{1}H NMR spectra of vinylidene resonance of complex **F** at (a) -50°C, (b) -55°C, (c) -60°C.

Although the slow exchange limit could not be reached because of the freezing of the solution below -60°C, the free energy of activation for rotation about the C(1)-C(2) bond was estimated to have an upper limit of ~47 kJ/mol.

One result of the intramolecular exchange of the two terminal vinylidene hydrogens of the coordinated olefin of complex **F**, and of the intermolecular exchange between the free and coordinated alkene, would be that the vinylidene hydrogens of the free alkene would also undergo mutual exchange. Indeed, the intramolecular exchange between the two terminal vinylidene hydrogens of 2,4-Me_2-1-pentene was confirmed by a one-dimensional NOESY.[29] To our knowledge, the zirconocene catalyzed exchange of the vinylidene hydrogens of an olefin has not been observed previously. The

intramolecular exchange of the two terminal vinylidene hydrogens of the coordinated olefin through a $Cp_2Zr(Me)CH_2C^+(Me)CH_2CHMe_2$ carbocation intermediate can constitute a mechanism for chain end epimerization.

Although complex **F** was observed as an intermediate species during the reaction between $[Cp_2ZrMe][B(C_6F_5)_4]$ and 2,4-Me_2-1-pentene by low-temperature NMR experiments, it was not observed in the NMR spectra of the reaction between $[Cp_2ZrMe][MeB(C_6F_5)_3]$ and 2,4-Me_2-1-pentene. This may be due to the different coordination ability of the two counter anions; thus, the $[MeB(C_6F_5)_3]$ anion is expected to compete more effectively with the alkene for the coordination site than the $[B(C_6F_5)_4]$ anion does and consequently, the concentration of [**F**][$MeB(C_6F_5)_3$] at any one time might be much lower than that of [**F**][$B(C_6F_5)_4$].

The presence of the $[Cp_2Zr(Me)(CH_2C(Me)CH_2CHMe_2)]^+$ complex as an intermediate species during the reaction of $[Cp_2ZrMe][B(C_6F_5)_4]$ with 2,4-Me_2-1-pentene indicates that a vinylidene group, although sterically unfavorable, does coordinate to the vacant site of the metal center. The vinylidene group cannot insert into the Zr-Me bond most likely due to steric hindrance. However, the polarization of the double bond in the coordinated vinylidene makes the protons of the groups attached to the internal vinylidene carbon, which is more electron deficient, strongly acidic and therefore they can be more easily transferred to the adjacent methyl group on the metal center to form Zr-allyl complexes and eliminate methane. These results are of fundamental importance as they can explain the catalyst deactivation in Ziegler-Natta polymerization: the vinylidene end groups of the polymeryl chains obtained following β-hydrogen

elimination reactions, can similarly recoordinate to the active catalyst and eventually deactivate it by slowly being converted to Zr-allyl polymeryl species.

4.2.2. The Dynamic Behavior of $Cp_2Zr(\eta^3$-allyl) species

Previous studies on several zirconocene η^3-allyl complexes have shown that the allyl ligand of these complexes, in solution, exhibits dynamic behavior.[15,16] Two main mechanisms have been proposed to account for the dynamic behavior of the metal(η^3-allyl) complexes.[32] The first one, shown in Scheme 4.10(a), involves a metal(η^1-allyl) intermediate and consists of an η^3- to η^1-allyl rearrangement by dissociation of one of the allyl carbon-carbon π bonds, rotation of the C=C unit about the allyl carbon-carbon σ-bond and possibly of the η^1-allyl unit about the metal-carbon σ-bond, and a reversion to the η^3-allyl coordination mode by recoordination of the allyl carbon-carbon π-bond to the metal center.[32,33] Alternatively, the allyl carbon-carbon π-bond dissociation can be followed by the rotation of the η^1-allyl unit about the metal-carbon σ-bond and recoordination of the allyl carbon-carbon π-bond to the metal center, as shown in Scheme 4.10(b).

Scheme 4.10. Dynamic behaviour of metal-allyl complexes via η^3/η^1 allyl interconversion.

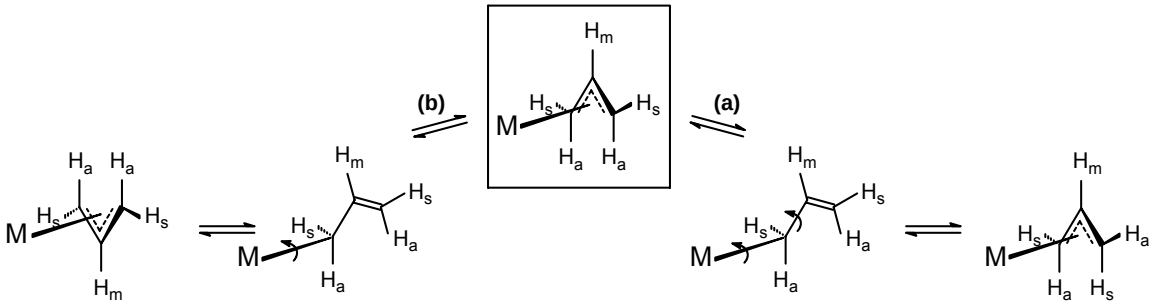

The second mechanism proposed to account for the dynamic behavior of the metal-allyl complexes involves a 180° rotation of the η^3-coordinated allyl ligand about the metal-allyl bond as shown in Scheme 4.11.[32]

Scheme 4.11. Dynamic behaviour of metal-allyl complexes via rotation of the η^3-coordinated allyl ligand about the metal-allyl bond.

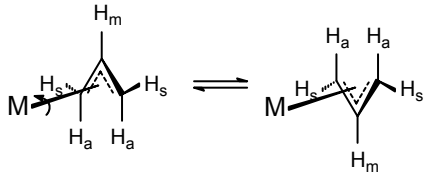

For a particular metal-allyl complex, the dynamic behaviour of the allyl ligand can involve any one of these processes, or a combination of them, which makes the mechanistic interpretation of experimental results rather difficult.[32a]

In a previous section (Section 4.2.1), the synthesis and characterization of a series of $[Cp_2Zr(\eta^3\text{-allyl})]^+$ complexes (**A-E**) were reported. Variable temperature ^1H NMR spectra of the zirconium-allyl complexes **A-E** revealed that the allyl ligands of these species are fluxional. In this section, the dynamic behaviour of the zirconium-allyl complexes **A-E** is studied. The ^1H NMR spectra of all Zr-allyl complexes studied were recorded on a 600 MHz spectrometer in chlorobenzene-d_5 over a temperature range from -40°C to 70°C.

a. Dynamic Behavior of $[Cp_2Zr(\eta^3\text{-}CH_2C(CH_2CHMe_2)CH_2)][MeB(C_6F_5)_3]$ (complex A) and $[Cp_2Zr(\eta^3\text{-}CH_2C(Me)CHCHMe_2)][MeB(C_6F_5)_3]$ (complex B)

At -40°C, the ^1H NMR spectrum of complex **A** consists of one singlet for the CH_2 allyl *syn* hydrogens at 2.5 ppm, one singlet for the CH_2 allyl *anti* hydrogens at 3.24 ppm and two singlets for the Cp ligands at 5.61 and 5.52 ppm. This spectrum is consistent with a static structure of the η^3-allyl ligand of complex **A** relative to the Cp_2Zr^+ moiety. By increasing the probe temperature, the Cp resonances decrease in intensity and broaden to coalesce at 20°C (Figure 4.11).

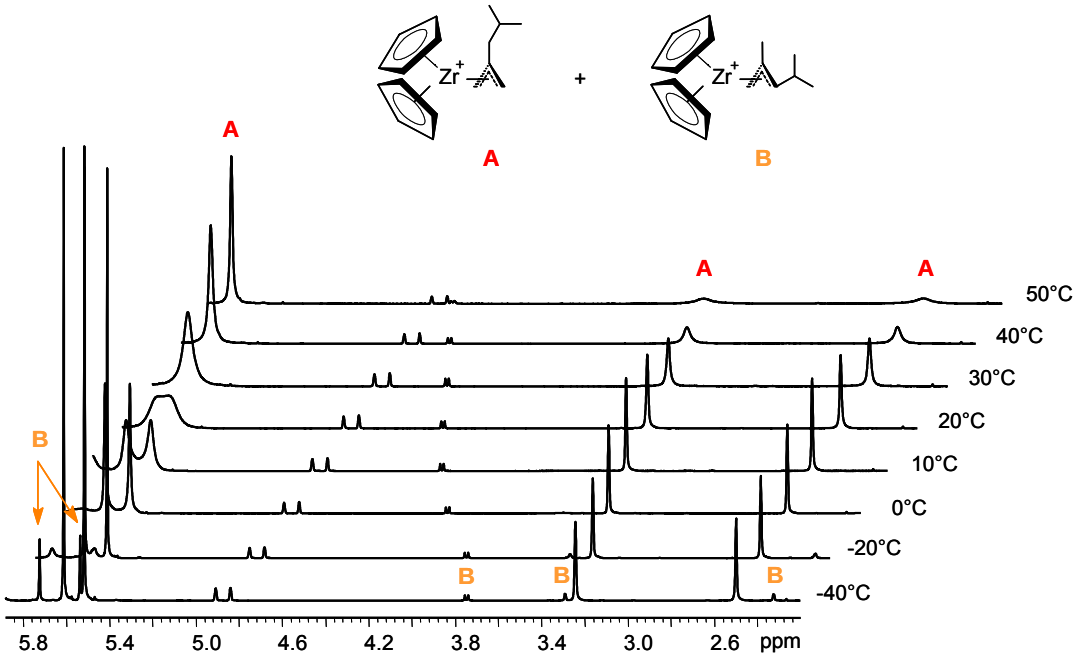

Figure 4.11. Variable temperature ^{1}H NMR spectra of the mixture of **A** and **B** complexes (counterion, $[MeB(C_6F_5)_3]^-$) in the Cp and allylic regions.

Up to 20°C, the *syn* and *anti* hydrogen resonances of the two CH_2 allyl groups remain narrow. By increasing the probe temperature further, the broad, averaged Cp resonance narrows and shifts slightly downfield ($\Delta\delta = 0.14$); the *syn* and *anti* hydrogen resonances, on the other hand, start to broaden and rather diverge than converge such that, although they broaden considerably up to 50°C, they do not coalesce up to 70°C, a temperature for which decomposition also begins to occur. This behavior indicates that the *syn* and *anti* hydrogens of the η^3-coordinated allyl unit of complex **A** as well as the Cp ligands of complex **A** undergo intramolecular exchange. A mechanism which would account for the *syn* and *anti* hydrogen exchange consists of η^3- to η^1-allyl rearrangement, rotation of the C=C unit about the allyl carbon-carbon σ-bond and reversion to the η^3-allyl coordination mode, as shown in Scheme 4.12. On reversion from η^1- to η^3-allyl coordination mode,

the CH_2CHMe_2 group of **A** can become closer to any one of the two Cp ligands. A result of this would be that the two Cp ligands of complex **A** appear to have exchanged positions although they do not in fact move (apparent Cp ligand exchange, see Scheme 4.12).

Scheme 4.12. Proposed mechanism of *syn-anti* hydrogen exchange and apparent Cp ligand exchange in complex **A**.

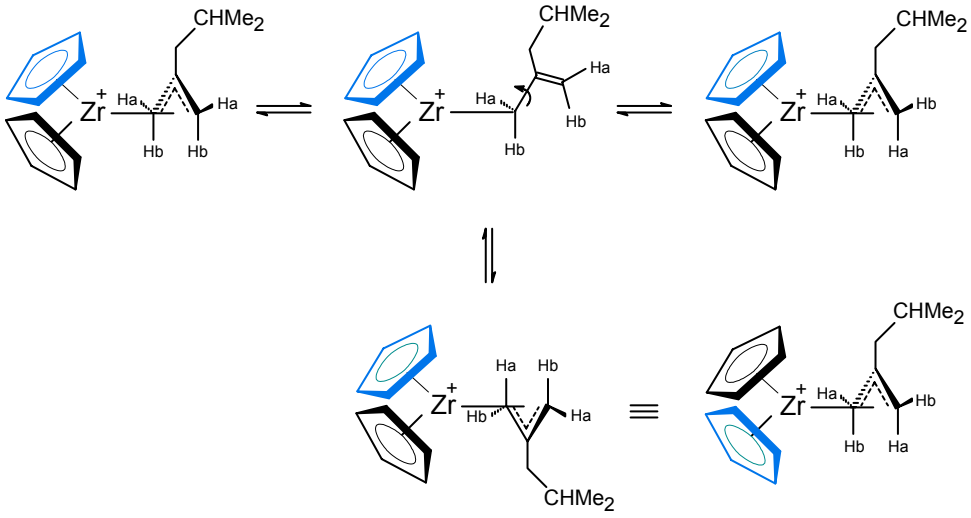

The *syn-anti* hydrogen exchange was also confirmed by a NOESY spectrum recorded at 0°C. A NOESY spectrum showing the exchange between *syn/anti* hydrogens of the allylic CH_2 groups of complex **A,** recorded at 0°C, is presented in Figure 4.12.

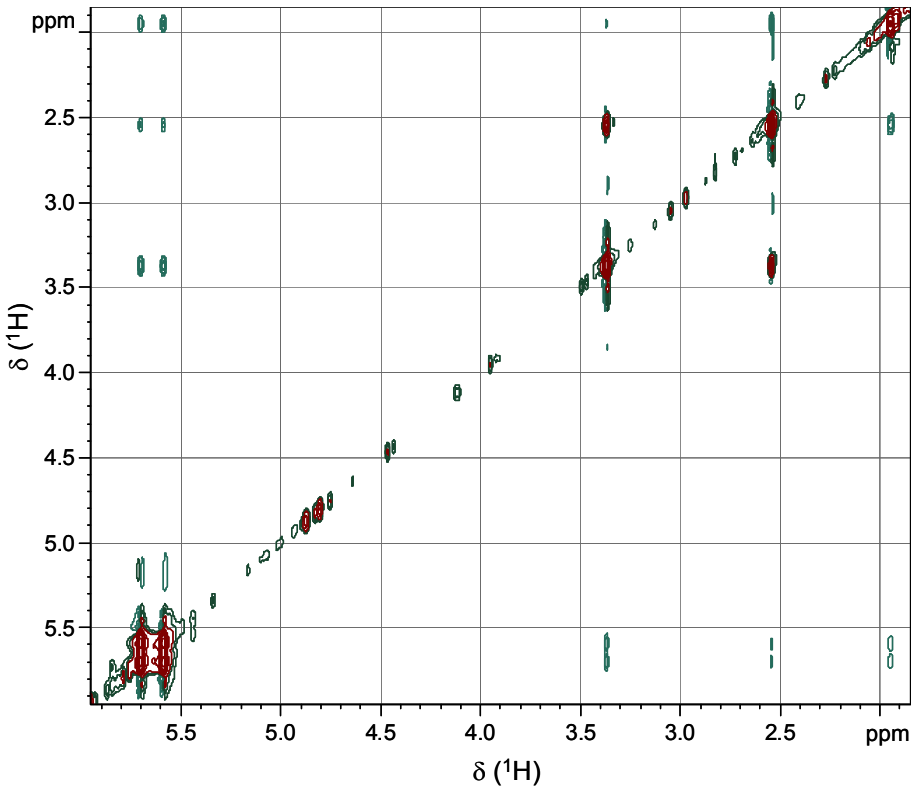

Figure 4.12. The NOESY spectrum of complex **A** at 0°C (600 MHz, mixing time = 0.4 sec), showing the exchange between the *syn* and *anti* hydrogens of the allylic CH_2 groups and the exchange between the two Cp ligands (brown = exchange cross peaks, green = NOE cross peaks).

Processes involving the rotation of the η^3-allyl group about the Zr(η^3-allyl) bond may also be contributing to the observed dynamic behavior of complex **A** ligands. This exchange mechanism is depicted in Scheme 4.13 and it would result in apparent Cp ligand exchange only. The free energy of activation for the intramolecular exchange processes of complex **A**, as estimated from the coalescence temperature of the two Cp ligands, is 59.9 kJ/mol.

Scheme 4.13. Proposed mechanism for apparent Cp ligand exchange in complex **A**.

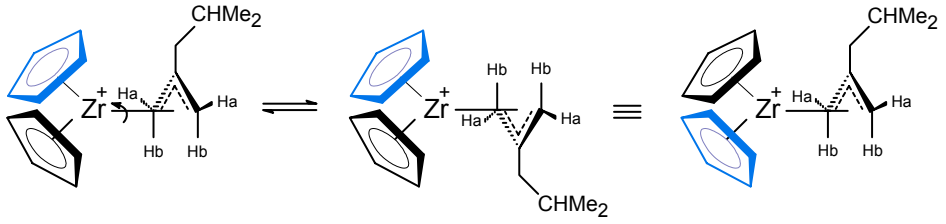

As can be seen from Figure 4.11, the complex **B** resonances are also present in the ^{1}H NMR spectra of the reaction mixture. The low temperature (-40°C) ^{1}H NMR spectrum of complex **B** exhibits two sharp resonances for the two nonequivalent Cp ligands at 5.72 and 5.54 ppm, one doublet for the allylic CH hydrogen at 3.75 ppm, one doublet for the *syn* hydrogen of the CH_2 allyl group at 2.32 ppm and one doublet for the *anti* hydrogen of the CH_2 allyl group at 3.29 ppm, consistent with a static structure of the η^3-allyl ligand of complex **B** at this temperature (see Figures 4.11 and 4.13). Upon warming, coalescence of the Cp signals at ~5.8 ppm occurs at 0°C yielding a free energy of activation for the Cp ligand exchange of 54.1 kJ/mol. The allylic *syn* and *anti* CH_2 hydrogen resonances, on the other hand, diverge rather than coalesce and broaden considerably such that, at 0°C, they could not be detected anymore. By increasing the probe temperature further, the averaged Cp resonance becomes narrow and shifts downfield ($\Delta\delta$ = 0.36).

These changes indicate that the allyl ligand of complex **B** undergoes a dynamic process in which both the allylic *syn* and *anti* CH_2 hydrogens and the two Cp ligands are exchanging, respectively. The *syn* and *anti* hydrogen exchange at the CH_2 allyl terminus probably proceeds by a mechanism involving the dissociation of the carbon-carbon π bond at the monosubstituted CH allyl end, rotation about the allyl carbon-carbon σ-bond

and recoordination of the carbon-carbon π-bond to zirconium. This mechanism can also be responsible for the apparent Cp ligand exchange.

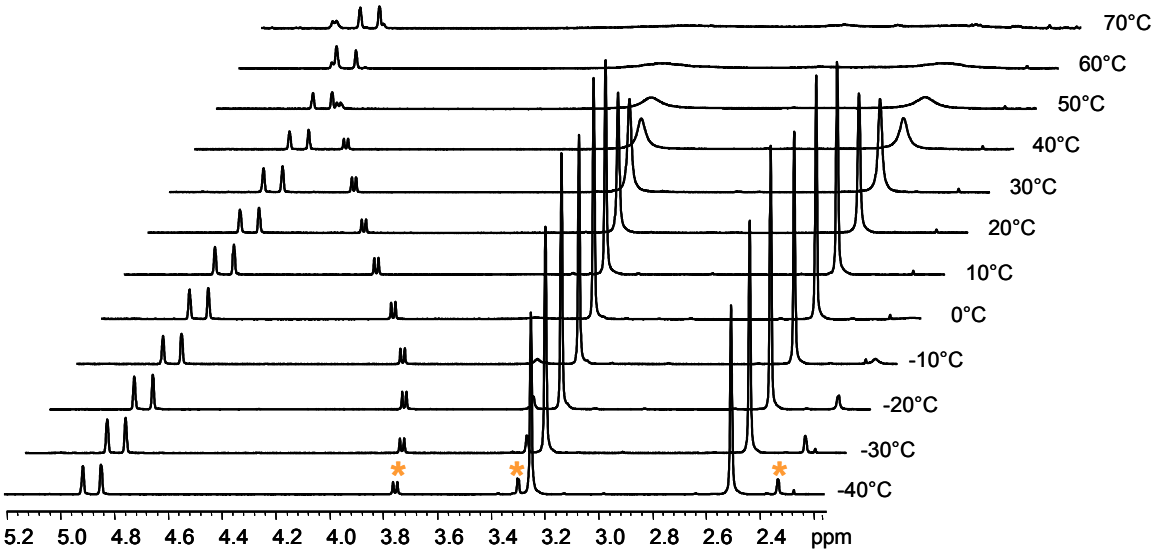

Figure 4.13. Variation of H_{syn} and H_{anti} resonances of the **A** and **B** complexes with temperature. The peaks marked with asterisk (*) represent *syn* and *anti* hydrogen resonances of complex **B**.

Aside from the exchange processes described above, another phenomenon becomes evident from the variable ^{1}H NMR spectra of complex **B**: by raising the probe temperature, the allyl C**H** resonance of **B** is significantly shifted downfield from 3.75 ppm at -40°C toward a free olefin resonance (4.93 ppm) at 70°C; on cooling the probe temperature, the same chemical shift changes occur in reverse. This dramatic change of the *anti* CH allyl hydrogen resonance with temperature coupled with the change of the averaged Cp chemical shift with temperature can be rationalized on the basis of a fast equilibrium between the η^1- and η^3-coordinated allyl complexes of **B**, as shown in Scheme 4.14. The presence of a fast equilibrium between the η^1- and η^3- coordinated

allyl complexes of **B** might also explain the divergence of the *syn* and *anti* allyl hydrogens of complex **B** with increasing temperature.

Scheme 4.14. The equilibrium between the η^1- and η^3-coordinated allyl complexes of **B**. The counterion, $[MeB(C_6F_5)_3]^-$, is omitted for simplicity.

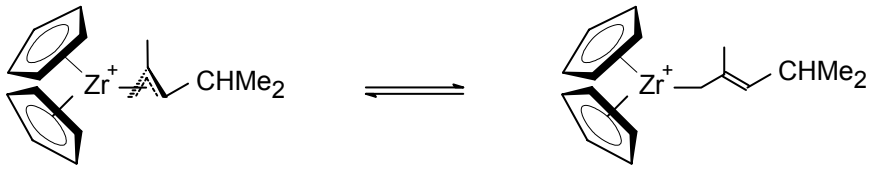

low temperature high temperature

Thus, the chemical shift position of the averaged CH allyl resonance observed depends on the composition of the equilibrium mixture at various temperatures, namely

$$\delta_{obs} = p_1\delta_1 + p_2\delta_2$$

where p_1 and δ_1 are the mole fraction and chemical shift, respectively, of the Zr(η^3-allyl) complex, and p_2 and δ_2 are the mole fraction and chemical shift of the Zr(η^1-allyl) complex, respectively ($p_1 + p_2 = 1$). Considering that the proton resonance at 3.75 ppm, recorded at -40°C, corresponds mostly to the monosubstituted CH allyl hydrogen of the η^3-coordinated allyl ligand of **B** and that the proton resonance at 4.93 ppm, recorded at 70°C, corresponds mostly to the =CH hydrogen of the η^1-coordinated allyl ligand of **B**, temperature dependent mole fractions of η^3- and η^1-coordinated allyl complexes can thus

be estimated. For instance, at 20°C, roughly 55% of the **B** complexes are predicted to be as η^1.

As mentioned above, the Cp and allyl hydrogen resonances of complex **A** are also shifted by changing the probe temperature. These chemical shift changes can also be attributed to the presence of a fast equilibrium between the η^1- and η^3- coordinated allyl complexes of **A**. From the comparison between the chemical shift changes of the averaged Cp resonances of complexes **A** and **B**, it can be inferred that at high temperatures, the mole fraction of η^1-coordinated allyl complex present at equilibrium is much lower for complex **A** than for complex **B**. The free energy of activation for the exchange process in the case of complex **B** is lower than that estimated in the case of complex **A** and this is consistent with **B** having a larger fraction of η^1-allyl complexes.

b. Dynamic Behavior of $[Cp_2Zr(\eta^3\text{-}CH_2C(CH_2CH(Me)(Pr))CH_2)][MeB(C_6F_5)_3]$ (complex C) and $[Cp_2Zr(\eta^3\text{-}CH_2C(Me)(CHCH(Me)(Pr))][MeB(C_6F_5)_3]$ (complex D)

At -40°C, the ^{1}H NMR spectrum for complex **C** shows two sharp resonances at 5.62 and 5.54 ppm for the hydrogens of the two inequivalent Cp rings, two singlets at 2.55 and 2.53 ppm for the two *syn* hydrogens and two singlets at 3.31 and 3.24 ppm for the two *anti* hydrogens of the terminal methylene groups. As the probe temperature is increased, the two Cp resonances broaden to coalesce at 20°C. The *syn* and *anti* hydrogen resonances are also broadened at this temperature (see Figure 4.14). As for **A**, by increasing the probe temperature further, the averaged Cp resonance becomes narrow and shifts slightly downfield while the allyl *syn* and *anti* hydrogen resonances broaden

considerably but the coalescence of these resonances does not occur up to 60°C, a temperature close to the decomposition temperature.

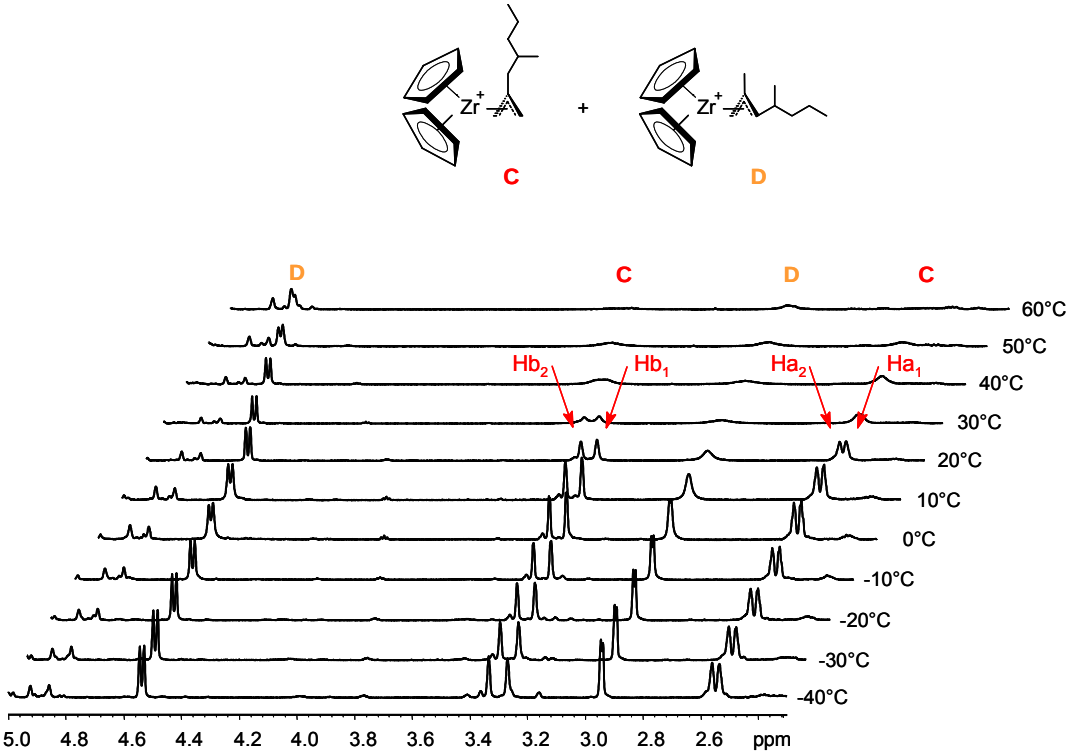

Figure 4.14. Variable temperature ^{1}H NMR spectra of the mixture of **C** and **D** complexes in the allyl region in chlorobenzene-d_5, 600 MHz (counterion, $[MeB(C_6F_5)_3]^-$).

These variable temperature ^{1}H NMR spectra indicate that the η^3-allyl ligand of **C** undergoes a dynamic behaviour in which the *syn* and *anti* hydrogens are exchanging.

The *syn/anti* hydrogen exchange is confirmed by a NOESY experiment acquired in the slow exchange regime (0°C). The NOESY spectrum of complex **C** in the allyl region is depicted in Figure 4.15. As can be seen, the *syn* hydrogen of the C_1 at 2.56 ppm (Ha_1) exchanges with the *anti* hydrogen of the C_2 at 3.42 ppm (Hb_2), while the *syn* hydrogen of the C_2 at 2.58 ppm (Ha_2) exchanges with the *anti* hydrogen of the C_1 at 3.36 ppm (Hb_1).

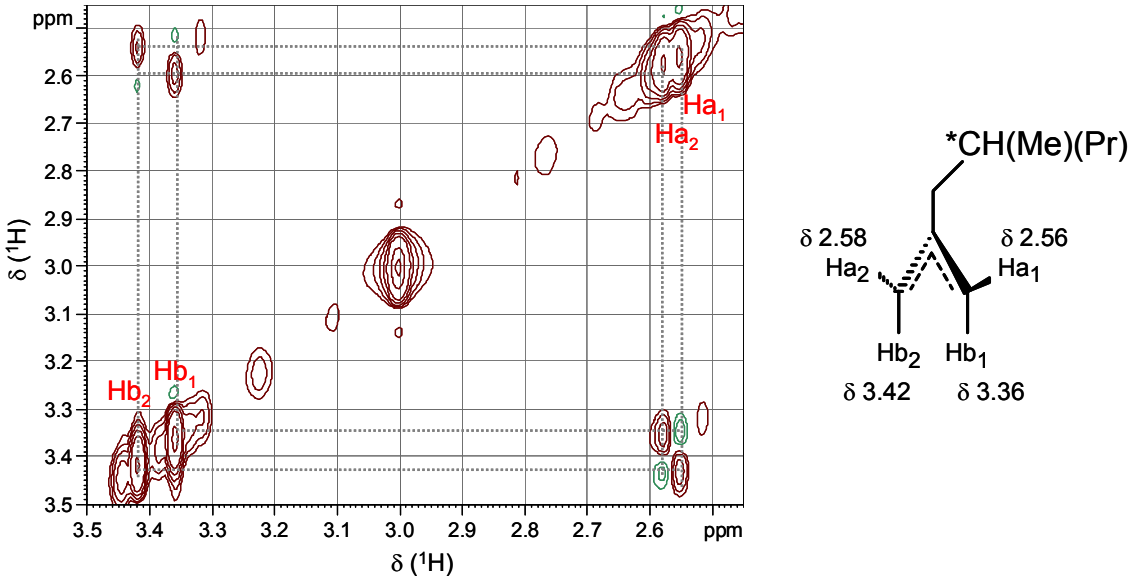

(a) (b)

Figure 4.15. (a) The NOESY spectrum of complex **C** in the allylic region, under slow exchange regime (at 0°C, 600 MHz, mixing time = 0.4 sec). The exchange cross peaks are in brown while the NOE cross peaks are in green. (b) The chemical structure of complex **C**, with chemical shift assignments (δ in ppm). Ha_1 and Hb_1 are *syn* and *anti* hydrogens, respectively, on carbon C_1, and Ha_2 and Hb_2 are the *syn* and *anti* hydrogens on carbon C_2.

This type of exchange can be explained by the dissociation of the carbon-carbon π bond at one CH_2 allyl end, rotation of the C=C unit about the allyl carbon-carbon σ-bond as well as zirconium-carbon σ-bond, in a concerted mechanism, and recoordination of the carbon-carbon π-bond to zirconium, as shown in Scheme 4.15. Depending on the direction of rotation of the η^1-coordinated allyl unit about the zirconium-carbon σ-bond, there is a roughly equal probability that the Cp ligand exchange also takes place (compare Scheme 4.15(a) with Scheme 4.15(b))

Scheme 4.15. Proposed mechanism of *syn-anti* hydrogen exchange and apparent Cp ligand exchange in complex **C**.

(a) *syn/anti*, *syn/syn*, and *anti/anti* hydrogen exchange ($Ha_2 \rightarrow Ha_1$, $Ha_1 \rightarrow Hb_2$, $Hb_2 \rightarrow Hb_1$, $Hb_1 \rightarrow Ha_2$)

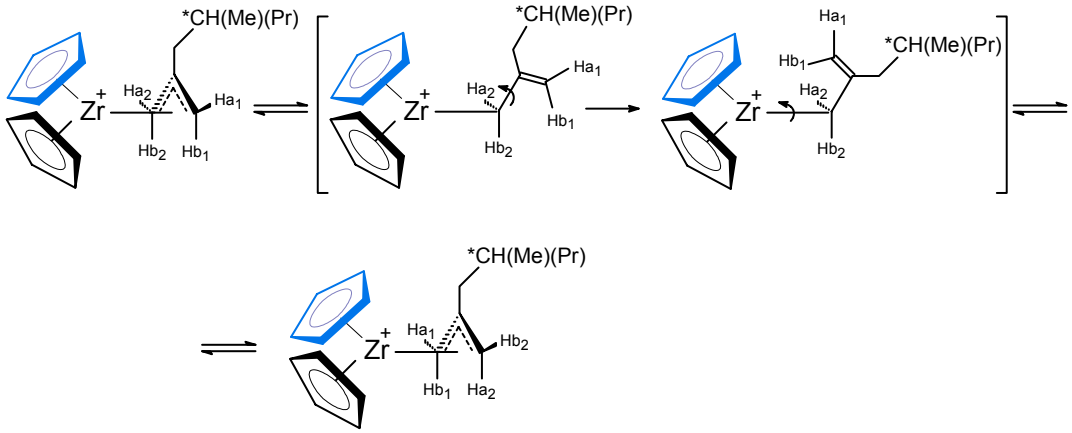

(b) *syn/anti*, *syn/syn*, and *anti/anti* hydrogen exchange ($Ha_2 \rightarrow Ha_1$, $Ha_1 \rightarrow Hb_2$, $Hb_2 \rightarrow Hb_1$, $Hb_1 \rightarrow Ha_2$) as well as apparent Cp ligand exchange

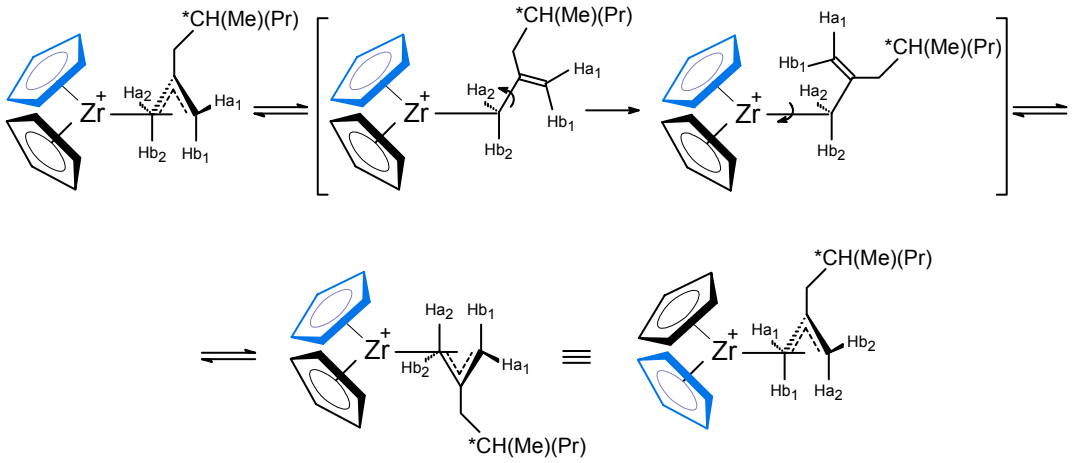

It is worth noting that rotation of the C=C unit about the allyl carbon-carbon σ-bond also results in a change of the allyl coordination face relative to the Cp_2Zr^+ moiety, and, as a result, the two CH_2 allyl end groups also exchange. The reversal of the η^3-allyl coordination face relative to zirconium might actually be a common feature in the complexes which undergo *syn/anti* hydrogen exchange. However, this type of exchange cannot be detected in the metal(η^3-allyl) complexes in which the two CH_2 allyl ends are equivalent.

Besides *syn/anti* hydrogen exchange, the exchange mechanisms displayed in Schemes 4.15(a) and (b) also result in *syn/syn* and *anti/anti* hydrogen exchange: this exchange cannot be observed in the NOESY spectrum most probably due to the poor resolution of the spectrum. As for complex **A**, a mechanism involving the rotation of the η^3-coordinated allyl ligand about the metal-carbon bond, which would result in apparent Cp ligand exchange, cannot be ruled out for complex **C**. The experimental free energy of activation for the exchange processes of complex **C**, as calculated from the coalescence of the two Cp resonances at 20°C, was estimated at $\Delta G^{\ddagger} = 60.2$ kJ/mol.

The ^{1}H NMR spectrum of complex **D** at -40°C, shows the presence of the two Cp resonances at 5.83 and 5.56 ppm (two singlets), the allyl methine hydrogen at 4.52 ppm (doublet) and the two allyl methylenic *syn* and *anti* hydrogen resonances at 1.83 and 2.93 ppm (doublets), respectively. By increasing the probe temperature to 0°C, the two Cp resonances and the allyl H_{syn} and H_{anti} resonances start to broaden and while the two Cp resonances coalesce at about 30°C, the coalescence for the two *syn* and *anti* hydrogens of the terminal methylenic group does not occur up to 60°C (Figure 4.14). The averaged Cp resonance, on the other hand, becomes narrow and shifts slightly downfield as the

temperature is increased. The free energy of activation, as calculated from the coalescence of the two Cp resonances of complex **D**, is 60.2 kJ/mol.

Interesting, the chemical shift of the substituted CH allyl hydrogen of complex **D** at -40°C is close to an olefinic chemical shift and it moves slightly downfield as the temperature is increased. This behavior indicates the presence of a fast equilibrium between the η^1- and η^3-coordinated allyl complexes of **D**, similar with that found for complex **B**. However, a much deshielded chemical shift of the unsubstituted CH allyl hydrogen of complex **D** at -40°C (4.52 ppm for complex **D** as compared with 3.75 ppm for complex **B**) coupled with the smaller variation in the chemical shift observed when the temperature is increased to 60°C ($\Delta\delta$ = 0.26 for complex **D** as compared with $\Delta\delta$ = 1.18 for complex **B**) might indicate that while complex **B** is found predominantly as a η^3-allyl complex at -40°C, complex **D** is found mostly as a η^1-allyl complex.

The intramolecular *syn/anti* hydrogen exchange in this case is expected to occur by dissociation of the carbon-carbon π bond at the monosubstituted CH allyl end, rotation about the allyl carbon-carbon σ-bond and recoordination of the carbon-carbon π-bond to zirconium.

c. Dynamic Behavior of $[Cp_2Zr(\eta^3\text{-}CH_2C(CH_2CHMe_2)CH_2)][B(C_6F_5)_4]$

The dynamic behavior of the complex **E** is similar with that of complex **A**, except that by increasing the sample temperature, the coalescence of the nonequivalent Cp resonances of complex **E** occurs at a much higher temperature (about 60°C) as compared with the coalescence of the Cp resonances of complex **A** (20°C). The free energy of activation for the exchange processes in the first case, as estimated from the coalescence of the Cp

resonances, is 68.6 kJ/mol. The difference between the free energy of activation of complexes **A** ($\Delta G^{\ddagger}$ = 59.9 kJ/mol) and **E** ($\Delta G^{\ddagger}$ = 68.6 kJ/mol) arises from the different coordination ability of the two counteranions.

To summarize, this study shows that the allyl ligand of complexes **A** - **E** manifest dynamic behavior. The fluxional behavior in these complexes is mainly due to the η^3- to η^1- isomerization, rotation of the allyl carbon-carbon π unit about the carbon-carbon σ-bond and reversion to the η^3-allyl coordination mode, when the allyl *syn/anti* hydrogen exchange occurs. A second mechanism which may account for the apparent Cp ligand exchange in the $Cp_2Zr^+(\eta^3$-allyl) complexes under investigation and which consists of rotation of the η^3-coordinated allyl ligand about the metal-allyl bond may also occur. Aside from the intramolecular allyl exchange described above, this study also shows that the η^1- and η^3-coordinated allyl forms of a particular Zr-allyl complex coexist in solution and that the equilibrium composition of these species is temperature dependent.

4.2.3. Kinetic Study of Cp_2Zr^+-allyl Species Formation

There is now growing experimental evidence for formation of Zr-allyl complexes during α-olefin polymerization by zirconocene catalysts. Formation of Zr-allyl species have attracted considerable attention over the last years as they are assumed to remain 'dormant' to further olefin insertions and therefore to profoundly affect the catalyst activity. In Section 4.2.1, we investigated the possibility of Zr-allyl species formation from the reaction between Cp_2ZrMe_2, activated with either $B(C_6F_5)_3$ or $[Ph_3C][B(C_6F_5)_4]$, and two different alkenes (2,4-Me_2-1-pentene and 2,4-Me_2-1-heptene) used as model compounds for a vinylidene terminated polymeryl chain. Under the selected conditions,

the formation of Zr-allyl species was found to be rather facile. These experiments imply that the vinylidene end groups of polymeryl chains, released during propylene polymerization as a result of β-hydrogen elimination reactions, can also recoordinate to the active catalyst to form Zr-allyl polymeryl species. These reactions are supposed to become dominant toward the end of the polymerization reaction when a high concentration of vinylidene terminated chains accumulates in the polymerization system. Thus, the catalyst deactivation via formation of Zr-allyl polymeryl species in propylene polymerization reactions is a side reaction which cannot be avoided and therefore a kinetic study for the formation of Zr-allyl species can provide useful information regarding the energy barrier that this reaction must overcome in order to form the dormant Zr-allyl species. This is therefore an important step in assessing the impact of the vinylidene end groups on the catalytic activity. To our knowledge, no experimental data on the activation energy for formation of Zr-allyl species are available.[12b]

In the following, the experimental data of a kinetic study on the Zr-allyl species formation are presented. Specifically, the formation of $[Cp_2Zr(\eta^3\text{-}C_7H_{13})]^+$ complex from the *in situ* reaction between 1.5 equivalents of 2,4-Me_2-1-pentene and either $[Cp_2ZrMe][MeB(C_6F_5)_3]$ or $[Cp_2ZrMe][B(C_6F_5)_4]$, in chlorobenzene-d_5 was studied by ^{1}H NMR spectroscopy at different temperatures. The progress of the reaction was followed by monitoring the decrease of the Cp resonance intensity of the $[Cp_2ZrMe]^+$ catalyst. Figure 4.1 provides an example of ^{1}H NMR spectra showing the progress of the reaction between $[Cp_2ZrMe][MeB(C_6F_5)_3]$ and 2,4-Me_2-1-pentene in chlorobenzene-d_5 at room temperature.

The reaction between $[Cp_2ZrMe][MeB(C_6F_5)_3]$ and 2,4-Me_2-1-pentene was monitored at 293, 298, 303, 308, 313, and 318 K. Figure 4.16 shows plots of $[10^{-3}/(a_0-b_0)]\ln(ab_0/a_0b)$, at various temperatures versus time. a_0 and b_0 designate the initial concentrations of the two reactants, $[Cp_2ZrMe]^+$ and 2,4-Me_2-1-pentene, respectively, while a and b represent the concentrations of the two reactants at time t.

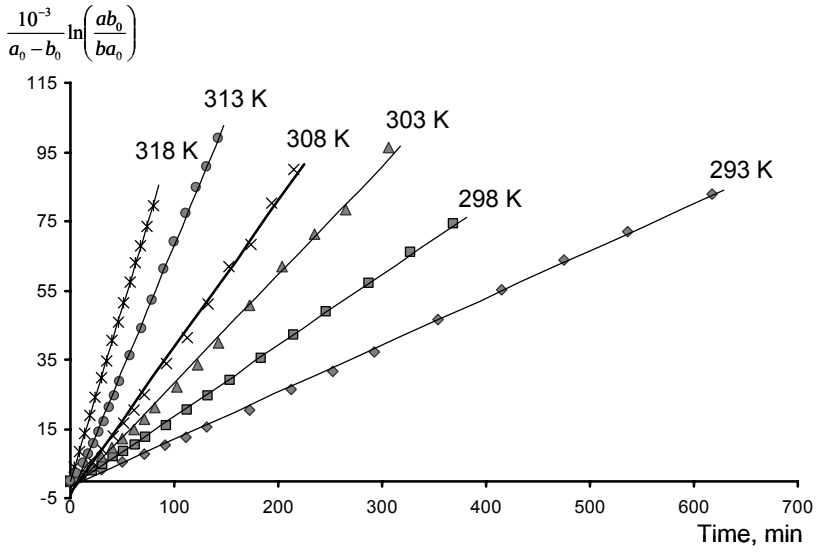

Figure 4.16. Plots of $[10^{-3}/(a_0-b_0)]\ln(ab_0/a_0b)$ versus time for the formation of $[Cp_2Zr(\eta^3\text{-}C_7H_{13})]^+$ from $[Cp_2ZrMe][MeB(C_6F_5)_3]$ and 2,4-Me_2-1-pentene in chlorobenzene-d_5.

The plots are clearly linear indicating that the reaction obeys a second-order rate expression,[30] given by the equation :

$$-\frac{d[Cp_2Zr^+Me]}{dt} = k[Cp_2Zr^+Me][2,4-Me_2-1-pentene] \qquad (\mathbf{4.4})$$

where k is the temperature dependent rate constant for the reaction. The slopes of these plots (determined by linear least-square fit) afforded the values for the reaction rate constants at various temperatures. Using the Arrhenius equation:

$$k = A \cdot \exp\left(-\frac{E_a}{RT}\right) \qquad \textbf{(4.5)}$$

where E_a is the activation energy, A is the pre-exponential factor, R is the gas constant and T represents the temperature, from the dependence of ln k on T^{-1} (Fig 4.17), an activation energy of 50.9 kJ/mol was obtained.

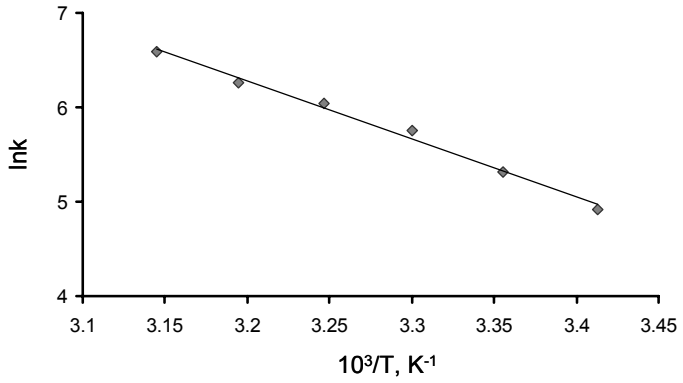

Figure 4.17. Arrhenius plot for the formation of $[Cp_2Zr(\eta^3\text{-}C_7H_{13})]^+$ from $[Cp_2ZrMe][MeB(C_6F_5)_3]$ and 2,4-Me_2-1-pentene in chlorobenzene-d_5.

Using Eyring's equation:

$$k = \frac{k_b T}{h} \exp\left(\frac{-\Delta H^{\ddagger} + T\Delta S^{\ddagger}}{RT}\right) \qquad \textbf{(4.6)}$$

where $\Delta S^{\ddagger}$ and $\Delta H^{\ddagger}$ represent the activation entropy and enthalpy, respectively, k_b is Boltzmann's constant, h is Plank's constant, T represents the temperature, and R is the gas constant, the activation parameters ($\Delta H^{\ddagger}$ and $\Delta S^{\ddagger}$) can now be determined. The activation entropy and enthalpy determined from the intercept and slope, respectively, of an Eyring plot, are -72.5 J/mol K and 48.3 kJ/mol, respectively. The large, negative activation entropy suggests a highly ordered transition state, consistent with an associative mechanism.[30]

To investigate the effect of the counterion on the rate of the Zr-allyl species formation reaction, the rate constants for the reaction between $[Cp_2ZrMe][B(C_6F_5)_4]$ and 2,4-Me_2-1-pentene in chlorobenzene-d_5 were also determined. As noted in Section 4.2.1.3, when Cp_2ZrMe_2 was reacted with $[Ph_3C][B(C_6F_5)_4]$ (1.1-1.2 equivalents) in chlorobenzene-d_5, besides the active ion pair $[Cp_2ZrMe][B(C_6F_5)_4]$, small amounts of methyl bridged binuclear cation $[(Cp_2ZrMe)_2(\mu\text{-}Me)][B(C_6F_5)_4]$ were also formed. To avoid its interference in this kinetic study, the methyl bridged binuclear cation was slowly converted to the mononuclear species, before the reaction with alkene was started, by warming the NMR tube at 40°C for 30 min.

The reaction between $[Cp_2ZrMe][B(C_6F_5)_4]$ and 2,4-Me_2-1-pentene is much faster than that between $[Cp_2ZrMe][MeB(C_6F_5)_3]$ and 2,4-Me_2-1-pentene. Consequently, for the former, the kinetics was followed at low temperatures in order to slow down the reaction and allow *in situ* monitoring of Cp resonance decay. A complication which could not be avoided in this case was that the reaction is very fast and hard to control in the first few minutes after the two reactants (the active catalyst and alkene) are mixed and until the

temperature is equilibrated. The second order rate constants for Zr-allyl formation from $[Cp_2ZrMe][B(C_6F_5)_4]$ and 2,4-Me_2-1-pentene were again determined from the plots of $[10^{-3}/(a_0-b_0)]\ln(ab_0/a_0b)$ versus time (Figure 4.18).

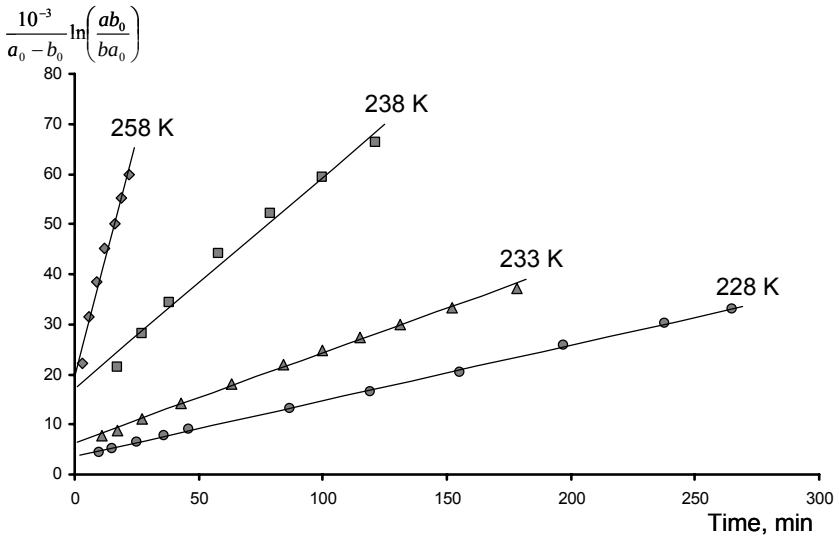

Figure 4.18. Plots of $[10^{-3}/(a_0-b_0)]\ln(ab_0/a_0b)$ versus time for the formation of $[Cp_2Zr(\eta^3\text{-}C_7H_{13})]^+$ from $[Cp_2ZrMe][B(C_6F_5)_4]$ and 2,4-Me_2-1-pentene in chlorobenzene-d_5.

The small deviations from linearity for some plots might indicate that the reaction is more complicated than a simple second order reaction probably due to a slight interference from the formation of the intermediate complex **F**. The dependence of ln k on T^{-1} is satisfactorily described by the Arrhenius equation (Figure 4.19) from which an activation barrier of 46.4 kJ/mol was determined.

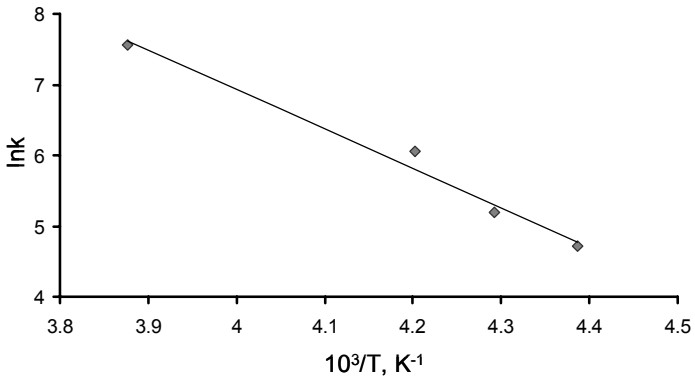

Figure 4.19. Arrhenius plot for the formation of $[Cp_2Zr(\eta^3\text{-}C_7H_{13})]^+$ from $[Cp_2ZrMe][B(C_6F_5)_4]$ and 2,4-Me_2-1-pentene in chlorobenzene-d_5.

The activation parameters $\Delta H^{\ddagger}$ and $\Delta S^{\ddagger}$ determined from an Eyring's plot are 44.4 kJ/mol and -42.4 J/mol·K, respectively. The enthalpy of activation for the reaction between $[Cp_2ZrMe][B(C_6F_5)_4]$ and 2,4-Me_2-1-pentene is lower than that for the reaction between $[Cp_2ZrMe][MeB(C_6F_5)_3]$ and 2,4-Me_2-1-pentene which is expected considering that the $[B(C_6F_5)_4]^-$ anion has a lower coordination ability as compared with $[MeB(C_6F_5)_3]^-$. The entropy of activation is also less negative for the first reaction, consistent with a less structured transition state.

Overall the activation energy obtained for the Zr-allyl formation from $[Cp_2ZrMe][B(C_6F_5)_4]$ and 2,4-Me_2-1-pentene is lower than that obtained for the Zr-allyl formation from $[Cp_2ZrMe][MeB(C_6F_5)_3]$ and 2,4-Me_2-1-pentene, as expected when an anion with less coordinating ability is used. Thus, the $[MeB(C_6F_5)_3]^-$ anion, which is more tightly associated with the metal center than $[B(C_6F_5)_4]^-$, will hinder the access of the bulkier vinylidene group at the active site of the metal center, in this way slowing down the reaction.

Theoretical studies show that the insertion of olefin into Zr-C σ-bond during the propagation polymerization occurs with an activation energy between 25-30 kJ/mol.[31] In this context, assuming that the pre-exponential factors are of about the same magnitude, this kinetic study suggests that the formation of Zr-allyl intermediates during the polymerization may occur with a relative probability as often as one out of every 1,000 as compared with olefin insertion, especially in systems where noncoordinating anions are used.

4.2.4. *In situ* Propylene Polymerization using zirconocene catalysts; Identification of Cp_2Zr^+-allyl Polymeryl Intermediates.

As stated in Section 4.1, zirconocene-catalyzed polymerization processes are adversely affected by slow conversion of the active catalysts to relatively dormant or even unreactive species.[1] As a possible deactivation pathway, the relatively unreactive Zr-allyl polymeryl intermediates were previously postulated to arise during propylene polymerization and remain inert to further propylene insertions.[2b,15b] In the following, a series of *in situ* propylene polymerization reactions as catalyzed by $Cp_2ZrMe_2/B(C_6F_5)_3$ and $Cp_2ZrMe_2/[Ph_3C][B(C_6F_5)_4]$, rerspectively, in chlorobenzene-d_5 at room temperature are reported. The purpose of this study is to find out if Cp_2Zr^+-allyl polymeryl intermediates are present in the polymerization mixture.

Treatment of Cp_2ZrMe_2 with 1.1 equivalents of $B(C_6F_5)_3$ in chlorobenzene-d_5 at room temperature resulted in fast generation of the $[Cp_2ZrMe][MeB(C_6F_5)_3]$ ion pair via abstraction of one methyl anion from the neutral dimethyl zirconocene by $B(C_6F_5)_3$. A

typical spectrum of the *in situ* generated chlorobenzene-d_5 solution of $[Cp_2ZrMe][MeB(C_6F_5)_3]$ ion pair is shown in Figure 4.20(a).

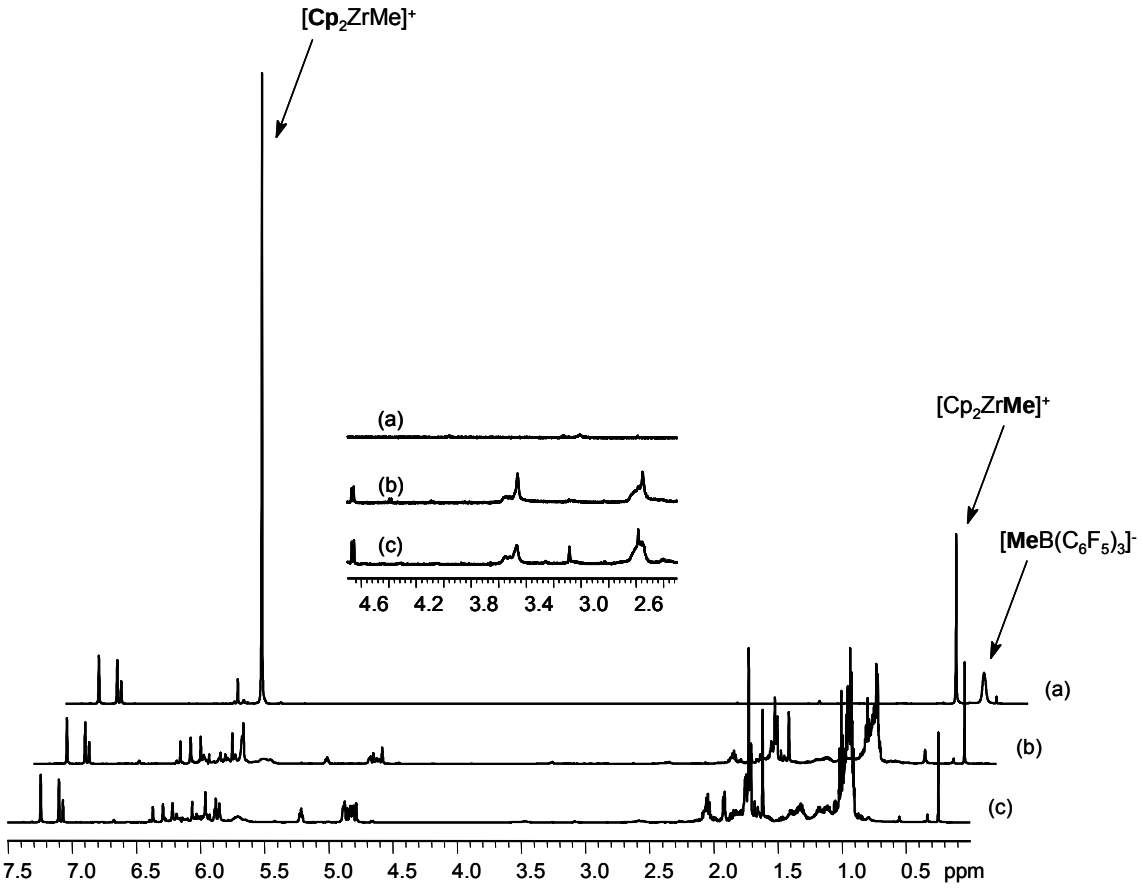

Figure 4.20. ^1H NMR spectra of the *in situ* propylene polymerization by $[Cp_2ZrMe][MeB(C_6F_5)_3]$ in chlorobenzene-d_5 (room temperature, 600 MHz). (a) The $[Cp_2ZrMe][MeB(C_6F_5)_3]$ ion pair, (b) after addition of 5 equivalents of propylene, (c) after addition of 10 equivalents of propylene. The inset shows the allylic region.

In this spectrum, the **Cp** and Zr-**Me** resonances of the cationic methyl zirconocene $[Cp_2ZrMe]^+$ complex are present at 5.97 and 0.56 ppm, respectively, while the $[\mathbf{Me}B(C_6F_5)_3]^-$ resonance is present at 0.34 ppm.

Upon addition of a roughly 5-fold excess of propylene to the above ion pair solution, the **Cp** resonance at 5.97 ppm and Zr-**Me** resonance at 0.56 ppm decreased in intensity while the backbone resonances of short chain atactic polypropylene oligomers appeared between 0.7 and 2.2 ppm (Figure 4.20(b)). The **Me**-B resonance at 0.34 ppm was not evident any more and it seems reasonable that it is overlapped with the backbone polypropylene oligomer resonances after being shifted downfield toward a free $[\mathbf{Me}B(C_6F_5)_3]^-$ resonance (1.1-1.2 ppm) (see Section 4.2.1.1). The ^1H NMR spectrum of the reaction mixture also shows the presence of a series of broad exchange resonances in the allyl region between 2.5 and 4.8 ppm and a resonance at 0.25 ppm attributable to methane, in addition to the olefinic end group resonances between 4.8 and 5.4 ppm. Also, a series of low relative intensity resonances are present in the Cp region between 5.9 and 6.4 ppm. While no attempt to identify all these resonances was done, it seems reasonable that they belong to various Zr-alkyl oligomers present in the reaction mixture. Subsequent addition of another 5-fold excess of propylene resulted in the complete disappearance of the **Cp** and Zr-**Me** resonances of the initial cationic zirconocene $[Cp_2ZrMe]^+$ catalyst and an increase in the intensities of all new resonances formed following the addition of propylene (Figure 4.20(c)).

The ^1H NMR spectra in the olefinic end group region of the obtained atactic polypropylene oligomers is shown in Figure 4.21.

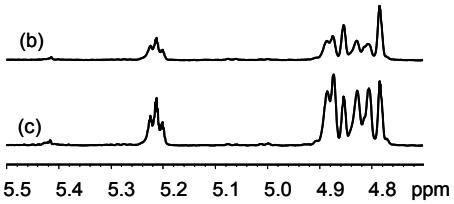

Figure 4.21. ^{1}H NMR spectra, in the olefinic end group region of atactic polypropylene oligomers obtained from $[Cp_2ZrMe][MeB(C_6F_5)_3]$ in chlorobenzene-d_5 at room temperature, using (b) 5 equivalents of propylene and (c) 10 equivalents of propylene.

As can be seen, the spectra show the presence of multiple olefinic resonances between 4.78 and 4.94 ppm. These resonances were attributed[34] to the vinylidene end groups and possibly internal vinylidene groups of different length, short chain atactic polypropylene oligomers. A terminal vinylidene group arises from β-hydride elimination following a primary (1,2) propylene insertion into Zr-alkyl chains while an internal vinylidene group is the result of propylene insertion into a Zr-allyl bond, as explained in Section 2.2.4.

Interestingly, a closer look to the ^{1}H NMR spectra in the olefinic region of atactic polypropylene oligomers also reveals the presence of a triplet resonance at ~5.2 ppm (J_{HH} = 7 Hz). As indicated by Resconi *et al.*,[7b,35] a triplet resonance at ~5.2 ppm has been previously observed in the ^{1}H NMR spectra of isotactic polypropylene and it was assigned to an internal unsaturation group of type $CH_3CH_2CH_2CH=C(CH_3)P$, where P is a polymeryl chain. Because this resonance was observed[7b,35] to arise only in conjunction with the *cis*-2-butenyl end group resonance[36] at ~5.4 ppm, it was proposed to be connected to the presence of secondary (2,1) insertions.[7b,35] A possible mechanism which could explain the occurrence of an internal olefinic group of the type $-CH_2CH_2CH=C(CH_3)-$ on the polymer chain is depicted in Scheme 4.16 and would

involve a secondary propylene insertion into a primary Zr-polymeryl bond, followed by a 2,1 to 3,1-isomerization and further primary propylene insertion, when a chain defect consisting of four methylene units would be incorporated into the polymer chain. Subsequent β-hydrogen elimination, followed by allylic C-H activation of the vinylidene chain end at the methylene group and further propylene insertion into Zr-allyl bond would incorporate an internal unsaturation of the type -C(Me)=CHCH$_2$CH$_2$CH$_2$- into the polymer chain.

Scheme 4.16. Possible mechanism for formation of an internal olefinic group of the type -C(Me)=CHCH$_2$CH$_2$CH$_2$-

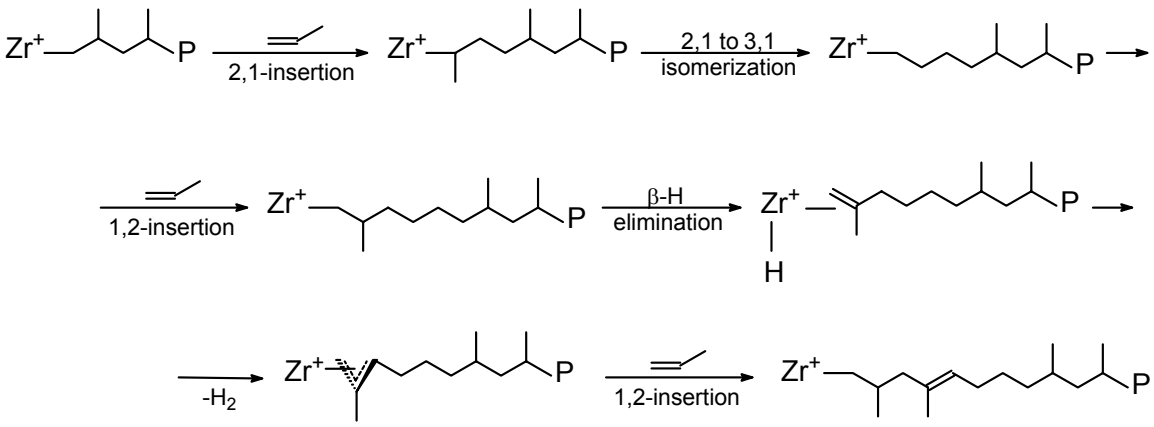

However, while isotactic polypropylene is known to incorporate small amounts of regiodefects as a result of occasional secondary propylene insertions,[7b] so far there is no evidence of the presence of secondary insertions in atactic polypropylene. Another possible mechanism which might account for the formation of an olefinic group of type -CH$_2$CH$_2$CH=C(Me)(alkyl) is shown in Scheme 4.17. This mechanism involves two

consecutive primary insertions of propylene into a Zr-H bond, followed by β-hydrogen elimination and allylic C-H activation of the vinylidene chain end at the methylene group to form a cationic Zr(η^3-$CH_2C(Me)CHCH_2CH_3$) species. Subsequent propylene insertion into the Zr-allyl bond would result in a polymeryl chain with a $CH_3CH_2CH=C(Me)$- end group. To the best of our knowledge, the presence of a 3-propenyl end group on polypropylene chains has not been reported previously.

Scheme 4.17. Possible mechanism for formation of a $CH_3CH_2CH=C(Me)$- end group.

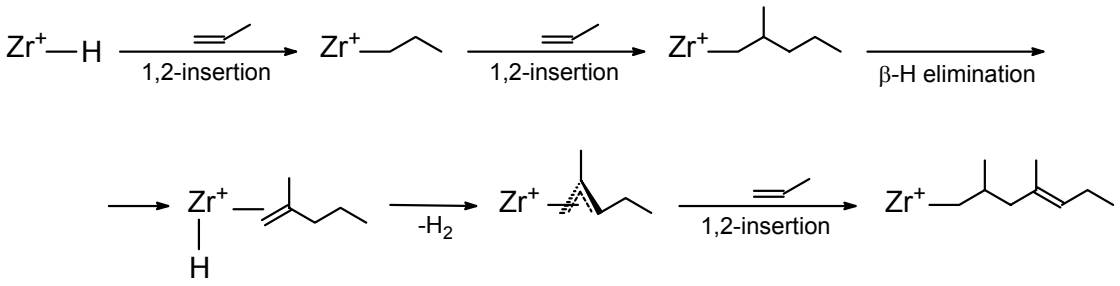

This latter mechanism shows that the presence of a triplet resonance at ~5.2 ppm in the ^{1}H NMR spectra of polypropylene can be connected with the presence of the Zr(η^3-allyl) species during the polymerization and does not necessarily need the presence of a secondary insertion. Indeed, as shown in Figure 4.20, the ^{1}H NMR spectra of *in situ* propylene polymerization by $[Cp_2ZrMe][MeB(C_6F_5)_3]$ in chlorobenzene-d_5 shows also the presence of allylic resonances between 2.5 and 4.8 ppm, in addition to the olefinic resonances between 4.78 and 4.94 ppm. Also, a closer examination of the ^{1}H NMR spectra of isotactic polypropylene in references [7b] and [35] indicates the presence of internal vinylidene groups, which were ascribed to the presence of Zr-allyl species during

the polymerization, in addition to the triplet resonance at 5.2 ppm; however, no connection between the presence of the triplet at 5.2 ppm and that of internal vinylidene groups was previously made.

As stated above, the ^{1}H NMR spectra of atactic polypropylene (Figure 4.20) shows the presence of weak resonances in the allylic region between 2.5 and 4.8 ppm. On the basis of comparison with the ^{1}H NMR spectra of complexes **A** - **D** (see Figures 4.1 and 4.4), these resonances were attributed to various Zr-allyl oligomer intermediates of the type $[Cp_2Zr(\eta^3\text{-}CH_2C(CH_2P)CH_2)]^+$ (major) and $[Cp_2Zr(\eta^3\text{-}CH_2C(Me)CHP)]^+$ (minor), where P is a short chain alkyl or polymeryl group, formed during the propylene oligomerization reaction. The presence of the methane resonance at 0.25 ppm in the reaction mixture is also diagnostic of the formation of Zr-allyl species. Specifically, it suggests that Zr-allyl oligomers were formed in the early stages of the oligomerization reaction, before even the first ^{1}H NMR spectrum was acquired, by recoordination of the vinylidene end groups of short chain oligomers to the unreacted cationic zirconocene $[Cp_2ZrMe]^+$ catalyst followed by C-H activation. However, an additional mechanism for Zr-allyl species formation in which β-H elimination of Zr-polymeryl species is followed directly by C-H activation, without alkene dissociation (Scheme 4.1(b)), cannot be ruled out.

In order to establish whether Zr-allyl species formation during propylene polymerization by zirconocene catalysts represents a general reaction pathway, *in situ* propylene polymerization by Cp_2ZrMe_2 activated with $[Ph_3C][B(C_6F_5)_4]$ was also investigated. In this regard, the neutral dimethyl zirconocene catalyst was reacted with 1.1-1.2 equivalents of $[Ph_3C][B(C_6F_5)_4]$ in chlorobenzene-d_5 at room temperature to form

Ph_3CMe (2.13 ppm (**Me**) and 7.1-7.4 ppm (**Ph**)) and the solvated complex $[Cp_2ZrMe][B(C_6F_5)_4]$ (5.99 ppm (**Cp**) and 0.78 ppm (Zr-**Me**)). For this catalytic system, small amounts of methyl bridged binuclear cations $[(Cp_2ZrMe)_2(\mu\text{-}Me)]^+$ were also formed and they were slowly converted to the mononuclear species by warming the NMR tube at 40°C for 30 min. A typical ^1H NMR spectrum of the solvated $[Cp_2ZrMe][B(C_6F_5)_4]$ complex is shown in Figure 4.22(a).

Addition of roughly 5 equivalents of propylene to the chlorobenzene-d_5 solution of $[Cp_2ZrMe][B(C_6F_5)_4]$ at room temperature resulted in complete conversion of propylene to low molecular weight polypropylene chains as indicated by the broad resonances present in the aliphatic region (0.9–2 ppm) of the ^1H NMR spectrum while a majority of the initial cationic zirconocene catalyst $[Cp_2ZrMe]^+$ remained unconsumed (Figure 4.22(b)). This implies a very fast propagation and very low degrees of catalyst initiation.[12b] Also present in the ^1H NMR spectrum are the Zr-allyl resonances between 2.5 and 4.7 ppm and a resonance at 0.25 ppm attributed to methane. Subsequent addition of another 5 equivalents of propylene to the reaction mixture resulted again in quantitative consumption of propylene while the resonances of the initial cationic zirconocene catalyst at 5.99 ppm (**Cp**) and 0.78 ppm (Zr-**Me**) are still present (Figure 4.22(c)). As expected, the allyl and methane resonances all have increased in intensity. The presence of Zr-allyl oligomers in the reaction mixture is also evident from the two Cp resonances at 5.69 and 5.78 ppm attributable to nonequivalent Cp groups of $Cp_2Zr^+(\eta^3\text{-allyl})$ oligomers (compare with Figure 4.6(b)).

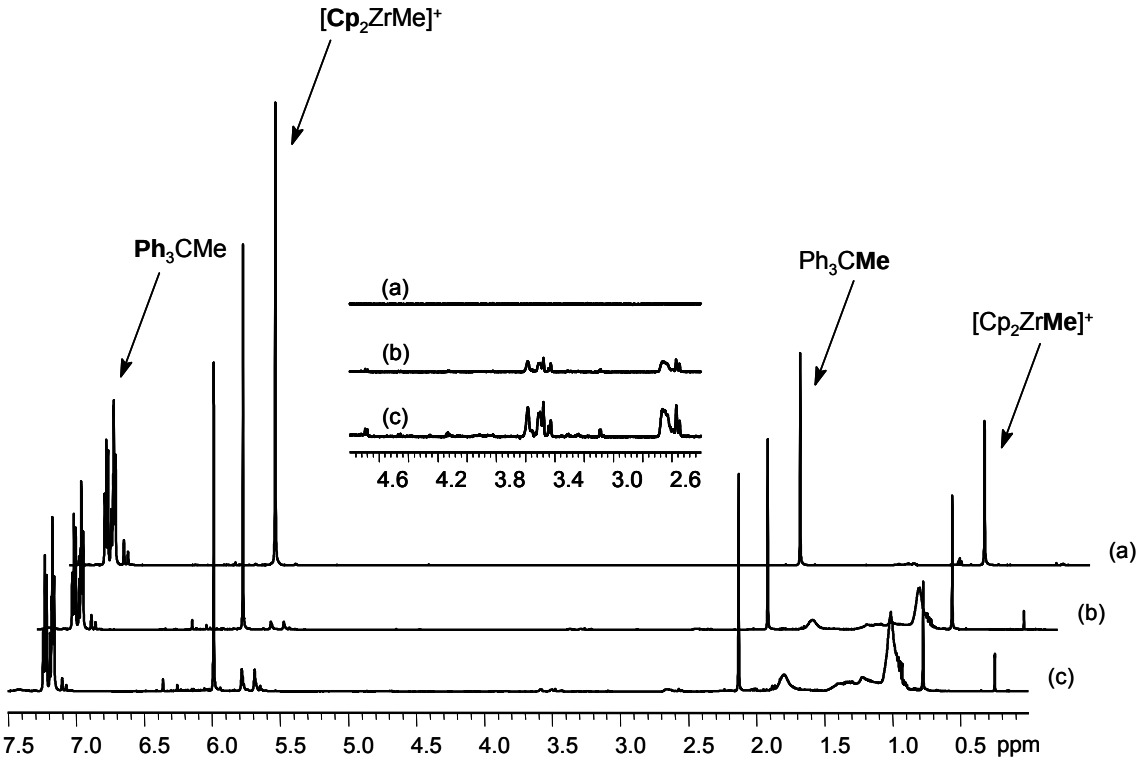

Figure 4.22. ^{1}H NMR spectra of the *in situ* propylene polymerization by $[Cp_2ZrMe][B(C_6F_5)_4]$ in chlorobenzene-d_5 (room temperature, 600 MHz). (a) the $[Cp_2ZrMe][B(C_6F_5)_4]$ ion pair, (b) after addition of 5 equivalents of propylene, (c) after addition of 10 equivalents of propylene. The inset shows the allylic region.

The olefinic resonances resulting from chain transfer reactions are absent from the ^{1}H NMR spectra of the reaction mixture. The lack of olefinic end group resonances, coupled with the observation of a methane resonance at 0.25 ppm and of Zr-allyl resonances between 2.5 and 4.7 ppm, implies that while β-elimination reactions occur during the polymerization, any olefinic end group of the polymeryl chains recoordinated to the metal center to be further converted to Zr-allyl species with elimination of methane before the first NMR spectrum was recorded.

The allylic region of the ^{1}H NMR spectra in Figures 4.20 and 4.22 looks complicated due to different chain length Cp_2Zr^+-allyl oligomers. As a result, a clear identification of individual oligomeric Cp_2Zr^+-allyl species by ^{1}H NMR spectroscopy is difficult. In order to identify individual Cp_2Zr^+-allyl oligomer species present in the polymerization system, the polymerization reaction mixture was analyzed by using electrospray ionization tandem mass spectrometry.

In a typical experiment, the propylene oligomerization reaction has been carried out by adding 5 equivalents of propylene to a room temperature $[Cp_2ZrMe][MeB(C_6F_5)_3]$ ion pair solution ($4x10^{-2}$ M) generated *in situ* in chlorobenzene, from activation of the Cp_2ZrMe_2 precursor catalyst by $B(C_6F_5)_3$. The resulted polypropylene oligomer mixture was further diluted 2-fold with chlorobenzene and then fed continuously into the first quadrupole of a QSTAR XL QqTOF mass spectrometer via an electrospray ionization interface.

The ESI-MS spectra of the reaction mixture obtained in positive ion mode by scanning the first quadrupole were complex and of low quality due to many overlapping peaks. Indeed, a typical ESI-MS spectrum of a zirconocene complex displays a distinct isotopic pattern of seven peaks, due to contribution of the five principal natural isotopes of zirconium and along with the natural isotopes of carbon and hydrogen.[37] Due to the large variety of Cp_2Zr^+ containing reaction intermediates which can form during the polymerization and which can differ by an m/z less than 7, extensive overlapping of peaks is expected to occur, such that the isotopic pattern of individual zirconocene containing intermediates present in the reaction mixture cannot be clearly distinguished.

A typical ESI-MS spectrum of a polypropylene oligomer mixture in chlorobenzene is shown in Figure 4.23.

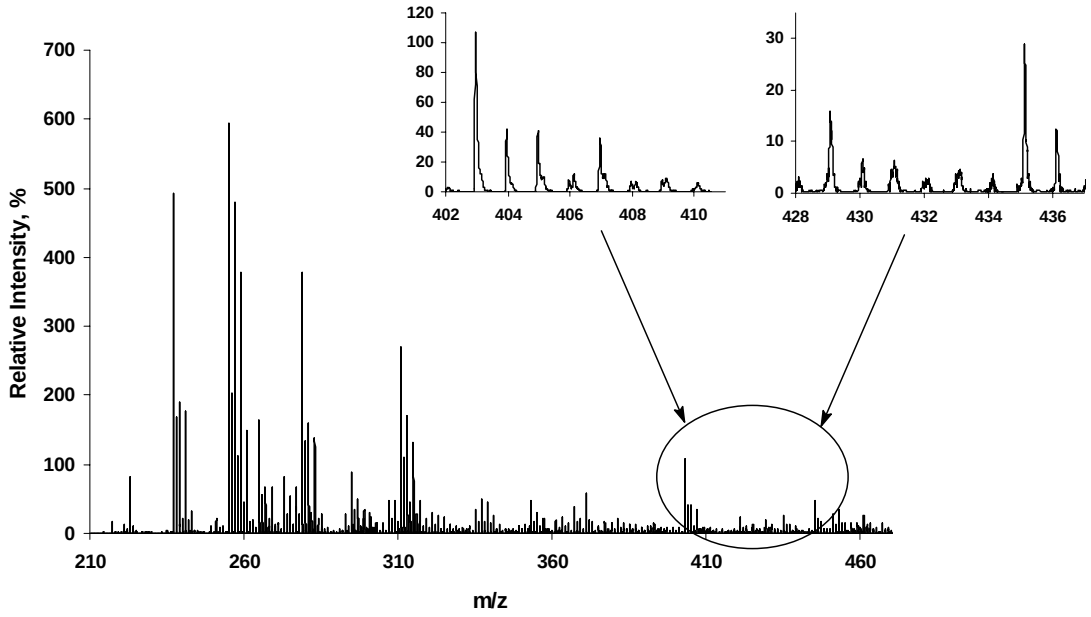

Figure 4.23. Positive mode ESI-MS spectrum of a polypropylene oligomer mixture in chlorobenzene. Insets show isotopic patterns for peaks at m/z 403-410 and m/z 429-436 which may be assigned to $[Cp_2Zr(C_3H_6)_4CH_3]^+$ and $[Cp_2Zr(C_3H_4)(C_3H_6)_4H]^+$, respectively.

The complexity of the ESI-MS spectra is further enhanced by some decomposition of the reaction intermediates due to impurities and traces of water present in the instrument. For instance, the presence of traces of water was evident from the presence of a large peak at m/z 237, with an isotopic pattern consistent with the Cp_2Zr^+OH complex,[38] as shown in Figure 4.24. As a result, direct identification of various oligomeric zirconocene intermediates present in reaction mixture by ESI-MS is very difficult.

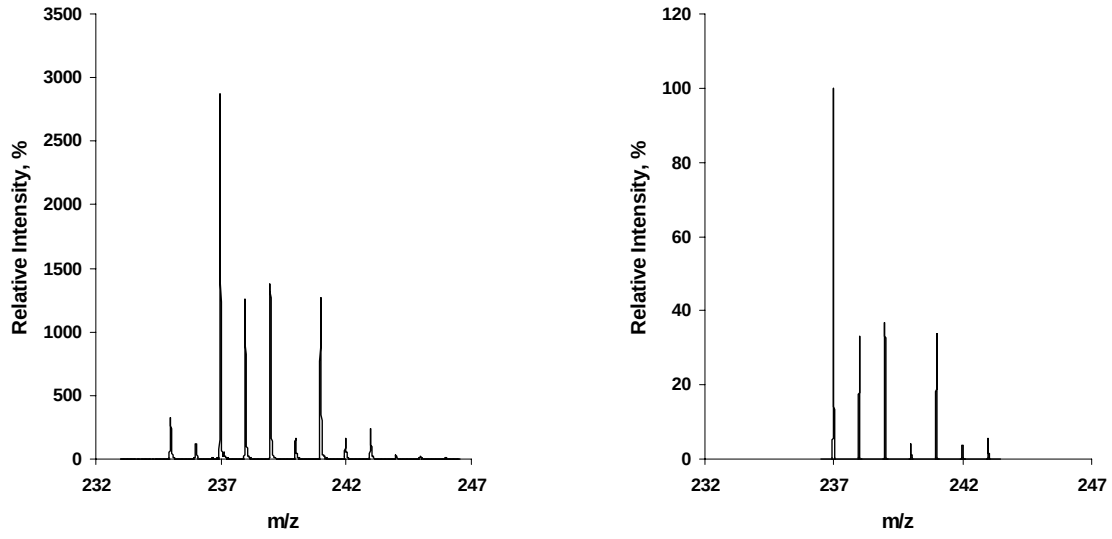

(a) (b)

Figure 4.24. (a) Positive mode ESI-MS spectrum of the peak at m/z 237, (b) The theoretical isotopic product distribution of $C_{10}H_{10}ZrOH$.

In order to identify the cationic polymerization intermediates of interest, specific m/z peaks corresponding to particular zirconocene complexes were isolated from first quadrupole and further examined by collision-induced dissociation (CID) experiments. A single m/z value, corresponding to the isotopic species having the most abundant ^{90}Zr isotope, was selected for each particular zirconocene complex. An example of an ion fragmentation experiment by CID is shown in Figure 4.25.

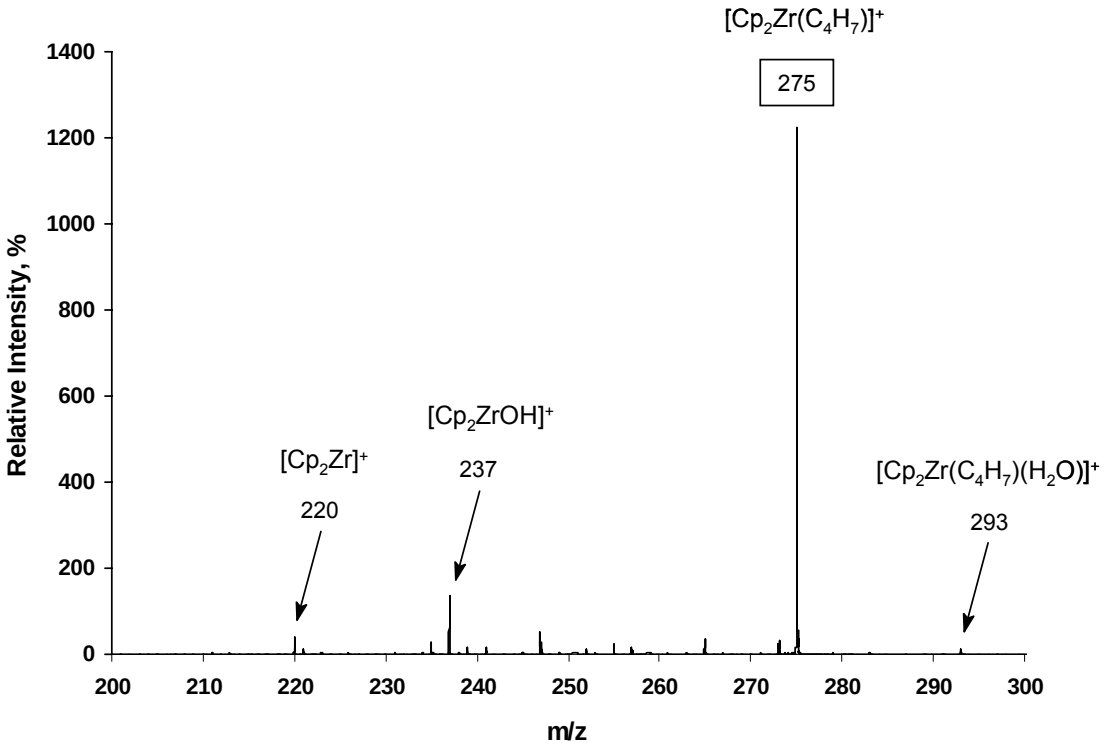

Figure 4.25. Positive mode ESI-MS/MS spectrum of the oligomeric zirconocene intermediate cation of m/z 275.

As can be seen, the selected ion of m/z 275, corresponding to $[Cp_2Zr(C_4H_7)]^+$, shows a loss of C_4H_7 ligand[37] to give an ion of m/z 220 corresponding to the $[Cp_2Zr]^+$ fragment ion. The $[Cp_2Zr]^+$ fragment ion is diagnostic for identification of a zirconocene complex.[37,39] Also present in the spectrum are ions of m/z 237 corresponding to the $[Cp_2ZrOH]^+$ complex[38] and m/z 293 which can be assigned to the $[Cp_2Zr(C_4H_7)(H_2O)]^+$ adduct ion. These ions are the reaction products formed in the collision cell from the zirconocene cation of m/z 275 with traces of water as shown in Equation 4.7.

$$[Cp_2Zr(C_4H_7)]^+ + H_2O \rightarrow [Cp_2Zr(C_4H_7)(H_2O)]^+ \rightarrow [Cp_2ZrOH]^+ + C_4H_8 \quad (\mathbf{4.7})$$

m/z 275 m/z 293 m/z 237

Similarly, the presence of ions of m/z 317, 359, 401, 443 and 485 corresponding to $Cp_2Zr^+(C_3H_4)(C_3H_6)_nCH_3$ species (n=1-5) and also the presence of ions of m/z 261 corresponding to $Cp_2Zr^+(C_3H_4)H$ species in the polymerization mixture could be detected. The CID experiments of the above mentioned ions always lead to formation of a fragment ion of m/z 220 corresponding to the $[Cp_2Zr]^+$ complex, an ion of m/z 237 corresponding to the $[Cp_2ZrOH]^+$, as well as the formation of ions of m/z corresponding to the selected ion-water adduct. The product ion distribution for the cationic allyl oligomers $[Cp_2Zr(C_3H_4)(C_3H_6)_nCH_3]^+$, (n=0-5) is shown in Figure 4.26. It should be mentioned here that a small contribution to the intensity of these peaks can also come from a $[Cp_2Zr\text{-polymeryl}]^+$ complex bearing an internal unsaturation. Such a species would result from further propylene insertion into a Zr-allyl bond during the polymerization. Therefore this study focuses only on qualitative identification of Cp_2Zr^+-allyl polymeryl complexes.

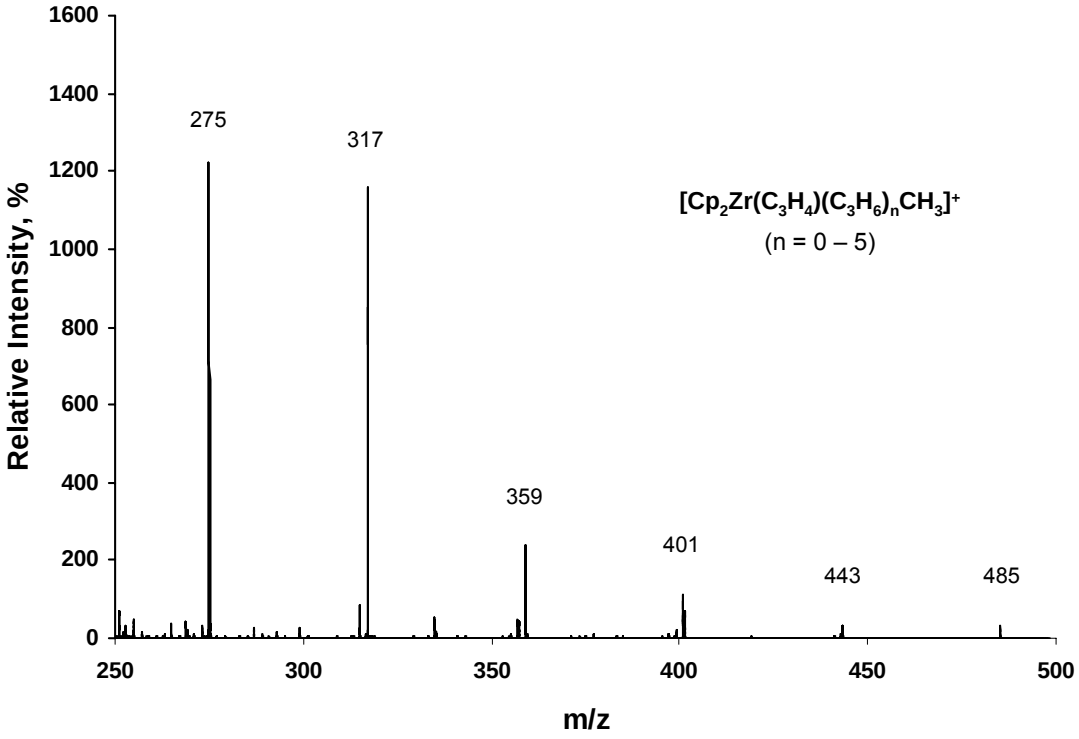

Figure 4.26. Positive mode ESI-MS/MS spectrum of the distribution of oligomeric zirconocene intermediate cations of m/z 275, 317, 359, 401, 443, and 485.

$[Cp_2Zr(allyl)]^+$ complexes were previously detected by MS/MS as the main reaction products of corresponding Zr-polymeryl species in the CID experiments via loss of H_2.[39] However, to our knowledge direct identification of oligomeric Zr-allyl intermediates preformed in solution under catalytic conditions by ESI-MS/MS was not reported previously.

4.3. Summary

In this chapter, a study regarding formation and characterization of Cp_2Zr^+-allyl complexes is reported.

Reactions between Cp_2ZrMe_2, activated with either $B(C_6F_5)_3$ or $[Ph_3C][B(C_6F_5)_4]$, and 2,4-Me_2-1-pentene and 2,4-Me_2-1-heptene, in chlorobenzene-d_5 at room temperature, result in the irreversible formation of $[Cp_2Zr(\eta^3\text{-allyl})]^+$ complexes and the release of methane. These complexes have been characterized in solution by NMR spectroscopy with respect to their structure and dynamic behaviour. The reactions imply that vinylidene end groups of the polymer chains released during the polymerization as a result of β-hydrogen elimination reaction may react in the same way with the active catalyst to form Cp_2Zr^+-allyl polymeryl intermediates which are considered to remain "dormant" and thus to affect the catalyst activity. Thus, the formation and characterization of $[Cp_2Zr(\eta^3\text{-allyl})]^+$ complexes can provide insight in the formation and characterization of similar Zr-allyl polymeryl intermediates which might arise during zirconocene catalyzed propylene polymerization reactions.

The formation of $[Cp_2Zr(\eta^3\text{-}CH_2C(CH_2CHMe_2)CH_2)][B(C_6F_5)_4]$ from the reaction between $[Cp_2ZrMe][B(C_6F_5)_4]$ and 2,4-Me_2-1-pentene in chlorobenzene-d_5 occurs via the $[Cp_2Zr(Me)(CH_2C(Me)CH_2CHMe_2)][B(C_6F_5)_4]$ intermediate which was detected by low temperature NMR spectroscopy. The identification of the $[Cp_2Zr(Me)CH_2C(Me)CH_2CHMe_2]^+$ complex represents the first direct experimental evidence of a $[Cp_2Zr(alkyl)(alkene)]^+$ complex as a reaction intermediate. Low temperature ^1H NMR experiments indicate that the two terminal vinylidene hydrogens of the coordinated olefin undergo intramolecular exchange. The intramolecular exchange of

the two terminal vinylidene hydrogens of the coordinated olefin can occur through a $Cp_2Zr(Me)CH_2C^+(Me)CH_2CHMe_2$ carbocation intermediate and this process can constitute a mechanism for chain end epimerization in stereoregular alkene polymerization.

Variable temperature ^1H NMR experiments indicate that all $[Cp_2Zr(\eta^3\text{-allyl})]^+$ complexes synthesized in this chapter are non-fluxional at low temperature; by increasing the temperature, however, they adopt a dynamic behavior. The free energy of activation for the exchange processes, as estimated from the coalescence temperature of the two Cp ligands, is between 54 and 70 kJ/mol.

The kinetic study indicates that formation of Cp_2Zr^+-allyl species from the active catalyst $[Cp_2ZrMe][MeB(C_6F_5)_3]$ and 2,4-Me_2-1-pentene requires an activation energy of ~50 kJ/mol. The activation energy required for the Cp_2Zr^+-allyl formation from $[Cp_2ZrMe][B(C_6F_5)_4]$ and 2,4-Me_2-1-pentene, on the other hand, is lower (~46 kJ/mol) as expected when an anion with less coordinating ability is used. These activation energy values for formation of Zr-allyl complexes imply that formation of similar Zr-allyl polymeryl intermediates during propylene polymerization is quite feasible and it can become competitive with chain propagation when a high concentration of vinylidene terminated polymeryl chains accumulate in the polymerization system.

In situ propylene polymerizations by $Cp_2ZrMe_2/B(C_6F_5)_3$ and $Cp_2ZrMe_2/[Ph_3C][B(C_6F_5)_4]$, respectively, in chlorobenzene-d_5 at room temperature allowed direct observation of various Cp_2Zr^+-allyl polymeryl intermediates formed under catalytic conditions.

This study provides clear evidence that vinylidene end groups of polymeryl chains released as a result of β-elimination reactions are not simply spectators of the polymerization process but they can recoordinate to the active catalyst to convert it to less reactive Zr-allyl intermediates and in this way to decrease the catalyst activity.

4.4. Experimental Section

4.4.1. General Considerations

All chemicals were purchased from Aldrich unless stated otherwise. 2,4-Me_2-1-pentene and 2,4-Me_2-1-heptene were purchased from ChemSampCo. Chlorobenzene was dried by distillation, under argon, from calcium hydride prior to use. Deuterated chlorobenzene was obtained from Cambridge Isotope Laboratories (>99% atom %D) and dried by vacuum distillation from CaH_2, stored over molecular sieves and handled in a glove box. Polymerization grade propylene (99.5wt% purity, liquid phase, Praxair), was dried by passage through a column of activated 4 Å molecular sieves prior to use. Cp_2ZrMe_2 and $B(C_6F_5)_3$ were synthesized as described in Sections 2.4.2 and 2.4.5, respectively. Handling and storage of air-sensitive organometallic compounds was done using an MBraun Labmaster glove box.

NMR spectra were run on a Bruker AV 600 spectrometer, chemical shifts being referenced using the residual proton signals of the deuterated chlorobenzene. Probe temperatures were calibrated using methanol (low temperature) and ethylene glycol (high temperature) samples as references. ^1H NMR spectra were acquired with a 45 degree pulse and 1 sec delay between pulses; 16 transients were stored for each spectrum. ^1H-^{13}C HSQC spectra were collected using Echo/Antiecho-TPPI gradient selection with

decoupling (or with no decoupling, respectively) during acquisition using shaped pulses for all 180 degree pulses on f2-channel. The HSQC acquisition parameters were: a 0.1705 sec acquisition time, a 10 ppm spectral window in f2, a 165.6 ppm spectral window in f1 and a 1 sec relaxation delay. ^{1}H-^{13}C HMBC spectra were obtained via heteronuclear zero and double quantum coherence optimized on long range couplings of 5 Hz, with low-pass J-filter to suppress one-bond correlations and no decoupling during acquisition using gradient pulses for selection. The HMBC acquisition parameters were: a 0.1705 sec acquisition time, a 10 ppm spectral window in f2, a 222.3 ppm spectral window in f1 and a 1 sec relaxation delay. NOESY spectra were recorded using 2D homonuclear correlation via dipolar coupling (due to noe or chemical exchange); phase sensitive using Echo/Antiecho-TPPI gradient selection, with gradient pulses in mixing time. The NOESY acquisition parameters were: a 0.1672 sec acquisition time, a 10.2 spectral window in f2 and f1, respectively, a 2 sec relaxation delay and a 0.4 sec mixing time. ROESY spectra were collected with cw spinlock for mixing; phase sensitive using Echo/Antiecho-TPPI gradient selection. The ROESY acquisition parameters were: a 0.1672 sec acquisition time, a 10.2 ppm spectral window in f2 and f1, respectively, a 2 sec relaxation delay and a 0.3 sec mixing time.

ESI-MS/MS experiments were performed on a MDS Sciex QSTAR XL QqTOF mass spectrometer in ESI positive mode and were run by Dr. Bernd Keller.

4.4.2. *In situ* Reaction between $[Cp_2ZrMe][MeB(C_6F_5)_3]$ and 2,4-dimethyl-1-pentene

A solution of Cp_2ZrMe_2 (40 μmole) in C_6D_5Cl (0.5 mL) was added to a solution of $B(C_6F_5)_3$ (1.1 equiv.) in C_6D_5Cl (0.5 mL) and the yellow ion pair solution thus formed

was transferred to an NMR tube. The NMR tube was sealed with a rubber septum and parafilm and removed from the glovebox. Prior to running the NMR spectrum, 2,4-dimethyl-1-pentene (1 to 5 equivalents) was injected in the NMR tube via a microsyringe at room temperature. The progress of the reaction was monitored by ^{1}H NMR spectroscopy. The reaction products could not be isolated and were characterized in solution by ^{1}H NMR and correlation spectroscopy.

NMR Spectroscopic Data of [$Cp_2Zr(\eta^3$-$CH_2C(CH_2CHMe_2)CH_2)][MeB(C_6F_5)_3]$

^{1}H NMR (600 MHz, C_6D_5Cl, 25°C): δ 5.7 (br s, C_5H_5, 10H), 3.47 (s, allyl H_a, 2H), 2.56 (s, allyl H_s, 2H), 1.99 (d, CH_2, 2H), 1.76 (m, CH, 1H), 0.98 (d, CH_3, 6H) ppm.

^{1}H NMR (600 MHz, C_6D_5Cl, 0°C): δ 5.7 (s, C_5H_5, 5H), 5.58 (s, C_5H_5, 5H), 3.36 (s, allyl H_a, 2H), 2.54 (s, allyl H_s, 2H), 1.94 (d, CH_2, 2H), 1.75 (m, CH, 1H), 1.01 (d, CH_3, 6H) ppm.

^{13}C NMR (600 MHz, C_6D_5Cl, 0°C): δ 111.7 (C_5H_5, $^{1}J_{C\text{-}H}$ = 175 Hz), δ 110.5 (C_5H_5, $^{1}J_{C\text{-}H}$ = 175 Hz), 67.2 (allyl CH_2, $^{1}J_{C\text{-}H\textit{anti}}$ = 145 Hz, $^{1}J_{C\text{-}Hsyn}$ = 159 Hz), 52 (CH_2, $^{1}J_{C\text{-}H}$ = 131 Hz), 31.1 (CH, $^{1}J_{C\text{-}H}$ = 126 Hz), 22.1 (CH_3, $^{1}J_{C\text{-}H}$ = 129 Hz) ppm.

^{1}H NMR (600 MHz, C_6D_5Cl, -40°C): δ 5.61 (s, C_5H_5, 5H), 5.52 (s, C_5H_5, 5H), 3.24 (s, allyl H_a, 2H), 2.5 (s, allyl H_s, 2H), 1.88 (d, $^{3}J_{HH}$ = 6.8 Hz, CH_2, 2H), 1.74 (m, CH, 1H), 1.02 (d, $^{3}J_{HH}$ = 6.8 Hz, CH_3, 6H) ppm.

NMR Spectroscopic Data of $[Cp_2Zr(\eta^3\text{-}CH_2C(Me)(CHCHMe_2))][MeB(C_6F_5)_3]$

^{1}H NMR (600 MHz, C_6D_5Cl, -40°C): δ 5.72 (s, C_5H_5, 5H), 5.54 (s, C_5H_5, 5H), 3.75 (d, $^3J_{HH}$ = 9.4 Hz, allyl CH, 1H), 3.29 (d, $^2J_{HH}$ = 1.9 Hz, allyl H_a, 1H), 2.32 (d, $^2J_{HH}$ = 1.9 Hz, allyl H_s, 1H) ppm. The other resonances are obscured.

4.4.3. *In situ* Reaction between $[Cp_2ZrMe][MeB(C_6F_5)_3]$ and 2,4-dimethyl-1-heptene

A solution of Cp_2ZrMe_2 (40 μmole) in C_6D_5Cl (0.5 mL) was added to a solution of $B(C_6F_5)_3$ (1.1 equiv.) in C_6D_5Cl (0.5 mL) and the yellow ion pair solution thus formed was transferred to an NMR tube. The NMR tube was sealed with a rubber septum and parafilm and removed from the glovebox. Prior to running the NMR spectrum, 2,4-dimethyl-1-heptene (1 to 10 equivalents) was injected in the NMR tube via a microsyringe at room temperature. The progress of the reaction was monitored by ^{1}H NMR spectroscopy. The reaction products could not be isolated and were characterized in solution by ^{1}H NMR and correlation spectroscopy.

NMR Spectroscopic Data of

$[Cp_2Zr(\eta^3\text{-}CH_2C(CH_2CH(Me)C_3H_7)CH_2)][MeB(C_6F_5)_3]$

^{1}H NMR (600 MHz, C_6D_5Cl, 0°C, the resonances were assigned by using correlation spectroscopy): δ 5.71 (s, C_5H_5, 5H), 5.61 (s, C_5H_5, 5H), 3.42 (s, allyl CH_2, H_a, 1H), 3.36 (s, allyl CH_2, H_a, 1H), 2.58 (s, allyl CH_2, H_s, 1H), 2.56 (s, allyl CH_2, H_s, 1H), 2.14 (dd, CH_2, 1H), 1.89 (CH_2, 1H), 1.64 (CH, 1H), 0.99 (CH_3, 3H), 1.18 (CH_2, 1H), 1.39 (CH_2, 1H) ppm, the terminal ethyl peaks are obscured.

^{1}H NMR (600 MHz, C_6D_5Cl, -40°C): δ 5.62 (d, $^3J_{HH}$ = 1.5 Hz, C_5H_5, 5H), 5.54 (d, $^3J_{HH}$ = 1.5 Hz, C_5H_5, 5H), 3.31 (s, allyl CH_2, H_a, 1H), 3.24 (s, allyl CH_2, H_a, 1H), 2.55 (s, allyl CH_2, H_s, 1H), 2.53 (s, allyl CH_2, H_s, 1H) ppm.

NMR Spectroscopic Data of $Cp_2Zr(\eta^3\text{-}CH_2C(Me)(CHCH(Me)C_3H_7)][MeB(C_6F_5)_3]$

^{1}H NMR (600 MHz, C_6D_5Cl, 0°C): δ 5.88 (s, C_5H_5, 5H), 5.62 (s, C_5H_5, 5H), 4.60 (d, $^3J_{HH}$ = 9.1 Hz, allyl CH, 1H), 3.01 (s, $^2J_{HH}$ = 4.5 Hz, allyl CH_2, H_a, 1H), 1.85 (s, allyl CH_2, H_s, 1H), 1.82 (s, CH_3, 3H), 1.70 (CH, 1H), 0.81 (d, CH_3, 3H), 1.17 (CH_2, 1H), 0.88 (CH_2, 1H), 0.78 (CH_2, 1H), 0.67 (CH_2, 1H), 0.77 (t, CH_3, 3H) ppm.

^{1}H NMR (600 MHz, C_6D_5Cl, -40°C): δ 5.83 (d, $^3J_{HH}$ = 1.5 Hz, C_5H_5, 5H), 5.56 (d, $^2J_{HH}$ = 1.5 Hz, C_5H_5, 5H), 4.52 (d, $^3J_{HH}$ = 9.1 Hz, allyl CH, 1H), 2.93 (d, $^2J_{HH}$ = 4.5 Hz, allyl CH_2, H_a, 1H), 1.83 (d, $^2J_{HH}$ = 4.5 Hz, allyl CH_2, H_s, 1H) ppm.

4.4.4. *In situ* Reaction between $[Cp_2ZrMe][B(C_6F_5)_4]$ and 2,4-dimethyl-1-pentene

A solution of Cp_2ZrMe_2 (40 μmole) in C_6D_5Cl (0.5 mL) was added to a solution of $[Ph_3C][B(C_6F_5)_4]$ (1.1 equiv.) in C_6D_5Cl (0.5 mL) and the orange ion pair solution thus formed was transferred to an NMR tube. The NMR tube was sealed with a rubber septum and parafilm and removed from the glovebox. Prior to running the NMR spectrum, 2,4-dimethyl-1-pentene (1.5 equivalents) was injected in the NMR tube via a microsyringe at room temperature. The progress of the reaction was monitored by ^{1}H NMR spectroscopy. The reaction products could not be isolated and were characterized in solution by ^{1}H NMR and correlation spectroscopy.

NMR Spectroscopic Data of $[Cp_2Zr(\eta^3\text{-}CH_2C(CH_2CHMe_2)CH_2)][B(C_6F_5)_4]$

^{1}H NMR (600 MHz, C_6D_5Cl, 0°C): δ 5.71 (s, C_5H_5, 5H), 5.60 (s, C_5H_5, 5H), 3.38 (s, allyl H_a, 2H), 2.56 (s, allyl H_s, 2H), 1.96 (d, CH_2, $^3J_{HH}$ = 6.5 Hz, 2H), 1.76 (m, CH, 1H), 1.01 (d, CH_3, $^3J_{HH}$ = 6.5 Hz, 6H) ppm.

^{13}C NMR (600 MHz, C_6D_5Cl, 0°C): δ 112.8 (C_5H_5, $^1J_{C\text{-}H}$ = 171 Hz), δ 111.2 (C_5H_5, $^1J_{C\text{-}H}$ = 171 Hz), 68.5 (allyl CH_2, $^1J_{C\text{-}H\textit{anti}}$ = 145 Hz, $^1J_{C\text{-}Hsyn}$ = 156 Hz), 163.6 (allyl C), 53 (CH_2, $^1J_{C\text{-}H}$ = 135 Hz), 31.2 (CH, $^1J_{C\text{-}H}$ = 127 Hz), 23 (CH_3, $^1J_{C\text{-}H}$ = 129 Hz) ppm.

4.4.5. *In situ* Reaction between $[Cp_2ZrMe][MeB(C_6F_5)_3]$ and CD_3CN

A solution of Cp_2ZrMe_2 (40 μmole) in C_6D_5Cl (0.5 mL) was added to a solution of $B(C_6F_5)_3$ (1.1 equiv.) in C_6D_5Cl (0.5 mL) and the ion pair generated was charged in an NMR tube. After the NMR tube was capped with a septum, it was removed from the glovebox and the yellow ion pair solution was characterized by ^{1}H NMR. After running the ^{1}H NMR, 3 equivalents of CD_3CN was injected into the NMR tube via a microsyringe at room temperature, the NMR tube was shaken vigorously after which a new ^{1}H NMR spectrum was acquired.

NMR Spectroscopic Data of $[Cp_2ZrMe][MeB(C_6F_5)_3]$

^{1}H NMR (600 MHz, C_6D_5Cl, 25°C): δ 5.97 (s, C_5H_5, 10H), 0.56 (s, Zr-CH_3, 3H), 0.34 (br.s, B-CH_3, 3H) ppm.

^{1}H NMR (600 MHz, C_6D_5Cl, 0°C): δ 5.93 (s, C_5H_5, 10H), 0.55 (s, Zr-CH_3, 3H), 0.33 (br.s, B-CH_3, 3H) ppm.

NMR Spectroscopic Data of $[Cp_2Zr(Me)(CD_3CN)][MeB(C_6F_5)_3]$

^1H NMR (600 MHz, C_6D_5Cl, 25°C): δ 5.83 (s, C_5H_5, 10H), 0.22 (s, Zr-CH_3, 3H), 1.16 (br.s, B-CH_3, 3H) ppm.

^1H NMR (600 MHz, C_6D_5Cl, 0°C): δ 5.80 (s, C_5H_5, 10H), 0.20 (s, Zr-CH_3, 3H), 1.21 (br.s, B-CH_3, 3H) ppm.

4.4.6. General procedure for Variable Temperature NMR experiments

Samples of $[Cp_2Zr(\eta^3\text{-allyl})]^+$ complexes used for variable temperature ^1H NMR studies were prepared as described in Sections 4.4.2, 4.4.3, and 4.4.4. Samples were brought to the indicated temperature and allowed to equilibrate for 7-10 minutes before the ^1H NMR spectra were acquired. All of the temperature-dependent changes are reversible, i.e. on cooling the probe temperature, the reverse chemical shift changes occur. Free energy of activations, $\Delta G^{\ddagger}$, were calculated in kJ/mol from the equation $\Delta G^{\ddagger} = R \cdot T[23.76 - \ln(k/T)]$, where R is the gas constant (8.3145 J/mol·K), T is the absolute temperature (K) and k is the rate constant (sec^{-1}). The rate constant at coalescence temperature was approximated using the relation $k_{coal} = \pi \cdot \Delta\nu / \sqrt{2} = 2.22 \cdot \Delta\nu$, where Δν is the frequency difference (Hz) of decoalesced resonances measured at the temperature of the frozen spectrum. Making the substitution, one obtaines $\Delta G^{\ddagger} = R \cdot T_c[23.76 - \ln(2.22 \cdot \Delta\nu / T_c)]$, where T_c is coalescence temperature (K).[18b]

4.4.7. General Procedure for Kinetics experiments

a) In a typical experiment, a solution of Cp_2ZrMe_2 (40 μmole) in C_6D_5Cl (0.5 mL) was added to a solution of $B(C_6F_5)_3$ (1.1 equiv.) in C_6D_5Cl (0.5 mL) and the yellow ion pair

solution thus formed was transferred to an NMR tube. The NMR tube was sealed with a rubber septum and parafilm and removed from the glovebox. The NMR tube was then placed in the probe of an NMR spectrometer at a predetermined temperature and allowed to equilibrate for 7-10 minutes before the ^{1}H NMR spectrum of the ion pair solution was acquired. The NMR tube was removed from the NMR spectrometer and 2,4-dimethyl-1-pentene (1.5 equivalents) was injected in the NMR tube via a microsyringe. The NMR tube was quickly shaken and placed in the NMR probe at the same predetermined temperature. ^{1}H NMR spectra were acquired automatically at certain time intervals in order to monitor the progress of the reaction.

b) A solution of Cp_2ZrMe_2 (40 μmole) in C_6D_5Cl (0.5 mL) was added to a solution of $[Ph_3C][B(C_6F_5)_4]$ (1.1-1.2 equiv.) in C_6D_5Cl (0.5 mL) and the orange ion pair solution thus formed was transferred to an NMR tube. The NMR tube was sealed with a rubber septum and parafilm and removed from the glovebox. The sample was heated at 40°C for about 30 min in order to convert the methyl bridged binuclear cation (minor amount) to the mononuclear species. The NMR tube was then placed in the probe of an NMR spectrometer at a predetermined temperature and allowed to equilibrate for 7-10 minutes before the ^{1}H NMR spectrum of the ion pair solution was acquired. The NMR tube was removed from the NMR spectrometer and placed in a dry ice bath set at a temperature of 3-5°C lower than the temperature of the NMR probe before the sample was treated with 2,4-dimethyl-1-pentene (1.5 equivalents). The NMR tube was quickly shaken, wiped, and placed in the NMR probe at the same predetermined temperature. ^{1}H NMR spectra were

acquired automatically at certain time intervals in order to monitor the progress of the reaction.

4.4.8. *In situ* Propylene polymerization by [Cp_2ZrMe][$MeB(C_6F_5)_3$]

A solution of Cp_2ZrMe_2 (40 μmole) in C_6D_5Cl (0.5 mL) was added to a solution of $B(C_6F_5)_3$ (1.1 equiv.) in C_6D_5Cl (0.5 mL) and the yellow ion pair solution thus formed was transferred to an NMR tube. The NMR tube was sealed with a rubber septum and parafilm, removed from the glovebox and the yellow ion pair solution was characterized by ^1H NMR. After running the ^1H NMR, roughly 5 equivalents of propylene was injected into the NMR tube via a syringe at room temperature, the NMR tube was shaken vigorously after which a new ^1H NMR spectrum was acquired. Subsequently, an additional 5 equivalents of propylene was injected into the NMR tube via a syringe at room temperature, the NMR tube was shaken again and a new ^1H NMR spectrum was acquired.

4.4.9. *In situ* Propylene polymerization by [Cp_2ZrMe][$B(C_6F_5)_4$]

A solution of Cp_2ZrMe_2 (40 μmole) in C_6D_5Cl (0.5 mL) was added to a solution of $[Ph_3C][B(C_6F_5)_4]$ (1.1 equiv.) in C_6D_5Cl (0.5 mL) and the orange ion pair solution thus formed was transferred to an NMR tube. The NMR tube was sealed with a rubber septum and parafilm, removed from the glovebox and the yellow ion pair solution was characterized by ^1H NMR. After running the ^1H NMR, roughly 5 equivalents of propylene was injected into the NMR tube via a syringe at room temperature, the NMR tube was shaken vigorously after which a new ^1H NMR spectrum was acquired.

Subsequently, an additional 5 equivalents of propylene was injected into the NMR tube via a syringe at room temperature, the NMR tube was shaken again and a new ^{1}H NMR spectrum was acquired.

4.4.10. General procedure for ESI-MS/MS experiments

A solution of Cp_2ZrMe_2 (40 μmole) in dry C_6H_5Cl (0.5 mL) was added to a solution of $B(C_6F_5)_3$ (1.1 equiv.) in dry C_6H_5Cl (0.5 mL) and the yellow ion pair solution thus formed was transferred to a vial. The vial was sealed with a rubber septum and parafilm, removed from the glovebox and a predetermined amount of propylene (either 5 or 10 equivalents) was injected into the NMR tube via a syringe at room temperature. The vial was quickly shaken, the reaction mixture was further diluted with an additional 1 mL of dry C_6H_5Cl and shaken again. The resulted reaction mixture was then fed continuously into the first quadrupole of a QSTAR XL QqTOF mass spectrometer, under an atmosphere of dry nitrogen, via a syringe. The flow rate could be varied between 5 and 20 μl/min.

4.4.11. ^{1}H NMR Spectroscopic Data of 2,4-Me_2-1-pentene

^{1}H NMR (600 MHz, C_6D_5Cl, 25°C) δ 4.86 (s, CH_2=, 1H), 4.78 (s, CH_2=, 1H), 1.92 (d, $^3J_{HH}$ = 7.6 Hz, CH_2, 2H), 1.77 (m, CH, 1H), 1.71 (s, CH_3, 3H), 0.93 (d, $^3J_{HH}$ = 6.8 Hz, CH_3, 6H) ppm.

4.4.12. ^{1}H NMR Spectroscopic Data of 2,4-Me_2-1-heptene

^{1}H NMR (600 MHz, C_6D_5Cl, 25°C) δ 4.87 (s, CH_2=, 1H), 4.81 (s, CH_2=, 1H), 2.07 (dd, J= 6.1 Hz, CH_2, 1H), 1.84 (dd, J = 8.1 Hz, CH_2, 1H), 1.73 (s, CH_3, 3H), 1.65 (m, CH, 1H), 1.40 and 1.32 (2m, CH_2, 2H), 1.33 and 1.11 (2m, CH_2, 2H), 0.96 (t, $^{3}J_{HH}$ = 7.3 Hz, CH_3, 3H), 0.92 (d, $^{3}J_{HH}$ = 6.7 Hz, CH_3, 3H) ppm.

References

1. (a) Brintzinger, H. –H.; Fischer, D.; Mülhaupt, R.; Rieger, B.; Waymouth, R. M. *Angew. Chem. Int. Ed. Engl.* **1995**, *34*, 1143. (b) Bochmann, M. *Topics in Catalysis*. **1999**, *7*, 9. (c) Fischer, D.; Mülhaupt, R. *J. Organomet. Chem*. **1991**, *417*, C7. (d) Chien, J. C. W.; Sugimoto, R. *J. Polym. Sci. A., Polym. Chem*. **1991**, *29*, 459. (e) Dornik, H. P.; Luft, G.; Rau, A.; Wieczorek, T. *Macromol. Mater. Eng*. **2004**, *289*, 475. (f) Janiak, C.; Lange, K. C. H.; Marquardt, P. *J. Molec. Catal. A. Chem*. **2002**, *180*, 43. (g) Stehling, U.; Diebold, J.; Kirsten, R.; Röll, W.; Brintzinger, H. –H. *Organometallics* **1994**, *13*, 964. (h) Thorshaug, K.; Støvneng, J. A.; Rytter, E.; Ystenes, M. *Macromolecules* **1998**, *31*, 7149.
2. (a) Wondimagegn, T.; Xu, Z.; Vanka, K.; Ziegler, T. *Organometallics* **2004**, *23*, 3847. (b) Margl, P. M.; Woo, T. K.; Ziegler, T. *Organometallics* **1998**, *17*, 4997.
3. (a) Moscardi, G.; Piemontesi, F.; Resconi, L. *Organometallics* **1999**, *18*, 5264. (b) Lin, S.; Kravchenko, R.; Waymouth, R. M. *J. Molec. Cat. A: Chem*. **2000**, *158*, 423. (c) Tsutsui, T.; Kashiwa, N.; Mizuno, A. *Makromol. Chem., Rapid Commun*. **1990**, *11*, 565. (d) Lahelin, M.; Kokko, E.; Lehmus, P.; Pitkänen, P.; Löfgren, B.; Seppälä, J. *Macromol. Chem. Phys.* **2003**, *204*, 1323. (e) Juengling, S.; Muelhaupt, R.; Stehling, U.; Brintzinger, H. –H.; Fischer, D.; Langhauser, F. *J. Polym. Sci. A: Polym. Chem*. **1995**, *33*, 1305.
4. (a) Busico, V.; Cipullo, R.; Chadwick, J. C.; Modder, J. F.; Sudmeijer, O. *Macromolecules* **1994**, *27*, 7538. (b) Busico, V.; Cipullo, R.; Ronca, S. *Macromolecules* **2002**, *35*, 1537. (c) Busico, V.; Cipullo, R.; Talarico, G. *Macromolecules* **1998**, *31*, 2387.

5. (a) Landis, C. R.; Sillars, D. L.; Batterton, J. M. *J. Am. Chem. Soc.* **2004**, *126*, 8890. (b) Vatamanu, M.; Boden, B. N.; Baird, M. C. *Macromolecules* **2005**, *38*, 9944.
6. (a) Rieger, B.; Mu, X.; Mallin, D. T.; Rausch, M. D.; Chien, J. C. W. *Macromolecules* **1990**, *23*, 3559. (b) Grassi, A.; Zambelli, A.; Resconi, L.; Albizzati, E.; Mazzocchi, R. *Macromolecules* **1988**, *21*, 617. (c) Stehling, U.; Diebold, J.; Kristen, R.; Röll, W.; Brintzinger, H-. H.; Jüngling, S.; Mülhaupt, R.; Langhauser, F. *Organometallics* **1994**, *13*, 964. (d) Jüngling, S.; Mülhaupt, R.; Stehling, U.; Brintzinger, H-. H.; Fischer, D.; Langhauser, F. *J. Polym. Sci., Pol. Chem.* **1995**, *33*, 1305.
7. (a) Song, F.; Cannon, R. D.; Bochmann, M. *J. Am. Chem. Soc*. **2003**, *125*, 7641. (b) Resconi, L.; Camurati, I.; Sudmeijer, O. *Topics in Catalysis* **1999**, *7*, 145. (c) Resconi, L.; Piemontesi, F.; Camurati, I.; Balboni, D.; Sironi, A.; Moret, M.; Rychlicki, H.; Zeigler, R. *Organometallics* **1996**, *15*, 5046. (d) Dang, V. A.; Yu, L.-C.; Balboni, D.; Dall'Occo, T.; Resconi, L.; Mercandelli, P.; Moret. M.; Sironi, A. *Organometallics* **1999**, *18*, 3781. (e) Resconi, L.; Fait, A.; Piemontesi, F.; Colonnesi, M.; Rychlicki, H.; Zeigler, R. *Macromolecules* **1995**, *28*, 6667.
8. Liu, Z.; Somsook, E.; White, C. B.; Rosaaen, K. A.; Landis, C. R. *J. Am. Chem. Soc.* **2001**, *123*, 11193.
9. Busico, V.; Cipullo, R.; Romanelli, V.; Ronca, S.; Togrou, M. *J. Am. Chem. Soc.* **2005**, *127*, 1608.
10. (a) Bukatov, G. D.; Goncharov, V. S.; Zakharov, V. A. *Macromol. Chem. Phys*. **1995**, *196*, 1751. (b) Spitz, R.; Masson, P.; Bobichon, C.; Guyot, A. *Makromol. Chem*. **1989**, *190*, 717.

11. (a) Resconi, L. *J. Molec. Cat. A: Chem.* **1999**, *146*, 167. (b) Moscardi, G.; Resconi, L.; Cavallo, L. *Organometallics* **2001**, *20*, 1918.

12. (a) Al-Humydi, A.; Garrison, J. C.; Mohammed, M.; Youngs, W. J.; Collins, S. *Polyhedron* **2005**, *24*, 1234. (b) Landis, C. R.; Christianson, M. D. *Proc. Natl. Acad. Sci. USA* **2006**, *103*, 15349.

13. Jeske, G.; Lauke, H.; Mauermann, H.; Swepston, P. N.; Schumann, H.; Marks, T. J. *J. Am. Chem. Soc* **1985**, *107*, 8091.

14. (a) Casey, C. P.; Carpenetti, D. W.; Sakurai, H. *J. Am. Chem. Soc.* **1999**, *121*, 9483. (b) Galakhov, M. V.; Heinz, G.; Royo, P. *Chem. Commun*. **1998**, *17*.

15. (a) Horton, A. D. *Organometallics* **1996**, *15*, 2675. (b) Lieber, S.; Prosenc, M. –H.; Brintzinger, H. –H. *Organometallics* **2000**, *19*, 377.

16. (a) Horton, A. D. *Organometallics* **1992**, *11*, 3271. (b) Jordan, R. F.; LaPointe, R. E. ; Bradley, P. K. ; Baenziger, N. *Organometallics* **1989**, *8*, 2892.

17. Tjaden, E. B.; Casty, G. L.; Stryker, J. M. *J. Am. Chem. Soc*. **1993**, *115*, 9814.

18. (a) Silverstein, R. M.; Webster, F. X. *Spectrometric Identification of Organic Compounds*, Sixth Ed., John Wiley & Sons, Inc. **1998**. (b) Günther, H. *NMR Spectroscopy: Basic Principles, Concepts, and Applications in Chemistry*, Second Ed., John Wiley & Sons, Ltd. **1995**.

19. (a) Benn, R.; Rufińska, A. *J. Organomet. Chem*. **1982**, *239*, C19. (b) Schlosser, M.; Stähle, M. *Angew. Chem. Int. Ed. Engl*. **1982**, *21*, 145. (c) Brownstein, S.; Bywater, S.; Worsfold, D. J. *J. Organomet. Chem.* **1980**, *199*, 1.

20. Erker, G.; Berg, K.; Angermund, K.; Krüger, C. *Organometallics* **1987**, *6*, 2620.

21. Benn, R. Rufińska, A.; Schroth, G. *J. Organomet. Chem*. **1981**, *217*, 91.

22. (a) Temme, B.; Erker, G.; Karl, J.; Luftmann, H.; Fröhlich, R.; Kotila, S. *Angew. Chem. Int. Ed. Engl.* **1995**, *34*, 1755. (b) Karl, J.; Erker, G.; Fröhlich, R. *J. Organomet. Chem.* **1997**, *535*, 59. (c) Dahlmann, M.; Erker, G.; Nissinen, M.; Fröhlich, R. *J. Am. Chem. Soc*. **1999**, *121*, 2820. (d) Karl, J.; Erker, G.; Fröhlich, R. *J. Am. Chem. Soc*. **1997**, *119*, 11165.

23. (a) Bochmann, M.; Lancaster, S. *J. Angew. Chem. Int. Ed. Engl.* **1994**, *33*, 1634. (b) Bochmann, M.; Lancaster, S. J. *J. Organomet. Chem*. **1995**, *497*, 55. (c) Zhou, J.; Lancaster, S. J.; Walker, D. A.; Beck, S.; Thornton-Pett, M.; Bochmann, M. *J. Am. Chem. Soc.* **2001**, *123*, 223.

24. (a) Chen, E. Y.-X.; Metz, M. V.; Li, L.; Stern, C. L.; Marks, T. J. *J. Am. Chem. Soc*. **1998**, *120*, 6287. (b) Chen, E. Y.-X.; Marks, T. J. *Chem. Rev*. **2000**, *100*, 1391.

25. Jordan, R. F.; Dasher, W. E.; Echols, S. F. *J. Am. Chem. Soc.* **1986**, *108*, 1718.

26. (a) Baird, M. C. *Chem. Rev*. **2000**, *100*, 1471. (b) Carr, A. G.; Dawson, D. M.; Bochmann, M. *Macromolecules* **1998**, *31*, 2035. (c) Carr, A. G.; Dawson, D. M.; Thornton-Pett, M.; Bochmann, M. *Organometallics* **1999**, *18*, 2933. (d) Song, X.; Thornton-Pett, M.; Bochmann, M. *Organometallics* **1998**, *17*, 1004.

27. (a) Stoebenau, E. J.; Jordan, R. F. *J. Am. Chem. Soc.* **2006**, *128*, 8162. (b) Stoebenau, E. J.; Jordan, R. F. *J. Am. Chem. Soc.* **2006**, *128*, 8638.

28. Stoebenau, E. J.; Jordan, R. F. *J. Am. Chem. Soc.* **2004**, *126*, 11170.

29. Vatamanu, M.; Stojcevic, G.; Baird, M. C. *J. Am. Chem. Soc*. **2008**, *130*, 454.

30. Wilkins, R. G. *Kinetics and Mechanism of Reactions of Transition Metal Complexes*, 2nd Edition, **1991**, Weinheim; New York.

31. (a) Yoshida, T.; Koga, N.; Morokuma, K. *Organometallics*, **1995**, *14*, 746. (b) Margl, P.; Deng, L.; Ziegler, T. *J. Am Chem. Soc*. **1998**, *120*, 5517. (c) Yoshida, T.; Koga, N.; Morokuma, K. *Organometallics* **1996**, *15*, 766. (d) Chien, J. C. W.; Razavi, A. *J. Polym. Sci. A; Polym. Chem.* **1988**, *26*, 2369.

32. (a) Abrams, M. B.; Yoder, J. C.; Loeber, C.; Day, M. W.; Bercaw, J. E. *Organometallics* **1999**, *18*, 1389. (b) Benn, R. Rufińska, A.; Schroth, G. *J. Organomet. Chem*. **1981**, *217*, 91. (c) Faller, J. W.; Incorvia, M. J.; Thomsen, M. E. *J. Am. Chem. Soc*. **1969**, *91*, 518.

33. (a) Krieger, J. K.; Deutch, J. M.; Whitesides G. M. *Inorg. Chem*. **1973**, *12*, 1535. (b) Wilke, G.; Bogdanović, B.; Hardt, P.; Heimbach, P.; Keim, W.; Kröner, M.; Oberkirch, W.; Tanaka, K.; Steinrücke, E.; Walter, D.; Zimmermann, H. *Angew. Chem. Internat. Ed.* **1966**, *2*, 151. (c) Becconsall, J. K.; Job, B. E.; O'Brien, S. *J. Chem. Soc. A* **1967**, *423*. (d) Faller, J. W.; Thomsen, M. E.; Mattina, M. J. *J. Am. Chem. Soc*. **1971**, *93*, 2642. (e) Cotton, F. A.; Faller, J. W.; Musco, A. *Inorg. Chem*. **1967**, *6*, 179.

34. Yang, P.; Baird, M. C. *Organometallics* **2005**, *24*, 6013.

35. Resconi, L. ; Piemontesi, F. ; Camurati, I. ; Sudmeijer, O. ; Nifant'ev, I. E. ; Ivchenko, P. V. ; Kuz'mina, L. G. *J. Am. Chem. Soc*. **1998**, *120*, 2308.

36. Schaverien, C. J.; Ernst, R.; Schut, P.; Dall'Occo, T. *Organometallics* **2001**, *20*, 3436.

37. Christ, Jr., C. S.; Eyler, J. R.;Richardson, D. E. *J. Am. Chem. Soc*. **1990**, *112*, 596.

38. Aksenov, A. A.; Contreras, C. S. ; Richardson, D. E. ; Eyler, J. R. *Organometallics* **2007**, *26*, 478.

39. Santos, L. S. ; Metzger, J. O. *Angew. Chem. Int. Ed*. **2006**, *45*, 977.

Chapter 5

Conclusions

In this thesis, a systematic study on the nature and relative concentrations of Zr-polymeryl intermediates present during ethylene and propylene polymerization by homogeneous zirconium-based olefin polymerization catalysts is reported. In this regard, the potential of bromine as a quenching agent to give polymers containing brominated end groups, Br-polymeryl, is investigated. Using NMR spectroscopy, the Br-polymeryl groups can be identified as primary or secondary, thus providing information concerning the nature of the Zr-polymeryl linkage(s). Via integration, information about the relative concentration(s) of the Zr-polymeryl linkage(s) is also obtained. Aside from bromine, conventional quenching agent CH_3OH and the deuterium-labeling agent CD_3OD, are also used.

Bromine quenching was examined for ethylene polymerization by $Cp_2ZrMe_2/B(C_6F_5)_3$, and for propylene polymerization by $Cp_2ZrMe_2/B(C_6F_5)_3$, by $(indenyl)_2ZrMe_2/B(C_6F_5)_3$, and by *rac*-$\{C_2H_4(1\text{-indenyl})_2\}ZrMe_2/B(C_6F_5)_3$. Polymers with primary alkyl bromide end groups were obtained. In the case of propylene

polymerization by [ONNO]Zr($CH_2C_6H_5)_2$/MAO/2,6-di-^{t}Butylphenol, both primary and secondary alkyl bromide end groups were detected in polymers obtained after quenching the polymerization with bromine. Primary alkyl bromide end groups result from the cleavage by bromine of primary Zr-CH_2~polymeryl linkages while secondary alkyl bromides are the result of the cleavage by bromine of secondary Zr-CH(Me)CH_2~polymeryl linkages.

The relative concentration of Zr-CH_2~polymeryl intermediates was found to be low, less than 10% of the initial catalyst in the case of ethylene and propylene polymerization by $Cp_2ZrMe_2/B(C_6F_5)_3$. In the case of propylene polymerization by $(indenyl)_2ZrMe_2/B(C_6F_5)_3$, on the other hand, a relatively high value of 84% was reached within 20 sec, after which it decreased to much lower values for longer polymerization times (32% after 4 min). For propylene polymerization in the presence of [ONNO]Zr($CH_2C_6H_5)_2$/MAO/2,6-di-^{t}Butylphenol, the concentration of Zr-CH_2~polymeryl groups was always lower than the concentration of the initial catalyst. These results suggest that in all cases the catalyst deactivates during the polymerization.

The catalyst deactivation is usually attributed to formation of secondary (2,1) Zr-polymeryl species, which are assumed to be slowly propagating and to therefore accumulate in the polymerization system rather than engage in subsequent propagation steps. However, no secondary alkyl bromide end groups were detected in polypropylenes obtained from $Cp_2ZrMe_2/B(C_6F_5)_3$ and $(indenyl)_2ZrMe_2/B(C_6F_5)_3$ in chlorobenzene suggesting that at least for the propylene polymerization by the metallocene catalysts under investigation, the secondary Zr-CH(Me)CH_2~polymeryl intermediates were not present in the polymerization mixture at the time of quench. For propylene

polymerization by [ONNO]Zr($CH_2C_6H_5)_2$/MAO/2,6-di-^{t}butylphenol, on the other hand, secondary insertions of propylene into a Zr-C bond were found to occur, but the fraction of deactivated catalyst by far exceeds the fraction that could reasonably be attributed to the secondary Zr-polymeryl groups at the time of quench and therefore, the latter cannot constitute the main cause of catalyst deactivation.

An additional pathway proposed for deactivation of the catalyst during the polymerization consists of formation of Zr-allyl intermediates. The analysis of olefinic end groups of atactic polypropylene obtained from (indenyl)$_2$ZrMe_2/B($C_6F_5)_3$ after quenching the polymerization with CH_3OH indicates the presence of internal vinylidene and isobutenyl end groups on the polymer chains, in addition to the usual vinylidene end groups; this suggests that aside from the primary Zr-CH_2CH(Me)~polymeryl intermediates, Zr-allyl polymeryl intermediates are also formed during the polymerization. The bromine quenching method cannot provide information about the presence of Zr-allyl polymeryl intermediates in the polymerization systems where a high degree of chain transfer reactions via β-elimination occur, due to the close structural similarity of the brominated polymer chain ends resulting from the bromination of both Zr-allyl polymeryl intermediates and the olefinic groups present on the polymer chains. Therefore, in order to assess the presence of Zr-allyl intermediates in the polymerization mixture other methods are required.

The presence of Zr-allyl polymeryl species in the polymerization mixture was proven from the quenching of the polymerization reaction with CD_3OD. Cp_2Zr^+-allyl polymeryl intermediates were also detected in *in situ* propylene polymerization mixture by [Cp_2ZrMe][X], where [X] is either [MeB($C_6F_5)_3$] or [B($C_6F_5)_4$]. Therefore, at least for

metallocene catalyst systems, formation of Zr-allyl intermediates may constitute a cause of catalyst deactivation. In situ NMR studies indicated that formation of Zr-allyl species occurs in the early stages of the polymerization process, even before the initial catalyst $[Cp_2ZrMe]^+$ is completely consumed. The presence of methane in the ^1H NMR spectra of the *in situ* polypropylene reaction mixture implies that formation of Zr-allyl polymeryls may occur via recoordination of the vinylidene end groups of the polymer chains followed by C-H activation. This study shows clear evidence that polypropylene-containing vinylidene end groups CH_2=C(Me)~P (P = polymeryl) formed as a result of β-H elimination reactions are not simply spectators of the polymerization processes but they may recoordinate to the active catalyst to slowly convert it into less reactive Zr-allyl polymeryl intermediates.

An issue of major interest in coordination (Ziegler-Natta) polymerization of olefins is related to the observation that these processes are adversely affected by the conversion of the active catalyst of the type $[Cp_2ZrMe]^+$ to relatively unreactive species of the type Zr-allyl polymeryl intermediates. Thus, a second objective of this research was to investigate the formation and characterization of Zr-allyl complexes. Compounds of type $[Cp_2ZrMe]^+$ were found to react slowly with the model propylene oligomers 2,4-Me_2-1-pentene and 2,4-Me_2-1-heptene in C_6D_5Cl to form methane and cationic allylic complexes of type $Cp_2Zr^+(\eta^3$-allyl). Variable temperature ^1H NMR experiments indicate that all Zr-allyl complexes under investigation are fluxional and that the η^3-coordinated allyl complexes are in equilibrium with η^1-coordinated allyls, the mole fraction of each one being temperature dependent. A kinetic study indicates that formation of Cp_2Zr^+-allyl species from either $[Cp_2ZrMe][MeB(C_6F_5)_3]$ or $[Cp_2ZrMe][B(C_6F_5)_4]$ and 2,4-Me_2-1-

pentene is facile. These experiments are important as they suggest that polypropylene containing vinylidene end groups may indeed react in the same way with the active catalyst. Thus, at least for propylene polymerization by zirconocenes, catalyst deactivation via recoordination of vinylidene end groups of the polymer chains with formation of Zr-allyl polymeryl intermediates is a side reaction which might not be avoided. The $Cp_2Zr^+(\eta^3$-allyl) intermediates synthesized in this thesis can serve as excellent models for similar Zr-allyl intermediates which form during Ziegler-Natta polymerization processes.

The reaction of $[Cp_2ZrMe][B(C_6F_5)_4]$ with $CH_2=C(Me)CH_2CHMe_2$ in C_6D_5Cl involves the unprecedented η^1- or near η^1-vinylidene intermediate $[Cp_2Zr(Me)(CH_2CMeCH_2CHMe_2)]^+$, detected by low temperature one- and two-dimensional ^1H NMR spectroscopy. Alkyl alkene intermediates of the type Cp_2Zr^+(alkyl)(alkene) are of great interest as they are considered key intermediates in olefin polymerization by metallocene catalysts. Despite intense research to date in this area, such an intermediate was never observed during the catalysis. Thus, the observation of the $[Cp_2Zr(Me)(CH_2C(Me)CH_2CHMe_2)]^+$ complex represents the first direct experimental evidence for a d^0 metal-alkyl-olefin complex, detectable apparently because migratory insertion does not readily occur with vinylidene ligands. As the $[Cp_2Zr(Me)(CH_2C(Me)CH_2CHMe_2)]^+$ complex was observed to form during the reaction between active catalyst and an vinylidene compound of the type $CH_2=C(Me)$(alkyl), it is anticipated that similar intermediates might form during the metallocene-catalyzed propylene polymerization. The $[Cp_2Zr(Me)(CH_2C(Me)CH_2CHMe_2)]^+$ complex represents an excellent model of an metal-alkyl-alkene intermediate present in propylene

polymerization and further investigation of this complex related to structure and reactivity may provide essential information in understanding the Ziegler-Natta polymerization mechanism.

Appendix A:

^{1}H NMR spectrum (600 MHz, 25°C, CD_2Cl_2) of atactic polypropylene obtained from (indenyl)$_2$ZrMe$_2$/B(C_6F_5)$_3$ in chlorobenzene after CD_3OD quenching.

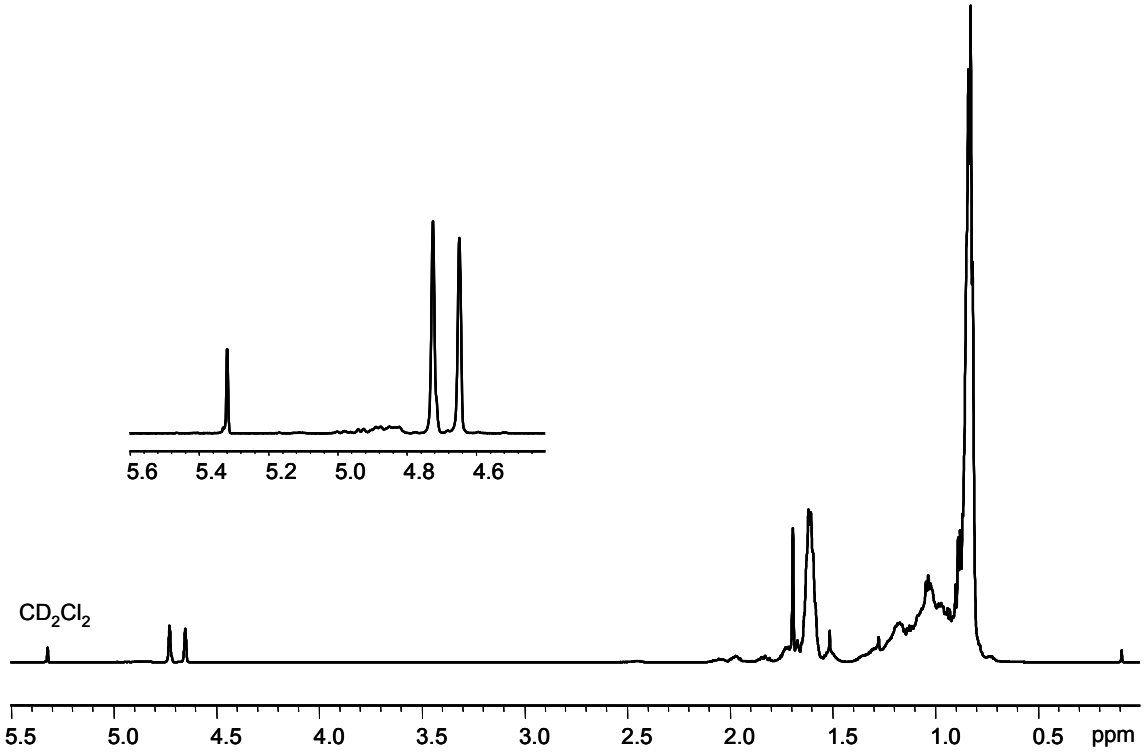

Appendix B:

^{13}C NMR spectrum in aliphatic region of iPP obtained from propylene polymerization by [ONNO]Zr($CH_2C_6H_5$)$_2$/MAO/2,6-di-^{t}butylphenol (4 min polymerization time, MeOH/HCl quenching, 1,1,2,2-tetrachloroethane-d_2, 120°C, 400 MHz).